NATIONAL COOPERATIVE HIGHWAY RESEARCH PROGRAM

NCHRP Report 411

Structural Supports for Highway Signs, Luminaires, and Traffic Signals

Transportation Research Board
National Research Council

NATIONAL COOPERATIVE HIGHWAY RESEARCH PROGRAM

Report 411

Structural Supports for Highway Signs, Luminaires, and Traffic Signals

FOUAD H. FOUAD
ELIZABETH A. CALVERT
EDGAR NUNEZ
The University of Alabama at Birmingham
Department of Civil and Environmental Engineering
Birmingham, AL

Subject Areas

Highway and Facility Design
Bridges, Other Structures, and Hydraulics and Hydrology

Research Sponsored by the American Association of State Highway and Transportation Officials in Cooperation with the Federal Highway Administration

TRANSPORTATION RESEARCH BOARD
NATIONAL RESEARCH COUNCIL

NATIONAL ACADEMY PRESS
Washington, D.C. 1998

NATIONAL COOPERATIVE HIGHWAY RESEARCH PROGRAM

Systematic, well-designed research provides the most effective approach to the solution of many problems facing highway administrators and engineers. Often, highway problems are of local interest and can best be studied by highway departments individually or in cooperation with their state universities and others. However, the accelerating growth of highway transportation develops increasingly complex problems of wide interest to highway authorities. These problems are best studied through a coordinated program of cooperative research.

In recognition of these needs, the highway administrators of the American Association of State Highway and Transportation Officials initiated in 1962 an objective national highway research program employing modern scientific techniques. This program is supported on a continuing basis by funds from participating member states of the Association and it receives the full cooperation and support of the Federal Highway Administration, United States Department of Transportation.

The Transportation Research Board of the National Research Council was requested by the Association to administer the research program because of the Board's recognized objectivity and understanding of modern research practices. The Board is uniquely suited for this purpose as it maintains an extensive committee structure from which authorities on any highway transportation subject may be drawn; it possesses avenues of communications and cooperation with federal, state and local governmental agencies, universities, and industry; its relationship to the National Research Council is an insurance of objectivity; it maintains a full-time research correlation staff of specialists in highway transportation matters to bring the findings of research directly to those who are in a position to use them.

The program is developed on the basis of research needs identified by chief administrators of the highway and transportation departments and by committees of AASHTO. Each year, specific areas of research needs to be included in the program are proposed to the National Research Council and the Board by the American Association of State Highway and Transportation Officials. Research projects to fulfill these needs are defined by the Board, and qualified research agencies are selected from those that have submitted proposals. Administration and surveillance of research contracts are the responsibilities of the National Research Council and the Transportation Research Board.

The needs for highway research are many, and the National Cooperative Highway Research Program can make significant contributions to the solution of highway transportation problems of mutual concern to many responsible groups. The program, however, is intended to complement rather than to substitute for or duplicate other highway research programs.

Note: The Transportation Research Board, the National Research Council, the Federal Highway Administration, the American Association of State Highway and Transportation Officials, and the individual states participating in the National Cooperative Highway Research Program do not endorse products or manufacturers. Trade or manufacturers' names appear herein solely because they are considered essential to the object of this report.

NCHRP REPORT 411

Project G17-10 FY'94

ISSN 0077-5614

ISBN 0-309-06271-3

L. C. Catalog Card No. 98-60938

Price $30.00

NOTICE

The project that is the subject of this report was a part of the National Cooperative Highway Research Program conducted by the Transportation Research Board with the approval of the Governing Board of the National Research Council. Such approval reflects the Governing Board's judgment that the program concerned is of national importance and appropriate with respect to both the purposes and resources of the National Research Council.

The members of the technical committee selected to monitor this project and to review this report were chosen for recognized scholarly competence and with due consideration for the balance of disciplines appropriate to the project. The opinions and conclusions expressed or implied are those of the research agency that performed the research, and, while they have been accepted as appropriate by the technical committee, they are not necessarily those of the Transportation Research Board, the National Research Council, the American Association of State Highway and Transportation Officials, or the Federal Highway Administration, U.S. Department of Transportation.

Each report is reviewed and accepted for publication by the technical committee according to procedures established and monitored by the Transportation Research Board Executive Committee and the Governing Board of the National Research Council.

Published reports of the

NATIONAL COOPERATIVE HIGHWAY RESEARCH PROGRAM

are available from:

Transportation Research Board
National Research Council
2101 Constitution Avenue, N.W.
Washington, D.C. 20418

and can be ordered through the Internet at:

http://www.nas.edu/trb/index.html

Printed in the United States of America

FOREWORD

By Staff
Transportation Research Board

This report contains the findings of a study undertaken to develop design specifications for structural supports for highway signs, luminaires, and traffic signals. The report reviews the specification development effort and explains the theoretical basis for the recommended design provisions. The contents of this report will be of immediate interest to highway and bridge designers.

Since the 1985 edition of the AASHTO *Standard Specifications for Structural Supports for Highway Signs, Luminaires, and Traffic Signals* was published, significant changes have occurred in design philosophies, material choices, and manufacturing processes for highway sign, luminaire, and traffic signal supports. These specifications lack comprehensive criteria for all materials, and some support components are not adequately addressed. In addition, design criteria for oscillation, fatigue, and deflection need improvement. Because of these deficiencies, revised specifications were needed.

The objective of this research was to develop up-to-date, comprehensive specifications, and an accompanying commentary, for structural supports for highway signs, luminaires, and traffic signals. Under NCHRP Project 17-10, the University of Alabama at Birmingham reviewed research reports, specifications, and related documents pertaining to design concepts and materials. This report provides detailed information on the development of wind loading criteria by using new isotach maps, revised allowable bending stresses for steel, deflection limitations, the analysis of second order effects, fatigue and vibration provisions, anchor bolt requirements, span wire design philosophies and new sections on composites and wood support structures. The report clearly identifies proposed changes to the specifications and provides an assessment of the impact of the change. The new specification reflects state-of-the-art design philosophies and manufacturing processes and includes guidance for poles fabricated from steel, aluminum, prestressed concrete, timber, and fiber-reinforced plastic composites.

CONTENTS

AUTHOR ACKNOWLEDGMENTS

The research reported herein was performed under NCHRP Project 17-10 by The University of Alabama at Birmingham, Department of Civil and Environmental Engineering. Fouad H. Fouad, Professor of Civil Engineering at The University of Alabama at Birmingham, was the principle investigator. The other authors of this report are Elizabeth A. Calvert, Research Associate, and Edgar Nunez, Research Assistant at the Department of Civil and Environmental Engineering, The University of Alabama at Birmingham.

Work related to wind loading provisions was spearheaded by Dr. W. Lynn Beason, Professor at Texas A&M University. The work undertaken at Texas A&M was under a subcontract with The University of Alabama at Birmingham.

Mr. John J. Panak, who served as a consultant to the project, provided invaluable advice throughout the work. His expertise and guidance resulted in major improvements to various sections of the proposed specifications.

Special thanks is extended to Mr. James H. Hatton, Jr., Mr. Ray Bailey, and Mr. Randy Kissell, who provided comments and reviews for selected sections of the specifications.

Finally, the authors are most grateful to the NCHRP Project 17-10 panel members and would like to acknowledge their patience and guidance throughout the study. The panel review sessions, chaired by Mr. Allen F. Laffoon, were particularly helpful to the researchers.

STRUCTURAL SUPPORTS FOR HIGHWAY SIGNS, LUMINAIRES, AND TRAFFIC SIGNALS

SUMMARY

NCHRP Project 17-10 was undertaken in an effort to update the 1985 AASHTO *Standard Specifications for Structural Supports for Highway Signs, Luminaires, and Traffic Signals* and its subsequent interim specifications (*1–5*). Because the 1985 *Supports Specifications* is based on studies and reports that were published in the late 1960s, a significant amount of work was performed to incorporate new information that is currently available in design codes as well as in new industry practices. Major revisions include introducing the new wind map and current wind engineering practice, incorporating the new breakaway provisions of *NCHRP Report 350* (*6*), including a new section on fiber-reinforced composites, providing a comprehensive section on wood structures, and converting the entire specification to Systeme Internationale (SI) units.

The research consisted of an extensive review and analysis of theoretical and experimental research investigations, with major emphasis on adding new technical information in the proposed specifications and commentary. Several technical areas, identified as needing the most research, were investigated with the purpose of developing improved design criteria. These areas included new wind load criteria, allowable bending stresses for steel and aluminum, alternative design procedures, allowable dead load deflections, final deflected position, fiber-reinforced composites, wood structures, prestressed concrete design, span wire design philosophies, breakaway devices, fatigue design, loading across the diagonal, anchorage systems, foundation design philosophies, and corrosion protection systems. Other topics were also addressed as deemed necessary by the researchers. The proposed *Supports Specifications* contains updates and state-of-the-art information on most of the topics listed above. New sections on fatigue resistant design, design of fiber-reinforced composites, and design of wood structures have also been added.

A comprehensive literature study, including the review of research on design concepts and materials for highway sign, luminaire, and traffic signal structures, was conducted as part of this study. A survey of all major manufacturers of structural supports, as well as state departments of transportation (DOTs), was performed to solicit their input on technical items of particular importance that needed to be included in the study. The research team visited major support manufacturers to obtain information on manufacturing, testing, and quality control procedures. DOTs with special expertise in structural supports were also contacted.

The updated *Supports Specifications* and commentary resulting from this study are presented in a format similar to the AASHTO *LRFD Bridge Design Specifications* (*7*). This format will provide the engineer with a uniform design methodology and a document that is easier to use. Several enhancements in the proposed specifications ensure its user friendliness, such as a detailed table of contents, a side-by-side specification and commentary format, and a list of references for each section.

This study also identified topics that need future research beyond what was accomplished in the project. A detailed discussion of these topics, as well as an approach for further investigating them, is presented in Chapter 4. The report also provides an implementation plan for moving the research into practice and discusses the work needed for future improvements to the proposed *Supports Specifications*.

CHAPTER 1

INTRODUCTION AND RESEARCH APPROACH

1.1 RESEARCH PROBLEM STATEMENT

The 1994 AASHTO *Standard Specifications for Structural Supports for Highway Signs, Luminaires, and Traffic Signals* (*Supports Specifications*) (*5*) needs significant revisions to incorporate the changes and new information that is currently available in design codes and new industry practices. Revisions are also needed to convert the specifications to SI units, to incorporate the new breakaway provisions of *NCHRP Report 350* (*6*), to include new materials such as fiberglass support structures, and to evaluate the increasingly used load-resistance factor design method of analysis and its applicability to the various structural support elements.

The 1994 *Supports Specifications* is based on studies and reports that were published in the late 1960s. Since that time significant research work has been performed that could highly impact the *Supports Specifications*. New wind loading provisions have been established by ASCE and the American National Standards Institute (ANSI), alternate design philosophies have been proposed, and new materials and design parameters are being used. This information should be incorporated in an updated *Supports Specifications* to achieve more economical and reliable designs. The new information should also be evaluated carefully to determine the effects of the revisions on the various types of support structures and the consequences of adopting such new material.

1.2 RESEARCH OBJECTIVES AND APPROACH

1.2.1 Objectives

The main objectives of this study are to

- Develop an up-to-date, comprehensive recommended *Supports Specifications*;
- Develop a detailed commentary for the specifications;
- Address fiberglass-reinforced plastic composite materials in the specifications and commentary;
- Investigate alternative design procedures and philosophies and propose an appropriate approach for the specifications;
- Provide an index and a section on definitions in the specifications;
- Provide a separate document containing numerous design examples illustrating the proper use of the specifications;
- Present the specifications and commentary in a user-friendly format similar to one used in the *LRFD Bridge Design Specifications* (*7*); and
- Adopt SI units in the development of the new specifications and commentary.

The specifications and commentary shall be suitably formatted for adoption consideration by the AASHTO Highway Subcommittee on Bridges and Structures.

1.2.2 Approach

The planned work for this project involved six tasks.

Task 1: Literature study. The research team made a comprehensive review of research reports and publications on design concepts and materials for highway signs, luminaires, and traffic signal structures. New design provisions, materials, and manufacturing processes were investigated. The current design methods were evaluated and compared to the alternative load-resistance factor design method. The team also surveyed various state DOTs and manufacturers.

Task 2: Develop and refine design criteria and considerations. To improve design criteria, the research team identified, investigated, and ranked in order of importance various technical items.

Task 3: Future research. The team identified and ranked those items that need future research and modification beyond what could be accomplished in this project.

Task 4: Interim report. The interim report includes documentation of Tasks 2 and 3. The report also included the intent and content of the proposed specifications, highlighting new additions and revisions.

Task 5: Draft of recommended specifications and commentary. A draft of the proposed *Supports Specifications and Commentary* was prepared and presented.

Task 6: Final report. The final report includes the proposed *Supports Specifications and Commentary*, illustrative design examples, a report with background for the additions and revisions to the specifications, and recommendations for future research.

1.3 SCOPE OF THE INVESTIGATION

In updating comprehensive specifications, several technical issues were studied and ranked in order of importance. These issues include:

1. Allowable bending stresses.
2. Wind loading criteria.
3. Fiberglass-reinforced composites.
4. Final deflected position.
5. Foundation design philosophies.
6. Wood structures.
7. Prestressed concrete design.
8. Alternative design procedures.
9. Span wire design philosophies.
10. Allowable dead load deflections.
11. Breakaway devices.
12. Oscillations, fatigue, and resonance.
13. Anchorage systems.
14. Connection techniques.
15. Loading across the diagonal.
16. Corrosion-protection systems.

1.4 ORGANIZATION OF THE REPORT

Chapter 2 summarizes the technical work performed, including the literature reviewed, studies made, and proposed revisions for the 16 major topics studied for the *Supports Specifications*. Chapter 3 discusses the overall impact of the changes of the proposed specifications. Chapter 4 provides suggested additional improvements to the specifications, topics for future research, and a summary and conclusion for the project. The appendixes provide more technical discussion of selected topics.

CHAPTER 2

RESEARCH FINDINGS

The project initially focused on 16 topics from the current *Supports Specifications* that needed revisions and updates. The research team reviewed the background of the current specifications and most recent research related to structural supports for highway signs, luminaires, and traffic signals. Comparisons were made between the current specifications and the most recent national codes and specifications to select up-to-date material. In addition to the 16 topics, some topics were added that were not specifically requested in the initial proposal to adequately address the proposed specifications.

The following topics were studied in this project:

- Alternative design procedures;
- Load combinations;
- Equity of safety factors among materials;
- Wind loading criteria;
- Ice loading;
- Allowable stresses for steel;
- Allowable stresses for aluminum;
- Prestressed concrete design;
- Wood design;
- Fiber-reinforced composites;
- Deflection limitations for dead loads and extreme loading conditions;
- Secondary moments;
- Oscillation, fatigue, and resonance;
- Connection techniques;
- Anchorage systems, emphasizing anchor bolt design;
- Foundation design;
- Breakaway devices;
- Span wire design philosophies; and
- Corrosion protection systems.

2.1 ALTERNATIVE DESIGN PROCEDURES

The current *Supports Specifications* adopts an allowable stress design (ASD) philosophy. Allowable stresses are specified for the materials, and computed service load stresses are required not to exceed the prescribed allowable stresses. The specification covers steel, aluminum, and prestressed concrete materials. With prestressed concrete, ultimate strength requirements must also be satisfied. The objective was to investigate whether a load and resistance factor design (LRFD) method would be more appropriate for the revised *Supports Specifications.*

The application of LRFD as a design philosophy is gradually increasing. Most design codes and specifications in United States, Canada, and Europe are moving toward the use of the LRFD design method as a replacement or alternative to the other more traditional design methods, such as ASD and load-factor design (LFD). Current design codes and specifications that adopt the LRFD design approach were reviewed as well as basic research works that introduced the LRFD approach.

A brief description of the work performed in evaluating the LRFD method and its application to the *Supports Specifications* is listed herein.

2.1.1 Specifications Using LRFD

In the United States, the LRFD philosophy has been introduced only in the last decade in the following specifications and standards:

- *Manual of Steel Construction—Load and Resistance Factor Design,* AISC, 1986 (*8*).
- AASHTO *LRFD Bridge Design Specifications,* 1994 (*7*).
- *Aluminum Design Manual,* "Specifications for Aluminum Structures—Load and Resistance Factor Design of Buildings and Similar Type Structures," 1994 (*9*).
- *LRFD Standard for Engineered Wood Construction* (Draft 1994), proposed by the American Forest & Paper Association, in cooperation with ASCE Standards Committee for Design of Engineered Wood Construction (*10*).

Most of these documents are recent publications. According to these documents, experience in the use of the LRFD method has not yet been well documented.

2.1.2 LRFD Philosophy

In the LRFD approach, factors are applied to loads and resistance. These factors adjust for uncertainties associated with the loads, materials, and various assumptions that are involved in the analyses. These factors are adjusted to ensure uniform reliability in the design.

The main characteristic of the LRFD philosophy is that it provides a consistent approach to strength evaluation and structural safety. The approach includes the variability in the behavior of structural elements and accounts for safety in a more rational way. The LRFD method assigns different overload factors to loads, depending on the type of load and the factored load combination that must be considered. The resistance factor, ϕ, is another safety-related provision that varies with the type of member, material, and limit state. These two factors, resistance and load, could be adjusted to ensure more uniform reliability in the design.

The development of the LRFD method is based on the following items:

- Probability-based model;
- Calibration with the allowable stress specifications;
- Judgment and past experience; and
- Comparative design studies of representative structures.

The LRFD approach requires a procedure that will determine values for the resistance and load factors. For a structural member or element designed according to its current specification, it is possible to compute the relative reliability of this design from data defining probability distribution and statistics of the resistance, loads, and load effects. The relative reliability is expressed as the reliability index. By repeatedly determining the reliability index for many structural designs, the relative reliability of different structural members built from different structural materials can be compared. For a selected value of the reliability index, using reliability analysis methods, it is possible to compute the resistance and load factors. The process requires a considerable amount of work, especially when new structural materials are investigated.

2.1.3 Documents Reviewed

The following publications were part of the review on the LRFD approach:

- Ellingwood et al., "Development of a Probability Based Load Criterion for American National Standard A58," 1980 (*11*).
- Ravindra et al., "Load and Resistance Factor Design for Steel," 1978 (*12*).
- Yura et al., "The Bending Resistance of Steel Beams," 1978 (*13*).
- Bjorhovde et al., "LRFD Criteria for Steel Beam-Columns," 1978 (*14*).
- Ravindra et al., "Wind and Snow Load Factors for Use in LRFD," 1978 (*15*).
- Galambos et al., "Properties of Steel for Use in LRFD," 1978 (*16*).
- Ellingwood et al., "Probability Based Load Criteria: Load Factors and Load Combinations," 1982 (*17*).
- Galambos et al., "Probability Based Load Criteria: Assessment of Current Design Practice," 1982 (*18*).
- Heger, F.J., "Public Safety—Is It Compromised by New LRFD Design Standards?" 1993 (*19*).
- Milford, R.V., "Load Factors for Limit States Codes," 1987 (*20*).
- Ang, A-H.S., and Cornell, C.A., "Reliability Bases of Structural Safety and Design," 1974 (*21*).
- Ravindra et al., "Illustrations of Reliability-Based Design," 1974 (*22*).
- Hasofer, A.M., and Lind, N.C., "Exact and Invariant Second-Moment Code Format," 1974 (*23*).

The research team also reviewed different LRFD specifications. Some of the pertinent specifications and standards are listed below:

- AASHTO *LRFD Bridge Design Specifications, First Edition*, 1994 (*7*).
- *Manual of Steel Construction—Load and Resistance Factor Design,* AISC, 1986 (*8*).
- "Specifications for Aluminum Structures—Load and Resistance Factor Design of Buildings and Similar Type Structures," *Aluminum Design Manual*, The Aluminum Association, 1994 (*9*).
- *LRFD Standard for Engineered Wood Construction,* Public Ballot Draft, ASCE, 1994 (*10*).
- *Ontario Highway Bridge Design Code*, Ministry of Transportation, Ontario, Canada, 1992 (*24*).
- *Design of Steel Transmission Pole Structures*, Second Edition, Manuals and Reports on Engineering Practice No. 72, ASCE, 1990 (*25*).

Discussions were also held with various individuals who were directly involved in LRFD specifications' development.

2.1.4 Comparison of ASD and LRFD

Numerical design examples for different support structures, using both the ASD and LRFD design philosophies, were prepared and compared. Load and resistance factors were obtained from AASHTO *LRFD Bridge Design Specifications* (*7*) and AISC *LRFD Manual of Steel Construction* (*8*). The load factors and resistance factors used in the comparisons were not specifically developed for highway support structures.

From these studies, the following conclusions were made:

- In high-level luminaires with tubular sections, the LRFD design approaches resulted in slightly larger cross-sectional areas than those obtained by using the ASD approach of the *Supports Specifications*. The maximum increase in required cross-sectional areas was about 2.1 and 5.3 percent for AASHTO *LRFD Bridge Design Specifications* and AISC *LRFD Manual of Steel Construction*, respectively.

- In roadside sign supports composed of W-shapes, all three methods gave comparable results. When comparing the ASD and the two LRFD methods, the selected W-shaped sections were the same for more than 90 percent of the cases considered.
- As the ratio of the wind load moment increases relative to the dead load moment, the LRFD design approaches resulted in a larger section than the section calculated by using the *Supports Specifications'* ASD design approach.
- The maximum increase in the required cross section modulus was for pure wind load and no dead load. The increases were 5 percent when using AISC *LRFD Manual of Steel Construction's* load combination and 2 percent when using AASHTO *LRFD Bridge Design Specifications.*
- For group I load combination (DL only), the required section modulus calculated by using the two LRFD approaches is less than the required section modulus calculated by using the ASD approach of the *Supports Specifications*. The reduction in the required section modulus is 19.1 and 22 percent for AISC LRFD *Manual of Steel Construction* and AASHTO *LRFD Bridge Design Specifications,* respectively. This load group seldom controls the design of the support structures.
- The load and resistance factors would need to be developed for an LRFD approach for support structures because it is improper to use factors developed for bridges or buildings.

2.1.5 ASD Design for the Proposed *Supports Specifications*

The researchers concluded that the application of the LRFD approach to the support structures cannot be achieved by simply adopting the load and resistance factors implemented in other specifications. Probability-based studies and calibrations with ASD designs are needed to establish the load and resistance factors for a certain reliability index. This could be achieved by establishing certain load factors for different load groups and varying the resistance factors depending on the type of material, load effect, and expected service life for each category of support structures.

To adopt an LRFD approach for support structures, an extensive study is needed to develop the load and resistance factors pertaining to this category of structures. Probability-based studies, considering the variables involved in the design of different categories of support structures, may result in design parameters that differ for each category of structures.

Several other factors add to the complexity of the needed work for establishing an LRFD approach. The *Supports Specifications* covers a wide variety of materials, including new materials such as fiber-reinforced composites. A thorough understanding of the various manufacturing methods of fiber-reinforced composites and an extensive testing program are needed to establish reliable strength equations for various cross sections. Strength equations must be developed for the new materials. Although an LRFD standard for wood (*10*) has just recently been drafted by ASCE, design of wood structures has been traditionally in ASD, and current design information is in this format. Experimental studies may also be needed to establish reliable strength equations for structural tubular shapes used extensively for support structures.

Considering the lack of vital information necessary to establish a rational LRFD design approach, the research team recommended that the proposed *Supports Specifications* remain in an ASD format for the following reasons:

- Significant time is needed to perform probability-based studies for various support structures. Total reliance on existing LRFD codes and specifications for obtaining the needed information is not possible.
- Information and literature on LRFD are lacking in the areas of fiberglass and wood design.
- None of the available LRFD codes and specifications adequately address tapered tubular poles, which is a category of structures used extensively for support structures.
- The LRFD approach usually results in a more economical design when dead loads are predominant. In support structures, where wind loads are usually predominant, the LRFD approach would probably result in a heavier and less economical design. Calibration of load and resistance factors is needed for all materials covered by the *Supports Specifications* to maintain economical designs and achieve the uniformity of safety among materials.
- The current ASD provisions and format of the *Supports Specifications* need significant revisions. It would therefore be advantageous to revise the current *Supports Specifications* in ASD format so that it is easily upgraded to LRFD in the future.
- Time constraints of this project prohibited the completion of all the work that is required for an LRFD specification.

2.2 LOAD COMBINATIONS

Group load combinations and their corresponding allowable stress increases were reviewed for consistency with specification documents such as the AISC *Manual of Steel Construction-Allowable Stress Design* (*26*), *Aluminum Design Manual* (*9*), and ASCE 7-95 *Minimum Design Loads for Buildings and Other Structures* (*27*). Load combinations remain the same, and an additional fatigue load combination has been added. The percentage of allowable stress for groups II and III load combinations has been modified.

2.2.1 Modification of Group Load Combinations in Section 1.2.6

The current *Supports Specifications* provides group loadings in Section 1.2.6, as shown in Table 1. The proposed *Supports Specifications* provides group loadings as presented in Table 2.

TABLE 1 Group loading in the current *Supports Specifications*

Group Load	Load Combination	Percent of allowable stress for all materials
I	*D*	100
II	*D + W*	140
III	*D + Ice +1/2(W)* for *W* based on the wind pressure formula with a minimum wind pressure value of 25 psf	140
Notation: *D* = dead load, *W* = wind load, *Ice* = ice load.		

2.2.2 Proposed Changes

The following changes were made in the proposed *Supports Specifications*:

- The percentage increase in allowable stress has been changed for group II loading from 40 to 33 percent. This change is consistent with the current increase in allowable stress for wind loads in the AISC—*Manual of Steel Construction—Allowable Stress Design* and *The Aluminum Design Manual.* Also, ASCE 7-95 *Minimum Design Loads for Buildings and Other Structures* allows a 25 percent reduction in forces for certain load combinations, which translates to a 33 percent increase in allowable stress.
- Similarly, the percentage increase in allowable stress has been changed for group III loading from 40 to 33 percent.
- Dead load should now be defined as the member weight and all material to be permanently supported by the member. Temporary loads during maintenance shall also be considered as part of the dead load.
- Group IV, a new load combination for fatigue loading, has been added to reflect the work of *NCHRP Report 412* (*28*).

As a result of the change in the allowable stress increase, a small reduction in allowable stresses (only about 5 percent) under extreme wind loading conditions will occur. This reduction should not result in overdesigning the structures, especially because the new wind map will result in generally lower wind loads across the majority of the United States.

All proposed changes are provided in Article 3.4, "Group Load Combinations," of the proposed *Supports Specifications.*

2.3 EQUITY OF SAFETY FACTORS

The safety factors for steel, aluminum, and prestressed concrete were evaluated and compared in flexure for two main reasons: to ensure equity in safety among materials and to calculate the new safety factors resulting from modifying the allowable stresses of the materials.

TABLE 2 Group load combinations for proposed *Supports Specifications*

Group Load	Load Combination	Percent of Allowable Stress (See Note 1)
I	*D*	100
II	*D + W*	133
III	*D + Ice +1/2(W)* (See Note 2)	133
IV	Fatigue	(See Note 3)

Notes:

1. No load reduction factors shall be applied in conjunction with these increased allowable stresses.
2. *W* shall be computed on the basis of the wind pressure formula. A minimum value of 1200 Pa (25.1 psf) shall be used.
3. See Section 12 for fatigue loads and stress range limits.
4. *D* = dead load, *W* = wind load, *Ice* = ice load.

TABLE 3 Yield safety factors in the current *Support Specifications**

	Safety factor on yield strength for Group I load combination.		
Material	**Steel**	**Aluminum**	**Prestressed Concrete**
In general	1.925 / K_p	1.65 min.	not applicable
Thin-walled round shapes	1.516 (K_p = 1.27)	1.65 min.	not applicable
Thin-walled square shapes	1.719 (K_p = 1.12)	1.65 min.	not applicable
* These values are the same in the proposed *Supports Specifications*.			

2.3.1 Safety Factors in the *Supports Specifications*

Table 3 shows the current safety factor based on yield. These values remain the same in the proposed specifications. The table provides an indication of serviceability requirements. Although serviceability requirements are important, emphasis should be placed on Table 4, which shows the safety factor based on ultimate strength for the current and proposed *Supports Specifications*. The first column provides safety factors for group I loading, and the last column shows the calculated safety factor based on 1.33 allowable stress increase under groups II and III loadings for the proposed specification. The proposed safety factors are higher than the current ones. This increase in safety factors does not necessarily mean additional conservatism in design, because the new wind load provisions are expected to result in a general reduction in forces for most areas.

2.3.2 Background for Calculation of Safety Factors for Steel

Figure 1a shows a typical stress-strain curve for steel. Figure 1b shows an idealized stress-strain curve used in plastic steel design. The idealized curve has an elastic portion with a slope equal to the modulus of elasticity and an inelastic portion with zero slope.

In Figure 2a when $\sigma = F_y$, the moment associated with this stress state is the yield moment, M_y. At moments in excess of M_y, as shown in Figure 2b, the stress-strain relationship is no longer linear. When half of a cross section has yielded in compression and half of a cross section has yielded in tension, as shown in Figure 2c, the plastic moment, M_p, is reached.

The plastic moment is the maximum moment of the cross section. M_p equals $\sigma_y Z$, where Z is the plastic section modulus. For sections that have the same yield point throughout the section and at least one axis of symmetry, $Z = Aa/2$, where a is the distance between centriods of two equal areas lying above and below the neutral axis and A is the cross-sectional area.

The ratio of the plastic moment, M_p, to the moment at the initiation of yielding, M_y, is $K_p = M_p/M_y = Z\sigma_y/S\sigma_y = Z/S$, where K_p is the shape factor and S is the section modulus for a particular section.

The ultimate safety factor for group I loading used for the current *Supports Specifications* for steel is 1.925, which is approximately $^1/_{12/23}$. The allowable bending stress for any compact section is $F_b = K_p F_y/1.925$. The safety factor for ultimate strength to allowable bending stress is

$$n_u = \frac{M_p}{M_b} = \frac{K_p F_y S}{F_b S} = \frac{K_p F_y S}{\frac{K_p F_y S}{1.925}} = 1.925$$

TABLE 4 Ultimate safety factors in the current and proposed *Supports Specifications*

	Current and Proposed	Current	Proposed
Material	**Safety factor without increase in allowable stress (Group I Load)**	**Safety factor with 1.4 increase in allowable stress (Group II & III Loads)**	**Safety factor with proposed 1.33 increase in allowable stress (Group II & III Loads)**
Steel	1.925	1.375	1.447
Aluminum	1.95 min.	1.393	1.466
Prestressed Concrete	N.A.	1.389	1.444

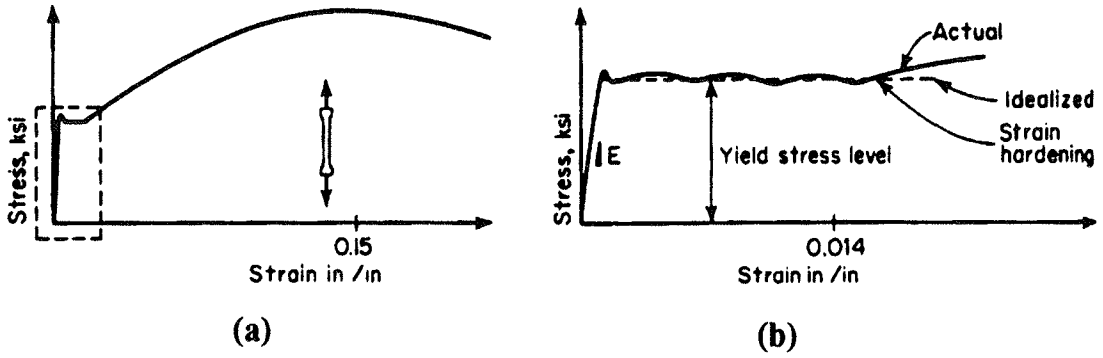

Figure 1. Typical stress-strain curve (29).

The safety factor for yield strength to the bending stress is n_y, where

$$n_y = \frac{M_y}{M_b} = \frac{F_y S}{F_b S} = \frac{F_y}{\frac{K_p F_y}{1.925}} = \frac{1.925}{K_p}$$

The safety factor, n_y, provides an indication of serviceability for the cross section.

For bending the safety factor for group I loading of 1.925 continues to be used for steel. Under groups II and III loading, the safety factor is 1.925/1.33 = 1.447, which includes a modification for a 33 percent increase in allowable stresses. These safety factors are consistent with current AISC and ASCE manuals (*26,27*).

2.3.3 Background for Calculation of Safety Factors for Aluminum

Figure 3 shows a typical stress-strain curve for aluminum. Because the stress distribution in a beam is nonlinear in the inelastic range for aluminum materials, the apparent stress for some types of beam cross sections can exceed the yield strength before significant yielding of the beam takes place. The yield strength for a beam is the apparent stress at which an offset equal to 0.2 percent is reached on the curve of apparent stress versus extreme fiber strain.

Safety factors, n_y and n_u, are calculated similar to the way that steel safety factors are calculated. For aluminum, K_y is the shape factor for the yield moment, and K_u is the shape factor for the ultimate moment. Precise values of the coefficients, K_y and K_u, depend on the shape of the section and on the shape of the stress-strain curves in tension and compression. The stress-strain curves vary somewhat for the different aluminum alloys. Table 5 provides typical values of K_y and K_u for aluminum.

The ultimate moment for aluminum is calculated as $M_u = K_u F_u S$, where F_u is the ultimate strength and S is the section modulus. The yield moment for aluminum is calculated as $M_y = K_y F_y S$, where F_y is the yield strength of the material.

The *Aluminum Design Manual* (*9*) uses equations involving bending of the member and tension and compression of its components (e.g., flanges and webs). These equations either reference the yield strength or the ultimate strength of aluminum. The minimum safety factor for yield is 1.65, and the minimum safety factor for ultimate is 1.95. In some cases, a conservative shape factor is used, resulting in higher actual safety factors. The *Aluminum Design Manual* uses conservative shape factors for K_y and K_u of 1.0 for rectan-

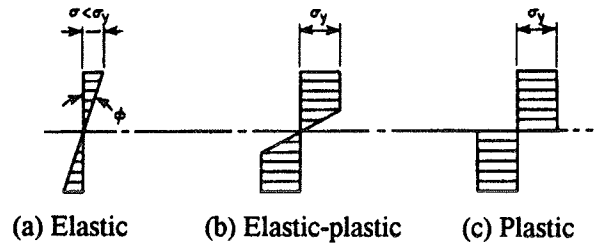

Figure 2. Flexural stress distribution (29).

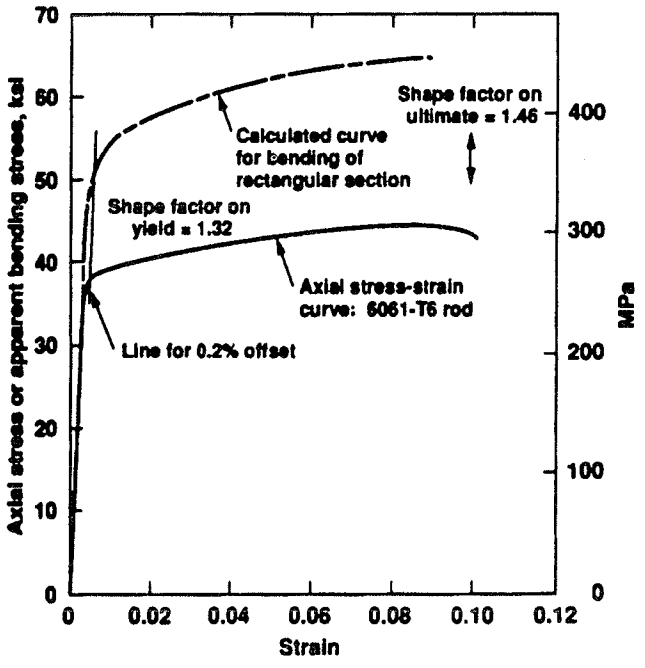

Figure 3. Typical stress-strain curve for aluminum (30).

TABLE 5 Shape factors for yielding and ultimate strength of aluminum beams (*9,30*)

Cross-section	K_y	K_u
Round tube	1.17	1.24
Rectangular tube	1.07	1.10
I-shape and channel bent about major axis	1.13	1.14
I-shape (minor axis)	1.33	1.44
Solid rectangle	1.32	1.46
Solid round	1.42	1.56

gular tubes; however, the actual shape factors are 1.07 for K_y and 1.10 for K_u.

2.3.4 Background for Calculation of Safety Factors for Prestressed Concrete

The moment allowed under groups II and III load combinations for prestressed concrete is currently calculated as $M \leq \phi M_n/1.25$. The safety factor for groups II and III loading is $1.25/\phi = 1.25/0.9 = 1.389$.

The proposed specification provides $M \leq \phi M_n/1.30$ for groups II and III load combinations, where $\phi = 0.9$. The safety factor is $1.30/0.9 = 1.444$. This modification adjusts the safety factor for prestressed concrete to be similar to steel and aluminum.

2.3.5 Other Materials

For wood and fiber-reinforced composite materials, global safety factors were used based on recommended practice or applicable specifications. These materials cannot be considered homogeneous and have physical properties that are highly dependent on the direction of loading. No attempt was made to differentiate between the safety factors at first yield and ultimate strength because the yield and ultimate strength may be so close that they can be considered identical.

2.4 WIND LOADING CRITERIA

The current specification on wind loading criteria is based primarily on information and procedures developed in the early 1960s and 1970s (*31,32*). These two documents are the predecessors to current wind load specification criteria presented by ASCE (*27*). Although some material contained in the current specification is outdated, it is based on sound engineering principles and judgments that were well thought out and presented. Therefore, changes to the specification are limited to those items that follow current wind engineering practice. Changes have been made to the specification that affect the presentation, terminology, and calculated wind loads. Major changes, primarily because of an updated wind map, include a significant increase in the magnitude of wind speeds in hurricane prone coastlines and a decrease in inland areas.

2.4.1 Documents Reviewed

Early information on the specification of wind loads for buildings and structures was compiled by an ASCE committee and was presented in 1961 (*31*). The gust coefficient of 1.3, incorporated in the existing specification, is discussed in this publication. During the late 1960s and early 1970s, the information in the ASCE publication was revised and published by ANSI as standard ANSI A58.1-1972 (*32*). This document presents the same fastest-mile wind speed data contained in the current AASHTO specifications. ANSI A58.1-1972 was revised in the early 1980s and a new version, entitled ANSI A58.1-1982, was published (*33*). ANSI A58.1-1982 contains an updated 50-year mean recurrence interval wind speed map and the introduction of the concept of the importance factor. The importance factor is used to convert 50-year mean recurrence wind speeds to those corresponding to other recurrence intervals. During the mid and late 1980s, ASCE rejoined ANSI in the maintenance of the wind load standard. In 1990, a revised version of ANSI A58.1, entitled ANSI/ASCE 7-88, was published by ASCE (*34*). In 1994, a revised version of this document, ANSI/ASCE 7-93, was published by ASCE (*35*). Changes in the wind load information during the period from the publication of ANSI A58.1-1982 through the publication of ANSI/ASCE 7-93 were minimal. However, in 1996, ASCE published a new version of ANSI/ASCE 7-95, which incorporated significant changes, including a move away from fastest-mile wind speeds to the 3-sec gust wind speeds and a redefinition of the importance factor. Previously, the importance factor, introduced in ANSI A58.1-82, was used to convert 50-year mean recurrence wind speeds to wind speeds corresponding to other mean recurrence intervals. The new importance factor, introduced in ANSI/ASCE 7-95, is used to convert wind pressures corresponding to a 50-year mean recurrence interval to wind pressures associated with other mean recurrence intervals.

Although other publications and documents were reviewed, the substantive revisions to the AASHTO specification are based primarily on this sequence of literature that serves as the core to wind load specification in the United States. The primary changes to the AASHTO specification include a move from fastest-mile design wind speeds to 3-sec gust wind speeds, the introduction of a new 50-year mean recurrence interval 3-sec wind speed map taken from ANSI/ASCE 7-95, the introduction of importance factors to convert wind pressures from 50-year mean recurrence intervals to other recurrence intervals, and the introduction of metric units as standard.

2.4.2 Wind Pressure Formula

The central element of this specification is the wind pressure formula. The wind pressure formulas presented in the current and the revised specifications are essentially the same. Both are based on the premise that the rise in pressure, p, on an immersed body, is given by the following expression:

$$p = wC_dV^2/2g \tag{1}$$

where

C_d = coefficient of drag,
w = specific weight of "standard air," 12.02 N/m^3 (0.0765 lb/cu ft) [at 15°C (59°F) and 760 mm (29.92 in.) of mercury],
V = wind speed expressed in meters per second (m/s) [miles per hour (mph) or kilometers per hour (kph)], and
g = 9.81 m/sec^2 (32.2 ft/ sec^2).

If these values are substituted into Equation 1, the following expression results:

$$p = \rho C_dV^2 \tag{2}$$

where p is expressed in pascals (Pa), if ρ is taken to be 0.613 and V is expressed in m/s; p is expressed in lb/ft^2, if ρ is taken to be 0.00256 and V is expressed in mph; and p is expressed in Pa, if ρ is taken to be 0.0473 and V is expressed in kph.

The value of the wind speed, V, that is used for a particular situation depends on a number of factors, including the characteristics of the terrain in the surrounding area, the height of the structural element above ground level, and the dynamic interaction of the structure and the wind. The current specification incorporates the assumption that the terrain in all directions is open with only scattered obstructions. This exposure is defined as an exposure C condition, which is explained later. The effect of the height of the element is taken into account with a coefficient of height, C_h. The geometric shape of the structural element is taken into account through the use of a drag coefficient, C_d, whose value depends on the geometric shape of the structural element and associated Reynolds number. The dynamic interaction of the structure with the wind is taken into account through the use of a gust effect factor equal to 1.3. These factors combine to result in the following equation for wind pressure that is incorporated in the current specification:

$$p_z = \rho(1.3V)^2C_dC_h \tag{3}$$

where the wind speed, V, is defined as the fastest-mile wind speed and the resulting pressure, p_z, is dependent on height above ground. In Equation 3, the proper value of the fastest-mile wind speed is taken from one of three different wind speed maps, depending on the desired recurrence interval.

Equation 3 is expressed in a unique form for the era in which it was introduced. The gust effect factor is expressed as a constant value of 1.3 with height, and the coefficient of height, C_h, reflects not only the increase of the fastest-mile wind speed with height but also the change in the ratio of the peak gust to fastest-mile wind speed with height. In analogous formulations of the same era, both the gust effect factor and the coefficient of height varied with height above ground level (*32,33*). This concept of a constant value for the gust effect factor was not introduced into the mainstream wind design standards until the introduction of ANSI/ASCE 7-95 (*27*).

One of the major proposed modifications to the specification is the use of 3-sec gust wind speeds instead of fastest-mile wind speeds. Examination of relationships between wind speed and duration originally advanced by Durst (*36*) and presented in ANSI/ASCE 7-95 suggests that the ratio of the fastest-mile to 3-sec gust wind speed is approximately equal to 0.82 (*27*). The ratio of the fastest-mile wind speed to the 3-sec gust wind speed is determined by using the ratio of probable maximum wind speed averaged over t seconds to an hourly mean speed in Figure 4 (*27*). The gust duration for fastest-mile wind speed is the time it takes a column of air at

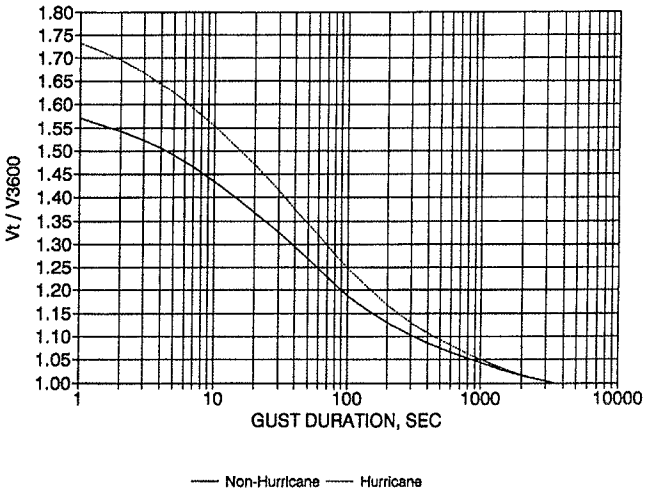

Figure 4. Ratio of probable maximum speed averaged over t sec to hourly mean speed (27).

a given velocity to travel one mile. The gust duration for the 3-sec gust wind speed is 3 sec. From Figure 4, the ratio, $V(t)$, to an hourly speed, $V_{3,600s}$, is determined for the fastest-mile wind speeds and the 3-sec gust wind speeds. These ratios are used to calculate the ratio of the fastest-mile wind speed to the 3-sec gust wind speed as follows:

$$\frac{V_{fm}(t)/V_{3,600s}}{V_{3\text{-sec}}/V_{3,600s}} = \frac{V_{fm}(t)}{V_{3\text{-sec}}} \approx 0.82$$

where

V_{fm} = fastest-mile wind speed,
$V_{3\text{-sec}}$ = 3-sec gust wind speed, and
$V_{3,600s}$ = hourly mean wind speed.

Table 6 provides ratios for V_{fm} to $V_{3,600s}$ and $V_{3\text{-sec}}$ $V_{3,600s}$ for various wind speeds, which were determined from Figure 4. With $V_{fm}/V_{3,600s}$ and $V_{3\text{-sec}}/V_{3,600s}$ known, the ratio, $V_{fm}/V_{3\text{-sec}}$, can be determined and is provided in Table 6. The values determined in Table 6 for $V_{fm}/V_{3\text{-sec}}$ are approximately equal to the selected value for $V_{fm}/V_{3\text{-sec}}$ of 0.82. Table 7 provides fastest-mile wind speed equivalents for the 3-sec gust wind speed of the proposed specifications for 50-, 25-, and 10-year mean recurrence intervals.

The relationship between the fastest-mile wind speeds and the 3-sec gust wind speeds may be represented by

$$\left(G_{fm}V_{fm}^2\right)^2 = G_{3\text{-sec}}V_{3\text{-sec}}^2$$

where G_{fm} is the gust effect factor associated with the fastest-mile wind speed and $G_{3\text{-sec}}$ is the gust effect factor associated with the 3-sec gust wind speed. The 3-sec gust can be determined as follows:

$$G_{3\text{-sec}} = \left(G_{fm}\frac{V_{fm}}{V_{3\text{-sec}}}\right)^2 = (1.3 \times 0.82)^2 = (1.066)^2 = 1.14$$

If the velocity, V, that is input into the wind speed equation is a 3-sec gust wind speed instead of a fastest-mile wind speed, then Equation 3 must be modified by multiplying 1.3 V by 0.82 as follows:

$$p_z = \rho(1.066V)^2C_dC_h \tag{4}$$

Equation 4 can then be written in terminology that is more consistent with ANSI/ASCE 7-95 as follows:

$$p_z = \rho K_z G V^2 C_d \tag{5}$$

where G, which is the gust effect factor, becomes $(1.066)^2$ or 1.14; K_z, which is the velocity pressure exposure coefficient, replaces C_h; and C_d is the drag coefficient.

In 1979, Simiu et al. *(37)* performed an analysis of wind speed data collected at 129 stations. Data from each of the 129 stations were analyzed, and wind speeds associated with different mean recurrence intervals were calculated. The ratio of the wind speed, V_r, associated with a mean recurrence interval of r years to the wind speed, V_{50}, associated with a mean recurrence interval of 50 years, is reasonably independent of the site *(37)*. Peterka and Shahid later confirmed this observation *(38)*. From these results, the following generalized relationship can be made:

$$V_r = V_{50}\sqrt{I_r} \tag{6}$$

where

V_r = wind speed associated with the r^{th} year return interval,

TABLE 6 Ratio of fastest-mile wind speed to 3-sec gust wind speed

Location	Fastest-Mile Wind Speed V_{fm} (mph)	Gust Duration for Fastest-Mile Wind Speed t (sec)	Ratio of Probable Maximum Speed Averaged Over t Seconds to Hourly Mean Speed $V_{fm(t)}/V_{3600s}$	Ratio of Probable Maximum Speed Averaged Over t Seconds to Hourly Mean Speed $V_{3\text{-sec}}/V_{3600s}$	$V_{fm}/V_{3\text{-sec}}$
Non-Hurricane	70	51.4	1.265	1.525	0.83
Non-Hurricane	80	45	1.285	1.525	0.842
Non-Hurricane	90	40	1.295	1.525	0.849
Hurricane	90	40	1.375	1.67	0.823
Hurricane	100	36	1.39	1.67	0.832
Hurricane	110	32.7	1.40	1.67	0.838
Selected Value					0.82

TABLE 7 Fastest-mile wind speed equivalents for 3-sec wind gust wind speed

3-Second Gust Wind Speed	Equivalent Fastest-Mile Wind Speed		
$V_{3\text{-sec}}$ Wind Speed (mph)	V_{fm} (mph) 50-year mean recurrence interval	V_{fm} (mph) 25-year mean recurrence interval	V_{fm} (mph) 10-year mean recurrence interval
85	69.7	65.0	58.7
90	73.8	68.8	62.1
100	82.0	76.5	69.1
110	90.2	84.1	76.0
120	98.4	91.8	82.9
130	106.6	99.4	89.8
140	114.8	107.1	96.7
150	123.0	114.7	103.6

V_{50} = wind speed associated with the 50-year mean recurrence interval, and
I_r = importance factor associated with the r^{th} year return interval.

Table 8 presents a set of importance factors corresponding to 10-, 25-, 50-, and 100-year mean recurrence intervals as given in ANSI/ASCE 7-95 (*27*). The definition of the importance factor presented in ANSI/ASCE 7-95 (*27*) is different from the definition presented in previous versions of ANSI/ASCE 7 (*34,35*).

Substituting the concept of the importance factor into Equation 5 results in the following revised wind pressure formula:

$$p_z = \rho K_z G V^2 I_r C_d \quad (7)$$

With the introduction of the importance factor in Equation 7, it is only necessary to have one wind speed map for a 50-year mean recurrence interval instead of the multiple wind speed maps contained in the current *Supports Specifications*.

2.4.3. Wind Speed Map

The current specification contains three wind speed maps based on work by Thom (*39*). The three individual maps present the variation of fastest-mile wind in the United States for mean recurrence intervals of 10, 25, and 50 years. These maps were widely recognized as authoritative into the early 1980s. The same maps were included in ANSI A58.1-72 (*32*). However, these wind speed maps have not been included in the major wind load standard since 1982.

TABLE 8 Importance factors, I_r

Return Period years	Importance Factor I_r
100	1.15
50	1.00
25	0.87
10	0.71

The wind speed maps developed by Thom (*39*) were replaced in general wind engineering practice in 1982 by a single fastest-mile wind speed map for a 50-year mean recurrence interval and a set of importance factors derived from analyses by Simiu et al. (*37*). The Simiu wind speed map and importance factors were incorporated into ANSI A58.1 in 1982 (*33*). The importance factors employed in this formulation were multiplied by the wind speed and not the wind pressure. Two different sets of importance factors were included in this presentation: one set for normal wind situations and one for hurricane prone areas. The Simiu wind speed map was developed by using similar techniques to those employed in the Thom maps. The major differences are that additional wind speed data were used in the analyses and a different extreme value distribution was used to model the wind speeds. In addition, a simulation technique was introduced to approximate the effects of hurricanes in coastal areas (*40,41*), which resulted in significant wind speed increases in the gulf coast areas. Although the increased wind speeds are not supported by statistical analyses of data recorded in coastal areas, the argument is made that the distances between official wind speed measurement stations are so great that it is not possible to reliably incorporate the effects of hurricanes on the basis of measured wind speed data. The Simiu wind speed map was referenced in wind speed standards through the presentation of ANSI/ASCE 7-93 (*35*).

In the mid 1990s, the ASCE Task Committee on Wind Loads decided to reference wind loads to 3-sec gust wind speeds instead of the traditional fastest-mile wind speeds. The design of structures for the effects of wind has always been

based on the pressures associated with gusts. However, in the past, fastest-mile wind speeds were increased to account for the increased gust speeds. The ANSI/ASCE 7-95 3-sec gust approach represents a philosophical simplification in the wind design process by dealing directly with gust wind speeds instead of factored fastest-mile wind speeds (*27*). The wind speed map presented in ANSI/ASCE 7-95 presents the variation of 3-sec gust wind speeds associated with a height of 10 m (33 ft) for a 50-year mean recurrence interval and open terrain conditions (*27*). This new wind speed map is based on a statistical analysis of peak gust data collected at 485 weather stations (*38,42*) and from predictions of hurricane wind speeds (*40,41,43*). The map contains a modified set of importance factors that are used to convert wind pressures corresponding to a 50-year mean recurrence interval to wind pressures associated with other mean recurrence intervals. These new importance factors are shown in Table 8. The new ANSI/ASCE 7-95 importance factors, which are multiplied by pressures, are not the same as the ANSI/ASCE 7-93 importance factors, which are multiplied by wind speeds. In addition, the 3-sec gust wind speeds in the hurricane-prone areas in the ANSI/ASCE 7-95 wind speed map have been increased so that only one set of importance factors is required for site locations inside or outside hurricane-prone areas.

The proposed specifications includes a modified version of the 3-sec gust wind speed map, shown in Figure 5, and the importance factors presented in ANSI/ASCE 7-95 (*27*). The modifications to the wind speed map consist of the metrication of the notes and labels. No substantive changes were made to the placement of the wind speed isotachs. The map in Figure 5 identifies several locations that are designated as special wind regions, which include mountainous terrain, gorges, and other special regions. If a structure is located in a special wind region, it may be subjected to wind speeds that are higher than indicated in the wind speed map. Therefore, care must be exercised in selecting the design wind speed. The design wind speed may be determined by consulting the authority that has jurisdiction over the special wind region. Otherwise, the appropriate wind speed can be determined through the analysis of local meteorological data, and ASCE 7-95 presents proper procedures for doing this. The wind speed should never be reduced below that presented in the wind speed map.

2.4.4 Variation of Wind Speed with Height

The variation of wind speed with height depends on the local exposure conditions and is caused by the frictional drag offered by various types of terrain. Since 1982, widely accepted wind design procedures have used four different terrain exposure conditions that are designated as exposures A, B, C, and D (*33*). The conditions associated with these four exposure conditions are defined as follows in ANSI/ASCE 7-95 (*27*):

> Exposure A. Large city centers with at least 50 percent of the buildings having a height in excess of 70 ft (21.3 m). Use of this exposure category shall be limited to those areas for which terrain representative of exposure A prevails in the upwind direction for a distance of at least one-half mile (0.8 km) or 10 times the height of the building or other structure, whichever is greater. Possible channeling effects or increased velocity pressures due to the building or structure being located in the wake of adjacent buildings shall be taken into account.
>
> Exposure B. Urban and suburban areas, wooded areas, or other terrain with numerous closely spaced obstructions having the size of single-family dwellings or larger. Use of this exposure category shall be limited to those areas for which terrain representative of exposure B prevails in the upwind direction for a distance of at least 1,500 ft (457.2 m) or 10 times the height of the building or structure, whichever is greater.
>
> Exposure C. Open terrain with scattered obstructions having heights generally less than 30 ft (9.1 m). This category includes flat open country and grasslands.
>
> Exposure D. Flat, unobstructed areas exposed to wind flowing over large bodies of water for a distance of at least 1 mi (1.61 km). This exposure shall apply only to those buildings and other structures exposed to the wind coming from over the water. Exposure D extends inland from the shoreline a distance of 1,500 ft (457.2 m) or 10 times the height of the building or structure, whichever is greater.

For a specified set of conditions, the wind pressures associated with the different exposures increase as the exposure conditions progress from A to D, with exposure A resulting in the least pressure and exposure D resulting in the greatest pressure. There are few areas that qualify as exposure A. Further, highway signs, luminaires, and traffic signals are generally located along roadways that provide corridors of open exposures that are more typical of exposure C, making it difficult to endorse the general use of either exposure A or B for the design of highway signs, luminaires, and traffic. This is particularly the case because the use of both exposures A and B results in lower design loads than the use of exposure C. Because of its limited area of applicability, exposure D has only been widely recognized in wind design procedures since the early 1980s (*33*). This specification has historically incorporated the general use of exposure C for all locations with no apparent difficulties. Therefore, it is recommended that highway signs, luminaires, and traffic signals continue to be designed for exposure C only.

The velocity pressure exposure coefficient, K_z, which appears in Equation 7, expresses the variation of wind speed with height and is calculated using the following relationship presented in ASCE 7-95:

$$K_z = 2.01(z/z_g)^{2/\alpha} \tag{8}$$

where z is height about the ground or 4.57 m (15 ft), whichever is greater, and z_g and α are constants that vary with the exposure condition (*27*). From information presented in ASCE 7-95, α should be taken to be 9.5 and z_g should be taken to be 274.3 m (900 ft) for exposure C. These values are

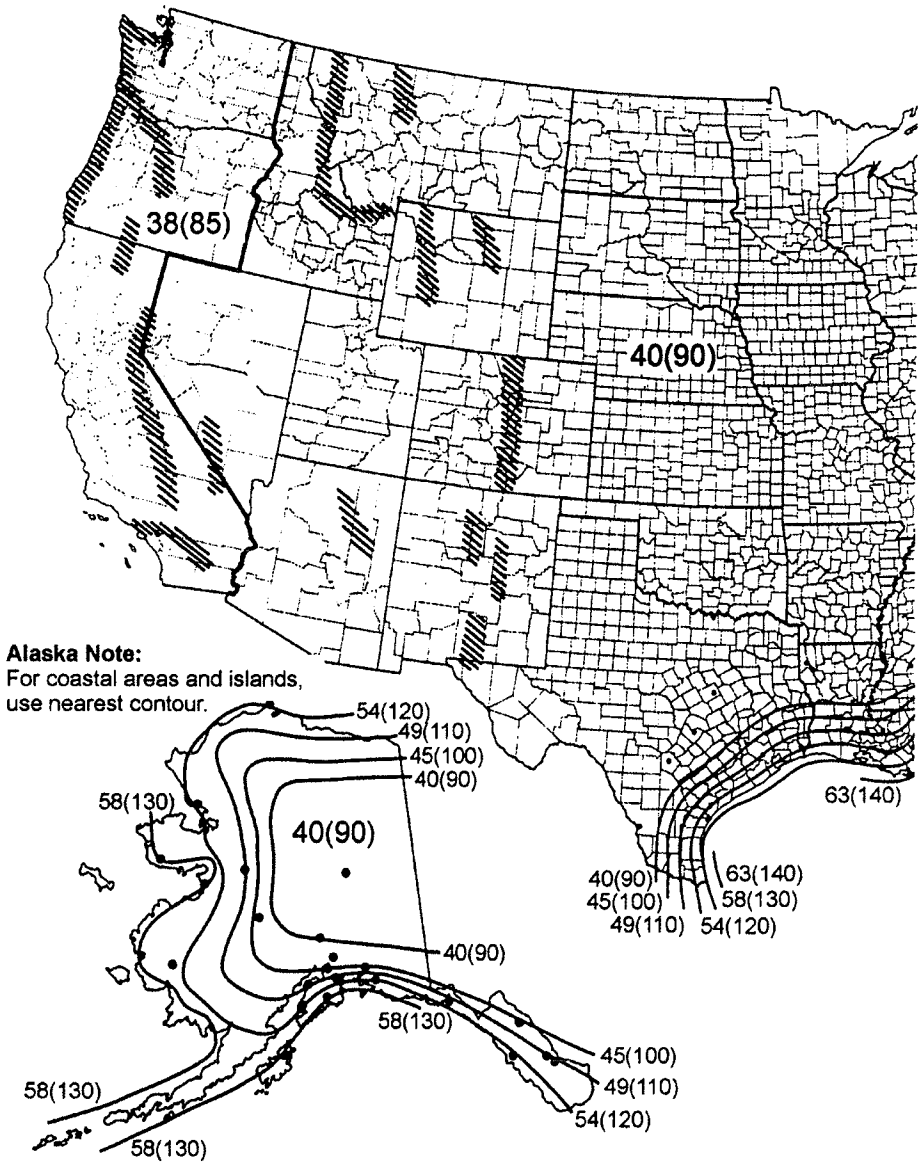

Figure 5. Basic wind speed, m/s (mph) (27).

for 3-sec gust wind speeds and are different to similar constants that have been used for fastest-mile wind speeds. Table 9 presents the variation of the velocity exposure coefficient, K_z, as a function of height based on the above relation. Figure 6 provides a comparison of the height factors from the proposed and current specifications. Figure 7 provides a ratio of the height factors from the proposed to the current specifications. On average, there is a 7 percent decrease in the height factor for the proposed specification compared to the current one.

2.4.5 Gust Effect Factor

The gust effect factor, G, corrects the effective velocity pressure, V, for the dynamic interaction of the structure with the gustiness of the wind. The gust effect factor, G, should not be confused with the gust coefficient that was incorporated in earlier versions of this specification. Although the two factors accomplish essentially the same purpose, the gust effect factor, G, is multiplied by the pressure, while the gust coefficient is multiplied by the wind speed. Because the wind pressure is a function of the square of the wind speed, the gust effect factor, G, is nominally equal to the square of the gust coefficient. The proper procedure to calculate either the gust effect factor, G, or the gust coefficient depends on whether a structure is classified as wind sensitive or not.

ASCE 7-95 states that if the fundamental frequency of a structure is less than 1 Hz, or if the ratio of the height to least horizontal dimension is greater than 4, the structure should

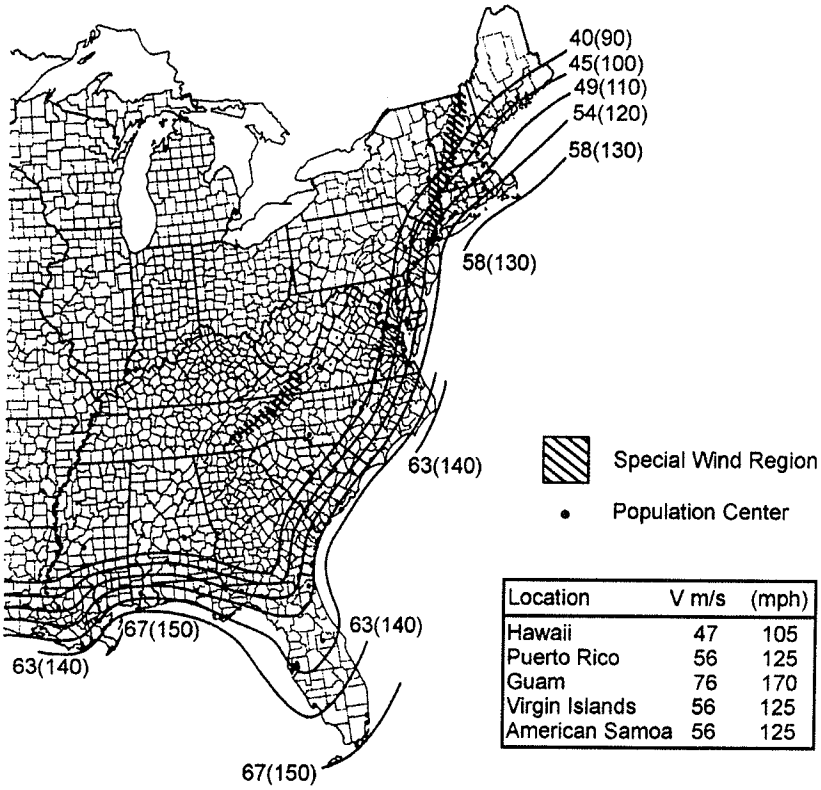

Location	V m/s	(mph)
Hawaii	47	105
Puerto Rico	56	125
Guam	76	170
Virgin Islands	56	125
American Samoa	56	125

Notes:
1. Values are 3-second gust speeds in m/s (mph) at 10 m (33 ft) above ground for Exposure C category and are associated with an annual probability of 0.02
2. Linear interpolation between wind speed contours is permitted.
3. Islands and coastal areas shall use wind speed contour of coastal area.
4. Mountainous terrain, gorges, ocean promontories, and special wind regions shall be examined for unusual wind conditons.

Figure 5. (continued).

be designed as a wind sensitive structure (*27*). From this definition, all structures covered by this specification should be classified as wind sensitive structures based on the height to least horizontal dimension ratio. Therefore, it is not appropriate to use the ANSI/ASCE 7-95 nonwind sensitive gust effect factor, G, of 0.85 for the design of signs, luminaires, and traffic signals. Special procedures are presented in the commentary of ANSI/ASCE 7-95 for the calculation of the gust effect factor for wind sensitive structures (*27*). The problem is that the use of the gust effect calculation procedure presented in ANSI/ASCE 7-95 for wind sensitive structures would significantly complicate this specification. The ANSI/ASCE 7-95 procedure requires accurate estimates of critical factors, such as the damping ratio and fundamental frequency of the structure. These factors are site and structure dependent. Relatively small errors in the estimation of these factors result in significant variations in the calculated gust effect factor. Therefore, even though signs, luminaires, and traffic signals are wind sensitive structures, the benefits of using the ANSI/ASCE 7-95 gust effect factor calculation do not outweigh the complexities and confusion introduced by its use.

Previous versions of this specification dealt with the wind sensitivity question by incorporating an increased gust coefficient of 1.3. This gust coefficient corresponds to a gust effect factor of 1.69 = (1.3)(1.3) for use with fastest-mile design wind speeds. The 1.3 gust coefficient has been with this specification since around 1959, and was intended to reflect the wind sensitivity of the types of structures addressed by this specification. Its origin was traced to work by Sherlock (*44*) and subsequent wind engineering literature through the 1950s and 1960s. Use of this factor results in higher wind loads than would be expected for structures that are not wind sensitive. However, signs, signals, and luminaires are wind sensitive. Thus, the types of structures addressed by this specification should be designed for wind loads that are higher than those used to design typical buildings. Finally, experience suggests that use of the traditional gust coefficient of 1.3 has resulted in successful designs. Therefore, the research team decided to use a 3-sec gust

TABLE 9 Velocity pressure exposure coefficient, K_z, for exposure C conditions

Height, m (ft)	K_z
5.0 (16.4) or less	0.87
7.5 (24.6)	0.94
10.0 (32.8)	1.00
12.5 (41.0)	1.05
15.0 (49.2)	1.09
17.5 (57.4)	1.13
20.0 (65.6)	1.16
22.5 (73.8)	1.19
25.0 (82.0)	1.21
27.5 (90.2)	1.24
30.0 (98.4)	1.26
35.0 (114.8)	1.30
40.0 (131.2)	1.34
45.0 (147.6)	1.37
50.0 (164.0)	1.40
55.0 (180.5)	1.43
60.0 (196.9)	1.46
70.0 (229.7)	1.51
80.0 (262.5)	1.55
90.0 (295.3)	1.59
100.0 (328.1)	1.63

effect factor, G, equal to 1.14 as derived from the traditional fastest-mile gust coefficient of 1.3 in the discussion surrounding Equation 5 (*27*). Signs, luminaires, and traffic signals that have been designed with this philosophy perform well. If designers wish to perform a more rigorous analysis, they should use the gust effect calculation procedure for flexible or dynamically sensitive structures presented in ANSI/ASCE 7-95 (*27*). The use of the ANSI/ASCE 7-95 gust effect calculation procedure for flexible or dynamically sensitive structures can result in a reduction or increase in the wind loads, depending on the dynamic characteristics of the structure.

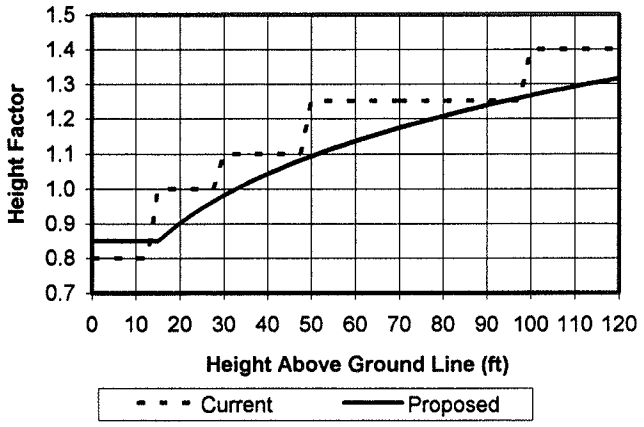

Figure 6. Comparison of height factor for the proposed and current specifications.

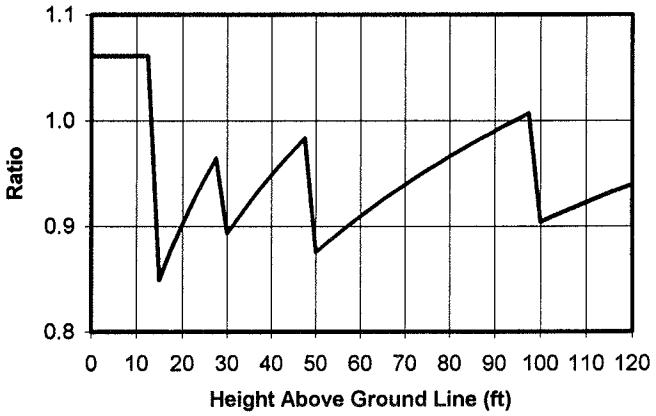

Figure 7. Ratio of proposed to current specifications for height factor.

2.4.6 Drag Coefficients

The current specification includes a table of well-documented drag coefficients that have been used successfully with this specification for many years. The validity of the drag coefficients presented in the current specification was examined by a group of researchers, including the chairman of the ASCE Task Committee on Wind Loads that supervised the development of ANSI/ASCE 7-95 (*45*). The group concluded that no change in the drag coefficient table was warranted. There has been no significant drag coefficient research presented since this effort. Therefore, while the drag coefficients presented in the current specification are not presented in the exact form of drag coefficients presented in other documents, the values presented appear reasonable for their intended use. In addition, the specification provides the user with the flexibility to use other sets of drag coefficients provided that the validity of the alternate drag coefficients is properly documented. Therefore, no substantive change needs to be made to the drag coefficient table.

It was necessary, however, to metricate the current drag coefficient table and revise the equations and limits to be consistent with 3-sec gust wind speeds, instead of fastest-mile wind speeds. The metrication is a simple matter of revising the various constants and limits to be consistent with wind speeds expressed in meters per second and dimensions expressed in meters. This exercise resulted in different constants that are presented in parenthesis in the current drag coefficient table because metric wind speeds in the current drag coefficient table are expressed in terms of kilometers per hour instead of meters per second. The conversion between fastest-mile wind speeds and 3-sec gust wind speeds was accomplished by simply incorporating the 0.82 conversion factor in an appropriate manner, and Table 10 shows the resulting drag coefficients. The information in Table 10 does not change the magnitude of the drag coefficient used in a particular situation.

2.4.7 Effective Velocity Pressure

To simplify the use of the revised specification, the wind pressure formula was simplified as presented in Equation 7. Table 11 shows the variation of the effective velocity pressure with height and wind speed as presented in the revised specification, for C_d and I_r equal to 1.0. Heights are presented in meters and wind speeds are presented in meters per second. Table 11 replaces table 1.2.5A in the current *Supports Specifications*.

To compare the proposed wind pressures in Table 11 with the wind pressures presented in the current specifications, the following exercise was conducted. First, the 3-sec gust wind

TABLE 10 Wind drag coefficients (C_d)

Type of Member[1]	Shape of Members[1]									
Structural Supports (Vertical & Horizontal) Single Member or Truss	Cylindrical	Flat[4]	Hexdecagonal		Dodecagonal[2]	Octagonal	Square[3]	Diamond	Elliptical	
			$0 \le r < 0.26$	$r \ge 0.26$					Broadside Facing Wind	Narrow Side Facing Wind
Vd ≤ 5.33 (39)	1.10	1.70	1.10	1.10	1.20	1.20	1.45	1.10		$C_{dd}[1 - .7(D/d_o - 1)^{1/4}]$
5.33(39) < Vd < 10.66(78)	9.69* /(Vd)$^{1.3}$	1.70	1.37 + 1.08r - Vd/19.8 - Vdr/4.94	0.55 + (10.66 - Vd)/9.67	3.28** /(Vd)$^{0.6}$	1.20	1.45	1.10		
Vd ≥ 10.66(78)	0.45	1.70	0.83 - 1.08r	0.55	0.79	1.20	1.45	1.10	1.7(D/d_o-1) + C_{dD}(2 - D/d_o)	
Two Members or Truss (one in front of other) and Trusses Forming Triangular Cross Section (all trusses with small solidity ratios)[6]	1.20	2.00								
Sign Panel (by ratio of length to width)										
L/W = 1.0	1.12									
2.0	1.19									
5.0	1.20									
10.0	1.23									
15.0	1.30									
Traffic Signals[5]	1.2									
Luminaries (with generally rounded surfaces)	0.5									
Luminaries (with rectangular flat side shapes)	1.2									

[1]Wind drag coefficients for members, sign panels and other shapes not included in this Table shall be established by wind tunnel tests (over an appropriate range of Reynolds numbers), in which comparative tests are made on similar shapes included in this Table.
[2]Valid for members having a ratio of corner radius to distance between parallel faces equal to or greater than 0.125.
[3]Valid for square dimensions no less than 0.076 m (3 inches). Valid for square shaped members with rounded corners. For shapes with sharp corners (no corner radius, such as extruded sections), use the drag coefficient for flat shaped members.
[4]Flat members are those shapes that are essentially flat in elevation, including plates and angles.
[5]Wind loads on free swinging traffic signals may be modified, as agreed by the owner of the structure, based on experimental data in Reference 46.
[6]Current data shows that the drag coefficients for a truss with a very small solidity ratio are merely the sum of the drags on the individual members that are essentially independent of one another. When two elements are placed in a line with the wind, the total drag depends upon the spacing of the elements. If the spacing is zero or very small, the drag is the same as on a single element; however, if the spacing were infinite, the total force would be twice as much as on a single member. When considering pairs of trusses, the solidity ratio is of importance because the distance downstream in which shielding is effective depends upon the size of the individual members. The effect of shielding dies out in smaller spacings as the solidity increases. Further documentation may be found in Reference 31.

Nomenclature:
V = Wind velocity (3 sec-gust) (m/s)(mph)
d = Depth (diameter) of member (m)(ft)
D/d_o = Ratio of major to minor diameter of ellipse (max 2)
C_{dD} = Drag Coefficient of cylindrical shape, diameter D
C_{dd} = Drag Coefficient of cylindrical shape, diameter d_o
r = Ratio of corner radius to inscribed circle

*In U.S. customary units this becomes 129

**In U.S. customary units this becomes 10.8

TABLE 11 Effective velocity pressures for structures

	Effective Velocity Pressure, p_z, Pa (psf) for Indicated Wind Velocity, m/s (mph)[1]							
Height, m (ft)	38 (85)	40 (90)	45 (100)	49 (110)	54 (120)	58 (130)	63 (140)	67 (150)
5.0 (16.4) or less	873 (18.2)	967 (20.4)	1224 (25.2)	1451 (30.5)	1763 (36.4)	2034 (42.7)	2399 (49.5)	2714 (56.8)
7.5 (24.6)	951 (19.9)	1053 (22.3)	1333 (27.5)	1581 (33.3)	1920 (39.6)	2215 (46.5)	2613 (53.9)	2955 (61.9)
10.0 (32.8)	1010 (21.1)	1119 (23.7)	1416 (29.2)	1679 (35.3)	2040 (42.1)	2353 (49.4)	2776 (57.3)	3140 (65.7)
12.5 (41.0)	1059 (22.1)	1173 (24.8)	1485 (30.6)	1760 (37.0)	2138 (44.1)	2466 (51.7)	2910 (60.0)	3291 (68.9)
15.0 (49.2)	1100 (23.0)	1219 (25.8)	1543 (31.8)	1829 (38.5)	2221 (45.8)	2563 (53.8)	3024 (62.4)	3420 (71.6)
17.5 (57.4)	1136 (23.7)	1259 (26.6)	1594 (32.9)	1889 (39.8)	2295 (47.3)	2647 (55.5)	3123 (64.4)	3533 (73.9)
20.0 (65.6)	1169 (24.4)	1295 (27.4)	1639 (33.8)	1943 (40.9)	2360 (48.7)	2723 (57.1)	3212 (66.2)	3633 (76.1)
22.5 (73.8)	1198 (25.0)	1327 (28.1)	1680 (34.6)	1992 (41.9)	2419 (49.9)	2791 (58.6)	3293 (67.9)	3724 (78.0)
25.0 (82.0)	1225 (25.6)	1357 (28.7)	1718 (35.4)	2037 (42.9)	2474 (51.0)	2854 (59.9)	3367 (69.4)	3808 (79.7)
27.5 (90.2)	1250 (26.1)	1385 (29.3)	1753 (36.1)	2078 (43.7)	2524 (52.0)	2912 (61.1)	3435 (70.8)	3885 (81.3)
30.0 (98.4)	1273 (26.6)	1410 (29.8)	1785 (36.8)	2116 (44.5)	2570 (53.0)	2965 (62.2)	3499 (72.2)	3957 (82.8)
35.0 (114.8)	1315 (27.5)	1457 (30.8)	1844 (38.0)	2186 (46.0)	2655 (54.8)	3063 (64.3)	3614 (74.5)	4088 (85.6)
40.0 (131.2)	1352 (28.3)	1498 (31.7)	1896 (39.1)	2249 (47.3)	2731 (56.3)	3150 (66.1)	3717 (76.7)	4204 (88.0)
45.0 (147.6)	1386 (29.0)	1536 (32.5)	1944 (40.1)	2305 (48.5)	2799 (57.7)	3230 (67.8)	3810 (78.6)	4310 (90.2)
50.0 (164.0)	1417 (29.6)	1571 (33.2)	1988 (41.0)	2357 (49.6)	2862 (59.0)	3302 (69.3)	3896 (80.3)	4406 (92.2)
55.0 (180.5)	1446 (30.2)	1602 (33.9)	2028 (41.8)	2405 (50.6)	2920 (60.2)	3369 (70.7)	3975 (82.0)	4496 (94.1)
60.0 (196.9)	1473 (30.8)	1632 (34.5)	2065 (42.6)	2449 (51.5)	2974 (61.3)	3431 (72.0)	4048 (83.5)	4579 (95.8)
70.0 (229.7)	1521 (31.8)	1686 (35.6)	2134 (44.0)	2530 (53.2)	3072 (63.4)	3544 (74.4)	4182 (86.2)	4730 (99.0)
80.0 (262.5)	1565 (32.7)	1734 (36.7)	2194 (45.3)	2602 (54.8)	3160 (65.2)	3645 (76.5)	4301 (88.7)	4865 (101.8)
90.0 (295.3)	1604 (33.5)	1777 (37.6)	2250 (46.4)	2667 (56.1)	3239 (66.8)	3737 (78.4)	4409 (90.9)	4987 (104.4)
100.0 (328.1)	1640 (34.3)	1817 (38.4)	2300 (47.4)	2727 (57.4)	3312 (68.3)	3821 (80.2)	4508 (93.0)	5099 (106.7)

[1] $p_z = 0.613\ K_z\ G\ V^2\ I_r\ C_d$ ($p_z = 0.00256\ K_z\ G\ V^2\ I_r\ C_d$) for I_r and C_d equal to 1.0.

speeds corresponding to the table headings in Table 11 were multiplied by 0.82 to convert them to equivalent fastest-mile wind speeds. Then, a double interpolation was performed on the wind pressure data presented in the current specifications to develop a set of wind pressures that correspond to the adjusted fastest-mile wind speeds and selected heights presented in Table 11. Table 12 shows this comparison and presents a range of heights from 5 to 90 m (16.4 to 295.3 ft) and 3-sec wind speeds ranging from 38 to 58 m/s (85 to 130 mph). Two pressure entries presented in pounds per square foot are presented for each wind speed/height. The pressures are presented in pounds per square foot because these units were used in table 1.2.5A. For example, the first entry in the table that corresponds to a 3-sec gust of 85 mph (fastest-mile wind speed of 69.7) and a height of 5 m (16. 4 ft) is expressed as 18.2 (17.5). The first number, 18.2, is the value of the pressure in pounds per square foot as presented in Table 11 and the second number, 17.5, is the interpolated value of the pressure in pounds per square foot from table 1.2.5A. Table 12 shows that the effective velocity pressures calculated for a given wind speed with the revised specification are very close to the current specifications' pressures. Some of the proposed pressures are a little higher than the current pressures, and some are a little lower; however, all of the pressures are very close. The major differences in the pressures could be the result of round-off errors made in the preparation of table 1.2.5A because the magnitude of the error tends to decrease with the magnitude of the pressure. Thus, the proposed changes in the wind pressure formula do not significantly alter design pressures for a specified wind speed.

TABLE 12 Comparison of proposed and current wind pressures

	Wind Speeds 3-Sec. Gust/Fastest-mile (mph/mph)					
Height (ft)	85/69.7	90/73.8	100/82	110/90.2	120/98.4	130/106.6
16.4	18.2 (17.5)	20.4 (19.7)	25.2 (24.2)	30.5 (29.3)	36.4 (35.1)	42.7 (41.1)
32.8	21.1 (21.2)	23.7 (24.1)	29.2 (30.0)	35.3 (35.9)	42.1 (42.6)	49.4 (50.0)
49.2	23.0 (22.8)	25.8 (26.1)	31.8 (32.6)	38.5 (39.2)	45.8 (46.6)	53.8 (54.6)
98.4	26.6 (26.7)	29.8 (30.0)	36.8 (36.8)	44.5 (44.1)	53.0 (52.3)	62.2 (61.8)
147.6	29.0 (29.7)	32.5 (33.3)	40.1 (40.9)	48.5 (49.1)	57.7 (58.9)	67.8 (68.7)
196.9	30.8 (31.7)	34.5 (35.7)	42.6 (44.1)	51.5 (53.1)	61.3 (62.9)	72.0 (74.0)
295.3	33.5 (33.7)	37.6 (37.7)	46.4 (46.3)	56.1 (56.2)	66.8 (66.8)	78.4 (78.7)

2.4.8 Comparisons of Current and Revised Wind Load Provisions

The revised wind load procedure involves the application of Equation 7, which is a function of the importance factor, I_r, and the coefficient of drag, C_d. As explained, the coefficients of drag have remained essentially unchanged. As Table 12 shows, the proposed procedure for calculating the effective velocity pressure, p_z, results in essentially the same pressures for a specified wind speed and height. The effect of the importance factor, I_r, is essentially the same as the use of multiple wind speeds for different mean recurrence intervals. Therefore, the maximum deviation of the current and revised wind pressures is about 4 percent for a specified pressure as presented in Table 12. Despite terminology changes, the mechanics of the revised wind load procedure are essentially equivalent to the current wind load procedure for a given wind speed. However, there are significant differences in calculated wind pressures as a result of differences in the current and revised wind speed maps.

The wind speed maps in the current version are based on research conducted in the late 1960s. As discussed earlier, wind speed data from different anemometer locations were modeled with extreme value statistics. Then contour lines were constructed that show the variation of the calculated fastest-mile wind speeds for 10, 25, and 50-year mean recurrence intervals. These maps were referenced in the ANSI A58.1-1972 wind load standard (*32*) and were later replaced by a single 50-year mean recurrence interval fastest-mile wind speed map and a set of importance factors in ANSI A58.1-1982 (*33*). A major difference in this later wind speed map was an increase of the wind speeds in coastal areas to reflect the occurrence of hurricanes. The 1982 wind speed map was replaced by the 50-year mean recurrence interval 3-sec gust wind speed map presented in ANSI/ASCE 7-95 (*27*). Hence, the current wind speed maps are two generations behind current technology. Therefore, it is essential that the specification be revised to reflect current wind speed maps regardless of the effect on design wind pressures.

The new 50-year mean recurrence interval 3-sec gust wind speed map presented in Figure 5 is a major departure from the current 50-year mean recurrence interval fastest-mile wind speed map reproduced in Figure 8. In the new wind

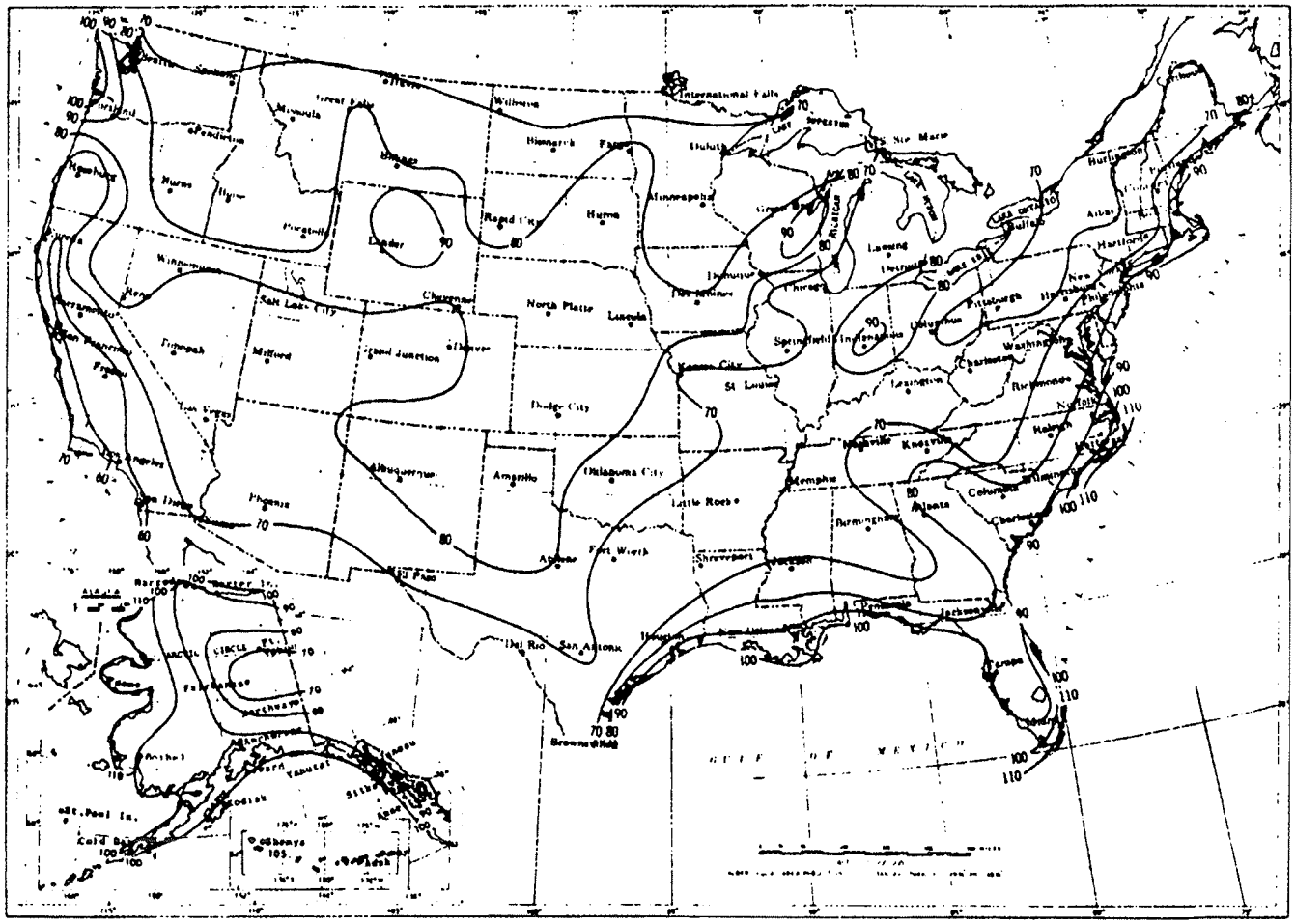

Figure 8. Fastest-mile wind speeds as presented in current specifications for 50-year mean recurrence interval (5).

speed map, the contiguous United States is divided into three distinct areas.

- Area I: the West Coast, including California, Oregon, and Washington;
- Area II: the hurricane-prone Gulf and East Coasts; and
- Area III: the area between the first two areas, which covers the largest land area.

The 3-sec gust design wind speed in area I is a recommended constant value of 38 m/s (85 mph). This 3-sec gust wind speed corresponds to a fastest-mile wind speed of about 31 m/s (70 mph). The current fastest-mile design wind speeds in this same area range from 27 m/s (60 mph) to 45 m/s (100 mph) as shown in Figure 8. Area I sites that are located in zones where the current fastest-mile design wind speed is less than 31 m/s (70 mph) will experience an increase in design wind loads, and area I sites that are located in zones where the fastest-mile design wind is currently greater than 31 m/s (70 mph) will experience a decrease in design wind loads. Table 13 presents the percentage increase and decrease in the design wind pressures as a function of the current fastest-mile wind speed presented in Figure 8. As shown in Table 13, a large portion of area I will experience a decrease in wind pressure up to a maximum value of 51 percent. At the same time, much of California and Oregon will experience an increase of design pressure of as much as 36 percent.

The 3-sec gust wind speeds in the hurricane-prone area II range from 40 to 67 m/s (90 to 150 mph), depending upon the proximity to the coast, and correspond to fastest-mile design wind speeds of 33 to 55 m/s (74 to 123 mph). A close examination of the two different wind speed maps shows that, in general, wind pressures in area II will increase. Increases for specific sites are presented in Table 14. The level of increase is very site specific.

The design area III, shown in Figure 5, is a constant 3-sec gust wind speed of 40 m/s (90 mph) that is to be applied throughout the entire area. This 3-sec gust wind speed corresponds to a fastest-mile wind speed of about 33 m/s (74 mph). The current fastest-mile design wind speeds in this same area range from 31 m/s (70 mph) to 40 m/s (90 mph) as shown in Figure 8. Area III sites that are located where the current fastest-mile design wind speed is less than 33 m/s (74 mph) will experience an increase in design wind loads, and area III sites that are located where the fastest-mile design wind is currently greater than 33 m/s (74 mph) will experience a decrease in design wind loads. Table 15 presents the percentage increase and decrease in the design wind pressures as compared to the current fastest-mile wind speed and shows that a large portion of area III will experience a decrease in wind pressure of up to 32 percent. Wind pressure increases in area III are limited to 12 percent.

There are several special wind regions throughout areas I, II, and III where the local authorities should be consulted for proper design wind speeds. It is anticipated that the recommended wind speeds in these special wind regions should be higher than the indicated wind speeds. The wind pressures based on the new 3-sec gust wind speed map may be significantly increased or decreased depending on the site location. This effect is the source of virtually all pressure variations between the current and proposed specifications. Because this effect will result in hardware changes in many cases, the information in the new wind speed map cannot be ignored.

TABLE 13 Percentage change in wind pressure in area I

Current Wind Speed, mph Fastest-mile (3-Second Gust)	Percentage Change in Wind Pressure[1]
100 (122)	-51 percent
90 (110)	-40 percent
80 (98)	-23 percent
70 (85)	0 percent
60 (73)	+36 percent

1. Compared to a fastest-mile wind speed of 31 m/s (70 mph).

2.5 ICE LOADING

The ice/wind load combination (group III load combination) of Section 1.2.6 in the current *Supports Specifications* was based on a similar load combination from the AASHTO *Standard Specifications for Highway Bridges* for forces due to sheets of ice in rivers bearing against piers. This load combination and the corresponding ice map are more than 20 years old and should be revised to reflect the latest information available on freezing ice accumulation on structural shapes and signs.

An ice load map is provided in the commentary of the recently published ANSI/ASCE 7-95 (*27*); however, it is believed to be incomplete and may not be used for all types of structural shapes. The ASCE Sub-Committee on Ice Loads is in the process of developing an ice load map, based on an historical weather model, that could be applicable to highway support structures. They are verifying and updating this map as ice storms occur, and the information is expected to be incorporated in the next revision of ASCE 7.

Freezing precipitation icing is the main type of ice loading that could be seen on traffic support structures. There is currently not enough information in the literature to warrant a change in the ice loading criteria in the current *Supports Specifications*, therefore the researchers have decided not to add any new material. Ice loading information should be followed over the next few years, and the *Supports Specifications* should be updated when adequate information becomes

TABLE 14 Percentage change in wind pressure in selected area II cities

City	Current Wind Speed, mph Fastest-mile (3-Second Gust)	Revised Wind Speed mph Fastest-mile (3-Second Gust)	Percentage Change in Wind Pressure
Houston, Texas	90 (110)	97 (118)	+16 percent
New Orleans, Louisiana	92 (112)	107 (130)	+35 percent
Miami, Florida	110 (134)	121 (148)	+21 percent
New York	85 (104)	92 (112)	+17 percent

available. Group III load combinations, which involves ice loading, and the ice load map remain unchanged.

2.6 ALLOWABLE STRESSES FOR STEEL

The allowable stresses for steel sections most commonly used in support structures were reviewed for the latest updates in codes and research. The study focused on round and multi-sided tubular sections, as well as I-shapes and channels. The most significant update pertained to allowable flexural stresses of multi-sided tubes. New formulas for the allowable flexural stresses were adopted on the basis of a study conducted at the Electric Power Research Institute (EPRI) (*47*). For other structural shapes, minor changes were made based on the recent AISC and AASHTO steel design specifications.

2.6.1 Documents Reviewed

Major research and specification documents reviewed included the following:

- *Design of Steel Transmission Pole Structures*, ASCE Manual No. 72, 1990 (*25*).
- Plantema, F.J., "Collapsing Stresses of Circular Cylinders and Round Tubes," 1946 (48).
- Schilling, C.G., "Buckling Strength of Circular Tubes," 1965 (49).
- Cannon, D.D., and LeMaster, R.A., *Local Buckling Strength of Polygonal Tubular Poles*, EPRI, 1987 (*47*).

TABLE 15 Percentage change in wind pressure in area III

Current Wind Speed, mph Fastest-mile (3-Second Gust)	Percentage Change in Wind Pressure[1]
90 (110)	-32 percent
80 (98)	-14 percent
70 (85)	+12 percent

1. Compared to a fastest-mile wind speed of 33 m/s(74 mph).

- AISC *Manual of Steel Construction-Allowable Stress Design*, 9th edition, 1989 (*26*).
- AISC *Manual of Steel Construction-LRFD*, 2nd Edition, 1994 (*50*).
- AASHTO *Standard Specifications for Highway Bridges*, 1996 (*51*).
- AASHTO *LRFD Bridge Design Specifications*, 1994 (*7*).

2.6.2. Allowable Bending Stress for Round Tubular Shapes

The research team found the background for the allowable bending stress equations in the current *Supports Specifications* for round tubular shapes in work by Plantema (*48*) and Schilling (*49*). In these papers, the local buckling of round tubular steel shapes under axial compression was studied. No reference, however, has been found that provided the development for the bending stress equation for local buckling of round tubular shapes as given in the current specification. It appears that this equation was based on Plantema's and Schilling's original research and then modified on the basis of test information.

Schilling's research suggested that Plantema's equations for axial compression be modified for bending and that the elastic local buckling stress for bending may be increased by 30 percent over the elastic buckling stress for axial compression. In this case, the possible approach for the development of the current *Supports Specifications'* equations may be outlined as follows:

1. Reference Plantema's axial compression equations, as shown in Table 16. The units of F_y and f_{cr} are in kips per square inch, D is the mid-thickness diameter, and t is the wall thickness.
2. Round end conditions of D/t as necessary to meet the end conditions of the three equations for bending.
3. Multiply Equation 9 by a shape factor of 1.27 for bending of round sections and divide by a safety factor of 23/12 to obtain Equation 12 (Table 17).

TABLE 16 Plantema's axial compression equations for round tubes (*49*)

$\frac{f_{cr}}{F_y} = 1.0 \text{ for } \frac{D}{t} \le \frac{3625}{F_y}$	Eq. 9
$\frac{f_{cr}}{F_y} = 0.75 + \frac{928}{F_y \frac{D}{t}} \text{ for } \frac{3625}{F_y} \le \frac{D}{t} \le \frac{11600}{F_y}$	Eq. 10
$\frac{f_{cr}}{F_y} = \frac{9280}{F_y \frac{D}{t}} \text{ for } \frac{D}{t} \ge \frac{11600}{F_y}$	Eq. 11

4. Multiply Equation 11 by 1.2 to estimate the increase in elastic local buckling stress for bending over the value for axial compression and divide by a safety factor of 23/12 to obtain Equation 14 (Table 17). (It appears that an increase for elastic buckling in bending over axial compression of 20 percent was used rather than the suggested 30 percent.)
5. Adjust Equation 10 to include a safety factor of 23/12 and to meet the end conditions of Equations 12 and 14, and the general form of Equation 10 to obtain Equation 13 (Table 17).
6. Equations 12–14 in Table 17 are the modified equations as given in the current *Supports Specifications* with the local buckling criteria presented in terms of D/t and F_y in terms of ksi.

2.6.2.1 Compact Limits

A compact section is a section capable of developing its full ultimate strength before locally buckling. Table 18 shows compact limits for round tubular shapes from various sources. Experimental work reported by Schilling indicated that $D/t \le 3{,}625/F_y$ would allow round tubes to reach their plastic moments. The limit for compact sections adopted by the current *Supports Specifications* ($D/t \le 3{,}654/F_y$) is slightly higher than this limit and is also higher than the limit adopted by the AISC *Manual of Steel Construction—Allowable Stress Design, 9th Edition*. Because these D/t limits are comparable, the compact limit for round tubular shapes in the proposed specification is given by $D/t \le 3{,}650/F_y$.

2.6.2.2 Allowable Bending Stress Equations

Table 19 compares allowable bending stress equations from various sources. These equations are based primarily on local buckling of sections in the inelastic range. Figure 9 compares the current *Supports Specifications* and the equations given in the literature. The current equation provides an upper bound for allowable stresses, except for a limited range of D/t ratios, where the AISC equation results in higher allowable stress values. The research team decided to retain the allowable stress equation of round tubular shapes in its present form without changes. A maximum limit of $D/t \le 13{,}000/F_y$ is specified because very limited test data is available for round tubes above this range.

In summary, the proposed *Supports Specifications* provides the following equations for round tubular steel sections:

TABLE 17 Allowable bending stress equations for round tubes in the current *Supports Specifications*

$\frac{f_{cr}}{F_y} = 1.0 \cdot \frac{\text{(Shape factor)}}{\text{(Safety factor)}}$ $\frac{f_{cr}}{F_y} = 1.0 * 1.27 * \frac{12}{23} = 0.66 \text{ for } \frac{D}{t} \le \frac{3654}{F_y}$	Eq. 12
$\frac{f_{cr}}{F_y} = 0.39 + \frac{986}{F_y \frac{D}{t}} \text{ for } \frac{3654}{F_y} \le \frac{D}{t} \le \frac{12180}{F_y}$	Eq. 13
$\frac{f_{cr}}{F_y} = \frac{9280 * \text{(elastic local buckling increase for bending)}}{F_y \frac{D}{t} \cdot \text{(safety factor)}}$ $\frac{f_{cr}}{F_y} = \frac{9280 * 1.19792}{F_y \frac{D}{t}} \cdot \frac{12}{23} = \frac{5800}{F_y \frac{D}{t}} \text{ for } \frac{D}{t} \ge \frac{12180}{F_y}$	Eq. 14

TABLE 18 Compact limits for round tubular shapes

	Compact Limit
Proposed *Supports Specification*	$\frac{D}{t} \le \frac{3650}{F_y}$
Current *Supports Specification* (*5*)	$\frac{D}{t} \le \frac{3654}{F_y}$
ASCE Manual No. 72 (*25*) (computed value)	$\frac{D}{t} \le \frac{4110}{F_y}$
Schilling (*49*)	$\frac{D}{t} \le \frac{3625}{F_y}$
AISC *Manual of Steel Construction - Allowable Stress Design* (*26*)	$\frac{D}{t} \le \frac{3300}{F_y}$
AISC *Manual of Steel Construction - LRFD* (*50*)	$\frac{D}{t} \le \frac{2070}{F_y}$

$$F_b = 0.66F_y \text{ for } \frac{D}{t} \le \frac{3{,}650}{F_y}$$

$$F_b = \left[0.39F_y + \frac{986}{\frac{D}{t}}\right] \text{ for } \frac{3{,}650}{F_y} \le \frac{D}{t} \le \frac{13{,}000}{F_y}$$

and $\frac{D}{t}$ shall not exceed $\frac{13{,}000}{F_y}$

2.6.3 Allowable Bending Stress for Multi-Sided Tubular Steel Shapes

The allowable stress equations for multi-sided tubular steel shapes in the current *Supports Specifications* were developed on the basis of a report by Brockenbrough (*52*) and were verified by Fiss (*53*). New equations are proposed on the basis of more recent research on multi-sided tubular sections by EPRI (*47*), which investigated the local buckling strength in bending of 8-, 12-, and 16-sided tubular steel sections. Full-scale testing of tubes in bending was performed and demonstrated that regular polygon-shaped tubes with different numbers of sides have different buckling capacities. Thus different equations are provided for polygonal shapes with different numbers of sides. Results of this study were adopted by the ASCE Manual 72 (*25*). These equations formed the basis for the equations for multi-sided steel tubes in the proposed *Supports Specifications*. Although the EPRI test program did not address rectangular tubular sections, ASCE Manual 72 treats such sections as equivalent to an octagonal section if the section is subjected primarily to bending.

The current *Supports Specifications* uses a constant safety factor of 1.925 against ultimate strength for bending of different shapes for compact, noncompact, and slender cross sections. The strength equations from ASCE Manual 72 were modified by using this safety factor to develop the proposed allowable stress equations.

2.6.3.1 Proposed Revisions

The proposed revisions and changes in the allowable bending stress equations for multi-sided tubular steel sections may be summarized as follows:

- Local buckling criteria are presented and defined. Steel sections are classified as being compact, noncompact, or slender element sections, according to their respective width-thickness ratio. Table 20 shows the proposed limiting width-thickness ratios.
- A new set of allowable stress equations for multi-sided tubular sections is proposed to replace the current equations. Table 21 shows the proposed allowable stress equations for different multi-sided tubular sections.
- An upper limit for the ratio for the width-to-thickness of $b/t = 365/\sqrt{F_y}$ for multi-sided tubular sections is proposed because of the lack of documented tests for multi-sided tubes with b/t above that ratio.
- The allowable bending stress for polygonal tubes shall not exceed the allowable stress for round tubes of equivalent radius.

2.6.3.2. Effect of the Proposed Changes

Figures 10–13 show comparisons between the allowable bending stresses for different multi-sided tubular sections as given by the current and proposed *Supports Specifications*. The following may be noted:

TABLE 19 Comparison of allowable bending stresses for noncompact round sections

	Allowable Bending Stress
Proposed *Supports Specification*	$F_b = \left[0.39F_y + \frac{986}{\frac{D}{t}}\right]$ for $\frac{3650}{F_y} \le \frac{D}{t} \le \frac{13000}{F_y}$
Current *Supports Specification*	$F_b = \left[0.39F_y + \frac{986}{\frac{D}{t}}\right]$ for $\frac{3654}{F_y} \le \frac{D}{t} \le \frac{12180}{F_y}$
ASCE Manual No. 72 (Plantema's Equation Modified for Bending)	$F_b = \left[\frac{12}{23}\right]\left[0.70F_y + \frac{1800}{\frac{D}{t}}\right]$ for $\frac{6000}{F_y} \le \frac{D}{t} \le \frac{12000}{F_y}$
Plantema's Equation for Axial Compression	$F_b = \left[\frac{12}{23}\right]\left[0.75F_y + \frac{928}{\frac{D}{t}}\right]$ for $\frac{3625}{F_y} \le \frac{D}{t} \le \frac{11600}{F_y}$
AISC *Manual of Steel Construction - Allowable Stress Design*	Not Provided.
AISC *Manual of Steel Construction - LRFD* (Modified to include a 23/12 safety factor)	$F_b = \left[\frac{12}{23}\right]\left[F_y + \frac{600}{\frac{D}{t}}\right]$ for $\frac{2070}{F_y} \le \frac{D}{t} \le \frac{8970}{F_y}$ $F_b = \left[\frac{12}{23}\right]\left[\frac{9570}{\frac{D}{t}}\right]$ for $\frac{8970}{F_y} \le \frac{D}{t} \le \frac{13000}{F_y}$
Note: Ultimate strength equations are multiplied by 12/23 to convert to an allowable stress form.	

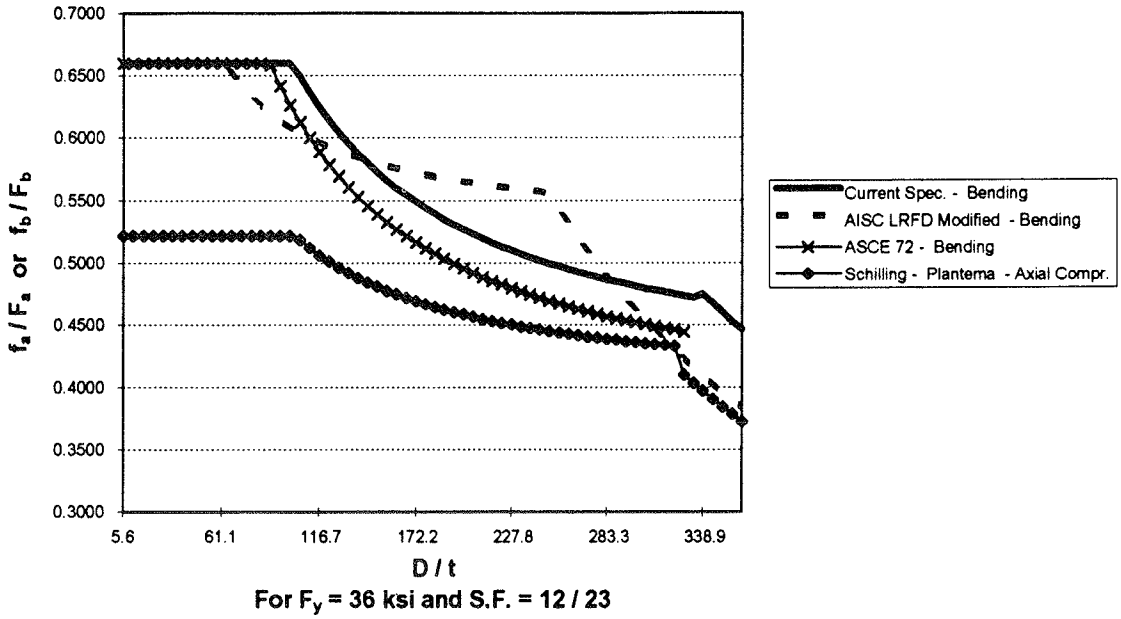

Figure 9. Allowable bending stresses for round tubular steel shapes.

TABLE 20 Width-thickness ratio limits for multi-sided steel tubes

Description of Section	Width-thickness ratio λ	λ_c Compact	λ_n Non-Compact	λ_s Slender
Hexdecagonal tube	$\frac{b}{t}$	$\frac{190}{\sqrt{F_y}}$	$\frac{215}{\sqrt{F_y}}$	$\frac{365}{\sqrt{F_y}}$
Dodecagonal tube	$\frac{b}{t}$	$\frac{190}{\sqrt{F_y}}$	$\frac{240}{\sqrt{F_y}}$	$\frac{365}{\sqrt{F_y}}$
Octagonal tube	$\frac{b}{t}$	$\frac{190}{\sqrt{F_y}}$	$\frac{260}{\sqrt{F_y}}$	$\frac{365}{\sqrt{F_y}}$
Square or rectangular tube	$\frac{b}{t}$	$\frac{190}{\sqrt{F_y}}$	$\frac{260}{\sqrt{F_y}}$	$\frac{365}{\sqrt{F_y}}$

- For noncompact and slender multi-sided tubular sections (dodecagonal, octagonal, and rectangular), the proposed allowable stresses are higher than the current allowable stresses. The increase in the allowable stress value ranges from zero to 12 percent, depending on the shape of the section and the ratio $b/t\sqrt{F_y}$.
- For noncompact and slender hexdecagonal tubular sections, the proposed stresses may be greater or lower than the current allowable stresses depending on the ratio $b/t\sqrt{F_y}$. The difference could vary from -11.3 to +1.2 percent.
- For multi-sided compact sections, no changes to the value of the allowable stresses are proposed.

2.6.3.3 Comparison of Multi-Sided Tubular Sections with Round Sections

The current *Supports Specifications* notes that the allowable bending stress of multi-sided tubes shall not exceed the allowable stress of the equivalent round section based on a diameter equal to the flat-to-flat dimension of the multi-sided tube. A study was conducted to determine if this restriction should be included in the current *Supports Specifications*. A comparison, using the proposed equations, was made between round tubular steel sections and 16-, 12-, 8-sided, and square tubular steel sections. A spreadsheet was developed to compare the allowable

TABLE 21 Proposed allowable bending stress F_b for multi-sided steel tubes

	$\lambda \le \lambda_c$ Compact Section	$\lambda_c < \lambda \le \lambda_n$ Non-Compact Section	$\lambda_n < \lambda \le \lambda_s$ Slender Section
Hexdecagonal Tube	$0.66F_y$	$F_b = 1.709F_y\left(1-.00323\frac{b}{t}\sqrt{F_y}\right)$	$F_b = 0.74F_y\left(1-.00137\frac{b}{t}\sqrt{F_y}\right)$
Dodecagonal Tube	$0.65F_y$	$F_b = 1.152F_y\left(1-.00229\frac{b}{t}\sqrt{F_y}\right)$	$F_b = 0.75F_y\left(1-.00129\frac{b}{t}\sqrt{F_y}\right)$
Octagonal Tube	$0.64F_y$	$F_b = 0.964F_y\left(1-.00177\frac{b}{t}\sqrt{F_y}\right)$	$F_b = 0.74F_y\left(1-.00114\frac{b}{t}\sqrt{F_y}\right)$
Rectangular Tube	$0.60F_y$	$F_b = 0.815F_y\left(1-.001394\frac{b}{t}\sqrt{F_y}\right)$	$F_b = 0.74F_y\left(1-.00114\frac{b}{t}\sqrt{F_y}\right)$

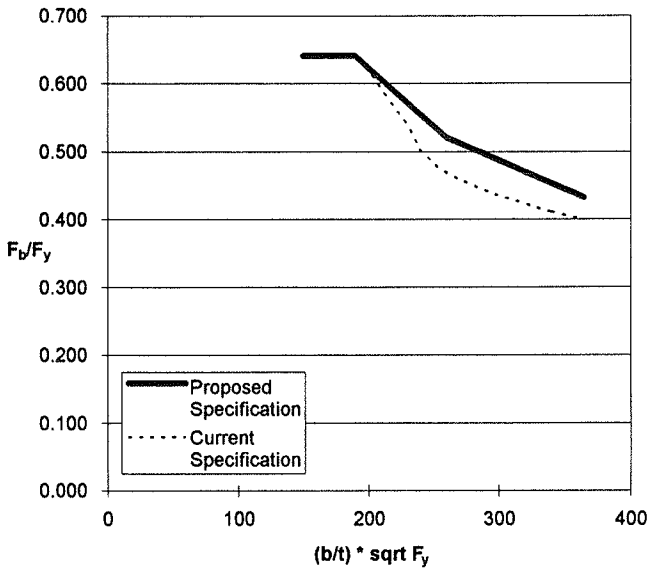

Figure 10. Allowable bending stresses for octagonal steel tubes.

stresses and bending moments for a 24-in. diameter section, with yield stresses of 36 and 70 ksi, to equivalent multi-sided 16-, 12-, 8-sided, and square sections (Figures 14–17).

The local buckling characteristics of a multi-sided steel tube should be similar to that of a round tube, particularly when the number of sides becomes large. The round section would have the highest allowable bending stress, the equivalent square section would have the lowest allowable bending stress, and the 8-, 12-, and 16-sided sections would have allowable bending stresses that range from those of the equivalent square section to the round section. However, for certain cross-sectional dimensions, as noted in Figures 14–17, the allowable stress equation for the multi-sided section exceeds the allowable stress equation for the round section. This case is mostly found in the compact and noncompact ranges of the multi-sided section.

The equations for round and multi-sided tubes were derived from different research studies. Additionally, the equations for the multi-sided tubes are developed from limited test data and do not include sufficient tests in the compact and noncompact ranges of the equations. Therefore, the researchers propose to limit the allowable bending stress for a multi-sided tube to that for a round tube until more research is performed.

As stated in the current *Supports Specifications*, multi-sided shapes need to be checked to determine if the allowable stress is greater than that of the round section for equivalent D/t of the multi-sided section greater than $3{,}650/F_y$, where D for a multi-sided tube is the flat-to-flat dimension and t is the wall thickness.

2.6.4 Allowable Bending Stress for Nontubular Shapes

The allowable stresses for nontubular sections in the current *Supports Specifications* were reviewed and updated. Comparisons were made with the allowable stresses given in

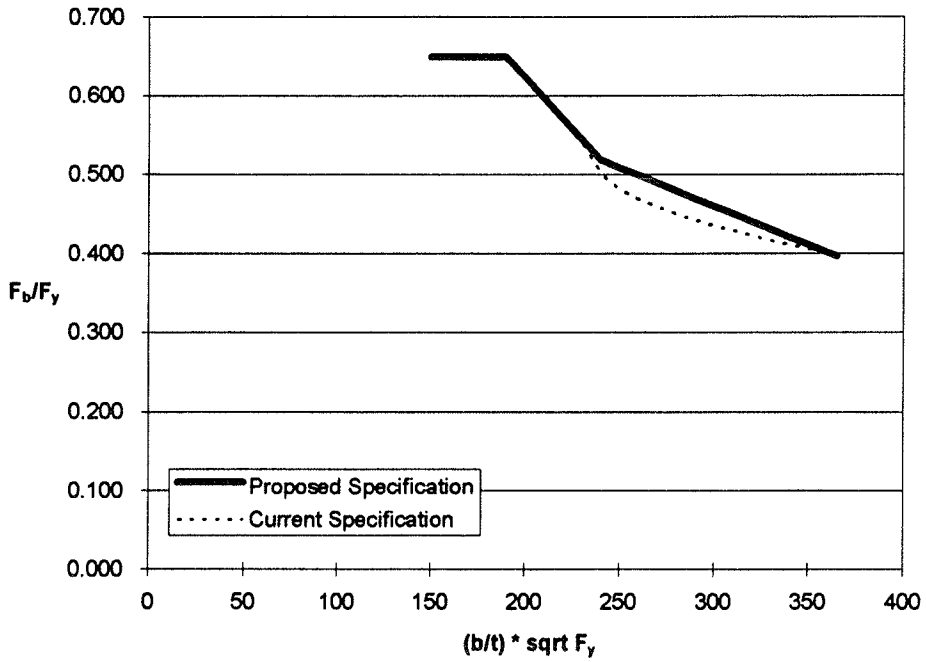

Figure 11. Allowable bending stresses for dodecagonal steel tubes.

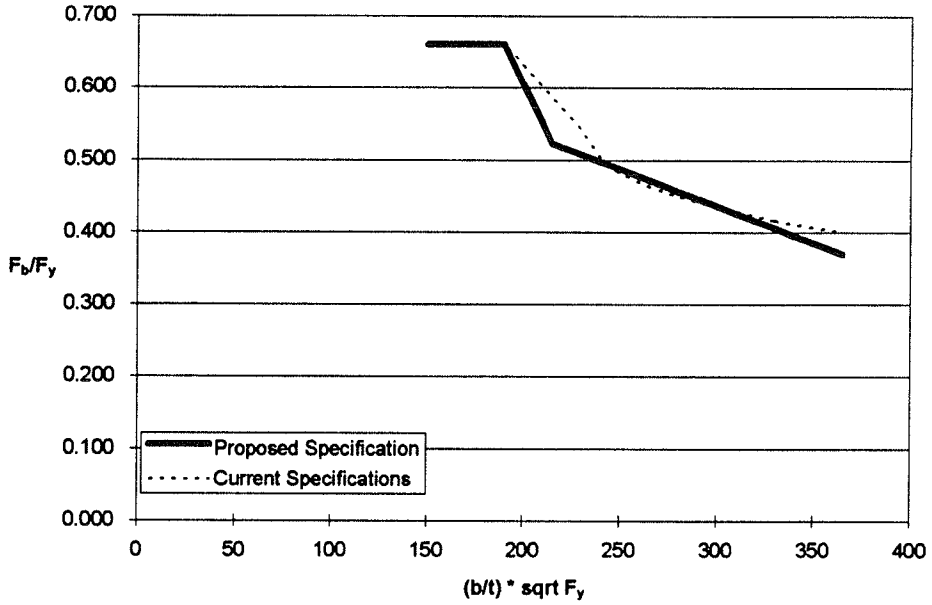

Figure 12. Allowable bending stresses for hexdecagonal steel tubes.

- AISC *Manual of Steel Construction—Allowable Stress Design*, 9th Edition, 1989 (*26*).
- AASHTO *Standard Specifications for Highway Bridges*, 1996 (*7*).

The current *Supports Specifications* adopts the allowable stresses of nontubular sections from the AISC specifications (*54*) with minor changes. While the AISC specification allows an allowable bending stress of $0.66F_y$ for compact I-shaped sections and channels, the current *Supports Specifications* allows only $0.60F_y$, which ensures the equity of safety factor between tubular and nontubular sections. The most recent edition of the AISC *Manual of Steel Construction* allows an increase in allowable stresses for I-shaped sections. However, to maintain comparable levels of safety among various steel cross sections, the research team decided not to change the allowable stress of $0.60F_y$ for compact I-sections with adequate lateral support. Allowable stress for channels remains at $0.60F_y$ for compact and noncompact sections. The equations for I-shaped sections and channels with inadequate lateral support remain unchanged.

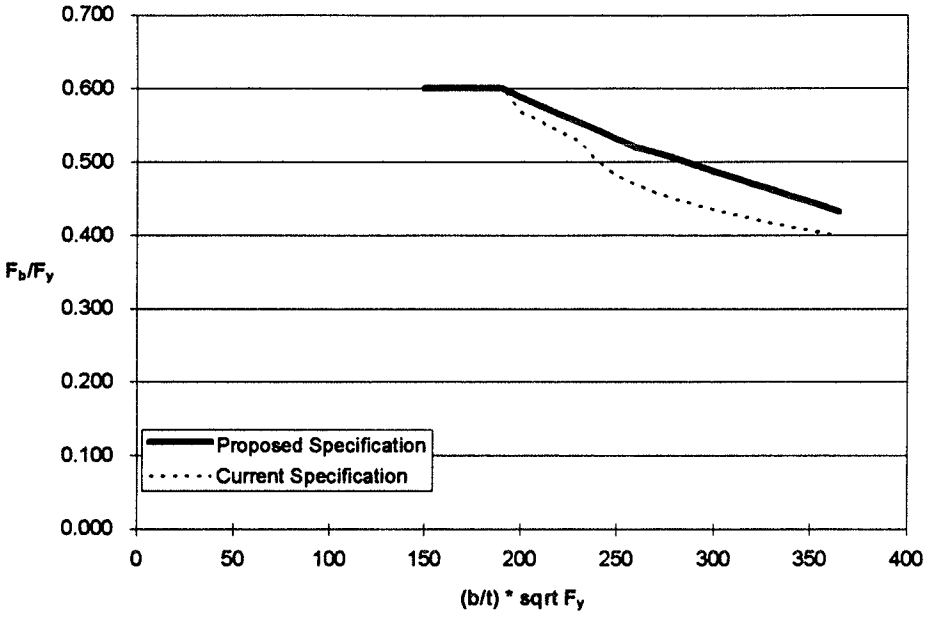

Figure 13. Allowable bending stresses for square and rectangular steel tubes.

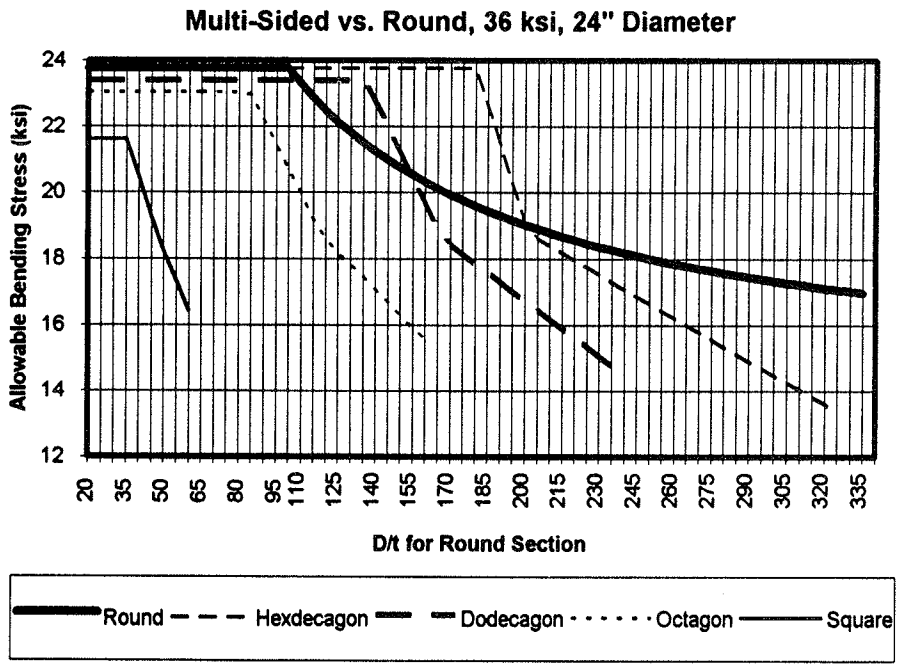

Figure 14. Comparison of allowable stresses for round and multi-sided tubes

2.6.5 Allowable Bending Stress About the Weak Axis

Allowable stresses for I-shaped sections with compact flanges bent about the weak axis have increased from 0.6 to $0.75F_y$. Allowable stresses for base plates have increased from 0.66 to $0.75F_y$. These changes are consistent with the AISC *Manual of Steel Construction.*

2.6.6 Allowable Compressive Stress

The allowable stress equation for inelastic buckling of axially loaded members with $KL/r < \sqrt{2\pi^2 E/F_y}$ currently employs a constant factor of safety of 1.92. This equation has been updated to comply with the current equation in AISC *Manual of Steel Construction—Allowable Stress Design* that employs a variable safety factor. The safety

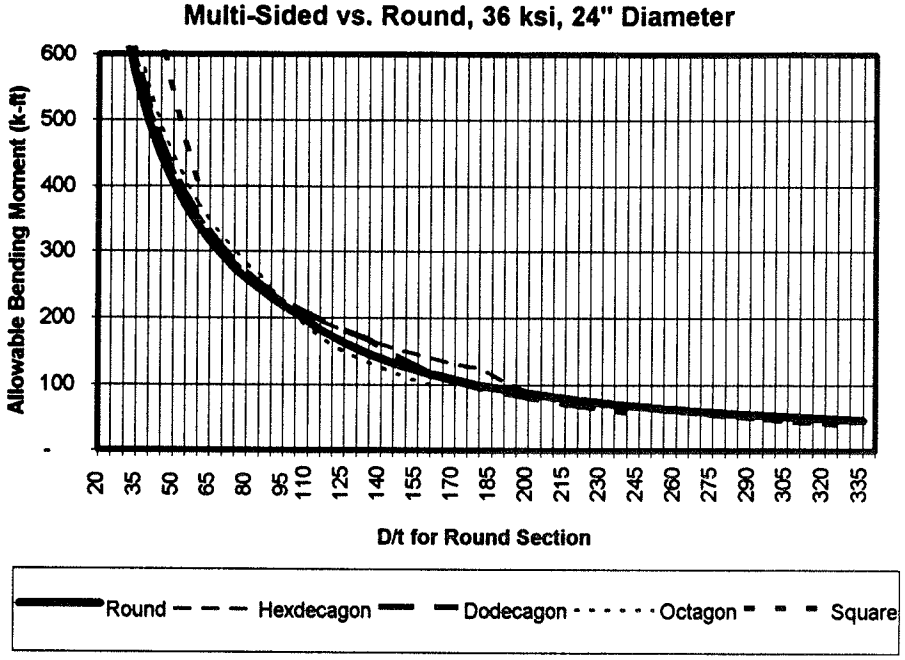

Figure 15. Allowable bending moments for round and multi-sided tubes.

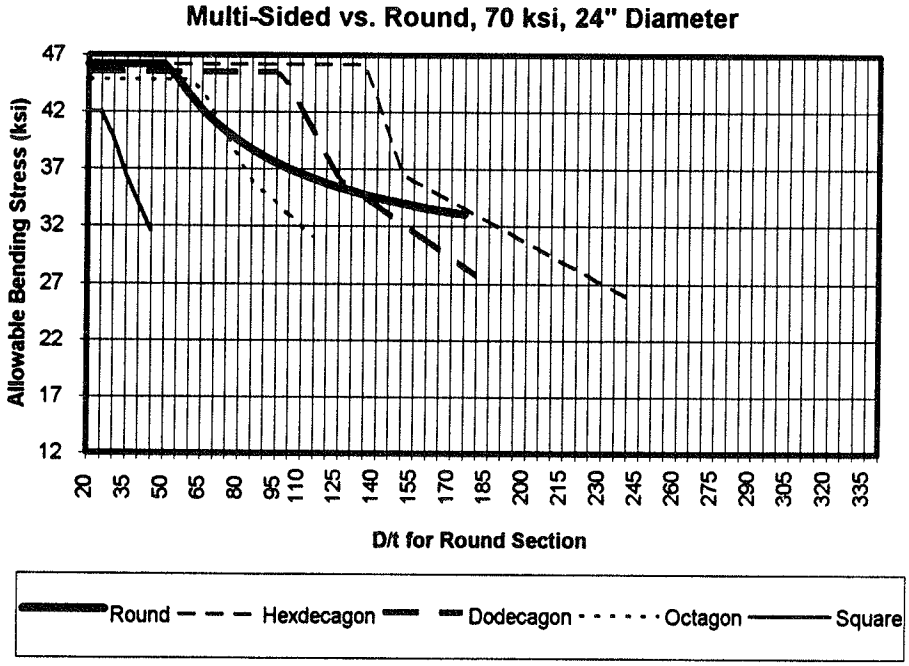

Figure 16. Comparison of allowable stresses for round and multi-sided tubes.

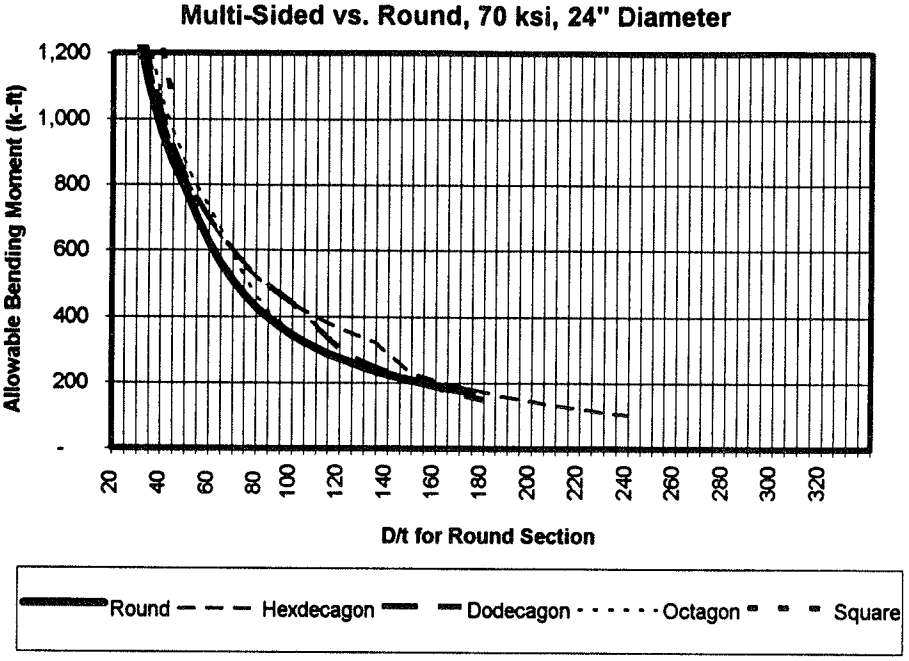

Figure 17. Allowable bending moments for round and multi-sided tubes.

factor varies from 1.67 at $KL/r = 0.0$ to 23/12 at $KL/r = \sqrt{2\pi^2 E/F_y}$. The proposed inelastic buckling equation is given by

$$F_a = \frac{\left[1 - \frac{\left(\frac{KL}{r}\right)^2}{2C_c^2}\right]F_y}{\frac{5}{3} + \frac{3\left(\frac{KL}{r}\right)}{8C_c} - \frac{\left(\frac{KL}{r}\right)^3}{8C_c^3}} \quad \text{for} \quad \frac{KL}{r} < C_c$$

where

$$C_c = \sqrt{\frac{2\pi^2 E}{F_y}}.$$

Figure 18 presents a comparison of allowable axial stresses for the current *Supports Specifications* and the proposed equations. An increase in the allowable axial stress occurs when using the proposed equation. This increase ranges from a 15 percent increase at $KL/r = 0.0$ to 0 percent at $KL/r = \sqrt{2\pi^2 E/F_y}$.

The allowable compressive stress equation in the elastic buckling range for $KL/r > \sqrt{2\pi^2 E/F_y}$ remains unchanged:

$$F_a = \frac{12}{23}\frac{\pi^2 E}{\left(\frac{KL}{r}\right)^2} \quad \text{for} \quad \frac{KL}{r} \geq C_c$$

2.6.7 Allowable Tensile Stress

The allowable tensile stress of $0.60F_y$ on the gross area has not changed. However, another criteria has been added that limits the allowable stress to $0.50F_u$ on the effective net cross-sectional area at bolted connections. This change is consistent with the allowable tensile stresses in the AISC *Manual of Steel Construction.*

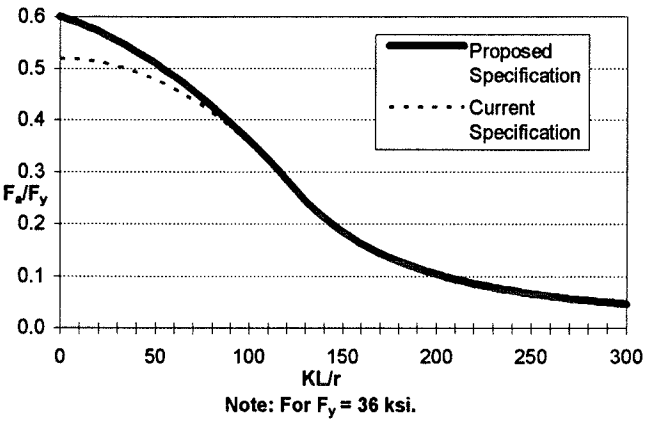

Figure 18. Comparison of allowable axial stress.

2.6.8 Allowable Shear Stress

For tubular steel, design equations for shear remain unchanged at this time. The allowable shear stress limit can be found in the ASCE Manual 72 (*25*). The ultimate shear stress in the ASCE manual is given as $0.58F_y$, which is based on the distortion-energy yield criterion. A factor of 12/23 is applied to obtain an allowable value of $0.30F_y$.

2.6.9 Combined Stress Ratio Equation (CSR)

Application of moment to axially loaded members causes additional deflection in the member. This deflection generates additional secondary moments that are equal to the product of the applied axial load and the eccentricity resulting from the maximum deflection generated by the moment. To account for the combined action of axial compression, bending, shear, and torsion, the current *Supports Specifications* provides the following equation:

$$CSR = \frac{f_a}{F_a} + \frac{f_b}{\left(1 - \frac{f_a}{F_a}\right)F_b} + \left(\frac{f_v}{F_v}\right)^2 \leq 1.0$$

where

f_a = calculated axial compressive stress,
f_b = calculated bending stress,
f_v = calculated stress due to shear or torsion or both,
F_a = allowable stress for members in axial compression,
F_b = allowable bending stress, and
F_v = allowable shear stress.

The current *Supports Specifications* states that sign support members, high-level lighting supports (truss type), and miscellaneous structural members, subjected to torsion, or any combination of bending, axial compression, shear and torsion, shall be proportioned to meet this limitation. The term $1/(1 - f_a/F_a)$ is an amplification factor for bending stress, f_b. This amplification factor is introduced in the equation to account for the secondary bending moment.

The amplification factor is similar to that used by the AISC *Manual of Steel Construction,* except that F_a is used instead of F'_e in the AISC equation. F'_e is an Euler elastic buckling stress that considers the slenderness ratio about the axis of bending rather than the maximum slenderness ratio of the member. The use of F_a in the amplification term is incorrect and results in extremely conservative moment magnifications, whereas the use of F'_e results in a better representation of the moment amplification. The research team proposes to adopt the term $1/(1 - f_a/F'_e)$ in the *Supports Specifications* instead of $1/(1 - f_a/F_a)$ because it provides more reasonable results and is consistent with the AISC *Manual of Steel Construction-Allowable Stress Design.* Therefore, the proposed combined stress ratio equation for member stability check may be written as follows:

$$\frac{f_a}{F_a} + \frac{f_b}{\left(1 - \frac{f_a}{F'_e}\right)F_b} + \left(\frac{f_v}{F_v}\right)^2 \leq 1.0 \qquad (15)$$

where

$F'_e = 12\pi^2 E/23(KL/r)^2$ = Euler stress divided by a factor of safety of 23/12,
E = modulus of elasticity,
L = actual unbraced length in plane of bending,
r = corresponding radius of gyration, and
K = effective length factor in the plane of bending.

This stability check is intended for slender members and applies generally at locations where large lateral displacements occur.

For cases when $f_a/F_a \leq 0.15$, the following equation, which ignores the amplification factor $1/(1 - f_a/F'_e)$, may be used:

$$\frac{f_a}{F_a} + \frac{f_b}{F_b} + \left(\frac{f_v}{F_v}\right)^2 \leq 1.0$$

Spreadsheets were developed to compare the interaction equation in Section 1.4.1.E.3 of the current *Supports Specifications* and the proposed Equation 15. Different slenderness ratios, KL/r, and yield stresses were considered in the comparisons. Figures 19–21 show interaction curves for bending and axial compression for different slenderness ratios and for yield stress, $F_y = 50$ ksi. The figures show the following:

1. For members with slenderness ratios, $KL/r \geq C_c$, where $C_c = \sqrt{2\pi^2 E/F_y}$, the interaction curves between bending and axial compression are the same as represented by the *Supports Specifications* or the AISC specifications, as shown in Figure 19. As long as the member is undergoing elastic buckling, the two equations yield the same results.
2. For members with slenderness ratios, $KL/r \leq C_c$, and with bending and buckling occurring in the same plane, the difference between the two interaction curves increases for shorter members, as shown by Figures 20 and 21. These short members can be found in a large percentage of structural supports (e.g., sign support members, high-level truss-type lighting supports, and miscellaneous structural members). The bending portion of the current interaction curve can result with

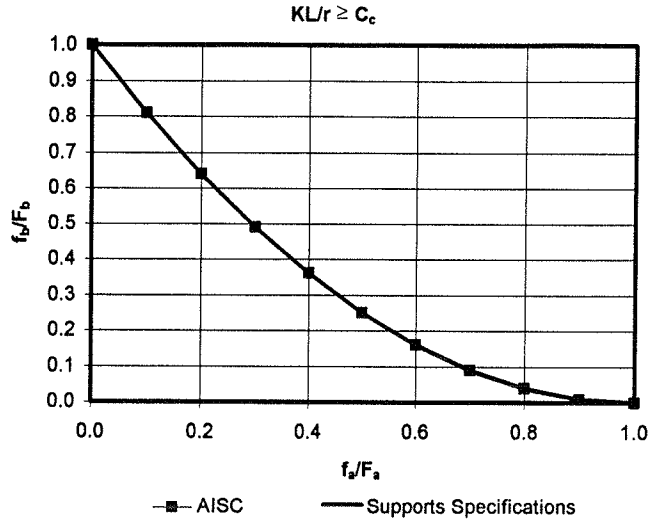

Figure 19. Interaction curves between axial and bending stresses for $KL/r \geq C_c$.

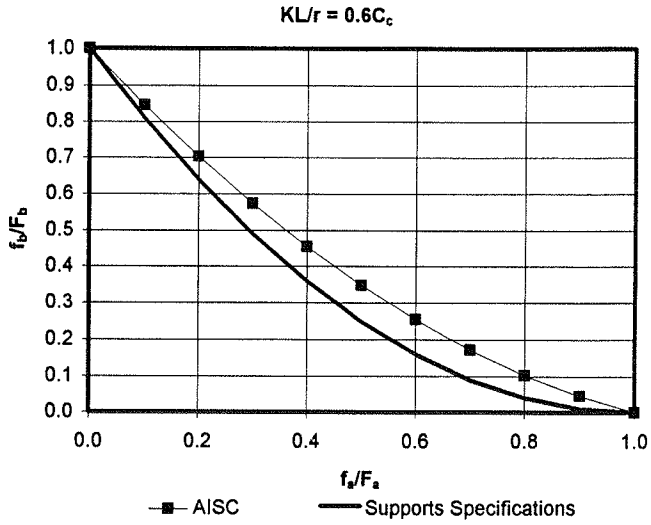

Figure 20. Interaction curves between axial and bending stresses for $KL/r = 0.6C_c$.

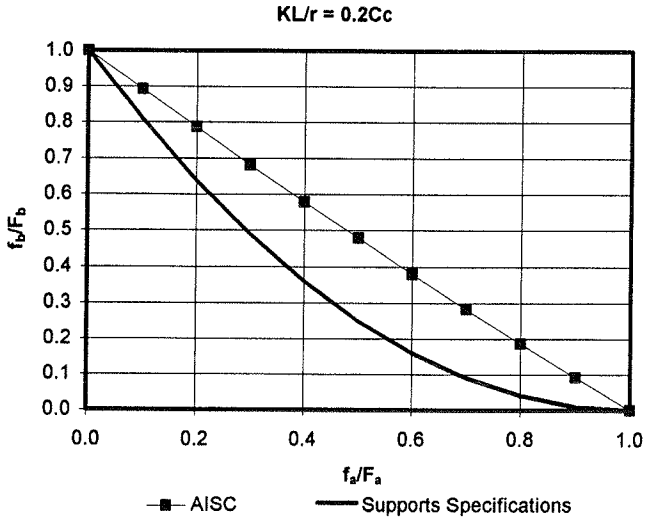

Figure 21. Interaction curves between axial and bending stresses for $KL/r = 0.2C_c$.

errors up to 100 percent for $f_a/F_a = 0.5$, and even higher errors for larger ratios of f_a/F_a.

The researchers therefore proposed to replace the interaction equation in Article 1.4.1(E)(3) with the following equations:

$$\text{For } f_a/F_a \geq 0.15, \quad \frac{f_a}{F_a} + \frac{f_b}{\left(1 - \frac{f_a}{F'_e}\right)F_b} + \left(\frac{f_v}{F_v}\right)^2 \leq 1.0$$

and

$$\text{for } f_a/F_a \leq 0.15, \quad \frac{f_a}{F_a} + \frac{f_b}{F_b} + \left(\frac{f_v}{F_v}\right)^2 \leq 1.0$$

A third interaction equation is also provided and is intended to check stresses at member end sections where buckling and secondary moments are not of concern. The equation is the same as in the current *Supports Specifications* and takes the form

$$\frac{f_a}{0.6F_y} + \frac{f_b}{F_b} + \left(\frac{f_v}{F_v}\right)^2 \leq 1.0$$

2.6.10 Loading Across the Diagonal for Rectangular Steel Tubes

The research team investigated the behavior of square and rectangular tubular steel sections loaded across the diagonal. Articles on this subject were obtained and reviewed to determine if the information is applicable for the proposed *Supports Specifications*.

The following documents were reviewed concerning biaxial bending of rectangular steel tubes:

- Brown, J.C., and Tidbury, G.H., "An Investigation of the Collapse of Thin-Walled Rectangular Beams in Biaxial Bending," 1983 (*55*).
- Duan, L., and Chen, W.-F., "A Yield Surface Equation for Doubly Symmetrical Sections," 1990 (*56*).
- Pekoz, T., "Combined Axial Load and Bending in Cold-Formed Steel Members," 1986 (*57*).
- Uchida, Y., and Morino, S., "Biaxial Bending Moment-Curvature Relation of Box Beam-Column with Degrading Stress-Strain Relation," 1986 (*58*).

Limited test data from a support manufacturer was reviewed. The data indicated that bending across the diagonal resulted in greater flexural strength than predicted by theoretical calculations. Although this may appear to justify increasing the allowable stresses in the case of bending about the diagonal, the researchers decided not to do so at this time because of the limited nature of the data. More research is needed to evaluate the strength of the rectangular section in bending about the diagonal.

2.7 ALLOWABLE STRESSES FOR ALUMINUM

The aluminum design section in the current *Supports Specifications* was reviewed and found to lack adequate information on design. Although no change in design philosophy has been made, new information has been added for the design of commonly used aluminum support structures. Another major weakness in the current section relates to presentation and format. The charts and design equations are difficult to read. The section has been revised to provide charts and design equations that are easier to read. The upgraded design information includes information on mechanical properties of welded and nonwelded aluminum alloys, allowable stress equations, formulas for buckling constants, allowable stresses for casting alloys, slenderness limits for truss members, minimum thickness of material, dimensional tolerances, allowable stresses for welds, anodizing, and painting provisions for corrosion prevention.

2.7.1 Documents Reviewed

The *Aluminum Design Manual* (*9*) provided a wealth of information on aluminum design. The manual includes a specification that covers design, allowable stresses, connection techniques, fabrication, and inspection of aluminum structures. It also includes information on aluminum materials, material properties, corrosion prevention, typical section properties, as well as a set of design examples that are provided to illustrate the application of the specification. In addition to the *Aluminum Design Manual*, several other publications on aluminum design were also reviewed, including:

- Sharp, M.L., *Behavior and Design of Aluminum Structures*, 1993 (*30*).
- Mazzolani, F.M., *Aluminum Alloy Structures,* 1985 (*59*).
- Clark, J.W., and Rolf, R.L., "Buckling of Aluminum Columns, Plates, and Beams," 1966 (*60*).
- Clark, J.W., and Rolf, R.L., "Design of Aluminum Tubular Members," 1964 (*61*).
- Clark, J., "Design of Aluminum Structural Members," *Structural Engineering Handbook*, 1990 (*45*).
- AASHTO *LRFD Bridge Design Specifications*, 1994 (*7*).
- *Standard Specifications for Highway Bridges*, AASHTO, 1996 (*51*).

Consultants and members of the Aluminum Association were also contacted to discuss specific issues related to aluminum support structures.

2.7.2 Allowable Stresses

The allowable stress equations in the current *Supports Specifications* were adopted from the fourth edition of the *Specifications for Aluminum Structures* (*62*). The sixth edition of the *Specifications for Aluminum Structures*, published in 1994, was reviewed and contained only minor changes to the previously published allowable bending stress equations for cross-sectional shapes extensively used for support structures (e.g., round and oval tubes, rectangular tubes, and structural shapes). Hence, the updates in the proposed *Supports Specifications* related to allowable stresses are only minimal.

The *Specifications for Aluminum Structures* provides general equations for allowable stresses that can be applied to any structure, with appropriate values for factor of safety (n_y, n_u) applied to the yield stress and the ultimate strength, respectively. Structures are divided into two general types (bridge type and building type), and different values for n_y and n_u are given for each structural type. The allowable stresses for aluminum in the 1985 edition of the *Supports Specifications* have been increased over those of the 1975 edition, which was a result of using the safety factors for building type structures rather than for bridge type structures. The proposed *Supports Specifications* adopts the same philosophy by using the safety factors for building type structures of 1.65 and 1.95 against yield and ultimate strength, respectively.

2.7.3 Increase in Allowable Stresses

The Aluminum Association specification allows a 33 percent increase in the allowable stresses when the stresses are produced by wind acting alone or in combination with dead and live load (Section 2.3.2, "Specifications for Aluminum Structures," fourth and sixth editions). The current *Supports Specifications* adopts the allowable stresses as given by the Aluminum Association specification but allows an increase of 40 percent for the allowable stresses. To be consistent, an increase in allowable stresses of 33 percent for wind loading is adopted in the proposed *Supports Specifications*.

2.7.4 Safety Factors for Aluminum Sections in Bending

A comparison was made between the safety factors for steel and aluminum in bending. The stress-strain curve for aluminum does not exhibit a definite yield point and, hence, cannot be idealized as elasto-plastic in a manner similar to steel. Shape factors for yield and ultimate strength are used in the case of aluminum to adjust the moment equation to reflect yielding and ultimate strength for a particular shape. The yield moment and ultimate moment for an aluminum section may be calculated as follows:

$$M_y(\text{alum.}) = K_y F_y S$$
$$M_u(\text{alum.}) = K_u F_y S$$

where K_y and K_u are the yield and ultimate shape factors, respectively. In comparison, the yield moment and ultimate moment for a steel section are calculated as follows:

$$M_y(\text{steel}) = F_y S$$
$$M_u(\text{steel}) = K_p F_y S$$

where S is the modulus of section and K_p is the plastic shape factor for a given section. Values for K_y and K_u, given in the *Aluminum Design Manual,* were compared to published values in the literature (*30*). The terms, K_y and K_u, have values always greater than 1.0 and will vary with cross-sectional shape and aluminum material properties. Typical values for K_y and K_u are presented in Table 22. The values given by the *Aluminum Design Manual* are either comparable or more conservative than values published in the literature (30).

In comparing the bending stresses in aluminum and steel, the comparison is made between the ratios of $1.4F_b/F_y$ and $1.33F_b/F_y$ for steel and ratios of $1.4F_b/K_yF_y$ and $1.33F_b/K_yF_y$ for aluminum, respectively. As mentioned previously, introduction of the term, K_y, is due to the fact that aluminum does not exhibit a purely elasto-plastic stress-strain curve. The yield strength, F_y, for aluminum is typically defined as the

TABLE 22 Shape factors for yielding and ultimate strength of aluminum beams

	Aluminum Design Manual		Estimated shape factors from *Behavior and Design of Aluminum Structures (30)*	
Cross-section	K_y	K_u	K_y	K_u
Round tube	1.17	1.24	1.16	1.22
Rectangular tube	1.00	1.00	1.07	1.10
I-shape (major axis)	1.00	1.00	1.13	1.14
I-shape (minor axis)	1.30	1.42	1.33	1.44
Solid rectangle	1.30	1.42	1.32	1.46
Solid round	1.30	1.42	1.42	1.56

stress corresponding to a 0.2 percent offset strain. The material is purely elastic only up to the proportional limit, and moments up to that level can be calculated by using the product of the stress, f, and the section modulus, S. For a stress value greater than the proportional limit, the corresponding moment can be calculated by using numerical integration and the actual stress-strain curve. For example, at a stress slightly higher than the proportional limit but less than the yield strength, the actual moment is greater than the product of f and S; or in other words, the actual stress corresponding to the moment $f \times S$ will be less than f. Thus the term, K_y, referred to as the shape factor, must be introduced to account for the effect of the shape of the cross section as well as the shape of the stress-strain curve. The shape factor, K_y, for yielding is defined as the ratio of the actual yield moment to the apparent moment at first yielding ($F_y S$). A discussion of the shape factor for ultimate strength is given in Section 2.3.

Table 23 shows the ratios of increased allowable stresses to the yield stress for steel, and to the yield stress multiplied by the shape factor for aluminum round tubes for different aluminum alloys. The table shows that the ratios are always lower for aluminum, which indicates a higher safety against yield.

2.7.5 Proposed Revisions

The new provisions of the sixth edition of the "Specifications for Aluminum Structures-Allowable Stress Design" are incorporated into the proposed *Supports Specifications*. Factors of safety of 1.65 for n_y and 1.95 for n_u, applied to the yield stress and the ultimate strength, respectively, as recommended by the Aluminum Association specifications for building type structures, have been adopted for the proposed *Supports Specifications*. The allowable stress increase for groups II and III load combinations has been limited to 33 percent instead of 40 percent, which is in agreement with the Aluminum Association specifications. The combined stress ratio equations have been revised and updated to be consistent with the *Aluminum Design Manual*.

Information has been added to the aluminum section to make it more comprehensive and user friendly. The following is a summary of the updated information:

- Minimum mechanical properties for different aluminum alloys;
- Minimum mechanical properties for different welded aluminum alloys;
- Allowable stress formulas for tension, compression, bending, and shear for various structural shapes;
- Formulas for buckling constants;
- Allowable stresses for casting alloys using safety factors for building type structures for permanent mold castings and sand castings; and
- Painting provisions for corrosion prevention.

New information to the proposed specification includes the following:

TABLE 23 Comparison of allowable bending stress with yield stress

	Yield Stress (ksi)	Allowable Stress F_b (ksi)	Increased Allowable Stress (40 percent) (ksi)	$\frac{1.4F_b}{F_y}$	$\frac{1.4F_b}{K_yF_y}$	$\frac{1.33F_b}{F_y}$	$\frac{1.33F_b}{K_yF_y}$
Steel							
A36	36	24	33.6	0.93	not applicable	0.89	not applicable
Aluminum Alloy							
6061 - T6	35	24	33.6	0.96	0.82	0.91	0.78
6063 -T6	25	18	25.2	1.01	0.86	0.96	0.82
6005 -T5	35	24	33.6	0.96	0.82	0.91	0.78
5086 - H34	34	24	33.6	0.99	0.84	0.94	0.80
5456 - H111	26	18	25.2	0.97	0.83	0.92	0.79
5083 - H111	24	17	23.8	0.99	0.85	0.94	0.81

1. Allowable stresses are calculated for compact round tubes in bending.
2. K_y = 1.17 for round aluminum tubes.

- Allowable stresses for bolts,
- Allowable stresses for welds,
- Slenderness limits for truss members,
- Minimum thickness of material,
- Dimensional tolerances, and
- Anodizing.

2.7.6 Effect of the Proposed Changes

Allowable stress equations for group I load combination remain unchanged; however, allowable stress values for groups II and III load combinations have been reduced by about 5 percent because of modifying the allowable stress increase from 40 to 33 percent. Technical information is more comprehensive and is presented in charts and tables that are user friendly.

2.8 PRESTRESSED CONCRETE DESIGN

The prestressed concrete design section has undergone major revisions. Information on allowable stresses for concrete and prestressing steel, ultimate moment and torsional capacities, development length, prestress losses, and durability considerations has been added. The section includes the latest information in design of prestressed concrete.

2.8.1 Documents Reviewed

The literature search focused primarily on concrete poles used for streetlighting and traffic signal applications. Documents reviewed included the following:

- ASCE/PCI "Guide for the Design of Prestressed Concrete Poles," Final draft, 1994 (*63*).
- "Guide for Design of Prestressed Concrete Poles," 1983 (*64*).
- "Guide Specifications for Prestressed Concrete Poles," 1982 (*65*).
- ASTM C1089, "Standard Specification for Spun Cast Prestressed Concrete Poles" (*66*).
- ASTM C935, "Standard Specification for Static Cast Prestressed Concrete Poles," 1995 (*67*).
- ACI 318-89 (Revised 1992), *Building Code Requirements for Reinforced Concrete*, 1992 (*68*).
- ACI 318-95, *Building Code Requirements for Structural Concrete,* 1995 (*69*).
- *Standard Specifications for Highway Bridges*, AASHTO, 1996 (*51*).
- AASHTO *LRFD Bridge Design Specifications,* 1994 (*7*).
- Proposed revisions to allowable stresses submitted to the AASHTO Subcommittee on Bridges and Structures (unpublished information).

2.8.2 Allowable Stresses for Concrete and Prestressing Steel

The allowable tensile and compressive stresses for concrete in the current *Supports Specifications* were adopted from the 1977 AASHTO *Standard Specifications for Highway Bridges* (*70*). The design philosophy does not allow the pole to be cracked under dead loads, but allows flexural cracking under temporary loading such as wind or handling. This philosophy has remained unchanged; however, the allowable tensile and compressive stresses have been updated on the basis of recent research. Permissible stresses in prestressing tendons have also been updated to reflect new tendon materials. These changes were based on AASHTO *Standard Specifications for Highway Bridges*, AASHTO *LRFD Bridge Design Specifications*, and ACI 318-95 *Building Code Requirements for Reinforced Concrete.*

2.8.3 Ultimate Moment and Torsional Capacities

The *Supports Specifications* provides equations for calculation of moment and torsional capacities. The flexural equations were adopted from research by Li and Liu (*71*). The torsion equations were based on ACI 318's torsion strength equation for concrete, with some modification factors applied for the effect of prestress and shape of section. The equations are empirical in nature and may provide nonconservative results in some cases. The equations are also limited to round cross sections with minimum wall thickness of one fourth of the outside diameter, which is not practical for typical concrete pole applications.

Equations for shear and torsional capacities, along with an interaction equation, have been provided. These equations have been updated based on ASCE/PCI "Guide for the Design of Prestressed Concrete Poles." The moment capacity equations have been replaced with the requirement to determine the moment capacity based on strain compatibility according to the assumptions of Section 5.7.2 in the AASHTO *LRFD Bridge Design Specifications.*

Safety factors for prestressed concrete have been reevaluated and found to be comparable to those of steel and aluminum (see Section 2.3 in this report for a discussion of safety factors). The strength requirements have been updated to reflect this change.

2.8.4 Additional Considerations

The current *Supports Specifications* does not include information on the calculation of development length, transfer length, and prestress losses. This information has been added for the proper design of concrete poles. Provisions are also included that require the designer to consider deflections, effects of cracking, and long-term effects.

General requirements, such as manufacturing tolerance, have been added based on ASTM C1089 "Standard Specifi-

cation for Spun Cast Prestressed Concrete Poles" (*66*). Information on corrosion protection, minimum cover requirements, and inspection has been added.

2.9 WOOD DESIGN

Section 10 of the current *Supports Specifications* on wood is extremely limited in scope and provides no information on design of wood structures. The only information provided is a statement that prohibits the use of permanent wood structures without pressure preservative treatment. Therefore, a completely new section with comprehensive design information has been prepared for the proposed specification. The new section addresses allowable stress design values for poles and posts for various wood species. Allowable stresses for flexure, shear, compression, and tension are prescribed. Interaction equations for members subjected to combined bending and axial compression as well as combined bending and axial tension are provided. Updated information on timber treatments and protection methods is also provided.

2.9.1 Documents Reviewed

The most important documents reviewed were:

- AASHTO *Standard Specifications for Highway Bridges*, 1996 (*51*).
- AASHTO *LRFD Bridge Design Specifications*, 1994 (*7*).
- ANSI/NFoPA NDS-1991, *National Design Specifications for Wood Construction* (*72*).
- ANSI 05.1-1992, "Specifications and Dimensions for Wood Poles" (*73*).
- AITC *Timber Construction Manual*, 1994 (*74*).
- *AWPA Book of Standards*, 1996 (*75*).

Since the NDS-1991 specification presents a more consistent wood design approach, it has been used as the basis for the section on wood structures in the proposed *Supports Specifications*. Some modifications, however, have been included to reflect particular design considerations specific to structural supports of highway signs, luminaires, and traffic signals. The wood sections of the AASHTO *Standard Specifications for Highway Bridges* and the AASHTO *LRFD Bridge Design Specifications* are also based primarily on the NDS-1991 specification.

2.9.2 Proposed Section on Wood

The wood section of the proposed *Supports Specifications* has been added to cover several species and grades of wood and two types of wood structures: *posts and poles*. These two types can be considered the most common applications of wood structural supports for highway signs, luminaires, and traffic signals.

The proposed specification includes:

- Design provisions and equations that cover bending, tension, compression, and shear, as well as combined stresses for members subjected to bending and compression and members subjected to bending and tension;
- Design procedures and design values for *posts* that include basic design values for bending, tension parallel to grain, shear parallel to grain, compression perpendicular to grain, compression parallel to grain, and modulus of elasticity;
- Design procedures and design values for *poles* that include tabulated design values for bending, shear parallel to grain, compression perpendicular to grain, compression parallel to grain, and modulus of elasticity;
- A set of modification factors to adjust the tabulated design stresses depending on moisture content, member size, cross-sectional shape, lateral stability, and location of critical section; and
- Preservative treatments required for permanent structures. The following AWPA Standards (*75*) are referenced in the proposed specification:
  - C2-90, "Lumber, Timbers, Bridge Ties and Mine Ties-Preservative Treatment by Pressure Process," to address the preservation treatment process of four sides sawn lumber;
  - C4-90, "Poles-Preservative Treatment by Pressure Process," to address the preservation treatment process of poles; and
  - C14-90, "Wood for Highway Construction-Preservative Treatment by Pressure Process," to address the preservation treatment process of poles and posts.

The proposed section on wood has been adapted for cantilever structures, such as posts and poles. NDS-91 does not directly address the design of poles. However, according to the *Timber Construction Manual*, allowable stresses for poles can be determined with the same equations used for piles based on single use. The proposed *Supports Specifications* adopts this philosophy and includes design equations for poles based on the NDS design equations for piles based on single use. The determination of basic design values for poles is required to be in accordance with standard ASTM D3200-74 (reapproved 1994) (*76*), which refers to standard ASTM D2899-86 (*77*) for the determination of those basic values.

2.10 FIBER-REINFORCED COMPOSITES

A new section has been introduced in the *Supports Specifications* on fiber-reinforced composites because of the emerging use of composites as support structures, specifically for streetlighting poles and posts for small signs. Benefits of fiber-reinforced composites include a high strength-weight ratio and corrosion resistant properties. Information

has been included on typical mechanical properties of fiberglass-reinforced polyester (FRP) laminates, allowable stress equations for tubular, polygonal, I-, and W-sections, a testing procedure for FRP poles, and minimum requirements for protection from ultraviolet radiation.

2.10.1 Documents Reviewed

An extensive literature review was conducted to gather the state-of-the-art information on the design of structural supports using fiber-reinforced composites. The review included journal articles, conference proceedings, lectures, textbooks, design and performance specifications of similar structures, and design manuals provided by various manufacturers. The *Structural Plastics Design Manual* (*78*) published by the ASCE served as a useful source of information.

2.10.2 Materials and Manufacturing Methods

FRP is the most widely used composite for structural supports and structural applications. It is composed of polyester resin (thermoset) and glass fiber reinforcement. The thermosetting polyester resin is brittle and must be reinforced with glass to provide structural strength. The glass reinforcement reduces shrinkage, increases toughness, improves abrasion resistance, and provides dimensional stability.

The glass reinforcement could be in one of three forms: chopped strand mat, roving, and woven fabrics. FRP reinforced with roving or woven fabric yields a strong composite with reliable properties, provided proper care has been taken in its manufacture. The properties of FRP are highly dependent on the glass/resin ratio. A higher glass/resin ratio results in stronger laminate.

The most common manufacturing methods applicable to FRP structural supports are filament winding, centrifugal casting, and pultrusion. A brief description of each of these three manufacturing procedures has been included in the proposed *Supports Specifications*. Material properties and behavior of a composite product depend highly on the manufacturing process. The strength and behavior of an FRP composite are directly related to the reinforcement type and orientation with respect to the applied load, which are a function of the manufacturing method. The orientation of the reinforcement within the section can be very complicated, making it difficult to estimate analytically the strength of the product.

2.10.3 Mechanical Properties of FRP Members

FRP material exhibits almost linear stress-strain behavior up to strains of about 0.005. The yield and ultimate strengths are almost identical, indicating the absence of plastic flow. The tangent modulus at the origin is typically used as the short-term modulus of elasticity and varies from 2×10^6 to 3×10^6 psi.

Designing with unreinforced plastics is very complicated because of the viscoelastic nature of the material, which is both time and temperature dependent. However, FRP products are less sensitive to temperature and can be assumed to be unaffected by loading or straining rates. For glass reinforcement in one direction, or two orthogonal directions, the behavior can be assumed as linear elastic and mechanics equations can be used. Because the behavior of the material is dependent on many parameters that vary among different manufacturers and/or manufacturing methods, experience and large testing databases are typically used as the basis for estimating the strength and behavior of the final product.

The proposed *Supports Specifications* requires determining the mechanical properties of FRP members by testing flat sheet samples manufactured in the same manner as the structural member. The testing of a flat sheet is to be in accordance with the appropriate ASTM standard. Because no equivalent AASHTO standards were found for FRP, minimum safety factors for bending, tension, compression, and shear are prescribed in the proposed *Supports Specifications*. These values are based mainly on experience and recommendations by major FRP product manufacturers. However, additional research is needed to evaluate the safety factors for FRP members in bending, tension, compression, and shear, considering the manufacturing method and the structure of the FRP laminate.

2.10.4 Design Equations

The proposed *Supports Specifications* addresses tubular (round and polygonal), I-, and W-sections. No design equations are provided for channels or angles because the use of these shapes is highly restricted because of their inherent lateral instability.

Design equations for I- and W-sections were obtained from the *Structural Plastics Design Manual*. They are limited to isotropic or nearly isotropic materials. Barbero and Ritchey (*79*) have proposed a general equation for the allowable bending stress of pultruded W- and I-members on the basis of the equations developed for the allowable bending stress of wood members. Because only very limited testing has been performed, these equations were not included in the proposed *Supports Specifications*.

Design equations for tubular round or polygonal members are included in the proposed *Supports Specifications* to consider the overall behavior of the member as well as the local behavior of the member at locations of critical stresses. Equations to determine the allowable compressive stress considering flexural buckling were taken from the *Structural Plastics Design Manual*. Equations to determine the allowable compressive stress considering local buckling were developed on the basis of the expressions for critical compressive stresses of orthotropic round or polygonal members presented by Johnson (*80*). Johnson also presents expres-

sions for the critical buckling moment of orthotropic round or polygonal members. From these expressions, the research team developed equations to determine the allowable bending stress of orthotropic tubular round or polygonal sections based on the premise that local buckling is the controlling parameter of tubular members under bending. The buckling equation of an orthotropic cylinder under bending was used as the basis for round tubular members. For polygonal sections, the buckling equation of a simply supported orthotropic plate representing the side of the polygon was used. Despite the model's simplicity, the researchers found it to be reasonably accurate for describing the behavior of polygonal sections in bending.

Shear strength equations for W- and I-sections were not found. Shear strength equations for tubular round or polygonal sections were developed on the basis of the torsional shear equation for tubular FRP members provided in the British standard BD 26/94 "Design of Lighting Columns" (*81*).

CSR equations were taken from the *Structural Plastics Design Manual*, which are similar to the ones used for steel structures. Although FRP does not fail according to the principal stress criteria, the simplified CSR equations should give conservative approximations. Research is needed to develop more reliable CSR equations for FRP members.

Because the proposed design equations for FRP members have not been fully calibrated for all the different fiber-resin combinations and manufacturing techniques, the proposed *Supports Specifications* recommends full-scale testing of FRP members. For FRP poles, a full-scale bending test based on the ASTM D4923 (*82*) procedure is recommended. The differences between the test recommended by the proposed *Supports Specifications* and the test specified by ASTM D4923 are:

- A safety factor of 2.0 against failure in bending is specified. The safety factor is greater than the 1.5 value specified by the ASTM standard to account for the inherent variability in mechanical properties of FRP.
- Fifteen percent of the pole height is specified as the maximum deflection limit for tested poles. This limit has been established for consistency with the deflection limit specified in the proposed *Supports Specifications*.

2.10.5 Durability Requirements

Because ultraviolet (UV) rays and heat from solar radiation degrade the natural molecular structure of FRP, and industrial pollutants and salt-spray can accelerate degradation, the proposed *Supports Specifications* provides requirements for weather protection for FRP members. Suitable protection against UV rays can be achieved with the use of surface veils, urethane coatings, and UV stabilizers (inhibitor). Protection provided by these methods can be evaluated by using the ASTM G53 test method.

2.10.6 New Section

At this time, the new section in the proposed *Supports Specifications* covers only FRP material; however, it should be expanded in the future to include new composites and practical applications for support structures.

2.11 DEFLECTION LIMITATIONS

The deflection limits that are set by the proposed *Supports Specifications* should provide an aesthetically pleasing structure under dead load conditions and an adequate structural stiffness that will result in acceptable serviceability performance under applied loads to ensure public confidence.

Research has addressed cantilevered structures and overhead monotube span-type structures. The following documents were reviewed:

- Kaczinski et al., "Fatigue-Resistant Design of Cantilevered Signal, Sign, and Light Supports,"; *NCHRP Report 412*, 1998 (*28*).
- McDonald et al., "Wind Load Effects on Signs, Luminaires, and Traffic Signals Structures," Texas Department of Transportation, 1995 (*83*).
- Lundgren, H.R., "Evaluation of Monotube Sign Support Structure," Report No. FHWA-AZ89-829, Arizona Department of Transportation, 1989 (*84*).
- Ehsani et al., "Static and Dynamic Behavior of Monotube Span-Type Sign Structures," Report No. FHWA/AZ-84/194-I, Arizona Department of Transportation, 1984 (*85*).
- Martin et al., "Field Testing of Monotube Sign Support Structures," Report No. FHWA/AZ-86/237, Arizona Department of Transportation, 1985 (*86*).
- AASHTO *LRFD Bridge Design Specifications,* First Edition, 1994 (*7*).

2.11.1 Dead Load Deflection for Cantilevered Support Structures

The only deflection limitation provided by the current *Supports Specifications* for cantilevered supports is a limit on the dead load (group I) deflection at the top of the vertical support. There is no limit on the deflection of the mast arm. The deflection limitations provided in the specifications are mainly for aesthetic reasons. The current *Supports Specifications* states that deflection resulting from group II (DL + wind) or group III (DL + ice + 1/2 wind) load combination is generally not critical, provided the structure satisfies the allowable stress requirements for the given material.

The current *Supports Specifications* provides two separate criteria for controlling dead load deflections. It differentiates between deflections due to dead load moments and those due to dead load transverse loads. For the dead load moment load

conditions, the angular deflection of the centerline at the top of the pole in relation to the centerline at its base is limited to 0.35 in. per 12 in., which is equivalent to a maximum angular rotation of 1:40 ft. For transverse load applications, the limit for the horizontal linear displacement at the top of the pole in relation to a tangent to the centerline of the structure's base is 2.5 percent of the structure height.

No references were found pertaining to dead load deflections for cantilever support structures. A more common industry standard value for the horizontal linear displacement under dead load is 1.5 percent of the structure height. The deflection limit of 2.5 percent of the structure height is excessive for certain materials and structure types. Therefore, the proposed specification adopts a revised deflection limit of 1.5 percent of the structure height and a slope limit of 0.35 in. per 12 in. under dead loads for vertical cantilevered pole structures. A statement is provided in the proposed *Supports Specifications*, however, that allows exceeding the deflection limits if allowed by the owner.

2.11.2 Dead Load Deflection for Overhead Span-Type Monotube Sign Support Structures

The 1985 *Supports Specifications* limits the vertical dead load deflection to the value of $d^2/400$ in feet, where d is the sign depth in feet. The limitation was developed primarily for truss span support structures. In the 1970s and 1980s monotube span support structures were becoming more popular because they were considered aesthetically pleasing and more economical than the truss-type span structures. Applying the deflection limit developed for truss span support structures provided too rigid a limitation on dead load deflection for long span monotube sign support structures. Although designers had difficulty meeting the $d^2/400$ deflection limit for overhead monotube sign supports, the deflection limit had in fact no relation to such structures.

Research, sponsored by the Arizona DOT (*85,86*), determined an appropriate deflection limitation for monotube span support structures. This research included field tests and analytical studies using computer modeling and investigated the static and dynamic behaviors of monotube span-type sign support structures. Based on this research, the 1994 edition of the *Supports Specifications* was revised to limit deflection to the span divided by 150 for dead and ice load applications. This limitation was intended to avoid dynamic responses because of vortex shedding by adding adequate stiffness to the structure. A later study by Lundgren (*84*) indicated that the limitation could be increased to the span divided by 100 because the dead load deflection criteria was not an aesthetic consideration and the structure could be cambered to eliminate the visual sag. However, no additional information has been found to justify changing the deflection limit to a more liberal value.

No other published works were found regarding the deflection of other types of overhead sign support structures, such as trichord and quadrichord trusses. These structures generally have higher stiffness than the monotube type, and the dead load deflection limit of the span divided by 150 could be adopted as a conservative limit for all types of overhead sign support structures.

The dead load plus ice load deflection limit of the span divided by 150 remains unchanged for the proposed *Supports Specifications* and still applies to overhead monotube and truss span-type sign support structures.

2.11.3 Proposed Deflection Criteria

The horizontal deflection limit for vertical supports, such as streetlighting poles, traffic signal structures, and sign structures, shall be limited as follows:

- Under group I load combination (dead load only), deflection at the top of the vertical support shall be limited to 1.5 percent of the structure height.
- Under Group I load combination (dead load only), slope at the top of the vertical support shall be limited to 0.35 inches per 12 inches.

For luminaire support structures under group II load combination (dead load plus wind), deflection shall be limited to 15 percent of the structure height.

The vertical deflection limit for a single-member mast arm for traffic signal and sign structures shall be limited as follows: Under group IV load combination (fatigue load), a deflection limitation of 8 in. for the range of vibration for galloping and truck-induced fatigue loads is provided.

The vertical deflection limit for horizontal supports for overhead bridge-type structures shall be limited as follows: Under dead load plus ice load, deflection shall be limited to span divided by 150.

2.11.4 Raking and Camber

A procedure to calculate the necessary raking for the verticals of cantilever sign structures has been introduced in the commentary of the proposed *Supports Specifications*. The current permanent camber provision that requires providing a camber equal to L/1,000, in addition to dead load camber for horizontal members of overhead sign and traffic signal structures, remains unchanged.

2.11.5 Summary of Proposed Changes

The following changes related to deflection limitations have been made in the proposed specification:

- The proposed *Supports Specifications* has incorporated a reduced deflection limit of 1.5 percent of height under dead load for vertical supports. The limitation on slope remains at 1°40 ft under dead load conditions. These

limiting values are now mandatory rather than optional for structural supports of all materials.
- The maximum deflection of the vertical support is specified at 15 percent of height for luminaire support structures under group II (dead load plus wind) load combination.
- Deflection limitations under dead load plus ice load for monotube and truss span-type support structures remains unchanged at span divided by 150.
- A limitation on the range of vibration for certain fatigue loads is provided for mast arms for sign and traffic signal support structures.

These requirements should provide supports that are aesthetically pleasing and will ensure public confidence by having acceptable serviceability performance under applied loads.

2.12 SECONDARY MOMENTS

Two methods are given in the current *Supports Specifications* to account for the secondary moments resulting from axially applied loads (P-delta moments). One method is approximate and uses a coefficient for amplification, C_A, to account for the P-delta effects. The second method, referred to as the "final deflected position" procedure, is an alternative that requires a detailed second order structural analysis considering the effects resulting from the change in eccentricity of the axial loads because of bending of the member. The second order analysis procedure outlined for the second method is not clearly written and could result in misinterpretation by the design engineer. In this study, both methods for the estimation of secondary moments were evaluated. A numerical study was conducted to check the accuracy of C_A; and a generalized step-by-step procedure is given for performing a second order analysis.

2.12.1 Approximate Method (C_A)

The current *Supports Specifications* states that steel vertical cantilever lighting and traffic signal supports (single members) subject to any combination of bending, axial compression, shear, and torsion shall be proportioned to meet the following combined stress ratio limit:

$$CSR = \frac{f_a}{0.6F_y} + \frac{f_b}{C_A F_b} + \left(\frac{f_v}{F_v}\right)^2 \leq 1.0 \qquad (16)$$

where

$$C_A = 1 - \frac{1}{0.52}\left[\frac{P_T \sqrt[3]{\frac{I_B}{I_T}} + 0.38D_p}{\frac{2.46EI_B}{L^2}}\right] \text{ for } F_a \leq 0.26F_y$$

and

P_T = vertical load at top of the pole,
I_B, I_T = moment of inertia for the cross sections at bottom and top of the pole,
L = height of the pole,
E = modulus of elasticity, and
D_p = weight of the pole.

A similar combined stress equation with C_A is also given for aluminum structures.

C_A applies to the bending stress term in the combined stress ratio of Equation 16. The coefficient estimates the effect of the secondary bending moments caused by an axial load applied at the top of a cantilever support. The method is approximate and simple to use because it involves only a single equation. In the current *Supports Specifications,* C_A is intended for cantilever supports over 50 ft in height, and for other conditions where secondary effects due to lateral deflection with an applied axial load are significant.

C_A was based on research by the USS Corporation (*87*), where a computer program, using a modified stiffness analysis, was developed to calculate the buckling load of a tapered column, supporting the column weight and a top vertical load. Solutions for 149 typical lighting standards were developed and then used to derive the following approximate equation to predict the buckling load for tapered cantilevered poles:

$$P_{cr} = \sqrt[3]{\frac{I_T}{I_B}\left(\frac{\pi^2 EI_B}{4L^2} - 0.38W\right)}$$

where P_{cr} is the critical buckling load at the top of the pole and W is the weight of the pole. By substituting $I_T = I_B$ and $W = 0$, P_{cr} equals $\pi^2 EI/4L^2$, which is the Euler buckling load for the particular case of a prismatic cantilevered pole with an axial load applied at the top.

To develop the approximate equation, the buckling equation for prismatic bars subjected to top load and distributed axial load presented by Timoshenko and Gere (*88*) was modified to fit the results of the 149 exact solutions analyzed by using the computer program. The effect of the column taper on the critical buckling load, as presented by Gere and Carter (*89*), was considered in the development of the equation.

The buckling strength was assumed to be independent of the effect of residual stresses. Consequently, the slenderness ratio was assumed to be within the Euler buckling range. These assumptions imply that the equation for C_A is applicable only to poles with slenderness ratio, KL/r, greater than $\sqrt{2\pi^2 E/F_y}$, which results in an allowable axial compression stress below $0.26F_y$.

An analytical study was performed to evaluate C_A, as given in the current *Supports Specifications,* and to compare it to exact solutions. Exact solutions were computed by using a commercial computer program (STAAD) that is capable of

performing second order analysis. A detailed description and conclusions of the study on C_A are given in Appendix A. As a result of this study, the current C_A is conservative for typical tubular lighting structures exceeding 50 ft. In some cases, overestimation of second order moments could exceed 50 percent by using the current C_A. The study proposed a modified C_A equation:

$$C_A = 1 - \left[\frac{P_T \sqrt[3]{\frac{I_B}{I_T}} + 0.38 D_P}{\frac{2.46 E I_B}{L^2}} \right]$$

The proposed equation provides results that are in closer agreement to those obtained from "exact solutions."

2.12.2 Final Deflected Position Procedure

As an alternative to C_A, a more exact nonlinear analysis for second order effects is permitted by the current *Supports Specifications*. This method requires the use of computer programs to perform the tedious calculations required to iterate the additional bending moments caused by vertical loads in a deflected position. To perform the analysis, all dead loads and wind loads are increased by the safety factor of 1.38 (safety factor for groups II and III load combinations in the current specification). The resulting stresses that include second order effects are divided by the same safety factor and substituted in the combined stress equation for the term, f_b/C_A.

The "final deflected position" procedure has been revised and rewritten for clarity. Because the safety factors for groups II and III load combinations have been revised and modified for the proposed *Supports Specifications*, the nonlinear analysis procedure was also modified to use a load factor of 1.45 rather than the current 1.38.

2.12.3 Summary of the Proposed Changes

The following changes have been introduced in the analysis of second order effects for the proposed *Supports Specifications*:

- The equation to compute C_A in the simplified method has been changed to produce more accurate results.
- The factor of safety has been changed from 1.38 to 1.45 for group II (dead load + wind) and group III (dead load + 1/2 wind + ice) load combinations, for consistency with other parts of the proposed *Supports Specifications*.
- The simplified and the detailed methods have been rewritten and an improved commentary has been added to provide clarity.

2.13 OSCILLATIONS, FATIGUE, AND RESONANCE

The current *Supports Specifications* provides little guidance for design considerations of fatigue and oscillation for the various support configurations. A load calculation due to vortex shedding for circular and multi-sided sections of single pole supports is provided in Section 1.9.6 on fatigue and vibration. This procedure is limited, however, to single pole supports with a top mounted luminaire and cannot be utilized for cantilever sign supports, cantilevered traffic signal supports, span wire supports, or overhead sign supports. The current specification requires that stress calculation for fatigue be determined as specified in the AASHTO *Standard Specifications for Highway Bridges*; however, the specification does not provide corresponding loading criteria for structure types other than top mounted luminaire supports. In this study, a major review of fatigue loads and fatigue design considerations was performed. As a result of this work, a new section on fatigue is provided in the proposed *Supports Specifications*, which requires the designer to investigate the effects of various fatigue loads acting on the support.

2.13.1 Research and Documents Reviewed

The following reports on fatigue of support structures were obtained from various DOTs for review:

- Kaczinski et al., "Fatigue-Resistant Design of Cantilevered Signal, Sign, and Light Supports," *NCHRP Report 412*, 1998 (*28*).
- McDonald et al., "Wind Load Effects on Signs, Luminaires, and Traffic Signals Structures," 1995 (*83*).
- Martin et al., "Field Testing of Monotube Sign Support Structures," Arizona DOT, 1985 (*86*).
- Ehsani et al., "Static and Dynamic Behavior of Monotube Span-Type Sign Structures," Arizona DOT, 1984 (*85*).
- Lundgren et al., "Evaluation of Monotube Sign Support Structure," Arizona DOT, 1989 (*84*).
- South, J.M., "Fatigue Analysis of Overhead Sign and Signal Structures," Illinois DOT, 1994 (*90*).
- Boulos et al., "Load Testing, Finite Element Analysis, and Design of Steel Traffic-Signal Poles," New York DOT, 1993 (*91*).
- Hahin, C., *Fatigue of Large Traffic Signal Structures*, Illinois DOT, 1989 (*92*).

The results of *NCHRP Report 412* (*28*) were studied in detail in this project. The study provided wind-induced fatigue design criteria for cantilevered support structures and proposed modifications for most of Section 1.9.6 on fatigue and vibration in the current *Supports Specifications*. Fatigue load criteria for vortex shedding and galloping because of wind on sign panels, as well as natural wind gusts

and truck-induced wind gusts, were formulated as part of the investigation.

2.13.2 Scope of *NCHRP Report 412*

NCHRP Report 412 focused on cantilevered sign, signal, and luminaire support structures. The project primarily studied steel structures; however, results also apply to aluminum structures. Table 24 summarizes the considerations covered by the project.

Several design examples were worked to compare designs based on the current *Supports Specifications* with the requirements proposed by *NCHRP Report 412*. Design examples included a mast arm, two nontapered streetlighting poles, and a high mast pole. A review of the report, how it would impact the design of support structures, and suggested modifications are provided in Appendix B.

2.13.3 Proposed Revisions

The fatigue and vibration section of the proposed *Supports Specifications* has been updated on the basis of information from *NCHRP Report 412*. The following information has been added:

- List of categories of connections for steel and aluminum. These categories include welded and bolted connections that are typical to support structures.

TABLE 24 Information provided by *NCHRP Report 412*

Applicable Materials	• Steel. • Aluminum.
Applicable Structure Types	• Cantilevered sign structures. • Cantilevered traffic signal structures. • Streetlighting poles. • High mast poles.
Design Loading Cases	• Natural wind gusts. • Truck-induced wind gusts. • Vortex shedding. • Galloping
Design Method	An equivalent static loading has been provided for each fatigue load case. Stresses produced by these loads shall be less than the fatigue limit for a particular detail. The method focuses on fatigue critical locations, such as member-to-member connection, base plate connection, and anchor bolt anchorages.
Connection Categories	Twenty welded and bolted connection types, specific to cantilever support structures and the corresponding fatigue resistance, have been provided. The presentation of this material follows the *AASHTO LRFD Bridge Design Specifications*.
Fatigue Limit	Each connection type has been provided with a corresponding allowable stress. The fatigue strength of the connection is checked by comparing the calculated maximum stress range to the CAFL (constant-amplitude fatigue limit) for the detail.
Anchor Bolts	The fatigue life for AASHTO M314 anchor bolts in tension has been provided. Guidance has been included on installation conditions that may be detrimental to the fatigue strength of anchor bolts, such as level of bolt preload or the level of misalignment in the bolts.
Deflection Limitations	The vertical deflection limit of the horizontal cantilever arm under galloping and truck-induced wind gusts has been proposed based on aesthetic reasons.

- Fatigue stress limits for each connection category.
- A fatigue load case, represented by an equivalent static load to estimate dynamic wind load effects, such as galloping, vortex shedding, natural wind gusts, and truck-induced wind gust. Stresses due to these loads are compared with specified fatigue limits.
- Fatigue life of AASHTO M314 anchor bolts in tension as well as guidance on installation procedures that may be detrimental to the fatigue strength.
- Maximum dynamic deflection range of 8 in. at the free end of the horizontal cantilever support.

Appendix B shows that the fatigue design criteria proposed are too stringent and could result in significant overdesign of support structures. The impact of the new provisions on design and the practicality of the design criteria needs to be further investigated. Because limited experience is available using the fatigue criteria of *NCHRP Report 412*, the proposed specification includes the following:

1. Only critical cantilevered structures are required to meet the proposed fatigue design criteria. These structure types include overhead cantilevered sign structures, overhead cantilevered traffic signal structures, and high-level lighting structures.
2. The specified structure types are required to meet fatigue design category III, which is the category with the lowest importance factors. Fatigue categories I and II result in larger structures that cannot be justified at this time.

2.13.4 Natural Frequency of Tapered Poles

The current *Supports Specifications* provides an approximate formula to compute the fundamental frequency of cantilever poles. The frequency obtained is used to compute the critical wind velocity at which Karman vortices may cause severe vibrations due to shedding of wind around the surface of the pole. The formula presented in the current *Supports Specifications*, however, does not consider the mass located at the top of the pole or the effect of the taper on nonprismatic poles. Hence, the results do not accurately estimate the fundamental frequency of poles and limit the applicability of this formula to simple configurations of prismatic poles with a small mass lumped at the top of the pole.

Therefore, an improved formula to compute the fundamental frequency of cantilever poles is proposed, which considers the mass located at the top of the pole. The results obtained are exact when the pole is prismatic. To extend the applicability of this formula to tapered members, the average moment of inertia is considered instead of using the moment of inertia of the average pole diameter as in the current specification. The average moment of inertia of the member provides better accuracy than the moment of inertia of the average diameter. The current and proposed formulas were evaluated and compared to results obtained from a commercial finite element analysis software for several common pole configurations.

2.14 CONNECTION TECHNIQUES

The current *Supports Specifications* contains limited information on connections and connectors. The information on design of welds and design of bolts has been updated using AISC *Manual of Steel Construction—Allowable Stress Design* (*26*) and the *Aluminum Design Manual* (*9*). Weld requirements have been updated to reference the most recent AWS codes.

The following documents were referenced pertaining to connections:

- *Manual of Steel Construction—Allowable Stress Design,* AISC, 1989 (*26*).
- *Aluminum Design Manual*, The Aluminum Association, 1994 (*9*).
- ANSI/AWS D1.1, *Structural Welding Code—Steel*, 1994 (*93*).
- ANSI/AWS D1.2, *Structural Welding Code—Aluminum*, 1990 (*94*).
- ANSI/NFoPA NDS-1991, *National Design Specifications for Wood Construction—Revised 1991 Edition*, 1993 (*72*).

Information in the proposed *Supports Specifications* pertaining to connections includes:

- Fabrication and allowable stresses of welds for steel, referencing ANSI/AWS D1.1, *Structural Welding Code—Steel*;
- Allowable stresses for steel bolts, referencing *Manual of Steel Construction—Allowable Stress Design*;
- Design of anchor bolts, which is further discussed in Section 2.15 of this report;
- Fabrication of welds for aluminum, referencing ANSI/AWS D1.2, *Structural Welding Code—Aluminum*;
- Allowable stresses of welded members and welds, based on the *Aluminum Design Manual*;
- Allowable stresses for aluminum bolts, referencing *Aluminum Design Manual*;
- Inspection of welds;
- Mechanical connections for wood, referencing ANSI/NFoPA NDS-1991, *National Design Specifications for Wood Construction—Revised 1991 Edition*;
- Procedures for the inspection of welds and quality control checks. These procedures are provided in accordance with the latest AWS requirements but with due consideration to the structural support covered by the proposed *Supports Specifications*;
- Testing requirements for welds; and

- Twenty connection types commonly used for support structures for welded and bolted steel and aluminum materials in conjunction with their fatigue strength. These connection types are provided as part of the fatigue design requirements proposed by *NCHRP Report 412*.

2.15 ANCHORAGE SYSTEMS

Information on anchor bolts contained in the current *Supports Specifications* is based on research studies performed in the late 1960s and late 1970s at the University of Texas at Austin. Little information is provided in the current specification on design of anchor embedments and the effect of edge distance. Information is also lacking on fatigue of anchor bolts in tension. The proposed section on design of anchor bolts addresses allowable tensile and shear stress of bolts. An appendix addresses minimum embedment length of headed cast-in-place anchor bolts, effect of edge distance, and effect of spacing between anchor bolts. Design for fatigue of anchor bolts in tension has been added.

2.15.1 Documents Reviewed

Approximately 60 references pertaining to anchor bolt design have been reviewed. The primary references were:

- ACI 349-90, "Code Requirements for Nuclear Safety Related Concrete Structures," Appendix B, "Steel Embedments," 1990 (*95*).
- AASHTO M 314-90, "Standard Specification for Steel Anchor Bolts," 1990 (*96*).
- ASTM F 1554-94, "Standard Specification for Anchor Bolts, Steel, 36, 55, and 105-ksi Yield Strength," 1995 (*97*).
- *Manual of Steel Construction—Allowable Stress Design,* AISC, 1989 (*26*).
- *Manual of Steel Construction—Load and Resistance Factor Design,* AISC, 1994 (*50*).
- Cook et al., *Design Guide for Steel-to-Concrete Connections*, 1989 (*98*).
- ACI 355.1R-91, "State-of-the-Art Report on Anchorage to Concrete," 1991 (*99*).
- Cannon, R.W., "Straight Talk About Anchorage to Concrete—Part I," 1995 (*100*).
- Jirsa et al., "Strength and Behavior of Bolt Installations Anchored in Concrete Piers," 1984 (*101*).
- Eligehausen et al., "Behavior of Fasteners Loaded in Tension in Cracked Reinforced Concrete," 1995 (*102*).
- Fuchs et al., "Concrete Capacity Design (CCD) Approach for Fastening to Concrete," 1995 (*103*).
- Kaczinski et al., "Fatigue-Resistant Design of Cantilevered Signal, Sign and Light Supports," *NCHRP Report 412*, 1998 (*28*).
- AASHTO *LRFD Bridge Design Specifications*, 1994 (*7*).
- AASHTO *Standard Specifications for Highway Bridges,* 1996 (*51*).
- Lynch, T.J., and Burdette, E.G., "Some Design Considerations for Anchors in Concrete," 1991 (*104*).
- Lee, D.W., and Breen, J.E., "Factors Affecting Anchor Bolt Development," 1966 (*105*).
- Hasselwander et al., "Strength and Behavior of Anchor Bolts Embedded Near Edges of Concrete Piers," 1977 (*106*).

2.15.2 Anchor Bolt Material Specifications

The current specification allows anchoring materials to be anchor bolts and bolts fabricated from reinforcing steel and other threaded parts. The proposed specification includes material information from AASHTO M314 (*96*), as well as several ASTM standards. The AASHTO specification lists three grades of anchor bolts, as shown in Table 25.

2.15.3 Allowable Stresses for Steel Anchor Bolts

The current specification provides an allowable tensile stress of $0.50F_y$ and an allowable shear stress of $0.30F_y$ applied to the tensile stress area. The commentary indicates that these values came from a widely accepted method for determining stresses in bolts, found in many textbooks and ASTM specifications. The use of the tensile stress area was included in the 1970 AISC *Manual of Steel Construction* (*107*) with an allowable tensile stress of $0.60F_y$. In the 1980 AISC *Manual of Steel Construction* (*54*), the equation was modified to reference the nominal area and the ultimate tensile stress of the bolt. The allowable tensile and shear equations of the current specification were compared to those in

TABLE 25 Anchor bolt material specification

Material Specification	Grade	Yield Strength (ksi)	Tensile Strength (ksi)	Size Range (in.)
AASHTO m314	36	36	58 - 80	1/4" - 4"
AASHTO m314	55	55	75 - 95	1/4" - 4"
AASHTO m314	105	105	125 - 150	1/4" - 3"

the current edition of the AISC *Manual of Steel Construction—Allowable Stress Design* (*26*). AISC specifies an allowable tensile stress of $0.33F_u$ and an allowable shear stress of $0.17F_u$ on the nominal area.

Table 26 shows the difference in allowable tensile forces for various bolt sizes and grades between the current and the AISC specifications. The difference is a function of

$$\frac{0.33}{0.50}\frac{F_u}{F_y}\frac{\text{(nominal area)}}{\text{(tensile stress area)}}$$

AISC allows a higher allowable tensile force per bolt. The greatest difference is for grade 36 bolts with small diameters, but the difference diminishes for higher grade bolts with large diameters.

Table 27 shows the difference in allowable shear forces for various bolt sizes and grades between the current and the AISC specifications. The difference is a function of

$$\frac{0.17}{0.30}\frac{F_u}{F_y}\frac{\text{(nominal area)}}{\text{(tensile stress area)}}$$

The difference in shear strength varies, depending on yield stress, ultimate stress, and diameter. The greatest difference is for grade 36 bolts with small diameters, and the greatest decrease is for higher grade bolts with large diameters.

Table 28 presents the allowable tensile stresses as a percentage of the yield stress based on the tensile stress area for the current specification, AISC, and the proposed specification. Percentages for group I load combination and groups II and III load combinations are presented. A similar trend follows for shear stresses with allowable stresses being higher than AISC. A decision was made not to use the AISC allowable stresses and to retain the values given in the current specification for the sake of conservatism. At this time, allowable stresses for anchor bolts remain unchanged under group I load combination. Allowable stresses are reduced by about 5 percent under groups II and III load combinations because the increase in allowable stress for these group loads has changed from 40 to 33 percent.

2.15.4 Use of J-Bolts

Although the use of J-bolts is common for support structures, most research has focused on design of headed cast-in-place anchor bolts. Limited testing has been done by Lee and

TABLE 26 Comparison of allowable tensile strength for AASHTO M314 bolts

Grade	Bolt Diameter (in.)	Current Spec. Allowable Force (k)	AISC (85) Allowable Force (k)	Percent Difference
36 ksi	0.50	2.55	3.76	47%
	0.75	6.02	8.46	40%
	1.00	10.90	15.03	38%
	1.25	17.44	23.49	35%
	1.50	25.29	33.82	34%
	1.75	34.19	46.04	35%
	2.00	44.97	60.13	34%
55 ksi	0.50	3.90	4.86	25%
	0.75	9.20	10.93	19%
	1.00	16.66	19.44	17%
	1.25	26.65	30.37	14%
	1.50	38.64	43.74	13%
	1.75	52.23	59.53	14%
	2.00	68.70	77.75	13%
105 ksi	0.50	7.45	8.10	9%
	0.75	17.56	18.22	4%
	1.00	31.80	32.40	2%
	1.25	50.88	50.62	-1%
	1.50	73.78	72.89	-1%
	1.75	99.72	99.22	-1%
	2.00	131.16	129.59	-1%

TABLE 27 Comparison of allowable shear strength for AASHTO M314 bolts

Grade	Bolt Diameter (in.)	Current Spec. Allowable Force (k)	AISC (85) Allowable Force (k)	Percent Difference
36 ksi	0.50	1.53	1.94	26%
	0.75	3.61	4.36	21%
	1.00	6.54	7.74	18%
	1.25	10.47	12.10	16%
	1.50	15.18	17.42	15%
	1.75	20.51	23.72	16%
	2.00	26.98	30.98	15%
55 ksi	0.50	2.34	2.50	7%
	0.75	5.52	5.63	2%
	1.00	9.99	10.01	0%
	1.25	15.99	15.65	-2%
	1.50	23.19	22.53	-3%
	1.75	31.34	30.67	-2%
	2.00	41.22	40.06	-3%
105 ksi	0.50	4.47	4.17	-7%
	0.75	10.54	9.39	-11%
	1.00	19.08	16.69	-13%
	1.25	30.53	26.08	-15%
	1.50	44.27	37.55	-15%
	1.75	59.83	51.11	-15%
	2.00	78.69	66.76	-15%

Breen (*105*) in which headed anchor bolts were compared to J-bolts. The research indicated that bolts with 90-deg bends did not develop their tensile strength as effectively as headed anchor bolts. Additional research by Jirsa et al. (*101*) compared bolts with a 90-deg hook to headed anchor bolts. The study determined that while yield stresses were developed in J-bolts made of grade 55 ksi material, yield stresses were not developed in grade 105 ksi material, indicating that the use of J-bolts should be limited to lower grade steels. The study showed that J-bolts with 90-deg bends yield in flexure at the bend. As a result, localized crushing of the concrete occurs at the bend and the bend gradually straightens as load or deformation is increased. The pull-out cones of concrete seen in anchorages with headed bolts or bolts with nuts and washers are not developed in hooked bars. The study concluded that an anchorage composed of a bolt with a nut is more effective in developing strength than a J-bolt.

Limitations on the use of hooked anchor bolts are also provided in the AISC *LRFD Manual of Steel Construction* (*50*). The manual states that "(h)ooked anchor rods should be used only for axially loaded columns to locate and prevent the displacement or overturning of columns due to erection loads or accidental collisions during erection. Additionally, high-strength steels are not recommended for use in hooked rods since bending with heat may materially affect their strength." ACI 355.1R-91 (*99*) does not recommend the use of J- or L-bolts because they "(h)ave been known to straighten out in pull-out tests." It also states that "(h)eaded anchors of the same size and length as L- and J-bolts have significantly higher capacities."

Because headed anchor bolts outperform J-bolts of the same size and length, the emphasis for the proposed *Supports Specifications* is placed on design of headed cast-in-place anchor bolts. Research on J-bolts is very limited; whereas, the majority of research on anchor bolts has been performed with headed cast-in-place anchor bolts. Nevertheless, because hooked anchor bolts have been commonly used in support structures applications, the proposed specification allows their use if the grade of steel does not exceed 55 ksi.

2.15.5 Allowable Loads for Embedment of Steel Anchor Bolts

The current specification does not provide for calculation of anchor bolt embedment. An appendix has been added for

TABLE 28 Comparison of allowable tensile stress for AASHTO M314 bolts

		Percentage of F_y on Tensile Stress Area					
		Under Group I Load Combination			Under Group II and III Load Combinations		
Grade	Bolt Diameter (in.)	Current Spec.	AISC (85)	Proposed Spec.	Current Spec.	AISC (85)	Proposed Spec.
36 ksi	0.50	50%	74%	50%	70%	98%	66.5%
	0.75	50%	70%	50%	70%	93%	66.5%
	1.00	50%	69%	50%	70%	92%	66.5%
	1.25	50%	67%	50%	70%	90%	66.5%
	1.50	50%	67%	50%	70%	89%	66.5%
	1.75	50%	67%	50%	70%	90%	66.5%
	2.00	50%	67%	50%	70%	89%	66.5%
55 ksi	0.50	50%	62%	50%	70%	83%	66.5%
	0.75	50%	59%	50%	70%	79%	66.5%
	1.00	50%	58%	50%	70%	78%	66.5%
	1.25	50%	57%	50%	70%	76%	66.5%
	1.50	50%	57%	50%	70%	75%	66.5%
	1.75	50%	57%	50%	70%	76%	66.5%
	2.00	50%	57%	50%	70%	75%	66.5%
105 ksi	0.50	50%	54%	50%	70%	72%	66.5%
	0.75	50%	52%	50%	70%	69%	66.5%
	1.00	50%	51%	50%	70%	68%	66.5%
	1.25	50%	50%	50%	70%	66%	66.5%
	1.50	50%	49%	50%	70%	66%	66.5%
	1.75	50%	50%	50%	70%	66%	66.5%
	2.00	50%	49%	50%	70%	66%	66.5%

design of cast-in-place headed anchor bolts that includes the effect of minimum embedment length, edge distance, and overlapping cone areas. The most commonly referenced document for design of steel embedments is ACI 349-90-Appendix B "Steel Embedments" (*95*). Cook's *Design Guide* (*98*) uses this document as background. Design of cast-in-place headed anchor bolts has been modified to an allowable stress design approach based on these documents and is found in Appendix C of the proposed specification.

The following figures present information on embedment calculations for cast-in-place headed anchor bolts, using the design method presented in the proposed specification. Figure 22 presents the allowable bolt force for various diameters of grade 55 bolts, based on full cone development. Figure 23 presents the minimum embedment depth for various diameters of grade 55 bolts, based on full cone development. Figure 24 presents the effect of edge distance of a 1½ in. diameter, grade 55 bolt on the allowable tensile force. The allowable tensile strength can be limited significantly by small edge distances. The effect of small edge distances varies with bolt grade and bolt diameter. Figure 25 shows the limiting tensile force of a 6-in. edge distance on grade 55 bolts for diameters greater than 1¼ in.

2.15.6 Fatigue of Anchor Bolts

Allowable tensile stresses for the new group IV fatigue load combination for anchor bolts have been added based on *NCHRP Report 412*.

2.15.7 Proposed Revision

A new article on anchor bolts has been included in Article 5.17 in the steel design section. A new Appendix C, "Anchorage of Cast-in-Place Headed Anchor Bolts," has been added to the proposed *Supports Specifications*. This appendix is based on information from ACI 349-90-Appendix B

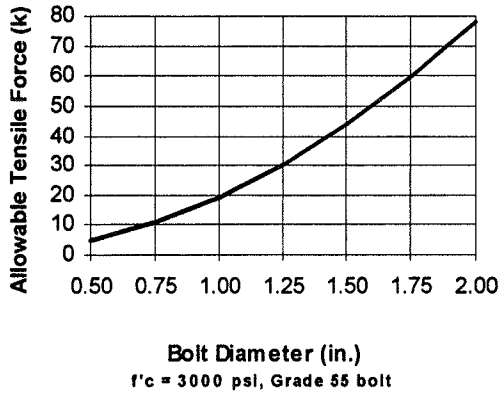

Figure 22. Allowable bolt force based on full cone development

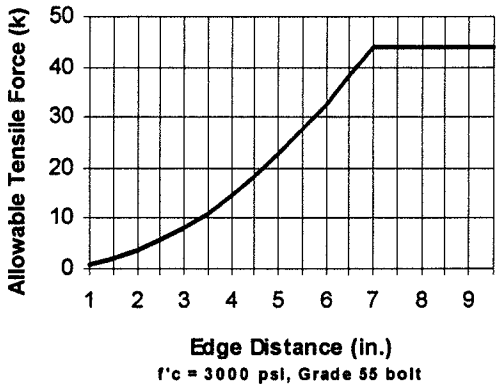

Figure 24. Effect of edge distance on 1½-in. diameter grade 55 bolts.

"Steel Embedments" and Cook's *Design Guide for Steel-to-Concrete Connections.*

Allowable stress equations for anchor bolts remain unchanged with the allowable tensile stress at $0.5F_y$ and the allowable shear stress at $0.3F_y$ based on the tensile stress area. Proposed revisions include:

- Changes in increase in allowable stress under groups II and III load combinations from 40 to 33 percent;
- Specified bolt materials per AASHTO M314 "Standard Specification for Steel Anchor Bolts," that include grades 36-, 55-, and 105-ksi bolts;
- Allowable tensile stress for group IV fatigue load combination, based on *NCHRP Report 412*;
- Minimum embedment length of headed cast-in-place anchor bolts;
- Effect of edge distance on the strength of embedments; and
- Effect of spacing between anchor bolts on the strength of embedments.
- Information on anchor pretensioning, misalignment and bending of anchor bolts, distribution of anchor bolt forces, and use of grout.

2.15.8 Effect of Proposed Revisions

No changes in allowable stress equations have been made for anchor bolts. The change in the increase in allowable stresses for groups II and III load combinations will result in a 5 percent decrease in allowable stresses. The proposed *Supports Specifications* provides a new appendix for detailed information on design of embedment of cast-in-place headed anchor bolts.

2.16 FOUNDATION DESIGN

The foundation design in the current *Supports Specifications* is too general and does not provide adequate information for the design engineer. Although the main foundation types

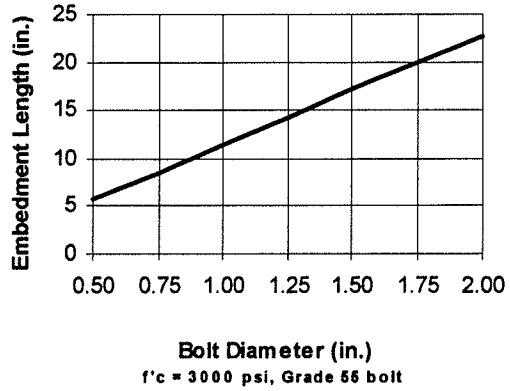

Figure 23. Minimum embedment for grade 55 bolts based on full cone development.

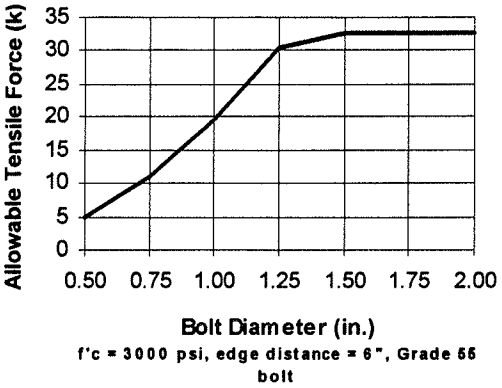

Figure 25. Allowable tensile force with a 6-in. edge distance for grade 55 bolts.

are referenced in the current *Supports Specifications*, guidance is not provided on the design of drilled shafts, spread footings, and piles. A nomograph is provided, however, for determining the embedment depth for small posts. One primary objective in updating the foundation design section was to provide guidance on the design of the main types of foundations used for support structures. Reference was made to AASHTO *Standard Specifications for Highway Bridges* where necessary for brevity and to avoid duplication of material.

2.16.1 Documents Reviewed

The documents that were reviewed included:

- AASHTO *Standard Specifications for Highway Bridges,* 1996 (*51*).
- AASHTO *LRFD Bridge Design Specifications,* 1994 (*7*).
- ACI 318-95 *Building Code Requirements for Structural Concrete* (*69*).
- ACI 336.3R-93, "Design and Construction of Drilled Piers," 1993 (*108*).
- ACI 336.2R-88, "Suggested Analysis and Design Procedure for Combined Footings and Mats," 1991 (*109*).
- Broms, B.B., "Design of Laterally Loaded Piles," 1965 (*110*).
- Broms, B.B., "Lateral Resistance of Piles in Cohesionless Soils," 1964 (*111*).
- Broms, B.B., "Lateral Resistance of Piles in Cohesive Soils," 1964 (*112*).
- *Design and Construction of Deep Foundations*, 1994 (*113*).
- DiGioia et al., "Statistical Analyses of Drilled Shaft and Embedded Pole Models," 1989 (*114*).
- Hansen, J.B., "The Ultimate Resistance of Rigid Piles Against Transversal Forces," 1961 (*115*).
- Ivey, D.L., and Hawkings, L., "Signboard Footings to Resist Wind Loads," 1966 (*116*).
- Poulos, H.G., *Pile Foundation and Design*, 1980 (*117*).
- Reese, L.C., and O'Neill, M.W., "Drilled Shafts: Construction Procedures and Design Methods," Report FHWA-HI-88-042, 1988 (*118*).
- Reese, L.C., *Handbook on Design of Piles and Drilled Shafts Under Lateral Load*, FHWA-IP-84-11, 1984 (*119*).
- Singh et al., "Lateral Load Capacity of Piles in Sand and Normally Consolidated Clay," (*120*).
- Teng, "Tapered Steel Poles Caisson Foundation Design," 1969 (*121*).
- Tomlinson, M.J., *Pile Design and Construction Practice*, 1977 (*122*).

2.16.2 Laterally Loaded Drilled Shafts

The current *Supports Specifications* does not provide adequate information on design of laterally loaded drilled shafts and direct embedded poles. The nomograph provided in the specification is intended for small posts for roadside signs. Attempts to use the nomograph for larger foundations could result in unnecessarily conservative designs. The proposed specification introduces a method for calculating the embedment depth based on work by Broms (*110–112*) on design of laterally loaded drilled shafts and direct embedded poles.

2.16.2.1 Methods Reviewed

The nomograph provided in the current *Supports Specifications* to calculate the embedment length for posts was based on work by Rutledge in 1947 for the Outdoor Advertising Association of America (*123*). This nomograph is limited to an embedment depth of 10 ft and provides excessively conservative results for structures with large bending moments. The soil parameters are not clearly represented in the nomograph. The method is outdated and is not referenced by the major researchers in the field of drilled shaft design.

A literature search showed more recent and detailed methods for embedment length calculations. The objective was to introduce a simplified procedure to be used in the absence of detailed soil information required for the more exact computer methods. The most frequently referenced method for estimating drilled shaft embedment depths due to lateral loads was based on work by Broms (*110–112*).

In 1964, Broms published two papers on the lateral resistance of piles in cohesive and cohesionless soils. He developed semi-empirical equations for the strength of piles in these soils. In 1965, he published another paper on the design of laterally loaded piles, where he recommended under-capacity and safety factors for the lateral resistance of laterally loaded piles. He suggested using an under-capacity factor of 0.7 for soil strength and an overload factor of 2 to 3. His method is still being used because it provides a simplified procedure for embedment depth calculation. The calculations only require knowledge of the angle of internal friction and the unit weight for cohesionless soils and the shear strength for cohesive soils. These parameters can be obtained from a typical geotechnical report or can be estimated from soil property charts.

More detailed methods for calculating strength of laterally loaded piles are based on load deflection curves. Computer programs, such as MFAD, LTBASE, and LPILE, have been developed by GAI Consultants (*124*), Borden and Gabr (*125*), and Reese (*126*), respectively. These programs, however, require the availability of more detailed soil properties. In 1989 DiGioia et al. (*114*) published a statistical study comparing four methods for embedment depth calculations (Broms, Hansen, Reese's LPILE, and GAI's MFAD). DiGioia indicated that GAI's MFAD computer model method had predicted the ultimate moment capacity very

well, on average. However, all methods had a wide variation in predicting results. In cases where detailed calculations are not necessary and in the absence of computer programs, Broms' method should yield acceptable results for estimating the embedment depths for laterally loaded piles.

2.16.2.2 Comparison of Current Method and Broms Method

Comparisons of embedment depths calculated according to the current *Supports Specifications* procedure and Broms' method were made for different types of soils, using safety factors of 2 and 3. The comparisons showed that the embedment depths calculated by using the current *Supports Specifications* approach are highly conservative. The only exception was for small posts embedded in clay soils, where for low working moments, embedment lengths calculated using Broms' method exceeded the current method in the *Supports Specifications*. The comparisons are shown in Figures 26–28. Design assumptions are provided in Table 29.

2.16.2.3 Proposed Revisions for Drilled Shafts

The embedment depth nomograph in the current specification is retained, but limited for use with small posts for roadside signs and lightly loaded poles. Refer to Ivey and Hawkings' paper (*116*) for further explanation on using the embedment depth nomograph. For laterally loaded drilled shafts with heavier loads, Broms' methods are recommended. It is proposed to use Broms' method to calculate the minimum embedment depth of laterally loaded drilled shafts in the absence of more exact methods of analysis that account for detailed soil properties, multiple soil layers, and the pile-soil interaction. The proposed method for embedment depth calculation should result in more economical design for most cases.

2.16.3 Spread Footings

The current *Supports Specifications* provides very limited information on spread footings and does not address the case of eccentrically loaded footings. The footing section in the proposed specification is revised to include more information on the design of spread footings and provide guidance for the case of eccentrically loaded footings. Uplift due to eccentricity of loading is specified to be limited to one corner and not to exceed 25 percent of the total bearing area of the footing. Design of spread footings is to be in accordance with the *Standard Specifications for Highway Bridges.*

2.16.4 Piles

The information on piles provided in the current *Supports Specifications* is very limited. The proposed specification includes a revised section that contains more detailed information on the design and applicability of piles. Piling should be considered on weak soils or when footings cannot be founded on rock, stiff cohesive or granular foundation material. Where potential erosion exists, piles may be used even if soil conditions permit the use of spread footings. Design of piles is specified to be in accordance with *Standard Specifications for Highway Bridges.*

TABLE 29 Soil parameters for bad, average, and good soils

Soil Parameter	Soil Type		
	Bad	Average	Good
Pile Diameter	3 feet	3 feet	3 feet
Clay - Cohesive Strength	325 psf (soft)	750 psf (medium)	1500 psf (stiff)
Sand - Saturated Unit Weight	60 pcf (wet)	65 pcf (wet)	75 pcf (wet)
Sand - Drained Unit Weight	110 pcf (dry)	120 pcf (dry)	125 pcf (dry)
Sand - Internal Angle of Friction	29 degrees (loose)	33 degrees (medium)	38.5 degrees (dense)

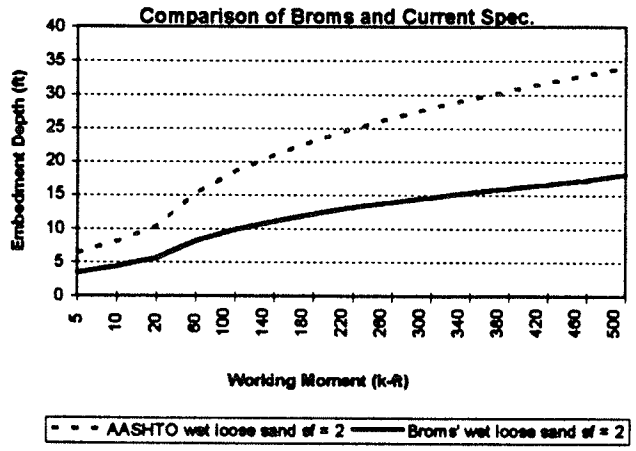

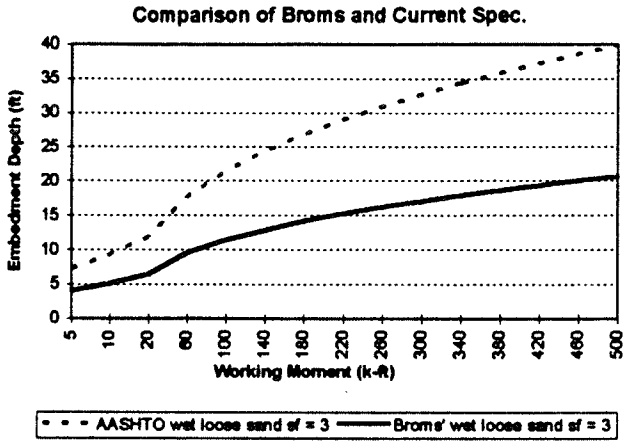

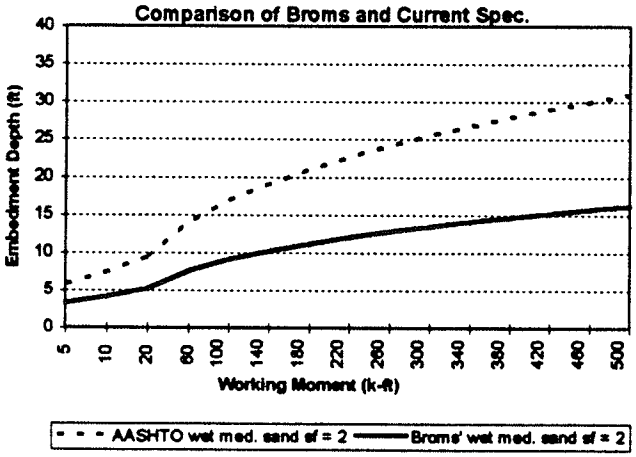

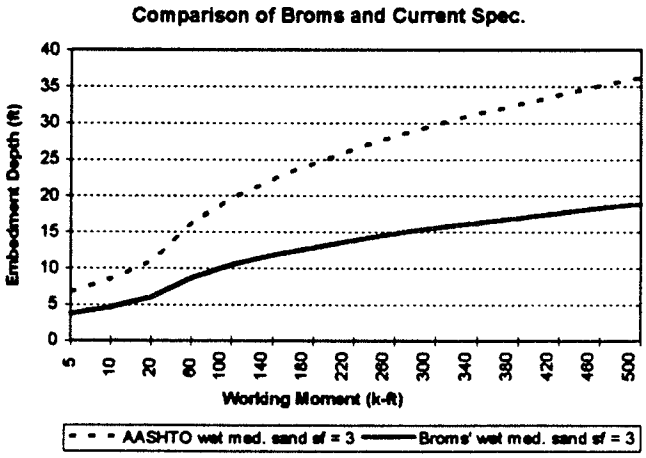

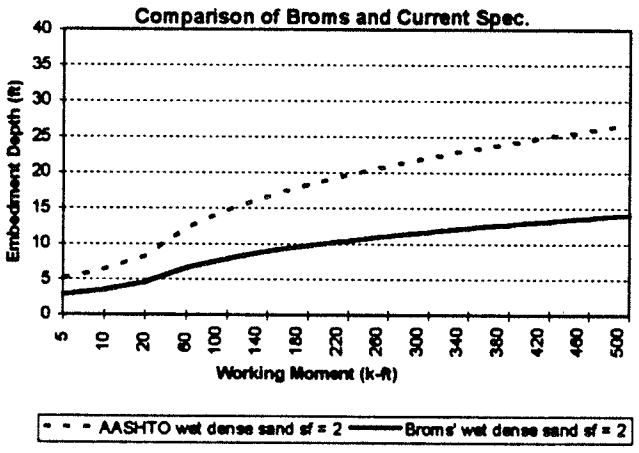

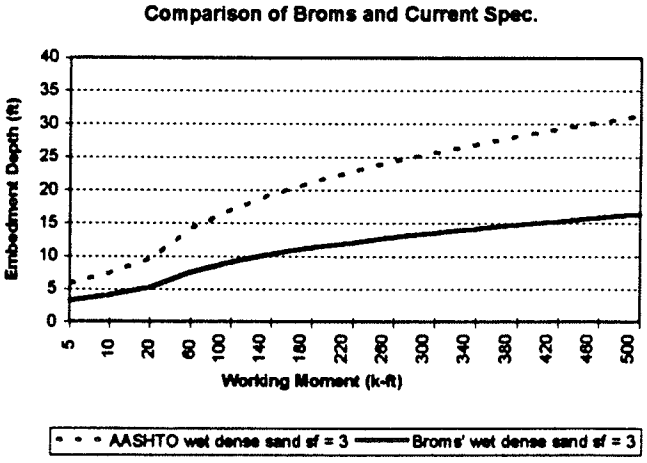

Figure 26. Comparison of methods for saturated sand.

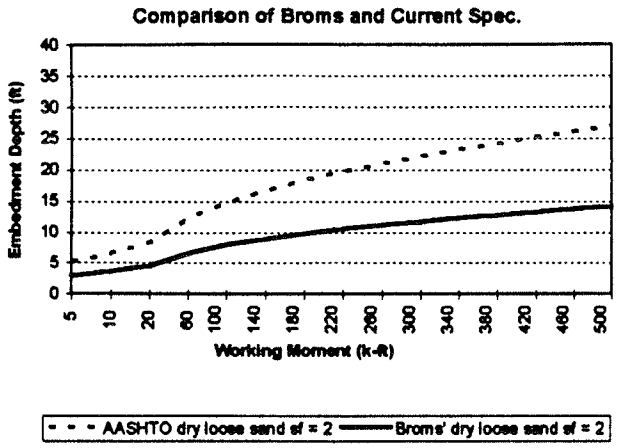

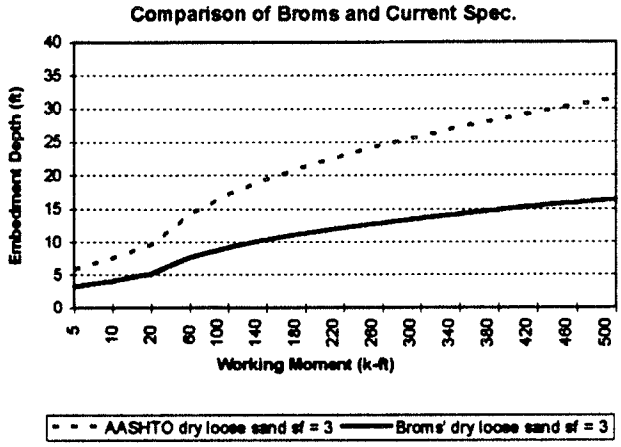

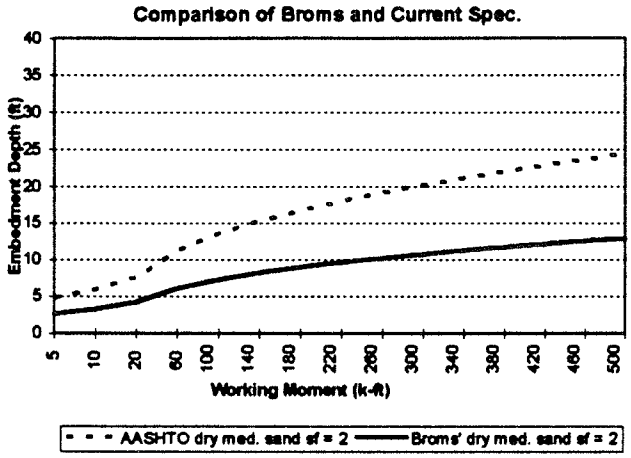

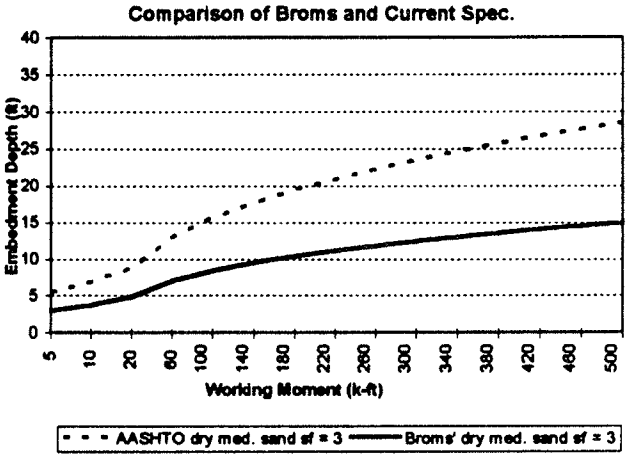

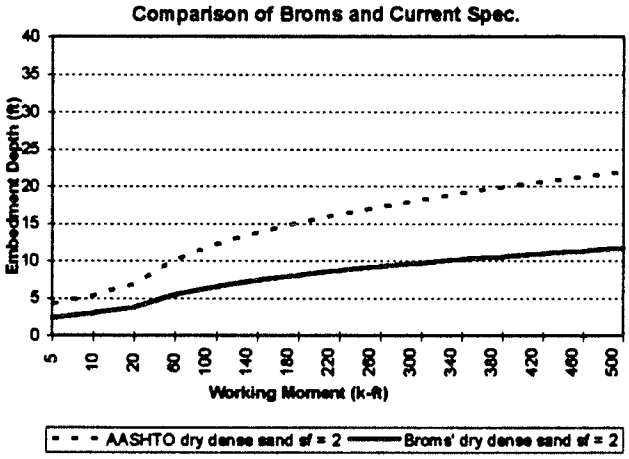

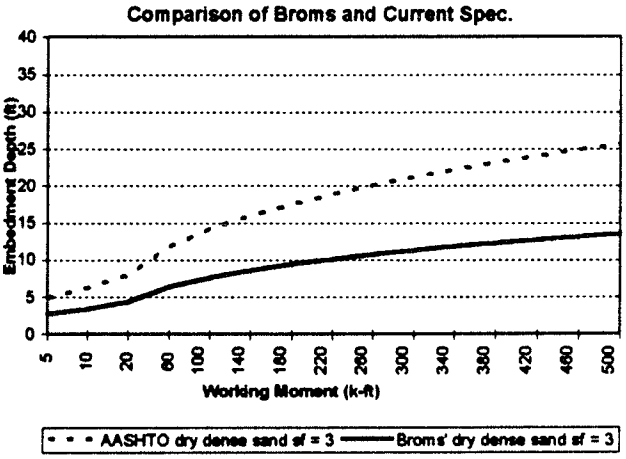

Figure 27. Comparison of methods for drained sand.

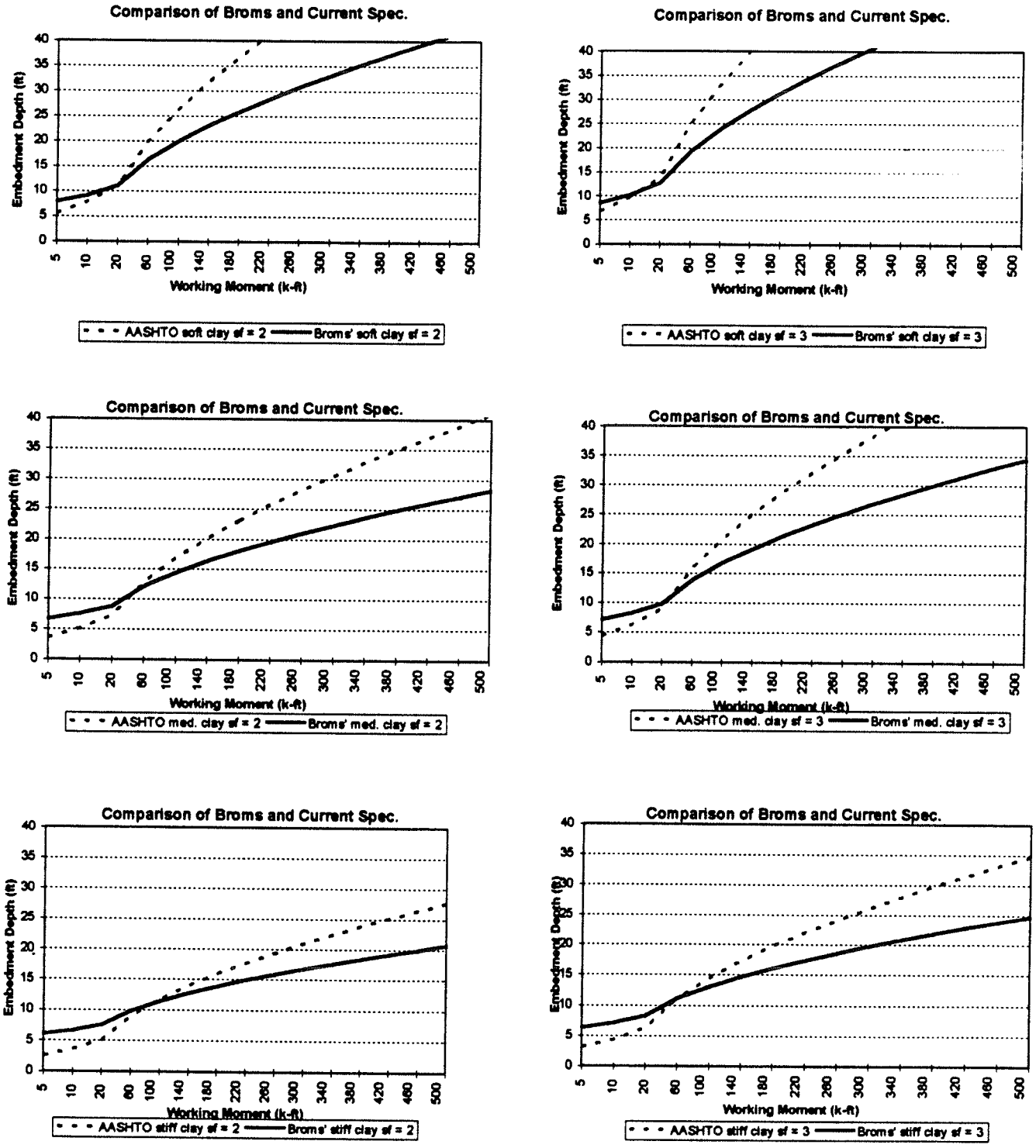

Figure 28. Comparison of methods for clays.

2.16.5 Proposed Changes

Changes to the foundation design section include:

- A detailed procedure for calculating embedment depth of laterally loaded drilled shafts and direct embedded poles,
- New material on eccentrically loaded spread footings, and
- Expanded information on pile foundations.

2.17 BREAKAWAY DEVICES

The breakaway requirements in Section 7 of the current *Supports Specifications* are based on *NCHRP Report 230* (*127*). This section has been updated to current breakaway test requirements, according to *NCHRP Report 350* (*6*). Dynamic testing and criteria for dynamic performance have been presented. Additionally, the test procedure for determining the structural strength of the members under static load has been expanded and clarified.

2.17.1 Documents Reviewed

Requirements for breakaway supports were first introduced in the 1975 edition of the *Supports Specifications* and were based on *NCHRP Report 153* (*128*). The 1985 *Supports Specifications* was updated on the basis of *NCHRP Report 230* (*127*). The most recent report on this topic, *NCHRP Report 350*, was published in 1993, and its procedures were based on research performed between 1981 and 1993.

2.17.2 Breakaway Requirements

Satisfactory dynamic performance is now indicated when the maximum change in velocity for a standard 820 kg (1,800 lb) vehicle, striking a breakaway support at speeds from 35 to 100 kmph (21.7 to 62.1 mph), does not exceed 5 m/s (16.4 fps), with a preferable value of 3 m/s (9.8 fps) (*6*).

2.17.3 Structural Testing Procedure

The breakaway section of the current *Supports Specifications* provides a structural test procedure for environmental loadings. This structural test procedure has been rewritten, clarifying the use of group load combinations and the appropriate safety factors to be used.

2.17.4 General Considerations

Additional information related to breakaway supports, such as stub remains, maximum weight for luminaire structures, electrical considerations, durability, use of torque-controlled bolts, and performance of breakaway roadside signs, has been included in the proposed *Supports Specifications*. No significant design changes are expected with these revisions to the breakaway section of the proposed specification.

2.18 SPAN WIRE DESIGN PHILOSOPHIES

The current *Supports Specifications* provides two methods to analyze span wire structures. The two methods were evaluated to investigate their accuracy and range of applicability and were rewritten for clarity.

2.18.1 Documents Reviewed

Literature on span wire and cable structures was studied. The literature covered classical simplified methods to calculate the tensile forces and reactions of cable structures with different configurations and different loads. Recent research on span wire tension calculations used for traffic signal and sign support structures was reviewed. The main references included:

- Florida Department of Transportation, *Strain Pole Program Version 1.65*, 1992 (*129*).
- McDonald, B., and Peyrot, A., "Sag-Tension Calculations Valid for Any Line Geometry," 1990 (*130*).
- Wang, C.M., "Optimal Shape of Cables," 1984 (*131*).
- Wang, C.M., and Jin, D., "Basic Problems on Optimal Spatial Cable Layout," 1989 (*132*).
- Watson, C.G., *Sags and Tension in Overhead Lines*, 1931 (*133*).
- Tatum et al., "Evaluation of Program to Calculate Traffic Signal Layouts," 1992 (*134*).

2.18.2 Span Wire Design Philosophies

The current *Supports Specifications* provides two methods to compute forces on span wire structures subjected to vertical loads as well as horizontal loads acting perpendicular to the wire. In the first method, referred to as the *simplified* method, the wire tension is obtained by equilibrium forces neglecting the lateral deflection of the vertical support. In the second method, referred to as the *detailed* method, the wire tension is obtained by equilibrium forces considering the lateral deflection of the vertical support due to the applied loads. The advantage of the simplified method lies in the simplicity of the calculations. Although the detailed method is tedious and requires the use of digital computers, it provides more precise and economical solutions.

2.18.3 Comparison of Methods

The two methods were evaluated, and the results were compared to the results obtained by other methods. A

description and recommendations of the study of the span wire procedures are presented in Appendix D. The study concluded the following:

1. The simplified method is significantly more conservative than the detailed method. Span wire forces calculated by both methods showed differences between the two methods that range between 30 and 40 percent for equivalent configurations. These differences can increase or decrease depending on the degree of flexibility of the vertical support. In fact, for ideal rigid supports with no flexibility, the detailed method converges with the simplified method. The opposite is also valid for very flexible supports, or in situations in which the vertical support experiences other excitations that cause it to deflect in the direction of the span. In these situations, the simplified method can provide values of tensions 100 percent greater or more than the detailed method. Based on these considerations, both methods can be used in the proposed specification, depending on the kind of analysis to be performed and subject to the designer's judgment.
2. Considering the results obtained using *COSMOS* software as being "exact," the simplified method is more conservative than *COSMOS* with rigid supports. The amount of error in the estimation of the tensions in the wires ranges from 2 percent for example 1, with a wind speed of 100 mph, to 23 percent for example 3, with a wind speed of 100 mph. Because the analysis with *COSMOS* or similar finite element programs requires specialized software as well as a solid background in nonlinear analysis from the designer, the simplified method offers an appropriate method for analysis of span wire structures when the flexibility of the supports is not included in the analysis.
3. Considering the results obtained using *COSMOS* software as being "exact," the detailed method is more conservative than *COSMOS* with flexible supports. The amount of error in the estimation of the tensions in the wires ranges from 30 percent for example 5, with a wind speed of 80 mph, to 67 percent for example 4, with a wind speed of 100 mph. Special considerations, such as deflection of the vertical supports, must be taken by the designer when using the detailed method. The deflection of the supports affects the magnitude of the induced tension in the wires and, hence, plays an important role in the determination of the member size of the vertical support.
4. For single span configurations, the critical loading condition for computing the wire tension occurs when the wind is acting normal to the wire.
5. Tethered configurations, where the tethered wires are considered as structural elements capable of taking wind loads, result in larger wire forces applied to the vertical support as compared to nontethered span wire configurations.

2.18.4 Other Revisions

For the design of *poles* on a span wire structure, Section 1.2.5(D)(4) of the current *Supports Specifications* requires evaluating the effects of wind from any direction. Accordingly, the current *Supports Specifications* requires that *half* of the total transverse component of the wind load on the exposed horizontal support (the wire) and on the sign panel or traffic signal be appropriately combined with the transverse tension component at the ends of the wire at each vertical support. This requirement is valid only for single span wire structures, and the transverse components of the wind load are equally distributed between the two vertical supports. Distribution of the transverse component of wind loads equally between the two poles is questionable because it implies that the wire is capable of transmitting compressive forces. Therefore, the total transverse component due to wind on the wire and attachments should be fully applied to only one of the vertical supports.

Section 1.2.5(D)(4) of the current *Supports Specifications* also stipulates that a parallel wind direction may be critical when the tension forces from the application of combinations 1 and 2 are small compared to the tension forces occurring from the vertical loads on the span wire. This is a hypothetical situation that can only occur when very heavy attachments with negligible wind exposed area are connected to a span wire that has a negligible wind exposed area. Because this case cannot occur in actual situations, this requirement has been eliminated in the proposed *Supports Specifications*.

2.18.5 Proposed Revisions

Based on the study presented in Appendix D, the following revisions have been made:

- Span wire tension calculations have been provided in a step-by-step format to provide clarity and assist the designers in their calculations (Appendix A, proposed *Support Specifications*).
- The provision that requires the application of *half* the transverse load due to wind on the wire and the attachments to each of the vertical supports has been modified to include the application of the full transverse load, and the sketches depicting the application of the transverse loads have been corrected accordingly.
- A new equation to compute the adjusted length of the wire when using the detailed method has been included (Equation A-6). Although this equation has been implied in the current *Supports Specifications*, it has been explicitly formulated in the proposed specification to provide clarity.
- The requirement to check the wind load applied parallel to the span wire has been eliminated.

2.19 CORROSION PROTECTION SYSTEMS

Corrosion protection against aggressive environments needs to be considered for all materials covered by the specification. Tubular support structures are particularly sensitive to corrosion in locations susceptible to moisture accumulation. The proposed *Supports Specifications* updates the sections on corrosion protection of steel and aluminum. These sections are based on the most recent specifications published by AASHTO and the Aluminum Association. Provisions for the durability of reinforced concrete structural supports have been added. A new section has been added on the preservative treatments for wood structures, based on the *Book of Standards* (*75*). Qualitative suggestions are made to delay and/or prevent the degradation of fiber-reinforced plastic composites.

2.19.1 Steel

Two codes and several technical references were reviewed to update the "Minimum Protection for Structural Steel" section of the *Supports Specifications*. The focus was primarily on galvanized and painted structures. The documents reviewed included:

- *Standard Specifications for Highway Bridges*, AASHTO, 1996 (*51*).
- AASHTO *LRFD Bridge Design Specifications,* 1994 (*7*).
- AASHTO M111-91 (ASTM A123-89a), "Standard Specification for Zinc (Hot-Dip Galvanized) Coatings on Iron and Steel Products" (*135*).
- AASHTO M111-87 (ASTM A123-84), "Standard Specification for Zinc (Hot-Dip Galvanized) Coatings on Iron and Steel Products" (*136*).
- AASHTO M232-84 (1993) (ASTM A153-82), "Zinc Coating (Hot-Dip) on Iron and Steel Hardware" (*137*).

For painted structures, the current *Supports Specifications* refers to the 1992 AASHTO *Standard Specifications for Highway Bridges* (*138*). In the proposed specification, the chapter on painting of the 1996 AASHTO *Standard Specifications for Highway Bridges* is referenced.

For structures galvanized after fabrication, the current *Supports Specifications* refers to AASHTO's "Standard Specification for Zinc (Hot-Dip Galvanized) Coatings on Iron and Steel Products" (*136*), which was updated to AASHTO M111-91 (ASTM A123-89a) (*135*). Bolts and similar threaded fasteners, castings, and rolled, pressed and forged items that are to be centrifuged, or otherwise handled to remove excess zinc, are to be galvanized in accordance with AASHTO's "Zinc Coating (Hot-Dip) on Iron and Steel Hardware" (*137*).

The proposed *Supports Specifications* refers to AASHTO M111-91 (ASTM A123-89a) (*135*) to address the galvanizing of steel structures and to AASHTO M232-84 (1993) (ASTM A153-82) (*137*) to address galvanizing bolts and other items that require special handling to remove excess zinc.

2.19.2 Aluminum

Several references were reviewed to update the aluminum protection section. The focus was primarily on galvanic corrosion (contact with dissimilar materials), although over-all painting, cleaning, and treatment of metal surfaces were also addressed. The reviewed documents included:

- The Aluminum Association, *Aluminum Design Manual*, 1994 (*9*).
- Davis, J.R., *Aluminum and Aluminum Alloys*, 1993 (*139*).
- Sharp, M.L., *Behavior and Design of Aluminum Structures,* 1993 (*30*).

Section 1.5.4 addressing contact of aluminum with dissimilar materials in the current *Supports Specifications* is based on *Specifications for Aluminum Structures* (*62*). This section has been updated and information has been added on overall painting, cleaning, and treatment of metal surfaces to complement the aluminum section in the proposed specification. The proposed specification has been updated with information from the 1994 *Aluminum Design Manual* (*9*) from the Aluminum Association.

2.19.3 Wood

The main documents reviewed were the 1996 AWPA *Book of Standards* (*75*) and the 1996 AASHTO *Standard Specifications for Highway Bridges* (*51*).

The current specification lacks a section on preservative treatments of wood. The new specification references the following AWPA standards:

- C2-90, "Lumber, Timbers, Bridge Ties and Mine Ties-Preservative Treatment by Pressure Process," to address the preservation treatment process of four sides sawn lumber;
- C4-90, "Poles-Preservative Treatment by Pressure Process," to address the preservation treatment process of poles; and
- C14-90, "Wood for Highway Construction-Preservative Treatment by Pressure Process," to address the preservation treatment process of poles and posts.

The proposed changes provide the new specification with a complete set of standards on preservative treatments of poles and posts used as supports for highway signs, luminaires, and traffic signals.

2.19.4 Prestressed Concrete

Concrete provides quality protection to prevent corrosion of reinforcing steel in normal environments. However, reinforced concrete can suffer deterioration in aggressive environments. Reinforcing steel can be attacked by chloride ion intrusion, which can produce rusting and cracking of the concrete. Concrete can be destroyed by alkali-aggregate reactions, chemical attacks, and freeze-thaw action. Material and design considerations can be provided to enhance the resistance of concrete to aggressive environments.

The current *Supports Specifications* provides no information on preventing deterioration of concrete. Specifying a minimum concrete cover is the only information that is related to corrosion protection in the current specification.

A significant amount of research on durability of concrete has become available in the last 20 years. Not all mechanisms of concrete deterioration are understood, but specific concrete quality improvements can be done to prevent or delay deterioration. The following documents on deterioration of concrete were reviewed:

- ACI 222R-89, "Corrosion of Metals in Concrete," 1995 (*140*).
- ACI 201.2R-92, "Guide to Durable Concrete," 1995 (*141*).
- ACI 212.3R-91, "Chemical Admixtures for Concrete," 1995 (*142*).
- ACI 318-95, *Building Code Requirements for Structural Concrete*, 1995 (*69*).
- Corley, W.G., "Designing Corrosion Resistance into Reinforced Concrete," 1995 (*143*).
- Hime, W.G., "The Corrosion of Steel—Random Thoughts and Wishful Thinking," 1993 (*144*).
- Rostam, S., "Service Life Design—The European Approach," 1993 (*145*).
- Campbell, G.M., and Detwiler, R.J., "Development of Mix Design for Strength and Durability of Steam-Cured Concrete," 1993 (*146*).
- Rasheeduzzafar et al., "Reinforcement Corrosion-Resisting Characteristics of Silica Fume Blended-Cement Concrete," 1992 (*147*).
- Yeomans, S.R., "Performance of Black, Galvanized, and Epoxy-Coated Reinforcing Steels in Chloride-Contaminated Concrete," 1994 (*148*).
- AASHTO *LRFD Bridge Design Specifications,* 1994 (*7*).
- AASHTO *Standard Specifications for Highway Bridges*, 1996 (*51*).

Protection of the reinforcing steel in concrete from corrosion can be improved by establishing a minimum concrete cover as well as providing quality concrete. The use of calcium chloride, other salts, or materials releasing chloride ions should be prevented. Considerations for enhancing the quality of the concrete include the use of quality materials, the use of low water-cement ratio, improvement of curing, and the use of mineral admixtures such as silica fume. Additional protection for the steel reinforcement includes the use of epoxy-coated reinforcement and the use of penetrating sealers.

For the proposed specification, minimum concrete cover for centrifugally cast and static cast poles is specified. Aggregates from sources known to have experienced alkali-silica reactions are prohibited. Portland cement with low alkali content, less than 0.6 percent, is required to be specified to ensure long-term durability.

2.19.5 Fiber-Reinforced Composites

Fiber-reinforced plastics provide exceptional corrosion resistance when proper coatings and resin formulations are used. A discussion of degradation due to UV exposure as well as moisture, salt-spray, chemicals, and temperature changes is in the section on fiber-reinforced composites. Measures to prevent degradation including surface veils, addition of UV inhibitors, and use of chemically resistant resins are specified.

2.19.6 Breakaway Supports

The previous edition of the specification did not address durability for breakaway supports. An article has been added specifying that breakaway supports shall meet the durability requirements for the material used.

CHAPTER 3

INTERPRETATION, APPRAISAL, AND APPLICATION

3.1 EVALUATION

The proposed *Supports Specifications* has been updated with the most recent technical information related to design of highway support structures. Technical updates were made to the wind load, steel, aluminum, prestressed concrete, and breakaway sections. Design information on wood and fiber-reinforced composites has been added. An important new section on fatigue design for steel and aluminum structures has also been added. The format includes side-by-side specification and commentary, similar to AASHTO *LRFD Bridge Design Specifications*. These updates provide the designer with a design specification that includes the most common materials used for highway support structures presented in an easy-to-use format. The following sections depict the major changes and updates that are recommended for the proposed *Supports Specifications*.

3.1.1 Alternative Design Procedures

The current *Supports Specifications* adopts an ASD philosophy. Allowable stresses are specified for the materials, and computed service load stresses are required not to exceed the prescribed allowable stresses. The specification covers steel, aluminum, and prestressed concrete materials. In prestressed concrete, ultimate strength requirements must also be satisfied. This design philosophy is continued with the proposed *Supports Specifications*.

The application of the LRFD approach to the support structures cannot be achieved by simply adopting the load and resistance factors implemented in other specifications. Probability-based studies and calibrations with ASD designs are needed to establish the load and resistance factors for a certain reliability index. The current revision of the *Supports Specifications* remains in an ASD format. An LRFD design approach should be considered for future updates of the specification because an updated ASD specification that considers the most recent research is now available.

3.1.2 Load Combinations

The load combinations remained unchanged, and an additional fatigue load combination has been added. The percentage increase in allowable stress has been changed for groups II and III load combinations from 40 to 33 percent. This change will result in a 5 percent reduction in allowable stresses for these load combinations. The fatigue load combination, group IV, has been added to reflect the work of *NCHRP Report 412* (*28*).

3.1.3 Wind Loading Criteria

The wind loading criteria in the current specification is based on procedures that were first advanced in the 1960s and 1970s. Significant changes have been made to the specification, which affect the presentation, terminology, and calculated wind loads. Major changes, primarily due to an updated wind map, include a significant increase in the magnitude of wind speeds in hurricane-prone coastlines and a decrease in inland areas.

Wind load calculations have been revised to be based on a 3-sec gust wind speed, rather than a fastest-mile wind speed. The number of maps, representing 10-, 25-, and 50-year mean recurrence intervals, have been reduced to one 50-year mean recurrence interval map with importance factors used to adjust the intervals. Height factors have also been adjusted for the 3-sec gust wind speed. The coefficient of drag essentially remains unchanged. Significant reduction or increase in calculated wind pressures may occur in wind pressures when updating the proposed *Supports Specifications* because of the result of differences in the current and revised wind speed maps.

When comparing the current with the proposed wind provisions, the changes in wind pressure, either decreasing or increasing, are highly site specific. Table 30 presents a comparison of wind pressures calculated at 30 ft above ground for various sites and mean recurrence intervals. The location marked "common" represents the largest land area for the United States. For the 50-year mean recurrence interval, the majority of the land area that has 70- and 80-mph fastest-mile wind speeds in the current specification will now have a 90-mph, 3-sec gust wind speed, with an importance factor of 1.0 in the proposed specification, which will result in changes in wind pressure varying from a 0 to 24 percent decrease. For the 25-year mean recurrence interval, the majority of the land area that has 70- and 80- mph fastest-mile wind speeds in the current specification will now have a 90-mph, 3-sec gust

TABLE 30 Comparison of wind pressures

Location	AASHTO 1994 Wind Speed	Proposed 3-Second Gust Wind Speed	Life / Importance Factor	AASHTO (1994) Pressure	AASHTO (Proposed) Pressure	Ratio Proposed to 1994
Common	70	90	50-years/1.0	23.3	23.22	1.00
Common	80	90	50-years/ 1.0	30.5	23.22	0.76
Common	70	90	25 years/0.87	23.3	20.2	0.87
Common	80	90	25 years/0.87	30.5	20.2	0.66
Common	60	90	10 years/0.71	17.1	16.5	0.96
Common	70	90	10 years/0.71	23.3	16.5	0.71
Lander, WY	90	90	50-years/1.0	38.5	23.2	0.60
	80	90	25 years/0.87	30.5	20.2	0.66
	70	90	10 years/0.71	23.3	16.5	0.71
Miami, FL	110	150	50-years/1.0	57.6	64.5	1.12
	100	150	25 years/0.87	47.6	56.1	1.18
	80	150	10 years/0.71	30.5	45.8	1.50
Fresno, CA	60	85	50-years/1.0	17.1	20.7	1.21
	50	85	25 years/0.87	11.9	18.0	1.51
	50	85	10 years/0.71	11.9	14.7	1.24
Assumptions: height at 30 feet above ground line; C_d = 1.0						

wind speed with an importance factor of 0.87 in the proposed specification, which will result in changes in wind pressure varying from 13 to 34 percent decrease. For the 10-year mean recurrence interval, the majority of the land area that has 60- and 70-mph fastest-mile wind speeds in the current specification will now have a 90-mph, 3-sec gust wind speed with an importance factor of 0.71 in the proposed specification, which will result in changes in wind pressure varying from 4 to 29 percent decrease.

Other locations that are site-specific depend mainly on changes between the wind maps of the current and proposed specifications. Some specific locations in the interior United States may have decreases in wind pressures of 40 percent or more, specifically locations that are 90-mph fastest-mile wind speed on the current map and 90-mph, 3-sec gust wind speed on the proposed map. Some coastal areas may experience increases in wind pressures of 50 percent or more. Despite these significant changes in wind speeds, it is essential that the specification be revised to reflect current wind speed maps and methodology, regardless of the effect on design wind pressures. These changes, representing over 20 years of changes in the wind technology, update the *Supports Specifications* to the most current wind methodology.

3.1.4 Allowable Stresses for Steel

The allowable stresses for steel in bending, axial tension, axial compression, shear, and torsion were reviewed for the latest updates in codes and research. The study focused on sections typically used in support structures, such as round tubular shapes, multi-sided tubular shapes, I-shapes, and channels. For other structural shapes, minor changes were made based on the recent AISC or AASHTO standards.

For round tubular sections in bending, the current allowable stress equations remain unchanged for compact and non-compact sections and a maximum limit of $D/t \leq 13{,}000/F_y$ has been specified. The proposed *Supports Specifications* provides the following equations for round tubular steel sections:

$F_b = 0.66F_y$ for $\frac{D}{t} \le \frac{3{,}650}{F_y}$, where F_y is in units of ksi,

$$F_b = \left[0.39F_y + \frac{986}{\frac{D}{t}}\right] \text{ for } \frac{3{,}650}{F_y} \le \frac{D}{t} \le \frac{13{,}000}{F_y},$$

and $\frac{D}{t}$ shall not exceed $\frac{13{,}000}{F_y}$

For multi-sided tubular steel sections in bending, a new set of allowable stress equations is proposed to replace the current equations. The proposed equations are as follows:

Hexdecagonal tube:

For $\frac{b}{t} \le \frac{190}{\sqrt{F_y}}$, $F_b = 0.66F_y$

For $\frac{190}{\sqrt{F_y}} \le \frac{b}{t} \le \frac{215}{\sqrt{F_y}}$, $F_b = 1.709F_y\left(1 - 0.00323\frac{b}{t}\sqrt{F_y}\right)$

For $\frac{215}{\sqrt{F_y}} \le \frac{b}{t} \le \frac{365}{\sqrt{F_y}}$, $F_b = 0.74F_y\left(1 - 0.00137\frac{b}{t}\sqrt{F_y}\right)$

Dodecagonal tube:

For $\frac{b}{t} \le \frac{190}{\sqrt{F_y}}$, $F_b = 0.65F_y$

For $\frac{190}{\sqrt{F_y}} \le \frac{b}{t} \le \frac{240}{\sqrt{F_y}}$, $F_b = 1.152F_y\left(1 - 0.00229\frac{b}{t}\sqrt{F_y}\right)$

For $\frac{240}{\sqrt{F_y}} \le \frac{b}{t} \le \frac{365}{\sqrt{F_y}}$, $F_b = 0.75F_y\left(1 - 0.00129\frac{b}{t}\sqrt{F_y}\right)$

Octagonal tube:

For $\frac{b}{t} \le \frac{190}{\sqrt{F_y}}$, $F_b = 0.64F_y$

For $\frac{190}{\sqrt{F_y}} \le \frac{b}{t} \le \frac{260}{\sqrt{F_y}}$, $F_b = 0.964F_y\left(1 - 0.00177\frac{b}{t}\sqrt{F_y}\right)$

For $\frac{260}{\sqrt{F_y}} \le \frac{b}{t} \le \frac{365}{\sqrt{F_y}}$, $F_b = 0.74F_y\left(1 - 0.00114\frac{b}{t}\sqrt{F_y}\right)$

Square or rectangular tube:

For $\frac{b}{t} \le \frac{190}{\sqrt{F_y}}$, $F_b = 0.60F_y$

For $\frac{190}{\sqrt{F_y}} \le \frac{b}{t} \le \frac{260}{\sqrt{F_y}}$, $F_b = 0.815F_y\left(1 - 0.001394\frac{b}{t}\sqrt{F_y}\right)$

For $\frac{260}{\sqrt{F_y}} \le \frac{b}{t} \le \frac{365}{\sqrt{F_y}}$, $F_b = 0.74F_y\left(1 - 0.00114\frac{b}{t}\sqrt{F_y}\right)$

An upper limit for the ratio for the width-to-thickness of $b/t = 365/\sqrt{F_y}$ for multi-sided tubular sections is proposed. The requirement that the allowable bending stress for polygonal tubes shall not exceed the allowable stress for round tubes of equivalent radius remains in the specification. In general, the allowable stresses for noncompact and slender multi-sided tubes will change by +/-15 percent, depending on the shape and width-thickness ratio, when comparing the current and proposed specifications. No change in allowable stresses is made for compact sections.

Allowable bending stresses for I-shaped sections with compact flanges bent about the weak axis have increased from 0.6 to $0.75F_y$. Allowable bending stresses for base plates have increased from 0.66 to $0.75F_y$.

The allowable stress equation for axial buckling has been changed so that the safety factor varies from 1.67 at KL/r = 0.0 to 1.92 at $KL/r = \sqrt{2\pi^2E/F_y}$. The resulting equation is:

$$F_a = \frac{\left[1 - \frac{\left(\frac{KL}{r}\right)^2}{2C_c^2}\right]F_y}{\frac{5}{3} + \frac{3\left(\frac{KL}{r}\right)}{8C_c} - \frac{\left(\frac{KL}{r}\right)^3}{8C_c^3}}$$

$$\text{for } C_c = \sqrt{\frac{2\pi^2E}{F_y}} \text{ and } \frac{KL}{r} < C_c$$

The change in allowable axial stress for the proposed equation relative to the current equation ranges from a 15 percent increase for KL/r = 0.0 to 0 percent at $KL/r = \sqrt{2\pi^2E/F_y}$.

The equation for allowable compressive stresses for $KL/r > \sqrt{2\pi^2E/F_y}$ remains unchanged. The equation is:

$$F_a = \frac{12}{23}\frac{\pi^2E}{\left(\frac{KL}{r}\right)^2} \text{ for } \frac{KL}{r} \ge C_c$$

The allowable tensile stress of $0.60F_y$ on the gross area has not changed. However, another criterion has been added that limits the allowable stress to $0.50F_u$ on the effective net cross-sectional area at bolted connection.

The combined stress ratio equations were updated. To account for the combined action of axial compression, bending, shear, and torsion, the current *Supports Specifications* provides the following equation:

$$CSR \le 1.0 \text{ where } CSR = \frac{f_a}{F_a} + \frac{f_b}{\left(1 - \frac{f_a}{F_a}\right)F_b} + \left(\frac{f_v}{F_v}\right)^2$$

The term $1/(1 - f_a/F_a)$ is an amplification factor for bending stress, f_b, introduced in the equation to account for the secondary bending moment. The derivation of the amplifica-

tion factor has been always based on using an elastic Euler load or stress F'_e, rather than the stress F_a, which may be elastic or inelastic depending on the value of KL/r. The use of F_a results in extremely conservative moment magnifications, whereas the use of F'_e results in a better representation of the moment amplification. It is proposed to adopt the term $1/(1 - f_a/F'_e)$ in the *Supports Specifications* in lieu of $1/(1 - f_a/F_a)$. Therefore, the proposed combined stress ratio equation for member stability check is written as follows:

$$\frac{f_a}{F_a} + \frac{f_b}{\left(1 - \frac{f_a}{F'_e}\right)F_b} + \left(\frac{f_v}{F_v}\right)^2 \leq 1.0$$

where

$F'_e = 12\pi^2 E/23(KL/r)^2$ = Euler stress divided by a factor of safety of 23/12;
E = modulus of elasticity;
L = actual unbraced length in plane of bending;
r = corresponding radius of gyration; and
K = effective length factor in the plane of bending.

For cases when the axial compression forces are small ($f_a/F_a \leq 0.15$), the following equation, which ignores the amplification factor $1/(1 - f_a/F'_e)$, may be used:

$$\frac{f_a}{F_t} + \frac{f_b}{F_b} + \left(\frac{f_v}{F_v}\right)^2 \leq 1.0$$

The following combined stress ratio equation for tension members has been added in the proposed specification:

$$\frac{f_a}{F_t} + \frac{f_b}{F_b} + \left(\frac{f_v}{F_v}\right)^2 \leq 1.0$$

The changes in allowable stresses for steel are dependent on cross section. However, for all shapes, the allowable stress increase for groups II and III load combinations has been limited to 33 percent instead of 40 percent, which reduces the permissible increase in allowable stress by about 5 percent. The increase in allowable stress equations for group I load combination remains unchanged.

3.1.5 Allowable Stresses for Aluminum

The aluminum design section in the current *Supports Specifications* lacks adequate information on design related considerations. No change in design philosophy has been made, but new information has been added for design of typical aluminum support structures. Major weaknesses of the current section were unreadable charts and design equations as well as incomplete design information. The section has been revised to provide easily readable charts and design equations. Design information has been included on mechanical properties of welded and nonwelded aluminum alloys, allowable stress equations, formulas for buckling constants, allowable stresses for casting alloys, slenderness limits for truss members, minimum thickness of material, dimensional tolerances, allowable stresses for welds, anodizing, and painting provisions for corrosion prevention.

The new provisions of the sixth edition of the "Specifications for Aluminum Structures—Allowable Stress Design" are incorporated into the *Supports Specifications*. Factors of safety of 1.65 for n_y and 1.95 for n_u, applied to the yield stress and the ultimate strength, respectively, as recommended by the Aluminum Association specifications for building type structures, have been adopted for the proposed *Supports Specifications*.

The allowable stress increase for groups II and III load combinations has been limited to 33 percent instead of 40 percent. The combined stress ratio equations have been revised and updated to be consistent with the *Aluminum Design Manual*. The increase in allowable stress equations for group I load combination remains unchanged; however, increases in allowable stress values for groups II and III load combinations have been reduced by 5 percent due to modifying allowable stress increase from 40 to 33 percent.

3.1.6 Prestressed Concrete Design

For the prestressed concrete design section, information on allowable stresses for concrete and prestressing steel, ultimate moment and torsional capacities, development length, transfer length, prestress losses, manufacturing tolerances, and durability has been added. The designer is required to consider deflections, effects of cracking, and long-term effects. Information on corrosion protection, minimum cover requirements, and inspection has been added. The overload factor for the ultimate strength equation has been modified from 1.25 to 1.3, to provide a safety factor that is more consistent with other materials of the specification as well as consistent with overload factors specified in other specifications.

3.1.7 Wood Design

Section 10 of the current *Supports Specifications* on wood is extremely limited in scope. The only information provided is that permanent wood structures shall not be used without pressure preservative treatment. No information is provided on design of wood structures. Therefore, a completely new section has been prepared for the proposed specification. The main document used in the development of the new section is the 1991 *National Design Specifications for Wood Construction*. The new section addresses allowable stress design values for poles and posts for various wood species. Allowable stresses for flexure, shear, compression, and tension are prescribed. Interaction equations for members subjected to combined bending and axial compression, as well as com-

bined bending and axial tension, are provided. Updated information on timber treatments and protection methods is also provided.

The wood section of the proposed *Supports Specifications* has been added to cover several species and grades of wood and two types of wood structures: *posts and poles*. These two types can be considered the most common applications of wood structural supports for highway signs and luminaires.

3.1.8 Fiber-Reinforced Composites

A new section has been introduced on FRP because of the emerging use of composites as support structures, specifically for streetlighting poles or posts for small signs. The proposed *Supports Specifications* addresses round tubular or polygonal sections, and I- or W-sections. Allowable stress design equations provided are limited to isotropic or nearly isotropic materials.

Because the proposed design equations for FRP members have not been fully calibrated for all the different fiber-resin combinations and manufacturing procedures, the proposed *Supports Specifications* recommends full-scale testing of FRP members. For FRP poles, a full-scale bending test based on the ASTM D4923 procedure is recommended. The following requirements are specified in the test:

- A safety factor of 2.0 against failure in bending is specified to account for the variability in mechanical properties of FRP.
- Fifteen percent of the pole height is specified as the maximum deflection limit for tested poles.

The proposed *Supports Specifications* also provides measures to protect against weathering of FRP members because of UV rays and heat from solar radiation.

3.1.9 Deflection Limitations

The following changes related to deflection limitations and permanent camber have been incorporated in the proposed specification:

- A deflection limit for vertical supports of 1.5 percent of height under dead load replaces the previously suggested limit of 2 percent. The limitation on slope remains at 1.67 deg under dead load conditions. These values are now required limits for all materials in the proposed specification.
- A maximum deflection for luminaire supports is specified at 15 percent of height under group II (dead load plus wind) load combination.
- Deflection limitations under dead load plus ice load for monotube and truss span-type support structures remains unchanged at span divided by 150.
- A limitation on the range of vibration for certain fatigue loads is provided for mast arm for sign and traffic signal support structures.
- The permanent camber of L/1,000 that is provided, in addition to dead load camber for horizontal members of overhead sign and traffic signal structures, remains unchanged.

These limitations provide supports that are aesthetically pleasing under dead load conditions and ensure public confidence by having acceptable serviceability performance under applied loads. These limits are consistent with current industry-accepted values.

3.1.10 Secondary Moments

The two procedures given in the current *Supports Specifications* (referred to as the simplified and detailed procedures) to account for the secondary moments resulting from axially applied loads (P-delta moments) were updated. The changes include:

- The C_A equation (simplified method) has been modified to produce better estimates of secondary moments.
- In the detailed method for calculating secondary moments, the factor of safety (or load multiplier) has been changed from 1.38 to 1.45 for group II (dead load + wind) and group III (dead load + 1/2 wind + ice) load combinations, for consistency with other parts of the proposed *Supports Specifications*.
- The simplified and the detailed methods have been rewritten and an improved commentary has been added to provide clarity and eliminate misinterpretations.

3.1.11 Oscillations, Fatigue, and Resonance

The current *Supports Specifications* provides little guidance on the design for fatigue and vibrations. A new section has been added to address fatigue design of cantilevered steel and aluminum support structures. Slenderness ratio limits have also been introduced to safeguard against excessive vibrations of steel and aluminum truss members.

The fatigue design section in the proposed *Supports Specifications* specifically addresses steel and aluminum cantilevered support structures. Applicable structure types include cantilevered sign structures, cantilevered traffic signal structures, streetlighting poles, and high mast poles. The following information is included:

- List of categories of connections for steel and aluminum. Twenty welded and bolted connection types, specific to cantilever support structures, and their corresponding fatigue resistance are provided. The presentation of this material follows the AASHTO *LRFD Bridge Design Specifications*.

- Fatigue stress limits, specified for each connection category. Each connection type has been provided with a corresponding allowable stress. The fatigue strength of the connection is checked by comparing the calculated maximum stress range to the CAFL (constant-amplitude fatigue limit) for the specific detail.
- Fatigue loads, represented by equivalent static load ranges, are provided to estimate the dynamic wind load effects. Equations for four wind loading phenomena are given: galloping, vortex shedding, natural wind gusts, and truck-induced wind gust. Stresses due to these loads are to be compared to a specified fatigue limit of a particular detail and should not exceed that fatigue limit for proper design. The fatigue design approach focuses on fatigue critical locations, such as member-to-member connection and base plate anchorage.
- A fatigue stress limit for AASHTO M314 anchor bolts in tension. Guidance on installation procedures that may be detrimental to the fatigue strength of anchor bolts, such as level of bolt preload or the level of misalignment in the bolts, are also provided.
- Maximum dynamic deflection limit at the free end of the horizontal cantilever support.

For the proposed specification only critical cantilevered structures are required to meet the proposed fatigue design criteria. These structure types include overhead cantilevered sign structures, overhead cantilevered traffic signal structures, and high-level lighting structures. The specified structure types are specified to meet the requirements of fatigue category III, which is the level with the lowest importance factors. Fatigue categories I and II result in larger structures that cannot be justified at this time.

3.1.12 Connection Techniques

The current *Supports Specifications* contains limited information on connections and connectors. The information on design of welds and bolts has been updated using the AISC *Manual of Steel Construction—Allowable Stress Design* and the *Aluminum Design Manual*. Weld requirements have been updated to reference the most recent AWS codes. A reference is provided for connections of wood members.

3.1.13 Anchorage Systems

No changes in allowable stress have been made for anchor bolts. The use of smooth hooked anchor bolts has been limited to steel grades not exceeding 55 ksi. Allowable tensile stresses for the new Group IV fatigue load combination for anchor bolts have been added based on *NCHRP Report 412* (*28*). The proposed *Supports Specifications* provides a new Appendix C "Anchorage of Cast-in-Place Headed Anchor Bolts" for detailed information on design of embedment of cast-in-place headed anchor bolts. The appendix includes information on minimum embedment length of headed cast-in-place anchor bolts, effect of edge distance, and effect of spacing between anchor bolts.

3.1.14 Foundation Design

Updates to the foundation design section include the following:

- Providing a more rational procedure for calculating embedment depth of laterally loaded drilled shafts and direct embedded poles;
- Adding new material on eccentrically loaded spread footings; and
- Expanding information on pile foundations.

The nomograph for calculating the embedment depth in the current *Supports Specifications* remains, but its use is limited to posts and lightly loaded poles. For laterally loaded drilled shafts with heavier loads, Broms' methods (*110–112*) have been added for the calculation of the minimum embedment depth of laterally loaded drilled shafts in the absence of more exact methods of analysis that account for detailed soil properties, multiple soil layers, and the pile-soil interaction. This method should result in more economical design.

The proposed specification includes more information on the design of spread footings and provides guidance for the case of eccentrically loaded footings. Design of spread footings is to be in accordance with the *Standard Specifications for Highway Bridges*. Uplift due to eccentricity of loading is limited to one corner of the footing and is not to exceed 25 percent of the total bearing area of the footing.

For piles, the proposed specification includes a revised section that contains more information on the design and applicability of piles. Design of piles is specified to be in accordance with AASHTO's *Standard Specifications for Highway Bridges*.

3.1.15 Breakaway Devices

The breakaway requirements in Section 7 of the current *Supports Specifications* are mainly based on *NCHRP Report 230* (*127*). This section has been updated to incorporate current breakaway test requirements in accordance with *NCHRP Report 350* (*6*). Dynamic testing and criteria for dynamic performance have been presented. Additionally, the test procedure for determining the structural strength of the members under static load has been clarified. Additional information related to breakaway supports, such as stub remains, maximum weight for luminaire structures, electrical considerations, durability, use of torque-controlled bolts, and performance of breakaway roadside signs, has been included. No

significant changes are expected with these revisions to the breakaway section of the proposed specification.

3.1.16 Span Wire Design Philosophies

The methods for analyzing span wire structures have been rewritten in a step-by-step format, and enhanced drawings have been included to provide clarity. The provision in Section 1.2.5(D)(4) of the current *Supports Specifications* that describes the application of the transverse load due to wind on the wire and the attachments has been revised. The full wire tension shall be applied to the vertical support instead of half the wire tension. The section that requires the designer to check the wind load applied parallel to the wire has also been eliminated, because the research team determined that this load case should not be critical for span wire structures. Changes related to span wire calculations will result in minimal or no change in design.

3.1.17 Corrosion Protection Systems

Corrosion protection and deterioration prevention updates have been provided for steel, aluminum, prestressed concrete, wood, and fiberglass. These updates include reference to the latest available standards from AASHTO, the Aluminum Association, ASTM, and the American Wood Preservers' Association.

3.1.18 Format of the Proposed Specifications and Commentary

The current AASHTO *Supports Specifications'* format does not conform to the AASHTO *LRFD Bridge Design Specifications*. The two documents are totally different in format as well as presentation of material. The proposed *Supports Specifications* and its commentary adopts a format similar to the AASHTO *LRFD Bridge Design Specifications*. This format provides the engineer with a uniform design methodology and a document that is easier to use.

3.1.19 Design Examples for the Proposed Specifications

Design examples in Appendix D of the proposed *Supports Specifications* cover a variety of structural support types that are commonly used. The examples are not intended to provide a complete design of each structure type; their main objective is to illustrate the use of specific design provisions of the proposed *Supports Specifications*.

3.2 SUMMARY

The proposed *Supports Specifications* has been updated and rewritten for design of highway support structures, implementing an allowable stress design philosophy. The format is presented in a side-by-side specification and commentary.

Technical changes were to made to each section, as necessary. Major changes implemented in the proposed *Supports Specifications* involve the following:

- Changing the basis of wind pressure calculations from fastest-mile wind speed to 3-sec gust, including updating the wind speed map;
- Changing the increase in allowable stress for groups II and III load combinations from 40 to 33 percent;
- Adding a new section on fatigue design criteria for steel and aluminum cantilevered structures;
- Adding a new section on wood design;
- Adding a new section on fiber-reinforced composite design;
- Updating the allowable stress equations for multi-sided tubular steel sections;
- Correcting the combined stress ratio equation for non-pole type members;
- Providing a revised equation for the coefficient for amplification, C_A;
- Adding an appendix on anchorage of cast-in-place headed anchor bolts; and
- Implementing a format that is similar to the AASHTO *LRFD Bridge Design Specifications*, including an SI version of the specification.

CHAPTER 4

SUMMARY, CONCLUSIONS, AND SUGGESTED RESEARCH

4.1 SUMMARY AND CONCLUSIONS

The proposed *Standard Specifications for Structural Supports for Highway Signs, Luminaires, and Traffic Signals* is the result of an extensive research study performed under NCHRP Project 17-10. The main objective was to update the previous edition of the specifications on the basis of state-of-the-art information for the design and use of structural supports. Considerable effort was made to specify the best practice, realizing the characteristics and limitations of each material. From a design safety standpoint, all materials for structural supports were treated on an equitable basis. Although safety, aesthetics, and economy were the three main guidelines in developing the provisions of the specifications, manufacturing practices and experiences were considered.

The document is presented in a specification/commentary side-by-side format. References are updated to provide a resource for the most recent research studies related to the structural behavior and performance of structural supports. The extensive table of contents will allow quick access to various provisions of the specifications.

Section 1, "Introduction," is a new section that will classify the type of structural supports covered by the specifications. Section 2, "General Features of Design," provides general guidelines and references other AASHTO specifications that cover the functional requirements of structural supports.

Section 3, "Loads" is revised in its entirety. A new wind speed map for the contiguous United States and Alaska based on a 3-sec gust is adopted. Only one map is provided as compared to three maps in the earlier editions of the specifications. This simplification is achieved by introducing an importance factor in the wind pressure formula that accounts for various mean recurrence intervals. The new map is based on the most recent wind research and, hence, could be updated as new information develops in the future. Group load combinations were revised to include a fatigue load case, and the increase in allowable stresses for groups II and III load combinations was modified to 33 percent.

Section 4, "Analysis and Design—General Considerations," provides the design basis that is used for all structural supports covered by the specification. Procedures for nonlinear second order analysis are clearly outlined. The approximate procedure to account for second order moments is revised to provide more accurate results that closely conform to exact calculations. A step-by-step procedure for span wire calculations is also outlined to provide a better understanding of the behavior of such structures and to simplify the engineer's calculations.

Section 5, "Steel Design," is revised to include new allowable stress equations for multi-sided tubular sections. Combined stress ratio equations are revised and corrected for various types of structural supports. Safety factors for axially loaded columns are also revised.

Section 6, "Aluminum Design," is updated to the latest edition of the Aluminum Design Manual. The section is presented in a user friendly format and contains considerable information needed for the design of aluminum structures.

Section 7, "Prestressed Concrete Design," is revised to include newly specified allowable stresses. A design philosophy considering both allowable stresses and ultimate strength is clearly presented. Ultimate strength design requirements and corresponding load and capacity reduction factors are specified. New shear and torsion formulations are provided.

Section 8, "Fiber-Reinforced Composites," is a new section that includes analytical procedures that are practical for design while at the same time adaptable to various FRP products. Full-scale testing and performance criteria are specified for evaluating FRP structures in case the analytical procedures have not been adequately verified by the product manufacturer.

Section 9, "Wood Design," is also a new addition to the specifications and provides direct and simplified procedures for wood design.

Section 10, "Serviceability Requirements," specifies requirements that are needed for aesthetics and ensures that the structures would function without excessive vibrations or undue deflections. A procedure for calculating camber and rake is provided in the commentary in an effort to improve field construction practices.

Section 11, "Fatigue," is a new section acknowledging the importance of wind induced vibration on the design of cantilevered support structures. Additional work is needed before its provisions can be applied to all types of cantilevered structures. Considerable effort has been expended to ensure that the fatigue provisions will not result in highly overdesigned structures.

Section 12, "Breakaway Supports," and Section 13, "Foundations," are both revised to include considerable additional information.

Four appendixes are also added to the specification. Appendix A, "Analysis of Span Wire Structures," includes step-by-step procedures for the analysis of span wire structures. Two procedures are outlined: a simplified procedure based on simple statics and a detailed procedure that considers the flexibility of the vertical support in span wire tension calculations. While the simplified procedure provides conservative results, the detailed procedure results in lower wire tensions and consequently more economical designs. Appendix B, "Design Aids," provides "cookbook" type formulas for the analysis and design of structural supports. Deflection equations for tapered hollow and solid members are also provided to assist the engineer in the design calculations. Appendix C, "Anchorage of Cast-In-Place Headed Anchor Bolts," provides detailed procedures for the calculation of embedment lengths of anchor bolts. Although rough estimates of anchor bolt embedment may be used, the detailed procedures are needed for proper design. Finally, Appendix D, "Design Examples," provides a step-by-step analysis and design calculations for various types of support structures. The examples illustrate the use and application of certain provisions of the specifications.

Overall, the proposed *Supports Specifications* represents an improvement over the previous editions and will hopefully assist the engineer by enhancing the design and use of structural supports for highway signs, luminaires, and traffic signals.

4.2 IMPLEMENTATION

The proposed *Supports Specifications* offers new information as well as significant updates in the design of highway signs, luminaires, and traffic signals over previous editions of the specification. The following suggestions are given to encourage and enhance the implementation of the proposed specifications:

1. Perform a study to compare design differences that occur on an overall structure level between the current and proposed specifications. This study would encompass major design evaluations of typical support structures across the country.
2. Develop a design guide that would provide detailed design information and design aids in support of the specification. Worked design examples depicting the use of the design aids would be performed.
3. Conduct a lecture series introducing the proposed *Supports Specifications*. A design handbook and course notes with detailed examples of typical as well as specific designs would be prepared for the workshop.

4.3 ADDITIONAL IMPROVEMENTS

The following list includes suggestions for improvements to the specifications that could be made without expending major research time or funds:

1. Provide an index for the proposed specification. A detailed table of contents has been provided for the proposed specification; however, the addition of an index would aid in searching for certain key words. This option could be implemented relatively easily with the use of a word processing program.
2. Modify the allowable bending stress equations for multi-sided steel tubes so that values produced by these equations will not exceed the allowable stresses for an equivalent round section. The current and proposed specifications have a provision that requires the designer to limit the allowable stresses of multi-sided steel tubes to that of the equivalent round section. Modifying the allowable stress equations to automatically provide the allowable stress in one computation should be a desirable simplification.
3. Review the allowable bending stress equations for round tubular equations. Some available research provides equations where the allowable stress is a function of the square root of the yield stress. Also, more detailed comparisons with ASCE 72 would be performed to ascertain the reasons for the lower allowable stresses specified by ASCE.
4. Provide an updated aluminum alloy materials table based on the 1997 edition of *Aluminum Standards and Data*.
5. Provide additional review of the prestressed concrete section. This review will include updating the shear and torsion equations for prestressed concrete, reflecting the new provisions of ACI 318-95. The review will also provide a detailed step-by-step flexural analysis procedure for round prestressed concrete members.
6. Include design aids for wood poles that specify an allowable top load for the different load combinations and different wood species.
7. Consider modifying the safety factor, used for calculating the second order effects, from 1.45 to 1.3 for consistency with load factors commonly used for second order analysis.
8. Add comments, drawings, and general information concerning variable message signs (VMS).
9. Review the concrete capacity design (CCD) method for calculating anchor bolt embedments and determine if it should replace the currently proposed method. This method has been recently introduced for calculating embedment lengths of anchor bolts and is in the process of being adopted by major codes.

10. Perform detailed design of various types of support structures to refine the fatigue design loads and categories.
11. Review the truck-induced wind gust load in the fatigue load criteria. The truck-induced wind gust should be modified to recognize the vertical separation distance between the sign panel and the top of standard trucks.
12. Review the following topics in the "Loads" section of the specification:
    a) Wind load analysis procedures for wind acting in any direction.
    b) Basic load combinations.
13. Consider modifying or removing the deflection limit for bridge-type truss horizontal supports. The previous values are based on monotube and were applied to trusses.
14. Add more information on cross-sectional properties, such as the following:
    a) Dimension of flat side for multi-sided tubes.
    b) Sectional properties for I-beams and channels.
    c) Deflection and slope calculations for nontapered beams, including cantilevered, simple support, and fixed beams.
    d) Exact equations for section properties of round, square, I-beam, and channel.
    e) Section properties for hexagonal (6-sided) shapes.
15. Work a variety of site specific design examples to compare between the current and proposed specifications with respect to safety and economy.

4.4 TOPICS FOR FUTURE RESEARCH

An objective of this project was to identify areas that need future research beyond what could be accomplished in this project. These topics include

- LRFD method for support structures;
- VMS;
- Behavior and strength of steel tubes;
- Strength and behavior of fiber-reinforced composite support structures;
- Mitigation techniques for vibration and oscillation; and
- Strength and deflection of prestressed concrete poles subjected to combined loadings.

4.4.1 LRFD Method for Support Structures

The current and proposed *Supports Specifications* present an allowable stress design approach. The recent trend for most specifications, including the AASHTO *LRFD Bridge Design Specifications*, AISC *Manual of Steel Construction* and the *Aluminum Design Manual*, is to adopt an LRFD method. This approach would provide a more consistent procedure to strength evaluation and structural safety. An LRFD *Supports Specifications* would also be easier to incorporate future engineering developments and test information because the *Supports Specifications* derives much of its information from national specifications that are based on LRFD. An LRFD approach for the design of structural supports is therefore needed for future versions of the *Supports Specifications.*

Although literature on the LRFD approach is available for different materials, the application of the approach to the support structures cannot be achieved by simply adopting the load and resistance factors implemented in other specifications. Probability-based studies and calibrations with ASD designs are needed to establish the load and resistance factors pertaining to support structures. An analytical research program, using computers, would be required to calibrate overload and resistance factors specific to highway support structures.

The LRFD method assigns different overload factors to loads depending on the type of load and the factored load combination that must be considered. A second factor used is the resistance factor, which accounts for the type of member, material, and limit state considered. The LRFD approach requires a procedure to determine values for the resistance factors and the load factors. For a structural member or element designed according to current specification, it is possible to compute the relative reliability index for many structural designs. The relative reliability of different structural members built from different structural materials can be compared. For a selected value of the reliability index, it is possible to compute the resistance and load factors by using reliability analysis methods.

Load and resistance factor design employs loads or load effects, which are multiplied by load factors and resistance factors in a set of checking equations. The checking equations have the following general form:

$$\phi R_n \geq U$$

where ϕR_n is the required design strength and U is the factored load effect.

The LRFD method is a probability-based design method, involving predicting the probability that loads imposed on a structure or member would cause it to cease its intended function. Load factors would be developed to account for uncertainties in estimating dead and live loads. Resistance factors would be developed to account for uncertainties in material strengths, dimensions, and workmanship. To develop load and resistance factors for support structures, a statistical study would need to be developed to simulate variations in materials and loadings that are unique to support structures. Variations in resistance of typical materials and shapes would need to be studied as well as variations in loadings.

The variations can be simulated using the Monte Carlo method, which generates random numbers to evaluate a function containing several variables expressing the scatter of material properties, physical dimension variations, and extreme loadings. The values are mapped to a resulting frequency distribution that allows for the probability of exceedance to be determined.

The variation in resistance can be determined by using Monte Carlo simulations. Statistics must be generated for limit states for support structures. Limit state describes a circumstance where a structure or one of its components does not perform its intended function in strength or serviceability. Statistical information on variations in material properties and physical dimensions of structural shapes is obtained. Individual variations in material properties and physical dimensions are combined to provide a probable resistance (e.g., bending moment, shear strength, tensile strength, and compressive strength) for a particular structural shape.

The variation in loading can also be determined by using Monte Carlo simulations. Statistical data on loadings will need to be reviewed in the context of support structures, especially statistics on extreme wind load effects on support structures. These extreme wind load effect statistics may be generated using Monte Carlo simulations. In addition, the most significant load ratios for support structures will need to be determined. These load ratios will be much different for support structures than for building or bridge structures.

Reliability is the percentage of times that the strength of a structure will equal or exceed the maximum loading applied during its estimated life. Reliability indices indicating the reliability associated with the *Supports Specifications* will be determined by using the statistical information generated on resistance and loadings. These indices will be determined by using the advanced first-order second-moment method (AFOSM). Then the AFOSM method will be used to determine load and resistance factors for support structures that optimally achieve the reliability overload ratios associated with these structures.

The calibration procedure would involve

- Selecting typical structures,
- Establishing a statistical database for load and resistance parameters,
- Developing load and resistance models,
- Developing a reliability analysis procedure,
- Selecting a target reliability index, and
- Calculating load and resistance factors.

Proper application of the LRFD method, developed with appropriate load and resistance factors specific to support structures, will provide a more consistent approach to strength evaluation and structural safety than any other design approach. The application of the LRFD approach in the *Supports Specifications* will put it in line with other specifications. Engineers would benefit from a unified design approach that is easier to use and more simple in application.

4.4.2 Variable Message Signs

VMS have been introduced in the past few years. Their use has been increasing rapidly, and their design and configuration are constantly changing. These structures have dimensions, configurations, and weights that differ significantly from those of usual signs and, thus, could highly impact the design of the supporting structure. Current VMS sizes have reached 36-ft long by 12-ft high by 4½-ft deep with a weight exceeding 5,000 lb. The current *Supports Specifications* does not address VMS or their supporting structures. With the increasing use of VMS, it is imperative that the *Supports Specifications* include guidance and provisions for the design of VMS supporting structures and their foundations.

Recently two failures of VMS supporting structures have been reported. One case was in Virginia in which the VMS was attached and supported by a cantilever structure. Another case was in California in which a Caltrans standard cantilever sign structure carrying a VMS failed because of unanticipated loadings.

VMS are heavier in weight and much larger in size compared to normal signs. They are attached to the supporting structure in a manner that torsional loads become significant. Because of their size, the effects of the aerodynamic forces are important and must be carefully evaluated. Truck-induced wind gusts and vortex shedding cause vibrations and fatigue. The presence of the torsional loads compounds the vibration and deflections induced by the wind and aerodynamic forces. The connection or method of attaching the VMS to the support structure is also important and must be addressed by the engineer.

Although the current AASHTO *Supports Specifications* does not address VMS or their supporting structures, engineers have erroneously used the current *Supports Specifications* in their design. The VMS was treated as a normal thin and flat sign, which could result in faulty designs. For example, the section on wind loads in the current *Supports Specifications* contains information that was developed mainly for wind pressures acting on thin flat-faced signs and not VMS. The wind pressure, drag coefficients, and uplift forces must be revised to reflect the much larger VMS structures (structures that could have a roof from 4 to 5 ft, and a bottom of 3 to 4 ft).

The engineer needs additional design information to provide safe and economical VMS structures. Both theoretical and field studies are needed to document the behavior of the VMS structures and to develop guidelines for their proper design and construction. Information on the effects of high torsional loads in combination with dead and live loads must be evaluated. Complex aerodynamic forces from wind and moving traffic as a result of the large physical dimensions of the sign warrant careful evaluation. The induced movements and vibrations cause fatigue and could be detrimental to the

sensitive electronic equipment of the VMS. Wind tunnel tests are needed to develop the necessary information on wind pressure and drag coefficients. Ice loads should be investigated, and water ponding on the flat surfaces should also be considered. The method of connecting the VMS to the supporting structure is an important design consideration. The center of gravity of the VMS is usually placed off the centerline of the horizontal support, which can produce significant torsional loads and deflections. The VMS could be integrated in the supporting truss structure to eliminate such torsional loads. Foundation design requirements must also be reviewed because of the larger loads. Finally, to achieve a safe and economical design, a mechanism is needed to provide interaction between the engineer/fabricator of the VMS and the engineer/fabricator of the support structure.

4.4.3 Behavior and Strength of Steel Tubes

Tubular steel members are used extensively in support structures. Allowable stress equations, compact section limits, and slenderness limits provided by the *Supports Specifications* are based on strength formulas and data obtained from experimental research, which was performed on a very limited number of tubular specimens. Some parameters were not adequately addressed. Further investigation is needed on the strength of round and polygonal tubular sections and bending about the diagonal of square and rectangular steel tubes.

4.4.3.1 Strength of Round and Polygonal Tubular Sections

The allowable stress formulas for steel polygonal tubes in the current *Supports Specifications* were based on analytical background and only limited experimental work. The allowable stress equations for bending of round tubular sections were mainly based on early work performed by Plantema (*48*) and Schilling (*49*) that was analytical in nature. Experimental work was very limited and addressed only round tubes with yield points of 36 to 52 ksi. On the other hand, the allowable stresses for polygonal cross sections were derived from testing sections made of higher strength steels (ASTM A572 plate steel material). This research program at the Transmission Line Mechanical Research Center, however, was limited to 16 test specimens. More tests are needed on polygonal tubes to verify the available strength equations. Typically, ASTM A595 coil steel is used for the manufacture of round tubes, and A572 Grade 55 or 65 plate steel is used for round or polygonal shapes. Preliminary test data indicate that the type of steel and fabrication process does have a significant effect on the bending strength of the cross section.

An experimental program is needed to determine the strength, and hence allowable stresses, for sections of different steels and fabrication processes. The experimental work would consider different cross-sectional shapes with the two types of steel commonly used. Updated strength equations (or allowable stress equations) would be derived from this work. Another parameter to consider in this study is the upper limit of D/t. No flexural strength test data is available for D/t greater than $12{,}000/F_y$. Information on the bending strength of tubes with D/t exceeding that limit is needed for the limited cases where such a slenderness may be used.

4.4.3.2 Bending About the Diagonal of Square and Rectangular Steel Tubes

In the design of cantilever support structures for lighting and similar applications, bending about the diagonal of square and rectangular steel tubes invariably controls the design. The reasons are the smaller section modulus and greater wind loads that the pole is subjected to when considering bending about the diagonal. The section modulus about the diagonal is about 30 percent smaller than that about the principal axis; and the calculated wind loading on the pole, according to the current *Supports Specifications*, is greater for wind applied along the diagonal.

Preliminary tests have shown that the strength of the square cross section is greater when bent about the diagonal than what is predicted by current calculations. One reason contributing to higher strengths is the fact that for compact sections the shape factor is higher for tubular sections bent about the diagonal than the shape factor for square sections bent about a principal axis. For noncompact and slender sections, the corner of the cross section provides added stiffness that results in the section resisting higher loads before locally buckling. It is inappropriate to apply allowable stresses for square tubular shapes bent about a principal axis for square tubular shapes bent about the diagonal. Tubular shapes bent about the diagonal would have a linearly varying stress distribution, while tubular shapes bent about a principal axis would have a uniformly compressed flange on one side that would contribute to a lower buckling stress.

Full-scale structural bending tests are needed to evaluate the performance and strength of cantilevered structures with square sections. The experimental program would consider various sizes as well as square sections with sharp and rounded corners. The objective would be to determine the effect of the corner on the strength of the square section when bent about the diagonal. The data would provide information on the usable strength of the section, and hence the allowable stresses that could be permitted when bending about the diagonal occurs. Compact, noncompact, and maximum slenderness width-thickness ratio limits for sections bent about the diagonal would also be determined.

4.4.4 Strength and Behavior of Fiber-Reinforced Composite Support Structures

The use of fiber-reinforced composites, specifically FRP, as support structures is rapidly growing. The FRP products, however, have varying physical properties that are dependent on the materials used and fabrication method. No design specifications or codes are currently available that cover the design requirements for FRP structures.

An experimental program is needed to evaluate the strength properties of various cross-sectional shapes typically used for support structures and to further verify the equations given in the proposed specification. The study would focus on commonly used materials, namely, polyester resin and glass fiber reinforcement. Products from the three major manufacturing methods (e.g., pultrusion, centrifugally casting, and filament winding) should be considered. For each of the manufacturing methods, the testing program would include several parameters such as cross-sectional shape, fiber orientation, glass/resin ratio, wall thickness, taper, etc. The tests would consist of full-scale structural testing, as well as material (coupon) testing, to develop generalized equations for predicting the strength of the cross section in flexure, shear, axial, and torsion applications for the different manufacturing processes. The experimental work will also establish local buckling criteria for the section. Information on the stiffness and deflection of these structures would be evaluated.

4.4.5 Mitigation Techniques for Vibration and Oscillation

The *Supports Specifications* should contain more qualitative information on mitigation and remediation techniques to prevent vibration and oscillation. Although *NCHRP Report 412* provides some information on mitigation techniques, the main focus of the project is on fatigue-resistant design of support structures. A study at Texas Tech suggests some techniques to reduce vibration and oscillation for traffic signal structures, such as removing back plates and installing a large damping plate. However, the study considered only a limited number of structures.

The proposed study should include mitigation techniques for all types of support structures. Topics might include:

- Creating new attachment types that incorporate mitigation techniques into their design without increasing the design load or affecting aesthetics,
- Determining if mesh signs are less susceptible to wind induced vortex shedding and galloping than solid signs,
- Proposing traffic signal and sign arrangements that may have low susceptibility to galloping and vortex shedding,
- Determining the effectiveness of tuned mass dampers on support structures, and
- Providing a synthesis of mitigation techniques from previous research studies that can be incorporated into design. The mitigation techniques would reduce the effects of fatigue as well as vibrations and oscillation.

4.4.6 Strength and Deflection of Prestressed Concrete Poles Subjected to Combined Loadings

Round prestressed concrete poles are commonly used for cantilever support structures. Such poles are typically subjected to a combination of axial force, bending moment, shear, and torsion. Very little information is available on the behavior of the poles under these combined forces. Reliable interaction equations need to be developed for round prestressed concrete poles. The literature information is limited particularly on the shear and torsional behavior of round prestressed concrete poles. An experimental and analytical test program is needed to determine the strength of the poles under combined loading and the interaction equations to aid in the analysis of the poles. The effect of cracking on the deflection behavior and stiffness should also be investigated as part of the study in an effort to develop simplified methods for predicting deflections after the pole cracks. This investigation should provide valuable information necessary for performing a reliable second order analysis for concrete poles.

APPENDIX A
ANALYTICAL STUDY FOR EVALUATION OF THE C_A FACTOR

A.1 INTRODUCTION

A preliminary study indicated that the coefficient for amplification, C_A, which estimates second order effects for cantilever supports, is overly conservative. To evaluate the C_A factor, 241 examples were analyzed by using a computer program developed for that purpose. Structural design parameters, such as the pole length, taper, steel strength, wind velocity, shape, and vertical top load, were varied to provide a whole spectrum of design situations. Based on the analysis of these examples, a modified equation to compute the C_A factor is proposed. The C_A factor, computed with the proposed equation, is found to estimate more closely the "exact" nonlinear moment resulting from second order effects in cantilever poles.

A.2 THEORETICAL BACKGROUND

A.2.1 Use of C_A as an Approximate Method

The current *Supports Specifications* provides C_A in the CSR equation. This coefficient amplifies the bending stresses in the CSR equation as a means to account for the effect of the secondary bending moments caused by an axial load applied to a cantilever support. This method for estimating the second order effects is easily calculated by a single equation. C_A was included in the current *Supports Specifications* for cantilever supports over 50 ft in height and for other conditions where secondary effects due to lateral deflection with an applied axial load were significant. The *Supports Specifications* states that steel vertical cantilever lighting and traffic signal supports (single members) subject to any combination of bending, axial compression, shear, and torsion shall be proportioned to meet the following combined stress ratio limit:

$$CSR = \frac{f_a}{0.6F_y} + \frac{f_b}{C_A F_b} + \left(\frac{f_v}{F_v}\right)^2 \leq 1.0$$

where

$$C_A = 1 - \frac{1}{0.52}\left[\frac{P_T\sqrt[3]{\frac{I_B}{I_T}} + 0.38D_P}{\frac{2.46EI_B}{L^2}}\right] \text{ for } F_a \leq 0.26F_y$$

and

P_T = vertical load at top of the pole,
I_B, I_T = moment of inertia for the cross sections at the bottom (groundline section) and top of the pole,
L = height of the pole,
E = modulus of elasticity, and
D_p = weight of the pole.

C_A was found to be based on previous research work (*87*). In that work, a computer program, using a modified stiffness analysis, was developed to calculate the buckling load of a tapered column, supporting the column weight and a top vertical load. Solutions for 149 typical lighting standards were developed and then used to derive the following approximate equation to predict the buckling load for tapered cantilevered poles:

$$P_{cr} = \sqrt[3]{\frac{I_T}{I_B}}\left(\frac{\pi^2 EI_B}{4L^2} - 0.38W\right)$$

where P_{cr} is the critical buckling load at the top of the pole and W is the weight of the pole. By substituting $I_T = I_B$ and $W = 0$, P_{cr} equals $\pi^2 EI/4L^2$, which is the Euler buckling load for prismatic cantilevered poles.

To develop the approximate equation, the buckling equation for prismatic bars subjected to top load and distributed axial load presented by Timoshenko and Gere (*88*) was modified to fit the results of the 149 exact solutions analyzed with the computer program. The effect of the column taper on the critical buckling load as presented by Gere and Carter (*89*) was considered in the development of the equation.

The buckling strength was assumed to be independent of the effect of residual stresses. Consequently, the slenderness ratio was assumed to be within the Euler buckling range. These assumptions imply that the equation for C_A is applicable only to poles with slenderness ratio, KL/r, greater than $\sqrt{2\pi^2 E/F_y}$, which results in an allowable axial compression stress below $0.26F_y$.

A.2.2 Final Deflected Position Procedure

As an alternative to C_A, a more exact, nonlinear analysis, considering the second order effect, may be performed. This method requires the use of a computer program to account for the additional bending moments caused by vertical loads in a

deflected position. Using this alternative method of design, all dead loads and wind loads are increased by the safety factor of 1.38 (safety factor for group II load combination in the current specification). The resulting stresses that include second order effects are divided by the same safety factor and substituted in the combined stress equation for f_b/C_A.

Because safety factors for groups II and III load combinations have been modified for the proposed *Supports Specifications*, the procedure outlining the more exact, nonlinear analysis specifies a safety factor of 1.45 rather than 1.38 for the proposed specification.

A.3 COMPUTER ANALYSIS OF THE C_A FACTOR

A.3.1 Preprocessor

Because of the large number of examples, a computer program was written to perform the static analysis and build the files required by the STAAD program (*149*) to perform the P-delta analysis. The computer program, CA.FOR, was written and compiled in Fortran 90, using full 32-bit architecture that delivers a performance similar to a workstation in a small PC. The program requires a simple input file in which the following data is required for each example:

- Wind speed (mph);
- Yield strength of steel (ksi);
- Bottom external diameter (in.);
- Top external diameter (in.);
- Thickness (in.);
- Shape code, an integer between 1 and 5 with the following meaning: 1 is a circular section, a 2 is a hexadecagonal section, 3 is a dodecagonal section, 4 is an octagonal section, and 5 is a square section;
- Length (ft);
- Vertical concentrated load at the tip of the pole (lb); and
- Effective projected area at the tip of the pole (psf).

With this data, the program performs the following operations:

- Wind forces computation;
- Self-weight computation;
- Static analysis;
- Axial, bending, and shear stress checking;
- C_A factor computation;
- Combined stress ratio checking;
- Second order moment estimation using the C_A factor; and
- Input data file preparation for second order analysis using STAAD.

A.3.2 STAAD Analysis

To perform the nonlinear analysis of the selected examples, the commercially available computer program STAAD was used. The STAAD analysis provided the final displacements and internal forces of the structure considering second order effects (P-delta analysis).

A.3.3 Postprocessor

Because of the large number of examples, the results provided by STAAD were located in more than 200 different files. To overcome this problem, a Fortran 90 computer program called CAR.FOR was written. CAR.FOR is able to build a single output file with a summary of the results by CA.FOR for the static analysis and STAAD for the P-delta analysis. The output file provided by CAR.FOR is written in fixed format, which converts easily to a spreadsheet format.

A.4 EXAMPLES

The research team analyzed 225 examples by using the C_A method and the exact method described in the current *Supports Specifications*. The parameters considered were grouped into three categories: geometry, material, and load parameters.

The geometry parameters considered were: length of the pole, taper, and shape. Three lengths were studied: 50, 100, and 150 ft, which corresponded to short, intermediate, and long poles, respectively. Two different tapers were studied: 0.06 and 0.15 in/ft. Three shapes were studied: round, hexadecagonal, and dodecagonal.

The material parameters considered were: type of material and strength. One material was studied: steel. Two steel strengths were considered in the study: 50 and 65 ksi.

The load parameters considered were the vertical top load and the wind load. Three vertical top loads were studied: 250, 750, and 1,500 lb, which corresponded to light, intermediate, and heavy axial loads, respectively, for normal applications. These three vertical top loads were associated with luminaire projected areas of 8, 12, and 16 sq ft, respectively, which were used to compute the wind load at the top of the pole for each example. Two wind pressures were considered in the computation of the wind forces: 27.7 and 52.3 psf. These pressures corresponded to wind speeds of 80 and 110 mph, respectively, according to the wind load provisions of the current *Supports Specifications*.

The total number of examples was given by the following formula:

Total No. = lengths × tapers × shapes × strengths × vertical top loads × wind loads

therefore,

Total No. = $3 \times 2 \times 3 \times 2 \times 3 \times 2 = 216$

Each example was analyzed by using the C_A method and the alternative method provided in the current *Supports Specifications*. Nine additional examples were analyzed considering the 1.45 factor of safety given in the proposed

Supports Specifications. Sixteen additional examples were analyzed to evaluate the effect of changing the top axial load over a wide range of values, while the other parameters are kept constant. The final number of examples was 241, which justified the development of the two computer programs described previously.

A.5 RESULTS

The C_A method can be explained by the following equation:

$$M_{NL} = \frac{M_L}{C_A} \tag{A-1}$$

where M_{NL} is the moment including second order effects, M_L is the static moment, and C_A is a coefficient for amplification defined as:

$$C_A = 1 - \alpha \frac{P}{P_e} = 1 - \frac{1}{0.52}\left[\frac{P_T\sqrt[3]{\frac{I_B}{I_T}} + 0.38D_P}{\frac{2.46EI_B}{L^2}}\right] \tag{A-2}$$

where P is the total axial compressive load acting on the member, P_e is the critical buckling load, and α is a factor of safety. In the current *Supports Specifications,* the value of α is 1.92.

In a preliminary study that included 35 examples, the application of the C_A factor resulted in an overestimation of the P-delta effect on high-level lighting poles. In fact, in one example with a very heavy axial load, the moment computed by using the C_A method was 60 percent higher than the actual moment obtained with a P-delta analysis. The ratio of the estimated moment by using the C_A factor to the nonlinear moment obtained with STAAD was 1.6.

From the results of these examples, the ratio of the static moment to the nonlinear moment obtained with STAAD was computed. This parameter was used to determine the specific value of α for each example as follows:

$$\alpha = \frac{1 - \frac{M_L}{M_{NL}}}{\frac{P}{P_e}} \tag{A-3}$$

The average value of α obtained for the first 33 examples was 0.93, and when the same procedure was applied to the 241 examples of the present study, the average value of α was 0.92. In contrast, a value of 1.92 is specified for α in the current *Supports Specifications*. The larger the value of α, the smaller the C_A factor and, hence, the more conservative the estimate of the nonlinear moments.

Cook and Young (*150*) outlined a method for the approximate analysis of beam columns. The method is based on the assumption that the deflection curve of the beam column has the same shape and can be expressed by the same function whether or not the axial force is present. This implies the assumption that the axial force changes only the amplitude of the lateral deflection of the beam column.

For a simply supported beam of length L, the moment equation including axial load may be written as

$$EI\frac{d^2y_{NL}}{dx^2} = M_L - Py_{NL} \tag{A-4}$$

and for $P = 0$, the equation takes the form

$$EI\frac{d^2y_L}{dx^2} = M_L \tag{A-5}$$

where the subscript, L, is the static component of the problem. The deflection curve may be approximated by a half sine wave as follows:

$$y_{NL} = Y_{NL}\sin\left(\frac{\pi x}{L}\right) \text{ and } y_L = Y_L\sin\left(\frac{\pi x}{L}\right) \tag{A-6}$$

where Y_{NL} and Y_L are amplitudes of lateral deflection with and without the presence of the axial force P, respectively.

Substitution of Equation A-6 into Equation A-4 yields

$$\frac{\pi^2 EI}{L^2}Y_{NL} = \frac{\pi^2 EI}{L^2}Y_L + PY_{NL} \tag{A-7}$$

Since $\pi^2EI/L^2 = P_e$, the Euler critical load, the deflection of the beam column may take the form

$$Y_{NL} = \frac{Y_L}{1 - \left(\frac{P}{P_e}\right)} \tag{A-8}$$

Assuming the bending moments are proportional to the deflections, the bending moment of the beam column including second order effects can be expressed as

$$M_{NL} = \frac{M_L}{1 - \left(\frac{P}{P_e}\right)} \tag{A-9}$$

This procedure applied to cantilever supports leads to the same result. Recognizing that $1 - (P/P_e) = C_A$ when $\alpha = 1$, the modified C_A equation would take the following form

$$C_A = 1 - \frac{P}{P_e} = 1 - \left[\frac{P_T\sqrt[3]{\frac{I_B}{I_T}} + 0.38D_P}{\frac{2.46EI_B}{L^2}}\right] \tag{A-10}$$

Comparisons of bending moments have been made for amplification factors with $\alpha = 1.0$ and $\alpha = 1.92$. In this

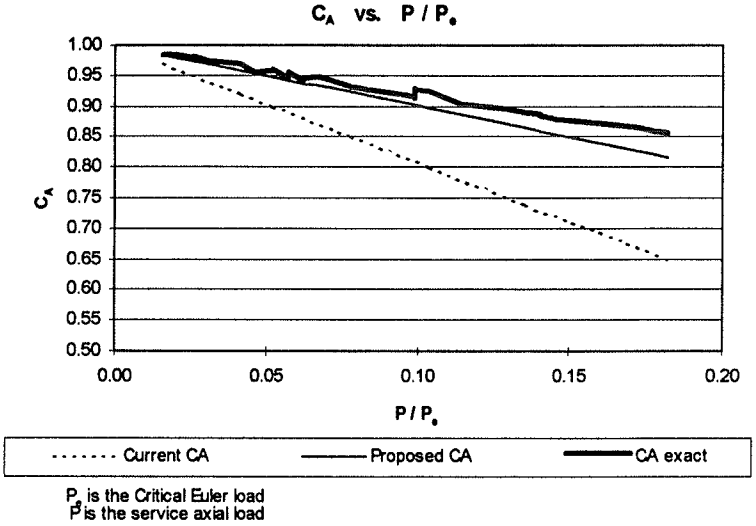

Figure A-1. Comparison of the current C_A, proposed C_A, and C_A exact.

study, C_A computed using Equation A-2 is the current C_A, C_A computed using Equation A-10 is the proposed C_A, and the ratio of linear moment to nonlinear moment is C_A exact. The static linear moment is denoted by M_L, the nonlinear moment computed with the alternative "detailed" method outlined in the current *Supports Specifications* is denoted by M_{NL}, the nonlinear moment computed with the current C_A is denoted by M_{NL}', and the nonlinear moment computed with the proposed C_A is denoted by M_{NL}''.

Figure A-1 provides a comparison of the current C_A, C_A exact, and the proposed C_A. The proposed C_A closely approximates C_A exact, while the current C_A shows significant differences for P/P_e values greater than 0.10. At the higher end of the curve, when P/P_e equals 0.172, C_A exact is 0.85, the proposed C_A is 0.82, and the current C_A is 0.65. There is an error of about 24 percent between the current C_A and C_A exact.

To perform a parametric study, the estimated moments were computed by substituting into Equation A-1 the values of the current and proposed C_A to obtain the M_{NL}' and M_{NL}'' moments, respectively. The nonlinear moment, M_{NL}, was obtained from the analysis performed using STAAD, and the linear moment, M_L, was obtained from the analysis performed with CA.FOR. In Figure A-2, the ratios of M_{NL}, M_{NL}', and M_{NL}'' to the linear moment, M_L, are compared. There is no appreciable difference between the proposed C_A moment

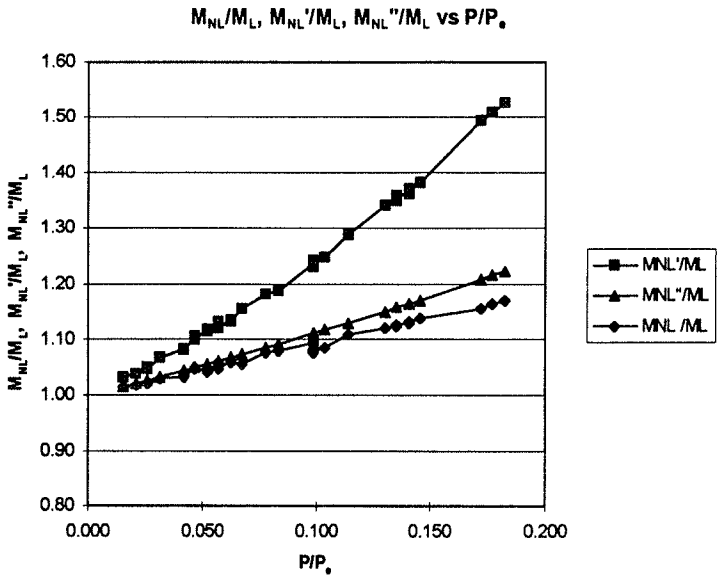

Figure A-2. Ratio of estimated and nonlinear moments to linear moments.

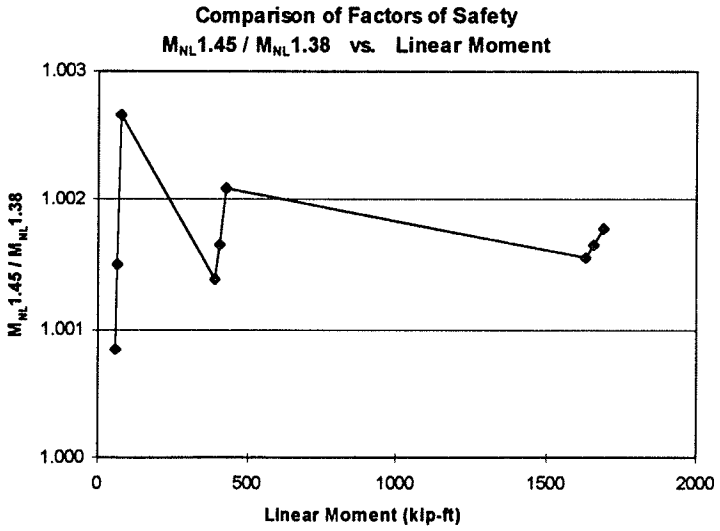

Figure A-3. Change of nonlinear moment with respect to linear moment when the safety factor is increased from 1.38 to 1.45.

curve, M_{NL}'' and the nonlinear moment curve, M_{NL}. On the other hand, the C_A moment curve, M_{NL}', diverges from the nonlinear moment curve, M_{NL}, for values of P/P_e as low as 0.05, reaching its maximum when P/P_e is greater than 0.172, where a difference of about 35 percent occurs between the two moment curves. The difference between the C_A moment curve, M_{NL}', and the nonlinear moment curve, M_{NL}, means that the current C_A coefficient produces a significant overestimation of the nonlinear moment. However, when the proposed C_A coefficient is used, the overestimation of the nonlinear moment is almost negligible.

The alternative method outlined in the current *Supports Specifications* states that the only way to ascertain that an overload factor of 1.38 has been furnished is to make the analysis with all axial loads and wind loads increased by a factor of 1.38 and then divide the resulting stresses by 1.38. However, in the proposed *Supports Specifications,* the factor of safety has changed from 1.38 to 1.45. To evaluate the impact of changing the overall safety factor from 1.38 to 1.45, a comparison of the nonlinear moments obtained by using these two safety factors was performed. As Figure A-3 shows, the maximum difference between the nonlinear moments computed with a safety factor of 1.38 (M_{NL} 1.38) and the nonlinear moments computed with a safety factor of 1.45 (M_{NL} 1.45) is only about 0.3 percent. From these results, the change of safety factor from 1.38 to 1.45 *does not* affect the results of nonlinear moments, when computed according to the alternative method described in the current *Supports Specifications.*

The variation of the current C_A moment, M_{NL}', and the proposed C_A moment, M_{NL}'', with respect to length of the pole was also evaluated. As Figure A-4 shows, the ratio of the

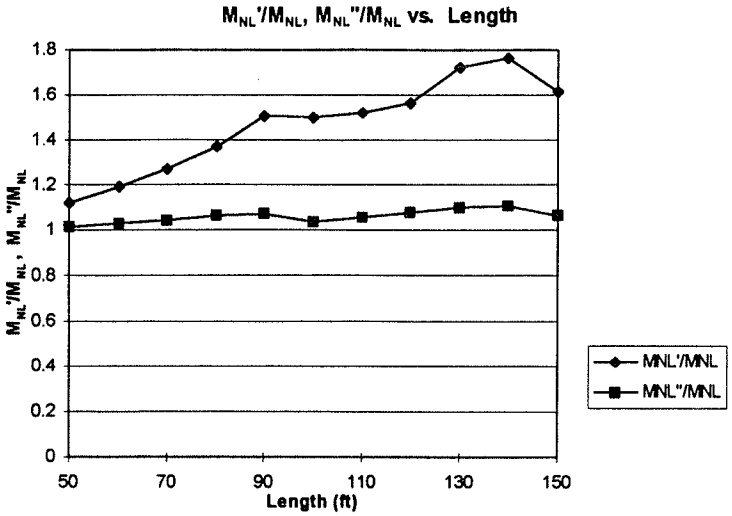

Figure A-4. Influence of the length in the estimation of the nonlinear moment.

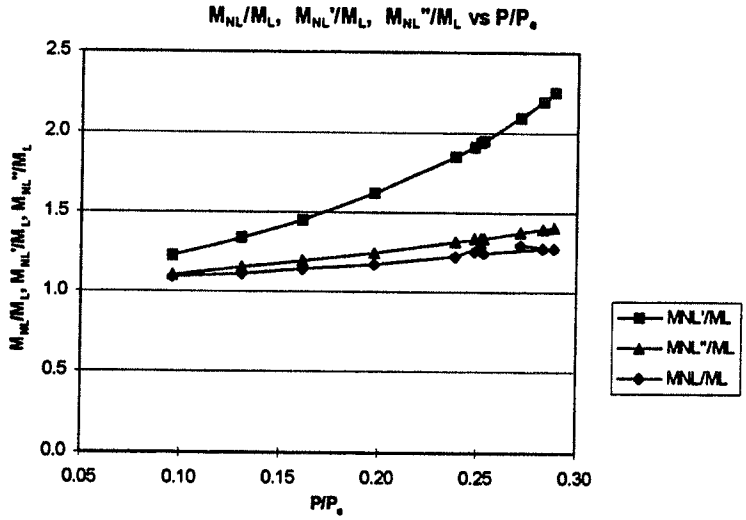

Figure A-5. Influence of the parameter P/P_e in the estimation of the nonlinear moment.

M_{NL}'' moment to the nonlinear moment, M_{NL}, is very close to 1, which means that M_{NL}'' moments, computed with the proposed C_A, provide a good estimate for the nonlinear moments in the length range of 50 to 150 ft. On the other hand, the ratio of the M_{NL}' moment to the nonlinear moment, M_{NL}, is always greater than 1 and, in some cases, can be as high as 1.80, which means that M_{NL}' moments computed with the current C_A clearly overestimate the nonlinear moments in the length range of 50 to 150 ft.

When the length of the pole changes and loads are kept constant, the ratio P/P_e changes because P_e, the critical buckling load, changes with the length. In Figure A-5, the ratios of M_{NL}, M_{NL}', and M_{NL}'' to M_L are plotted versus the P/P_e parameter, when the axial load is kept constant, but the length is changing between 50 and 150 ft. Figure A-5 shows that M_{NL}'' provides a good estimate for M_{NL}, while M_{NL}' clearly overestimates the nonlinear moment.

Finally, the effect of increasing the axial load was studied, keeping constant the other loads and geometric parameters of a given pole. In Figure A-6, the ratios of M_{NL}, M_{NL}' and M_{NL}'' to M_L are plotted versus the P/P_e parameter. The ratio of M_{NL} to M_L increases proportionally with the increase in axial load. The ratio of M_{NL}'' to the linear moment also increases, and this curve approximates the nonlinear moment curve. On the other hand, the ratio of M_{NL}' to the linear moment increases significantly when the parameter P/P_e exceeds 0.44. For this particular example, the valid range of the current C_A equation is for P/P_e less than 0.333. However, even in the valid range of the current C_A equation, C_A moments M_{NL}' overestimate nonlinear moments.

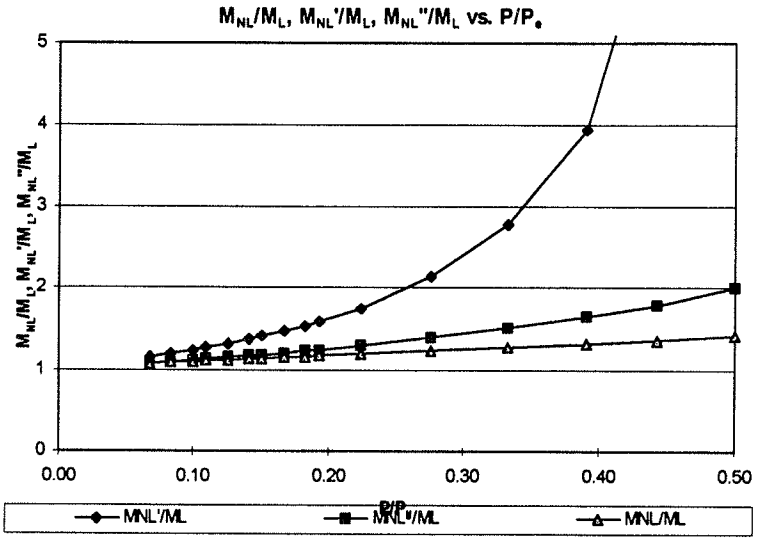

Figure A-6. Influence of the change in axial load in the estimation of the nonlinear moment.

A.6 CONCLUSIONS

After reviewing the results obtained from the analytical study of 241 examples, the following conclusions can be drawn:

1. The current C_A leads to a significant overestimation of the nonlinear moments that include second order effects. The magnitude of the error in the estimation of the nonlinear moment is dependent upon the length, stiffness, and magnitude of the axial load applied at the top of the pole.
2. To produce a better estimation of the nonlinear moments, the following modified equation for C_A is proposed:

$$C_A = 1 - \left[\frac{P_T \sqrt[3]{\frac{I_B}{I_T}} + 0.38 D_P}{\frac{2.46 E I_B}{L^2}} \right] \quad \text{for } F_a \leq 0.26 F_y \qquad \text{(A-11)}$$

3. The proposed C_A can predict with high accuracy the nonlinear moment. However, its use must be limited to cantilever supports, such as poles or posts. It is not intended to predict the nonlinear moments in other types of structures, such as trusses or overhead sign structures.
4. Because the proposed C_A is based on an approximate method, it can produce in some cases slightly nonconservative results, specifically for short stiff poles.
5. The overload factor of 1.38, which is to be used when performing the exact nonlinear analysis, has been changed to 1.45 for groups II and III load combinations. Results of analysis indicate that this change does not significantly affect the results of the calculated exact nonlinear moment, M_{NL}.

APPENDIX B

EVALUATION OF THE PROPOSED FATIGUE-RESISTANT DESIGN CRITERIA OF *NCHRP REPORT 412*

The proposed fatigue-resistant design criteria presented in the *NCHRP Report 412* (*28*) were evaluated. Fatigue limit stresses were compared with values found in other specifications, such as the AASHTO *LRFD Bridge Design Specifications* (*7*) and the AISC *Manual of Steel Construction* (*26*). Suggested modifications to the proposed fatigue-resistant design criteria are presented for consideration. Design examples, which show changes in member sizes because of the fatigue loads of galloping, vortex shedding, natural wind gusts, and truck-induced wind gusts, are presented for two streetlighting poles, a high mast pole, and a cantilevered traffic signal mast arm.

B.1 DESIGN CONSIDERATIONS

Design considerations for fatigue of a given detail include the number of load applications, the magnitude of the stress range, and the severity of stress concentrations. The number of cycles due to cyclic wind load is expected to exceed 100 million for a typical support structure over its lifetime. The report developed loadings that estimate the magnitude of stress range due to galloping, vortex shedding, natural wind gusts, and truck-induced wind gusts (*28*). Adjustments in the form of importance factors are made to the loadings that are dependent on the location, type of support structure, and type of loading. Typical connection details for support structures were categorized to address the severity of the stress concentrations. An allowable stress range is provided for each detail category for steel and aluminum.

B.1.1 Allowable Stress Range

The maximum stress range due to fatigue loading was selected on the basis of the constant-amplitude fatigue limit (CAFL) for a given detail and material. Constant-amplitude fatigue tests exhibit a CAFL after a certain number of cycles. The CAFL is the stress range below which the fatigue life appears to be infinite. The number of constant amplitude cycles at which the CAFL occurs is far less than the number of cycles that a typical support structure would experience. For practical purposes, a 25-year period is considered as infinite life for many support structures. The infinite life is a relative term that depends on the load history on the structure. Because a typical structure is expected to undergo an excessively large number of cycles, an infinite life design philosophy was adopted.

CAFL values for steel and aluminum, which are the same or similar to those values given in *NCHRP Report 412* can be found in the AASHTO *LRFD Bridge Design Specifications* (*7*), the AISC *LRFD Manual of Steel Construction* (*50*), AISC *Manual of Steel Construction -ASD* (*26*), and the *Aluminum Design Manual* (*9*). A comparison of CAFL for steel and aluminum to the CAFL of other specifications is presented in Tables B-1 and B-2, respectively.

B.1.2 Fatigue Loading

The current *Supports Specifications* only provides information on one type of fatigue loading: vortex shedding for a cantilevered pole. This arrangement is only applicable to post-top lighting poles. *NCHRP Report 412* determined that fatigue loading cases should be included for the following wind phenomena: galloping, vortex shedding, natural wind gusts, and truck-induced wind gusts.

The report also determined that certain structures are more susceptible to fatigue than other structures. Galloping and truck-induced wind gusts would need to be considered for cantilevered sign and traffic signal structures with rigidly attached traffic signals. Vortex shedding would need to be considered for nontapered cantilevered poles and arms. Natural wind gusts would need to be considered for all cantilevered structures.

B.1.3 Fatigue Categories

The importance factors are dependent on the location, structure type, and the type of fatigue loading. Three fatigue categories are defined as follows:

I: Critical cantilevered support structures installed on major highways.
II: Other cantilevered support structures installed on major highways and all cantilevered support structures installed on secondary highways.
III: Cantilevered support structures installed at other locations.

TABLE B-1 CAFL for steel

Detail Category	AISC - ASD (*26*) (ksi)	AISC - LRFD (*8*) (ksi)	AASHTO LRFD Bridge Spec. (*7*) (ksi)	NCHRP Report 412 (*28*) (ksi)
A	24.00	24.0	24.00	**24.00**
B	16.00	16.0	16.00	**16.00**
B'	12.00	12.0	12.00	**12.00**
C	10.00	10.0	10.00	**10.00**
D	7.00	7.0	7.00	**7.00**
E	5.00	4.5	4.50	**4.50**
E'	3.00	2.6	2.60	**2.60**
ET	--	--	--	**1.16**

The highest importance factors (i.e., most conservative) will be in fatigue category I and the lowest importance factors will be in fatigue category III.

B.1.4 Connection Categories

Twenty typical connections for highway support structures were categorized in *NCHRP Report 412*. The report includes sketches of each connection detail and the corresponding detail category, which has a given allowable stress range for steel and aluminum.

B.2 EXAMPLES

Stress range calculations for fatigue resistant design of a high mast pole, a cantilevered traffic signal mast arm, and two streetlighting poles are presented in this section. The examples illustrate changes in size because of imposing the fatigue requirements of *NCHRP Report 412*. Stresses are calculated for the shaft-to-base plate connections only. For the following examples, the only connection detail types presented are for stress category, E′ which was chosen because fillet-welded socket connections that are typically used in support structures fall into this category.

To simplify comparisons in the following examples, design for fatigue loading was addressed by increasing the size of the cross section. Wall thickness and the selected stress category for the shaft-to-base plate connection were kept unchanged for these examples. In general, stresses due to fatigue loads can be lowered by providing larger cross-sectional dimensions or increasing wall thickness. Allowable fatigue stress ranges can be increased by improving fatigue connection details. Also, the effects of galloping and vortex shedding can be reduced by adding damping devices.

TABLE B-2 CAFL for aluminum

Detail Category	Aluminum Design Manual (*9*) (ksi)	AASHTO LRFD Bridge Spec. (*7*) (ksi)	NCHRP Report 412 (*28*) (ksi)
A	10.20	9.42	**10.20**
B	5.40	5.80	**6.00**
B'	--	--	**4.60**
C	4.00	4.35	**4.10**
D	2.50	2.90	**2.50**
E	1.80	2.18	**1.90**
E'	--	--	**1.02**
ET	--	--	**0.44**

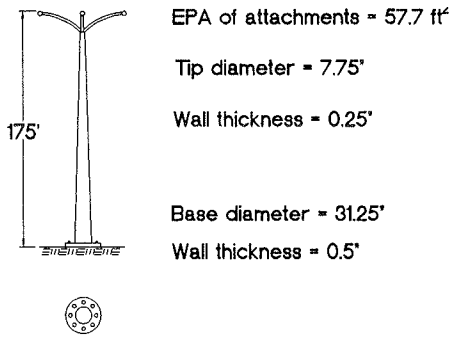

Figure B-1. Steel high mast pole example.

Sample stress calculations are provided for each example in this section. Sample calculations are provided for the high mast pole, the cantilevered traffic signal pole, and the two streetlighting poles. These calculations were done with a spreadsheet developed specifically to determine fatigue stresses for these three structure types on the basis of the fatigue loads proposed by *NCHRP Report 412*.

B.2.1 Example 1: Steel High Mast Pole

A typical steel high mast pole is shown in Figure B-1. The initial design is for a 175-ft high mast steel pole with a base plate. The attachment at the top has an effective projected area of 57.7 ft^2. The initial size, based on the design criteria of the current *Supports Specifications* for 80 mph, is a tapered eight-sided tubular pole with dimensions shown in Table B-3.

For a tapered steel high mast, only one fatigue load criterion is to be considered: natural wind gusts. The other three fatigue load cases, galloping, vortex shedding, and truck-induced wind gusts, are not relevant for this structure type.

A typical high mast pole would be located near a major highway and, therefore, would be designed for fatigue category I. For this example, a fillet-welded socket connection that corresponds to stress category E′ in *NCHRP Report 412* was selected as the base connection. This fatigue detail category has an allowable stress range of 2,600 psi for steel.

B.2.1.1 Fatigue Stress Due to Natural Wind Gusts

The stress range for natural wind gusts for fatigue category I is 5,197 psi, which is significantly above the 2,600 psi allowable fatigue stress for steel for stress category E'. The stress was calculated by using the initial pole size shown in Table B-3 and was designed based on the current *Supports Specifications* for 80 mph. In this case, the pole size or wall thickness would need to be increased, or the detail category modified to a higher level.

The required base width sizes can be obtained from Figure B-2. For this example, the tip diameters remain unchanged and the taper of the pole is modified. This example shows that a significant increase in pole size would be required to meet fatigue category I for a high mast pole. No increase in pole size would be required for fatigue category III, which is the lowest fatigue category. Increases in pole size for fatigue categories I and II, due to natural wind gusts, are shown in Table B-3.

B.2.1.2 Selection of High Mast Pole Size

This example of a high mast pole shows a significant increase in pole size to meet the proposed fatigue loading of natural wind gusts for fatigue categories I and II. The pole width at the base would need to be changed from 31.25 in. for the current *Supports Specifications* for 80 mph to 49.75 in. for fatigue category I and 39.25 in. for fatigue category II.

TABLE B-3 Summary of high mast steel pole sizes

	Fatigue Category I		Fatigue Category II	
Pole Size per:	Width Tip/Base (in.)	Tip/Base Thickness (in.)	Width Tip/Base (in.)	Tip/Base Thickness (in.)
Current *Supports Specifications* for 80 mph	7.75"/31.25"	0.25"/0.50"	7.75"/31.25"	0.25"/0.50"
Fatigue loading due to natural wind gusts	7.75"/49.75"	0.25"/0.50"	7.75"/39.25"	0.25"/0.50"
Selected Pole Size	**7.75"/49.75"**	**0.25"/0.50"**	**7.75"/39.25"**	**0.25"/0.50"**

Note: Width dimension refers to flat-to-flat dimension of the 8-sided pole.

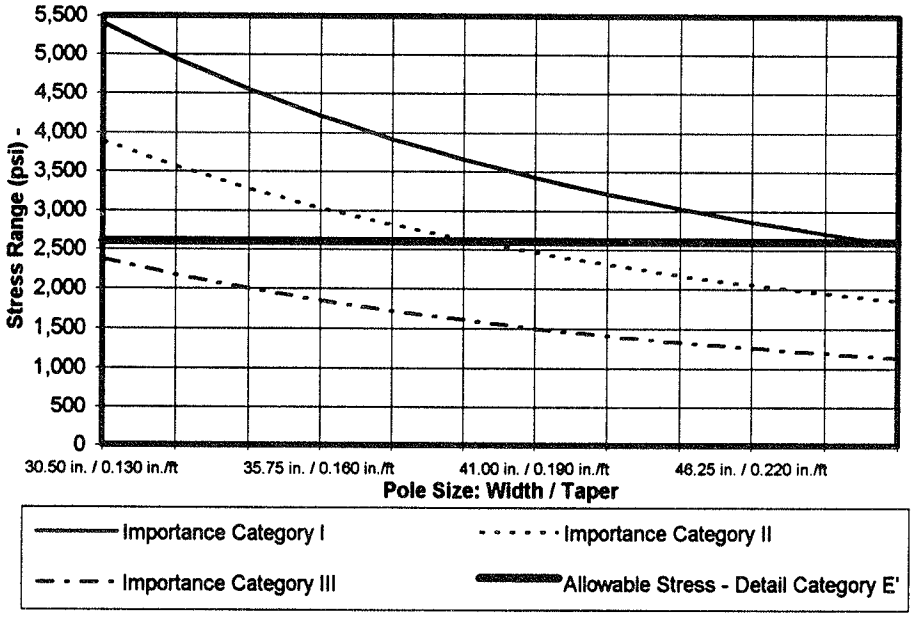

Figure B-2. Fatigue stresses due to natural wind gusts for 175-ft tapered high mast steel poles.

B.2.2. Example 2: Cantilevered Traffic Signal Steel Mast Arm

A cantilevered traffic signal pole is shown in Figure B-3. Stresses due to fatigue loadings were calculated at the mast arm's tube-to-base plate connection. The initial mast arm size is designed for the current *Supports Specifications* for 80 mph. The initial mast dimensions and attachments are presented in Tables B-4 and B-5.

For a tapered steel mast arm with a base plate, three fatigue load criteria were considered: galloping, natural wind gusts, and truck-induced wind gusts. The other fatigue load case, vortex shedding, does not need to be considered because excitation due to vortex shedding on a tapered arm is limited. Consistent shedding only occurs over a length of a few diameters because the critical velocity along the length of the member varies with the diameter. Therefore, vortex shedding over such a small length does not produce sufficient energy to induce large-amplitude vibrations (*28*).

A traffic signal mast arm would be designed for fatigue category I or II. The base connection for this type of structure is typically a fillet-welded socket connection that corresponds to stress category E′ in *NCHRP Report 412*. This fatigue detail category has an allowable stress range of 2,600 psi for steel.

B.2.2.1 Fatigue Stress Due to Galloping

The stress range for galloping is 13,023 psi for fatigue category I and 8,465 psi for fatigue category II, which is above the 2,600 psi allowable fatigue stress range for steel for stress

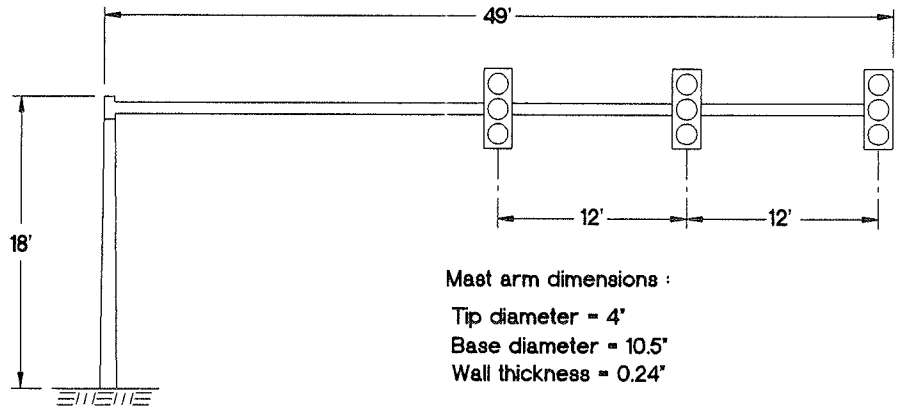

Figure B-3. Cantilevered traffic signal steel structure example.

TABLE B-4 Initial mast arm dimensions

Length	49 ft.
Tip Diameter	4.0 in.
Base Diameter	10.5 in.
Wall Thickness	0.24 in.

TABLE B-5 Traffic signal attachments

Quantity	3 ea.
Location	0', 12', 24' from end of arm
Projected area on vertical plane	9 ft^2, C_d=1.2
Projected area on horizontal plane	1 ft^2, C_d=1.2

category E′. The stresses were calculated using the initial mast arm size shown in Table B-4.

To meet the fatigue criterion for galloping, the mast arm size at the base would need to be increased to the following:

- 23 in. diameter × ¼ in. for fatigue category I, stress category E′;
- 19 in. diameter × ¼ in. for fatigue category II, stress category E′; and
- 13 in. diameter × ¼ in. for fatigue category III, stress category E′.

Each size would have a deflection within 2 to 3 in., which is less than the 8-in. limit required in the report. These sizes can also be selected in Figure B-4. A significant increase in cross-section would be required for the given mast arm to be designed for the fatigue requirements of fatigue categories I and II.

B.2.2.2 Fatigue Stress Due to Natural Wind Gusts

The stress range for natural wind gusts is 6,064 psi for fatigue category I and 4,851 psi for fatigue category II, which is above the 2,600 psi allowable fatigue stress for steel for stress category E′. The stresses were calculated using the initial pole size of Table B-4.

To meet the fatigue criterion for natural wind gusts, the mast arm diameter at the base would need to be increased to the following:

- 17 in. diameter × ¼ in. for fatigue category I, stress category E′;
- 15 in. diameter × ¼ in. for fatigue category II, stress category E′; and
- 12.5 in. diameter × ¼ in. for fatigue category III, stress category E′.

The required sizes are shown in Figure B-5.

B.2.2.3 Fatigue Stress Due to Truck-Induced Wind Gusts

The stress range for truck-induced wind gusts is 7,459 psi for fatigue category I and 6,266 for fatigue category II, which is above the 2,600 psi allowable fatigue stress for steel for stress category E′. The stresses were calculated using the initial mast arm size in Table B-4.

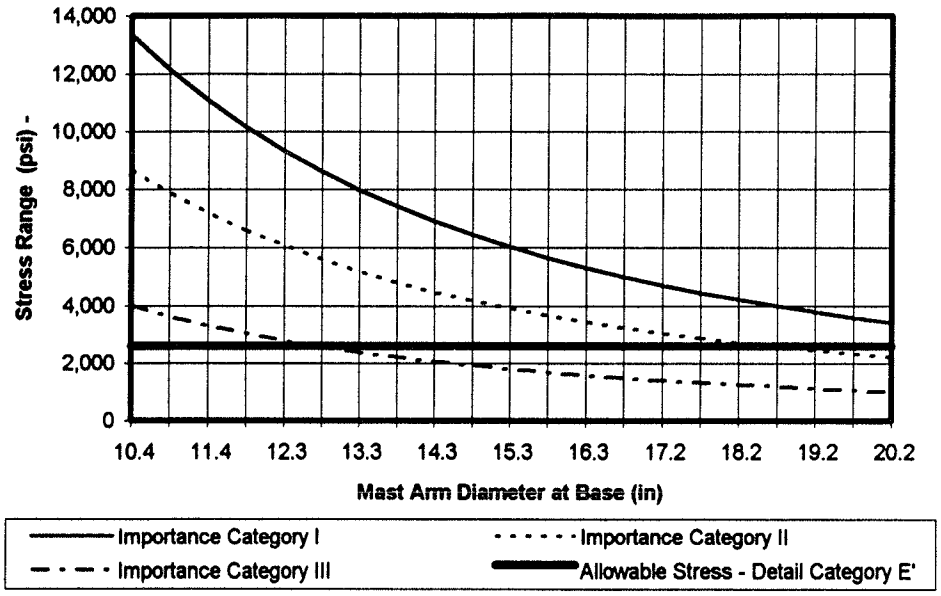

Figure B-4. Stress range due to galloping for traffic signal steel mast arms.

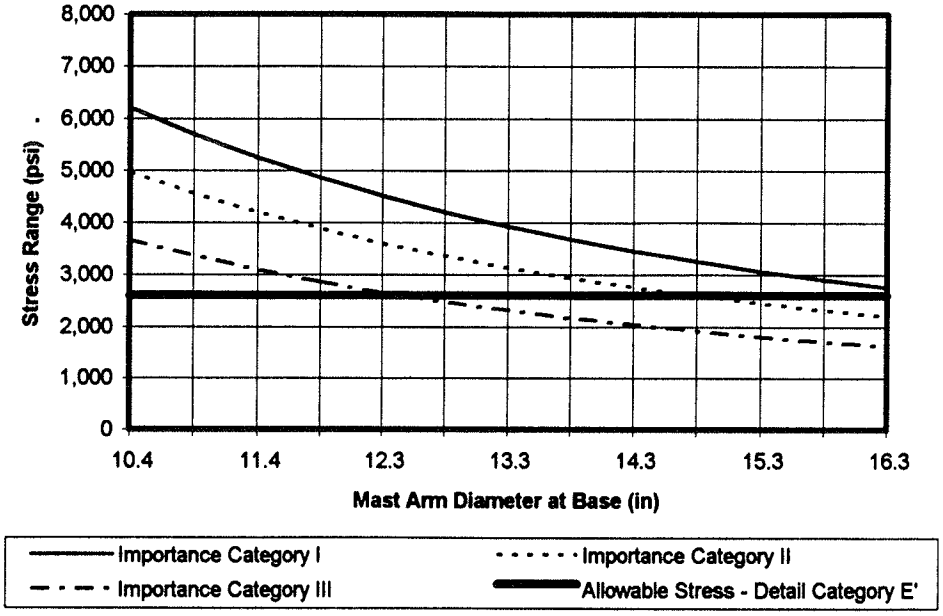

Figure B-5. Fatigue stresses due to natural wind gusts for traffic signal steel mast arms.

An increase in mast arm size at the base to meet the fatigue criterion due to truck-induced wind gusts would require the following:

- 18.75 in. diameter × ¼ in. for fatigue category I, stress category E′;
- 17 in. diameter × ¼ in. for fatigue category II, stress category E′; and
- 15 in. diameter × ¼ in. for fatigue category III, stress category E′.

Deflections for each of the modified sizes would be around 3 in., which is less than the 8-in. limit required by the NCHRP report. The sizes can also be selected graphically in Figure B-6.

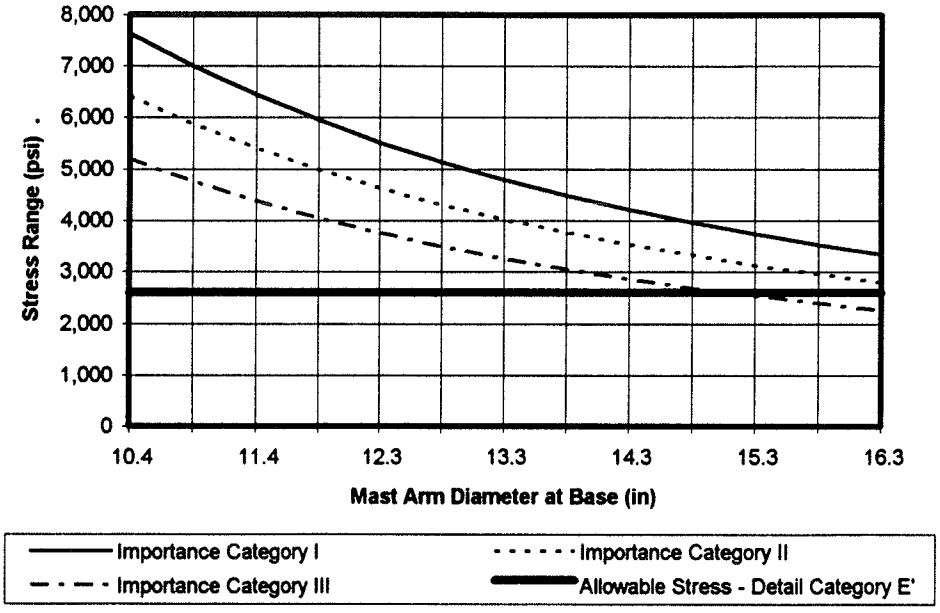

Figure B-6. Stress range due to truck-induced wind gusts for traffic signal steel mast arms.

TABLE B-6 Steel mast arm sizes at base

Pole Size per:	Fatigue Category I	Fatigue Category II
Current *Supports Specifications* for 80 mph	10.5" Diameter x 1/4"	10.5" Diameter x 1/4"
Fatigue loading due to galloping	23" Diameter x 1/4"	19" Diameter x 1/4"
Fatigue loading due to natural wind gusts	17.0" Diameter x 1/4"	15" Diameter x 1/4"
Fatigue loading due to truck-induced gusts	18.75" Diameter x 1/4"	17" Diameter x 1/4"
Selected Mast Arm Size	**23" Diameter x 1/4"**	**19" Diameter x 1/4"**

B.2.2.4 Selection of Steel Mast Arm Size

A summary of recommended mast arm sizes for the cantilevered traffic signal structure example is provided in Table B-6 for fatigue categories I and II. For importance categories I and II, the mast would require a significant increase in diameter to meet the fatigue loading criterion for galloping.

B.2.3 Example 3: Aluminum Streetlighting Pole

A typical aluminum post-top pole is shown in Figure B-7. The initial pole size is designed based on the current *Supports Specifications* for 80 mph. The overall pole length is 30 ft above ground. The attachment at the top of the pole has an effective projected area, including the drag coefficient, of 5 ft^2. The pole initial size, based on the design criteria of the current *Supports Specifications*, is a nontapered square tubular aluminum pole with a width of 6 in. and a wall thickness of ¼ in.

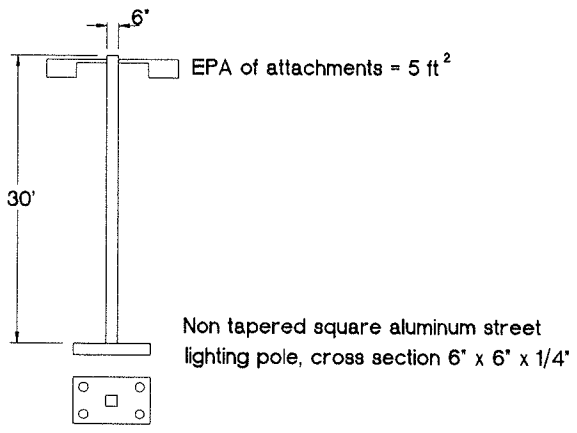

Figure B-7. Aluminum streetlighting pole example.

For a nontapered aluminum post-top pole with a base plate, two fatigue load criteria were considered: vortex shedding and natural wind gusts. The other two fatigue load cases, galloping and truck-induced wind gusts, are not relevant for this structure type.

Streetlighting poles would typically be designed for fatigue category II or III. The critical design location considered for discussion is where the shaft connects to the base plate. The base connection for this type of structure is typically a fillet-welded socket connection that corresponds to stress category E′ in *NCHRP Report 412*. This fatigue detail category has an allowable stress range of 1,015 psi for aluminum.

B.2.3.1 Fatigue Stress Due to Natural Wind Gusts

Stresses were calculated using the initial 6- × 6- × ¼-in. pole size. The stress range for the streetlighting pole example due to natural wind gusts is 2,027 psi for fatigue category II and 1,239 psi for fatigue category III, which is above the 1,015 psi allowable fatigue stress range for aluminum for stress category E′.

The required sizes to meet fatigue loading due to natural wind gusts can be obtained from Figure B-8. This graph shows that the pole size would need to be increased for all fatigue categories and would need to be greater than the 6- × 6- × ¼-in. initial pole size. An increase in pole size to meet the fatigue loading due to natural wind gusts would require the following:

- 13- × 13- × ¼-in. for fatigue category I, stress category E′;
- 10- × 10- × ¼-in. for fatigue category II, stress category E′; and
- 7- × 7- × ¼-in. fatigue category III, stress category E′.

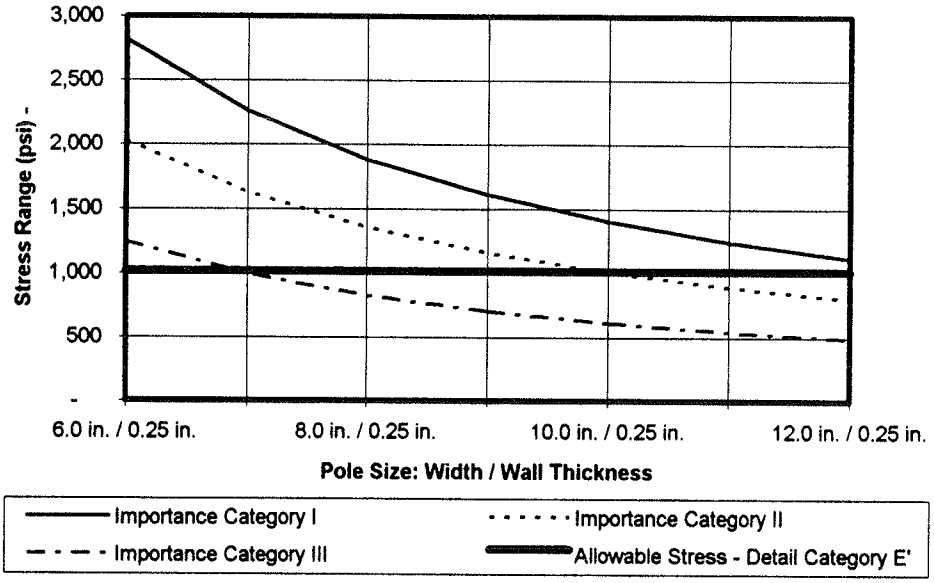

Figure B-8. Fatigue stresses due to natural wind gusts for a 30-ft nontapered aluminum streetlighting pole.

B.2.3.2 Fatigue Stress Due to Vortex Shedding

The stress range for vortex shedding is to be calculated when the critical wind velocity is less than 45 mph. Steadily repeating vortices do not typically form in winds over 45 mph. The critical velocity for the initial pole size in this example is 3.1 mph. The stress range for the initial pole size for fatigue category I is 906 psi, which is less than the allowable fatigue stress range of 1,015 psi for aluminum. Therefore, vortex shedding is not significant on a 30-ft pole that is 6- × 6- × ¼-in. in size.

However, as the pole width increases, the fatigue load stress increases at a significant rate and will need to be considered on pole widths greater than 6 in. for fatigue category I, 7 in. for fatigue category II, and 8.5 in. for fatigue category III. The stresses are proportional to the width and the frequency squared, which becomes larger for increasing widths.

Figure B-9 shows an increase in stress ranges as pole width increases. The critical wind velocities for the various pole sizes are shown in Table B-7 and in Figure B-10. The applied force per unit length in Table B-7 increases significantly as pole width increases.

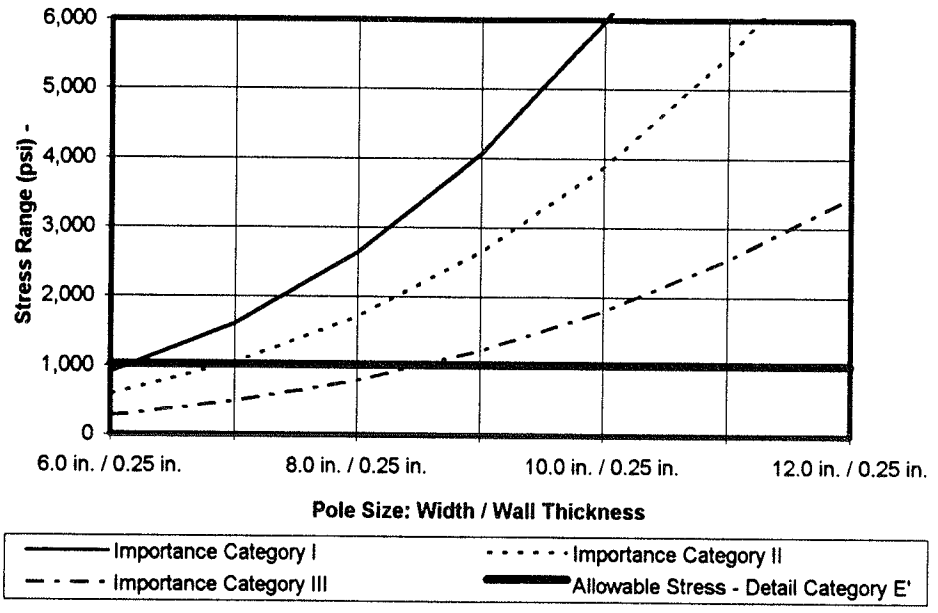

Figure B-9. Stress range due to vortex shedding for a 30-ft nontapered aluminum streetlighting pole.

TABLE B-7 Critical wind velocities

Pole Size	Est. Natural Frequency (Hz)	Critical Velocity (mph)	Applied Force Per Unit Length (lb/ft)
6" x 6" x 1/4"	1.00	3.1	1.77
7" x 7" x 1/4"	1.25	4.5	4.36
8" x 8" x 1/4"	1.50	6.2	9.47
9" x 9" x 1/4"	1.77	8.2	18.67
10" x 10" x 1/4"	2.04	10.5	34.14
11" x 11" x 1/4"	2.32	13.2	58.76
12" x 12" x 1/4"	2.45	16.2	96.23

B.2.3.3 Selection of Aluminum Streetlighting Pole Size

A summary of recommended pole sizes for the streetlighting pole example is provided in Table B-8 for fatigue categories II and III. For fatigue category III, the initial pole size will increase from 6 × 6 × ¼ in. to 7 × 7 × ¼ in. It will not be possible to design a square non-tapered pole for fatigue category II without the use of damping devices because this particular example would only allow a maximum size of 7 × 7 × ¼ in. to meet the vortex shedding fatigue criterion and a minimum size of 10 × 10 × ¼ in. is required to meet the natural wind gust fatigue criterion.

B.2.4 Example 4: Steel Streetlighting Pole

A typical steel streetlighting pole is shown in Figure B-11. The design criteria are the same as presented for the aluminum streetlighting pole example. The configuration is for a 30-ft steel pole with a base plate. The initial design criteria are based on the current *Supports Specifications* for 80 mph. The attachment at the top of the pole has an effective projected area of 5.0 ft^2. The initial size, based on the design criteria of the current *Supports Specifications*, is a nontapered square tubular steel pole with a width of 4 in. and a wall thickness of ¼ in.

For a nontapered steel post-top pole with a base plate, two fatigue load criteria were considered: vortex shedding and natural wind gusts. The other two fatigue load cases, galloping and truck-induced wind gusts, are not relevant for this structure type.

Streetlighting poles would typically be designed for importance category II or III. The critical location for design for discussion is where the shaft connects to the base plate. The base connection for this type of structure is typically a fillet-welded socket connection that corresponds to stress category E′ in the NCHRP report. This fatigue detail category has an allowable stress range of 2,600 psi for steel.

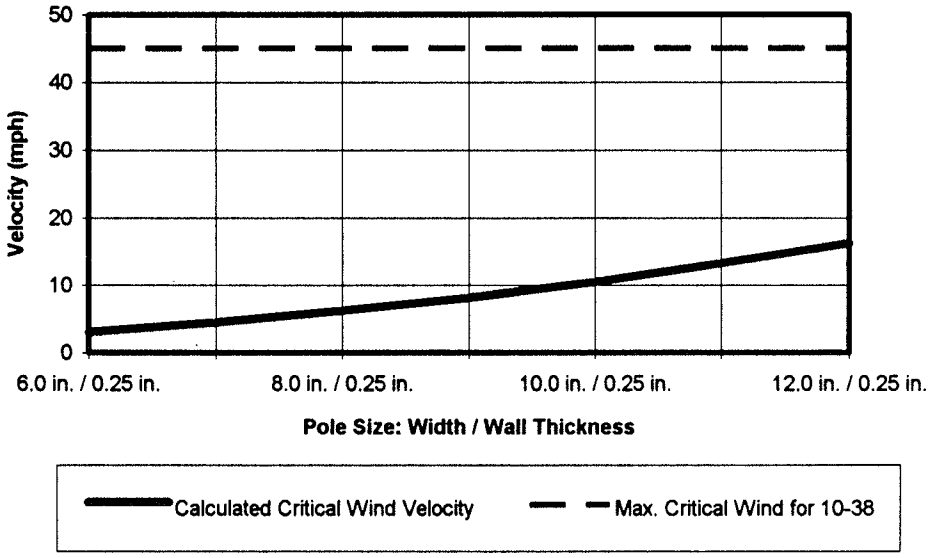

Figure B-10. Critical wind velocities for a 30-ft nontapered aluminum streetlighting pole.

TABLE B-8 Summary of aluminum streetlighting pole sizes

Pole Size per:	Fatigue Category II	Fatigue Category III
Current *Supports Specifications* for 80 mph	Square, 6" x 6" x 1/4"	Square, 6" x 6" x 1/4"
Fatigue loading due to natural wind gusts	Square, 10" x 10" x 1/4", min.	Square, 7" x 7" x 1/4", min.
Fatigue loading due to vortex shedding	Square, 7" x 7" x 1/4", max.	Square, 8.5" x 8.5" x 1/4", max.
Selected Pole Size	**Not possible without damping devices**	**Square, 7" x 7" x 1/4"**

B.2.4.1 Fatigue Stress Due to Natural Wind Gusts

Stresses were calculated by using the initial 4- × 4- × ¼-in. pole size. The stress range for the streetlighting pole example due to natural wind gusts is 3,760 psi for fatigue category II and 2,298 psi for fatigue category III, which is above the 2,600 psi allowable fatigue stress range for steel for stress category E′ for fatigue category II and below for fatigue category III.

The required size to meet fatigue loading due to natural wind gusts can be obtained from Figure B-12. The pole sizes that are required to meet the fatigue criterion for natural wind gust are:

- 6.5 × 6.5 × ¼ in. for fatigue category I, stress category E′;
- 5 × 5 × ¼ in. for fatigue category II, stress category E′; and
- Smaller than 4 × 4 × ¼ in. for fatigue category III, stress category E′.

B.2.4.2 Fatigue Stress Due to Vortex Shedding

The critical velocity for the initial pole size in this example is 1.68 mph. The stress range for the initial pole size for fatigue category I is 427 psi, which is less than the allowable fatigue stress range of 2,600 psi for steel. Therefore, vortex shedding is not significant on a 30-ft steel pole that is 4 × 4 × ¼ in.

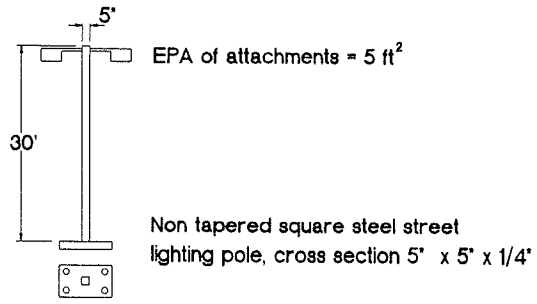

Figure B-11. Steel streetlighting pole example.

However, as the pole width increases, the fatigue load stress increases at a significant rate and will need to be considered on pole widths greater than 6.5 in. for fatigue category I, 7.5 in. for fatigue category II, and 9.5 in. for fatigue category III. The stresses are proportional to the width and the frequency squared, which becomes larger for increasing widths. Figure B-13 shows an increase in stress ranges as pole width increases. The critical wind velocities and force per unit length for the various pole sizes are shown in Table B-9. When Table B-7 from the aluminum streetlighting pole example is compared with Table B-9, the estimated natural frequency, the critical velocity, and the applied force per unit length are all higher for steel for similar section sizes. This is because steel has a higher modulus of elasticity.

B.2.4.3 Selection of Steel Streetlighting Pole Size

A summary of recommended pole sizes for the streetlighting pole example is provided in Table B-10 for fatigue categories II and III. For fatigue category III, the initial pole size will remain unchanged with a size of 4 × 4 × ¼ in. For fatigue category II, the pole size will need to be increased from 4 × 4 × ¼ in. to 5 × 5 × ¼ in. to meet the fatigue loading due to natural wind gusts.

B.3 ADDITIONAL DISCUSSION ON VORTEX SHEDDING FOR VARIOUS SHAPES

Calculations of critical wind velocities and forces per unit length for round, multi-sided, and square shapes were made due to vortex shedding. Critical wind velocities for natural frequencies up to 3 Hz are shown in Figure B-14 for round sections, Figure B-15 for multi-sided sections, and Figure B-16 for square sections. Higher natural frequencies have higher critical velocities for a given diameter or width. As

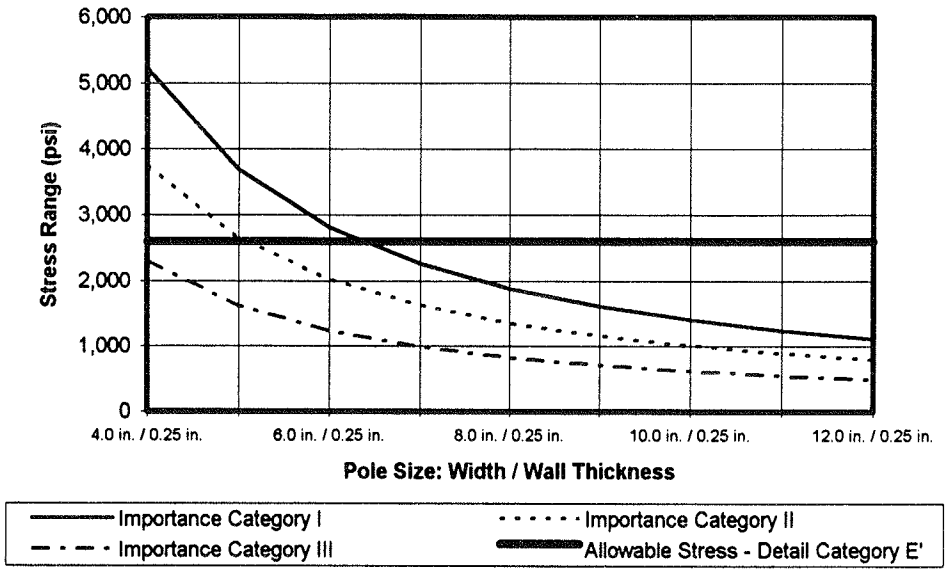

Figure B-12. Stress range due to natural wind gusts for a 30-ft nontapered steel streetlighting pole.

shown in these three figures, the critical velocity is below 10 mph for typical diameters of very flexible structures.

The fatigue load, which is calculated in terms of force per unit length of shaft for each shape at its critical wind speed, is shown in Figure B-17 for round, Figure B-18 for multi-sided, and Figure B-19 for square sections with a damping ratio of 0.005. The force per unit length is significantly higher for structures with a natural frequency of 3 Hz than for structures with a natural frequency of 1 Hz. The force per unit length also increases significantly with increasing diameter.

In general, typical support structures that might be subject to vortex shedding would have a natural frequency in the range of 0.5 to 2 Hz. Most of these structures will have dimensions that will have a corresponding critical velocity of less that 10 mph. The fatigue loading calculated for vortex shedding would only apply to nontapered cantilevered poles and arms, such as nontapered streetlighting poles. Critical velocities under 45 mph are the only velocities to be considered. Wind velocities above 45 mph do not allow steady shedding of vortices that induces significant excitation.

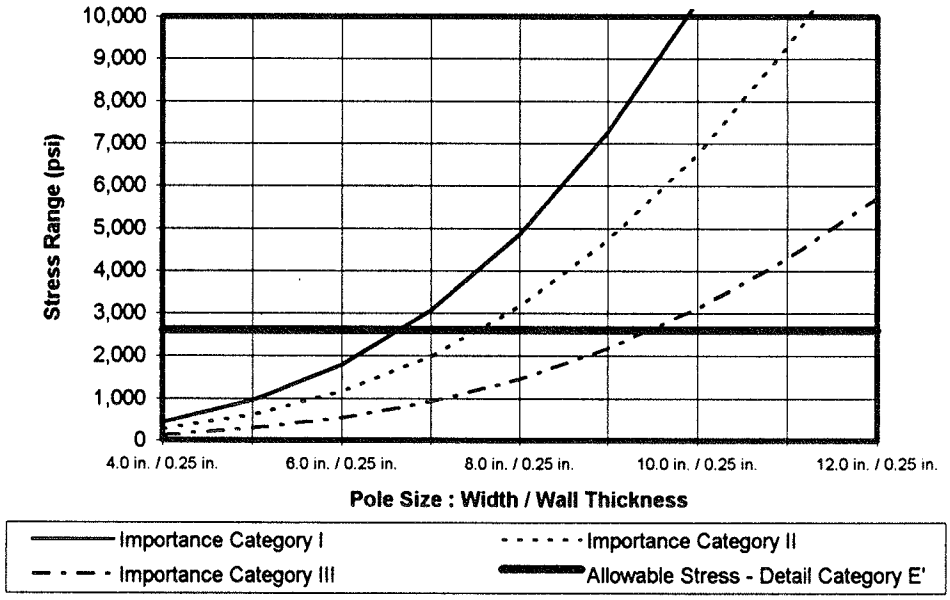

Figure B-13. Stress range due to vortex shedding for a 30-ft nontapered steel streetlighting pole.

TABLE B-9 Critical wind velocities

Pole Size	Est. Natural Frequency (Hz)	Critical Velocity (mph)	Applied Force Per Unit Length (lb/ft)
4" x 4" x 1/4"	0.81	1.68	0.35
5" x 5" x 1/4"	1.11	2.86	1.25
6" x 6" x 1/4"	1.41	4.37	3.51
7" x 7" x 1/4"	1.72	6.23	8.32
8" x 8" x 1/4"	2.04	8.43	17.44
9" x 9" x 1/4"	2.36	10.99	33.34
10" x 10" x 1/4"	2.69	13.90	59.29
11" x 11" x 1/4"	3.02	17.17	99.50
12" x 12" x 1/4"	3.36	20.80	159.25

TABLE B-10 Summary of steel streetlighting pole sizes

Pole Size per:	Fatigue Category II	Fatigue Category III
Current *Supports Specifications* for 80 mph	Square, 4" x 4" x 1/4"	Square, 4" x 4" x 1/4"
Fatigue loading due to natural wind gusts	Square, 5" x 5" x 1/4", min.	Square, less than 4" x 4" x 1/4", min.
Fatigue loading due to vortex shedding	Square, 7.5" x 7.5" x 1/4", max.	Square, 9.5" x 9.5" x 1/4", max.
Selected Pole Size	**Square, 5" x 5" x 1/4"**	**Square, 4" x 4" x 1/4"**

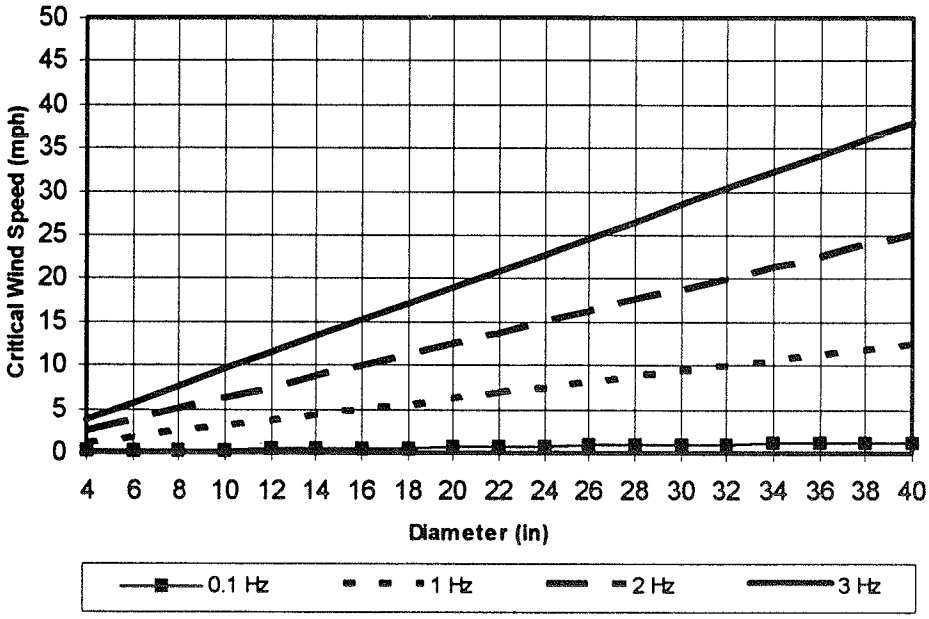

Figure B-14. Critical wind speed for round sections.

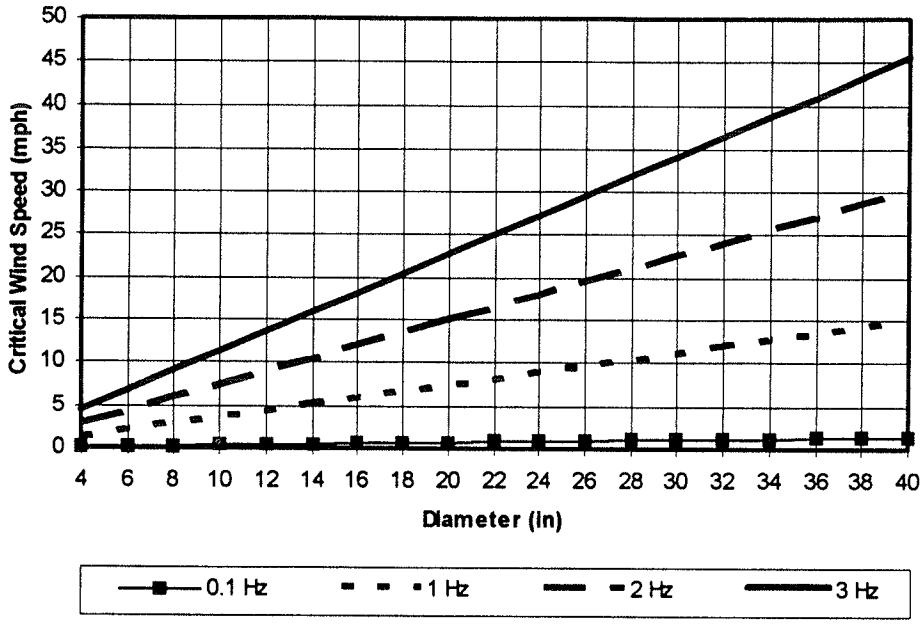

Figure B-15. Critical wind speed for multi-sided sections.

B.4 EVALUATION AND RECOMMENDED MODIFICATIONS

The following section contains recommended modifications to the proposed fatigue-resistant design criteria proposed by *NCHRP Report 412*. Additional comments are also made for future research.

B.4.1 Probability of Exceedence for CAFL Values

Based on *NCHRP Report 354*, if the maximum values of the stress range exceed the CAFL for more than 0.05 percent of the cycles, fatigue failure could occur (*151*). Also, if the maximum values of the stress range did not exceed the CAFL

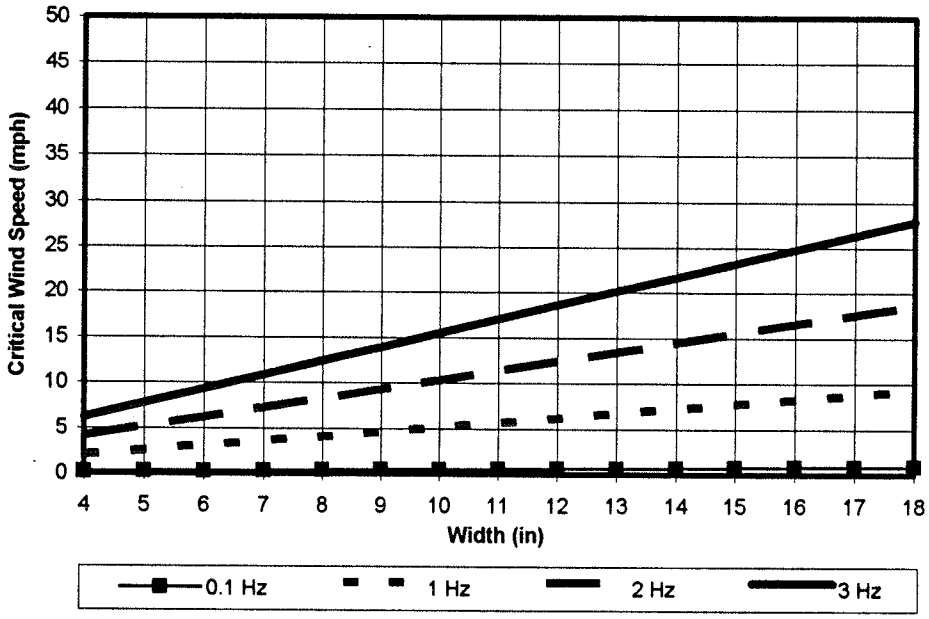

Figure B-16. Critical wind speed for square sections.

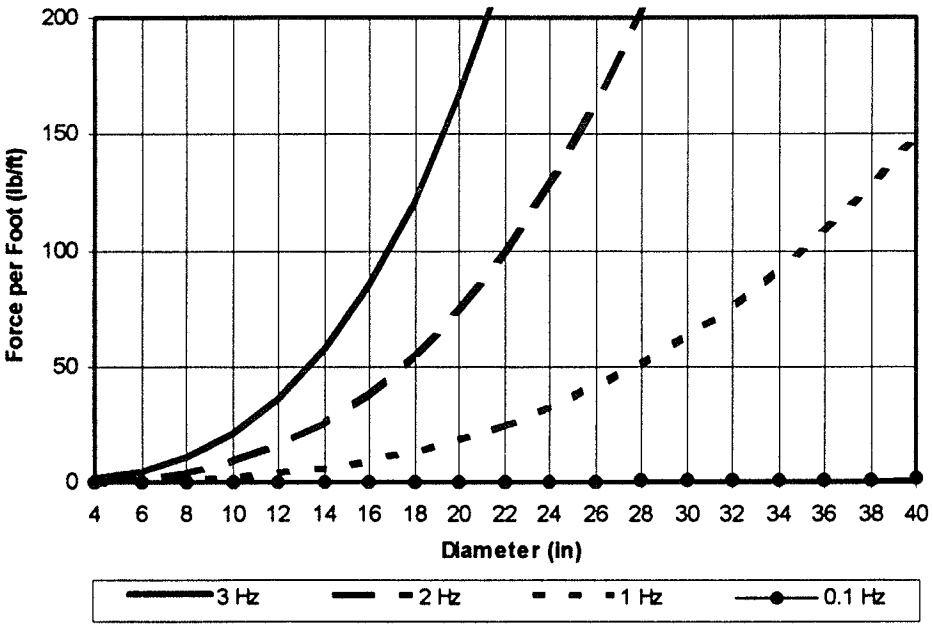

Figure B-17. Force per foot for round sections with a damping ratio of 0.005.

by more than 0.01 percent of the total number of cycles, an infinite fatigue life would result.

A review, which is beyond the scope of this study, will need to be made to determine how stringent is limiting the probability of exceedence of the CAFL to 0.01 percent of the total number of cycles and what the effects are of increasing the probability of exceedence of the CAFL. Because *NCHRP Report 354* indicates that if 0.05 percent of the cycles exceed the CAFL, a fatigue failure could occur, the percentage of fatigue failures needs to be provided for corresponding probabilities of exceedence of the CAFL of 0.05 percent and greater. An acceptable limit of structural fatigue failure will also need to be determined if the probability of exceedence is to be increased and less conservative designs allowed. If a higher probability of exceedence of the CAFL values, such as 2 percent, were allowed, calculated stress ranges due to

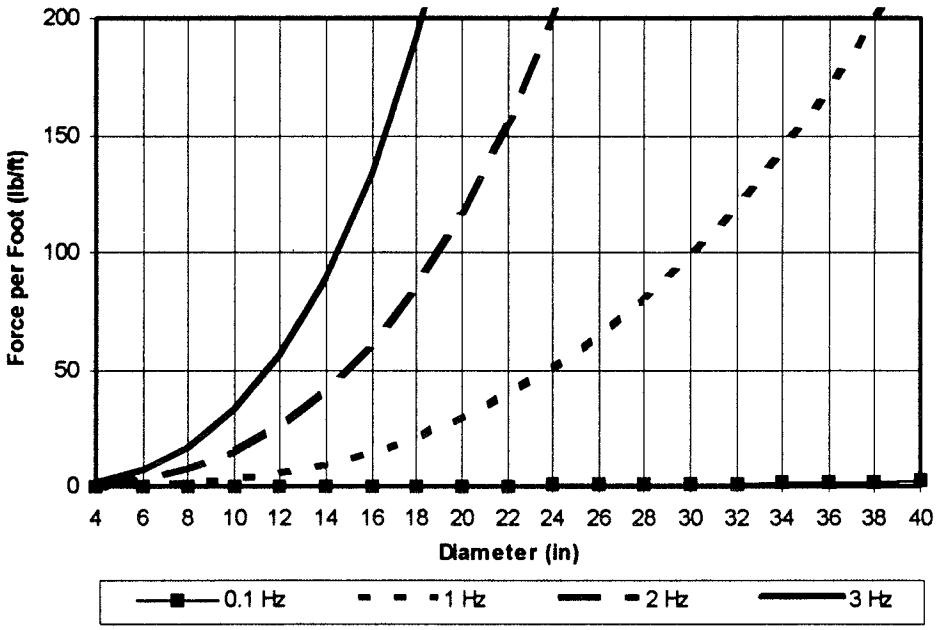

Figure B-18. Force per foot for multi-sided sections with a damping ratio of 0.005.

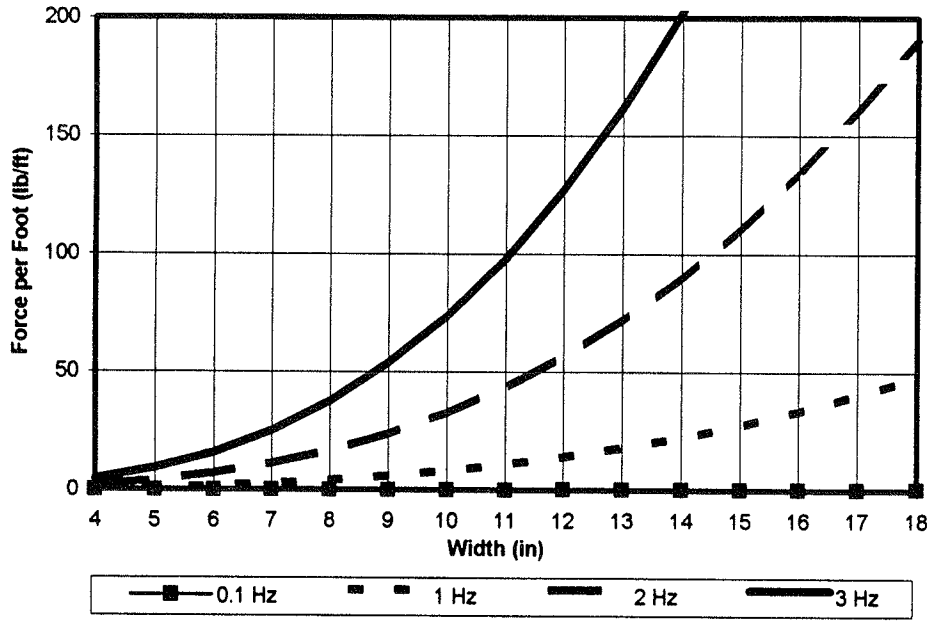

Figure B-19. Force per foot for square sections with a damping ratio of 0.005.

fatigue loading could be reduced, therefore, reducing the required cross sections to meet the fatigue load case.

In general, pole sizes will need to be increased to meet the proposed fatigue load criteria. This load criterion is based on limiting the probability of exceedence of the CAFL values to 0.01 percent. The galloping and natural wind gust loadings could be reduced if the probability of exceedence of the CAFL values could be increased from 0.01 to 2 percent.

B.4.2 Additional Structure Types and Materials

NCHRP Report 412 does not address fatigue of overhead span-type sign support structures, span-wire traffic signal structures, or roadside signs. The current *Supports Specifications* attempts to address fatigue of overhead span-type sign structures by limiting dead load deflection. The report also only addresses fatigue of steel and aluminum. A future research topic could develop fatigue loadings for these types of structures and for other materials represented in the *Supports Specifications*, specifically, concrete, wood, and fiberglass.

B.4.3 Fatigue Categories

The fatigue categories should be added in terms of years of design life. This presentation would make selecting an importance factor similar to selecting importance factors in the wind load section. Importance factors should be provided for 100-, 50-, 25-, and 10-year design lives.

B.4.4 Galloping

The fatigue load criterion for galloping will increase the base diameter of cantilevered traffic signal mast arms significantly. In the given example, the diameter would increase from 10.5 to 23 in. for fatigue category I and 19 in. for fatigue category II.

This loading could be reduced if the probability of exceedence for the CAFL values could be increased and, therefore, reduce the maximum wind speed that will need to be considered. Field observation has shown that the design pressure is a function of the wind speed. Because loads due to galloping are higher for higher wind speeds, the 21 psf force should be reviewed to determine the maximum wind speed that is associated with that load level. The pressure should be limited to maximum wind velocities associated with a higher probability of exceedence.

B.4.5 Vortex Shedding

Fatigue loads could be critical for certain streetlighting poles. Particularly, increases in width could cause significant increases in forces per unit length for vortex shedding. For the aluminum streetlighting pole example for fatigue category II, if pole sizes were increased due to the natural wind gust, the applied stress range due to vortex shedding could exceed the allowable fatigue limit. No provisions are given to mitigate natural wind gusts, but mitigation can be provided for vortex shedding and would be required for this case.

Fatigue category III did not require mitigation. Fatigue category II would require mitigation because the minimum pole size of 10 in. for natural wind gusts exceeds the maximum pole size of 7 in. that vortex shedding does control.

The upper bound of the critical wind speed is set below 45 mph. This upper bound could be further lowered, if higher probability of exceedences for the CAFL values are allowed. Lowering the upper bound of critical wind speeds would only be significant for large diameters. However, if higher probability of exceedences were allowed for the other fatigue load cases, lowering the upper bound of the critical wind speed would make it consistent with the other fatigue load cases.

The method described to calculate forces due to vortex shedding only includes the fundamental frequency. Higher natural frequencies may be significant and may be within the critical wind speeds that produce vortex shedding. No mention was made concerning these higher modes of vibration.

B.4.6 Natural Wind Gusts

Based on the given example, the fatigue load criterion for natural wind gusts will require significantly larger poles, in general. This would indicate that the natural wind gust fatigue criterion is extremely conservative for post-top street-lighting poles and high mast poles. The development of the fatigue design criterion for natural wind gusts should be reviewed.

The wind speed was developed as shown in equation 2.8 in *NCHRP Report 412*. A mean yearly wind speed of 11 mph has been selected. For this yearly mean wind speed, the 0.01 percent exceedence corresponds to a mean hourly velocity of 37 mph. This pressure corresponds to 5.2 psf for design.

The limit-state wind criterion was developed for a probability of 0.01 percent exceedence. The 0.01 percent probability of exceedence is very conservative and corresponds to a mean hourly wind velocity of 37 mph. If the percent exceedence were modified to 2 percent rather than 0.01 percent, the mean hourly wind velocity would reduce to 24.5 mph and pressure due to the modified limit state velocity could drop significantly.

B.4.7 Truck-Induced Wind Gusts

For truck-induced wind gusts, the wind velocity should probably be reduced based on roadway use, and therefore, be a function of the roadway speed because not all structures would be subjected to 65 mph speed zones.

B.5 SUMMARY

In general, the load criteria proposed by *NCHRP Report 412* will require structures to be designed for improved fatigue resistance, using a combination of the following: higher quality fatigue-resistant connection, larger widths, or thicker wall. The following modifications are suggested:

- Present importance factors in terms of 100-, 50-, 25-, and 10-year design lives;
- Determine if a higher probability of exceedence for the CAFL values can be provided;
- Provide probability of fatigue failure for the higher probability of exceedence of the CAFL values; and
- Provide lowered forces due to fatigue based on the higher probability of exceedence for the CAFL.

APPENDIX C

FUNDAMENTAL FREQUENCY OF TAPERED POLES

C.1 INTRODUCTION

Section 1.9.6 (A) in the current *Supports Specifications* proposes the following formula to compute the fundamental natural frequency of cantilever beams:

$$fn = \frac{1.75}{\pi}\sqrt{\frac{EI}{mL^4}} = \frac{1}{2\pi}\sqrt{\frac{3EI}{0.24ML^3}}$$

where

f_n = natural frequency (Hz);
E = modulus of elasticity of the pole material (psi);
I = moment of inertia (in.^{4});
m = pole mass per unit length (lb-sec^2/in per in.);
M = pole mass (lb-sec^2/in.); and
L = length of member (in.).

This equation, however, neglects the effect of the lumped mass usually attached at the top of the vertical support and is only applicable to prismatic poles. To compute the fundamental frequency of tapered poles, the current *Supports Specifications* uses the same equation, but computes the moment of inertia based on an equivalent diameter computed as

$$d_e = \frac{d_t + d_b}{2}$$

and an equivalent length computed as

$$L_e = L\sqrt{\frac{2d_t}{d_t + d_b}}$$

where d_t and d_b are the diameters at the top and bottom of the pole.

When a lumped mass is applied at the top of the pole, the above formula cannot be used to predict the exact frequency value. Therefore, a new equation that considers the effect of the lumped mass at the top of the vertical support is proposed.

C.2 EXISTING EQUATION

The equation in the current *Supports Specifications* is based on the following formula for computing the natural frequency of a one degree-of-freedom system:

$$f_n = \frac{1}{2\pi}\sqrt{\frac{k}{M_{eff}}}$$

where k is the stiffness of a cantilever beam, given as

$$k = \frac{3EI}{L^3}$$

and the term M_{eff} is the effective mass of the system. If the mass of the beam is considered in the analysis, the effective mass of the system becomes (*152*)

$$M_{eff} = M_{top} + 0.24M_{pole}$$

where M_{top} is the mass at the top of the pole and M_{pole} is the mass of the pole itself.

In the current *Supports Specifications*, the mass attached at the top of the beam is neglected and the equation takes the form of

$$M_{eff} = 0.24M_{pole}$$

Therefore, the application of this equation is limited to the analysis of single pole supports with top mounted luminaires, whose mass can be neglected.

C.3 PROPOSED EQUATION

To evaluate the natural frequency of a pole with a mass attached at its top, an equation considering the mass of the pole and the mass attached at the top of the pole must be proposed. When the mass of the pole is included in the computations of the frequency of the system, the effective mass takes the original form of

$$M_{eff} = M_{top} + 0.24M_{pole}$$

where M_{top} is the mass at the top of the pole and M_{pole} is the mass of the pole itself.

The equation for computing the frequency of the system may then take the form

$$f_n = \frac{1}{2\pi}\sqrt{\frac{3EI}{(M_{top} + 0.24M_{pole})L^3}}$$

TABLE C-1 Examples 1 through 4

Number	Example	Type	Material	Length (feet)	Bottom Diameter (inches)	Top Diameter (inches)	Wall Thickness (inches)	Tip Load (pounds)
1	Street Lighting Pole	Tapered	Steel	27	7	3.5	0.125	101
2	High Mast Pole	Tapered	Steel	100	22.25	7.75	0.375	1800
3	High Mast Pole	Tapered	Steel	125	25.375	7.75	0.438	1800
4	High Mast Pole	Tapered	Steel	150	28.375	7.75	0.500	1800

This equation is valid for prismatic poles. For tapered poles, the change in stiffness due to the taper must be considered. In addition, the change in location of the center of mass affects the natural frequency of the system. The exact formulation of the natural frequency of a cantilevered tapered pole is not available in a closed form format. Therefore, an approximate solution must be provided. Considering the frequency equation for prismatic poles, the same equation can be proposed for tapered poles, except that the inertia term is replaced by the average inertia of the tapered pole.

The proposed equation for tapered poles, thus, takes the form

$$f_n = \frac{1}{2\pi}\sqrt{\frac{3EI_{avg}}{(M_{top} + 0.24M_{pole})L^3}}$$

where

$$I_{avg} = \frac{I_{top} + I_{bottom}}{2}$$

and I_{top} is the moment of inertia at the top of the pole and I_{bottom} is the moment of inertia at the bottom of the pole.

C.4 COMPARISON OF RESULTS

To compare the results obtained with the current and proposed frequency equations, eight examples were analyzed. The first four examples were taken from plans of various DOTs, and can be viewed as practical examples. They are summarized in Table C-1.

The last four examples are the same as the first four examples, except that the poles are assumed to be prismatic rather than tapered. They are summarized in Table C-2.

Both sets of examples were analyzed using the *SAP90* computer program to obtain the "exact" natural frequencies, corresponding to the mode of bending vibration due to an excitation applied at the top of the pole. The results of the *SAP90* analysis were compared to the results obtained by using the current and the proposed equations to compute the fundamental natural frequency of a pole. The results and a comparison among the three methods are shown in Table C-3.

Table C-3 shows that the equation outlined in the current AASHTO *Supports Specifications* produces a significant overestimation of the fundamental frequencies of single vertical supports (poles). The overestimation increases as the mass attached at the top of the pole becomes comparable in magnitude with the mass of the pole itself, because the mass attached at the top of the pole is neglected in the equation outlined in the current *Supports Specifications*. This situation can be clearly observed in example 1, in which the mass attached at the top of the pole is 54 percent of the mass of the pole. In this case, the current equation overestimates the fundamental frequency of the system by 98 percent. On the other hand, when the mass attached at the top of the pole is small in comparison with the mass of the pole, the results obtained with the equation outlined in the current *Supports Specifica-*

TABLE C-2 Examples 5 through 8

Number	Example	Type	Material	Length (feet)	Bottom Diameter (inches)	Top Diameter (inches)	Wall Thickness (inches)	Tip Load (pounds)
5	Street Lighting Pole	Prismatic	Steel	27	7	7	0.125	101
6	High Mast Pole	Prismatic	Steel	100	22.25	22.25	0.375	1800
7	High Mast Pole	Prismatic	Steel	125	25.375	25.375	0.438	1800
8	High Mast Pole	Prismatic	Steel	150	28.375	28.375	0.500	1800

TABLE C-3 Results of examples 1 through 8

Example	Mass of the Pole (lb-s^2/in)	Mass attached at the top of the pole (lb-s^2/in)	Frequency from *SAP90* (Hz)	Frequency from AASHTO (Hz)	Frequency from Proposed Equation (Hz)	Ratio of AASHTO/*SAP90*	Ratio of Proposed Eq./*SAP90*
1	0.479	0.261	1.353	2.684	1.238	1.984	0.916
2	15.18	4.663	0.374	0.677	0.350	1.810	0.937
3	24.44	4.663	0.316	0.516	0.291	1.634	0.922
4	36.46	4.663	0.273	0.417	0.247	1.529	0.904
5	0.642	0.261	1.576	2.632	1.576	1.670	1.000
6	22.71	4.663	0.440	0.610	0.441	1.387	1.002
7	37.80	4.663	0.355	0.445	0.356	1.255	1.004
8	57.88	4.663	0.293	0.346	0.294	1.181	1.005

tions tend to converge to the results obtained with the exact analysis (*SAP90* analysis). This situation can be observed in Example 8, in which the mass attached at the top of the pole is 8 percent of the mass of the pole. In this case, the current equation overestimates the fundamental frequency of the system by 18 percent.

Another important observation is the effect of the taper in the estimation of the natural frequency of the system. The current equation can be applied directly to prismatic poles, and the results obtained are acceptable as seen in examples 5 through 8, where the error in the estimation of the natural frequency ranges from 18 to 67 percent. When the current equation is applied to tapered poles, the accuracy of the results decays rapidly, as seen in examples 1 through 4, where the error in the estimation of the natural frequency ranges from 53 to 98 percent, making these results worthless for engineering purposes.

The proposed equation includes the effect of the mass attached at the top of the pole. It produces more accurate results than those obtained with the current equation. For tapered poles, the proposed equation estimates the frequencies within 10 percent (examples 1 through 4), which should be acceptable for practical engineering purposes. For prismatic poles, the proposed equation produces "exact" results. This can be seen in examples 5 through 8, in which the differences between the results obtained from the *SAP90* model and the results obtained from the proposed equation are negligible.

C.5 CONCLUSIONS

The current equation for computing the fundamental frequency of vertical supports leads to an overestimation of the frequency because it does not consider the effect of the mass located at the top of the pole. The magnitude of the error in the estimation of the frequency is dependent upon the ratio of the mass located at the top of the pole with respect to the mass of the pole itself. If the mass at the top of the pole is comparable in magnitude with the mass of the pole, the error in the estimation can be considerable and the results obtained are useless for engineering purposes. If the mass at the top of the pole is small compared with the mass of the pole, the error in the estimation of the fundamental frequency is small and the results obtained can be used for engineering purposes. If the poles are tapered, the current equation for the estimation of the frequency is inaccurate and leads to erroneous results.

Because the proposed equation considers the effect of the mass of the pole and the mass at the top of the pole, the results are exact for prismatic poles. On the other hand, for tapered poles, the use of the average moment of inertia of the pole produces results within 10 percent of the exact frequencies, but with the advantage of requiring simplified calculations.

From these conclusions, the research team recommends replacing the current equation for estimating the fundamental frequencies of vertical support with the proposed equation.

APPENDIX D

EVALUATION OF SPAN WIRE ANALYSIS PROCEDURES

D.1 INTRODUCTION

The current *Supports Specifications* provides two methods for the analysis of span wire structures. In the *simplified* method, the wire tension is obtained by equilibrium forces neglecting the lateral deflection of the vertical support. In the *detailed* method, the wire tension is obtained by equilibrium forces considering the lateral deflection of the vertical support due to the applied loads.

Results obtained from the two methods differ appreciably; the simplified method produced conservative results when compared to the detailed method. The accuracy of these methods has been evaluated by comparing their results with those obtained from other methods.

D.2 OBJECTIVES

The objectives of this study are to

- Evaluate the simplified method;
- Evaluate the detailed method;
- Compare methods and establish differences and ranges of applicability;
- Compare the two methods to an exact nonlinear FEA analysis;
- Establish the accuracy of methods; and
- Rewrite the span wire calculation procedures for clarity and simplicity.

D.3 CURRENT *SUPPORTS SPECIFICATIONS'* SPAN WIRE DESIGN PHILOSOPHIES

The current *Supports Specifications* explains two methods for computing forces on span wire structures subjected to vertical loads as well as horizontal loads acting perpendicular to the wire.

D.3.1 Simplified Method

The simplified method neglects the deflection of the supports as a result of the applied loads on the wire. The forces in the wire are simply calculated by solving the equilibrium equations obtained from statics. To apply this method, a deflected shape of the wire under vertical loads must be assumed. A sag value of 5 percent of the span length at the point of maximum deflection due to dead loads is typically used. The wire's own loadings are then applied as a series of concentrated loads along the wire to represent the actual uniform loadings. For more accuracy, a minimum value of five concentrated loads is recommended. The vertical loads caused by signals and signs are also applied to determine the internal forces and reactions produced by gravitational loadings. The wind forces are then applied and the tension of the wire is determined, combining the effects of gravitational loads and wind loads.

The horizontal and vertical reactions of the wire perpendicular to the span are determined by statics, as shown in Figure D-1. The horizontal reaction of the wire parallel to the span, F_x, has to be determined with geometry, using the fact that the ratio of the vector length over the ratio of the vector force is proportional to the ratio of a component length over a component force. The total length of the wire may be expressed as:

$$\text{Length} = \sum_{i=1}^{n} \sqrt{F_{xi}^2 + F_{yi}^2 + F_{zi}^2}\, \frac{d_{xi}}{F_{xi}}$$

where

n = number of segments in the span;
F_{xi} = vector force component in the direction of the span acting in the ith segment, and constant for all the segments;
F_{yi} = vector force component in the vertical direction acting in the ith segment;
F_{zi} = vector force component in the horizontal direction perpendicular to the wire, acting in the ith segment; and
d_{xi} = vector length component in the direction of the span.

Because the length is established when the sag is assumed, F_x may be determined by a series of trial solutions, knowing that F_{xi} equals F_x and is constant over the span length.

D.3.2 Detailed Method

The detailed method follows the same procedure to compute the wire tension and reactions as the simplified method. However, to account for the horizontal deflection of the ver-

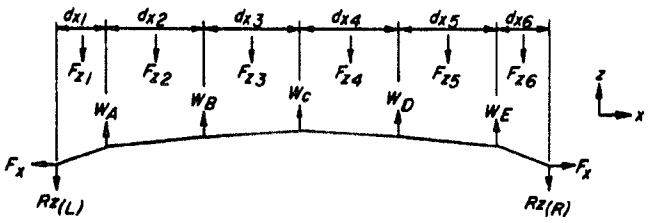

Figure D-1. Lateral forces on the wire.

tical support due to dead and wind loads, the following iterative procedure is provided:

1. Adjust the length of the wire according to the increase in horizontal deflection of the vertical supports, considering that the span length remains constant. The initial deflection of the vertical support may be calculated by using the wire's horizontal force component obtained by applying the dead load alone. All loads acting on the span wire structure must be considered to compute the horizontal deflection of the vertical support. However, to adjust the length of the wire, the deflection from dead load must be neglected, because it is already included in the analysis when the initial sag is determined under dead load.
2. Compute the magnitude of the horizontal reaction on the vertical support due to wire tension, considering the adjusted length of the wire.
3. Compute a new value for the deflection of the vertical support, considering the new value of the horizontal reaction.
4. Repeat steps 1 through 3 until the difference between the horizontal deflection of the vertical support obtained in two consecutive iterations is very small. At least two adjustments of the length of wire must be made to obtain a final force component.

D.4 COMPARISON OF METHODS

The two methods were evaluated on their correctness and range of applicability. Results obtained with the two methods differ appreciably, with the simplified method yielding highly conservative results. The differences between the two methods mainly stem from the consideration of the stiffness of the vertical supports. Both the simplified and detailed methods were also compared to the Strain Pole Program developed by the Florida DOT (*129*), and an approximate method used by the Georgia DOT (*134*). Additionally, the two methods were compared to a nonlinear static analysis performed by finite elements using the *COSMOS/M* software. In the finite element analysis, both rigid and flexible supports were considered in the determination of the tensions in the span wires.

D.4.1 Simplified and Detailed Methods of the Current *Supports Specifications*

Because the simplified and detailed methods require iterations to obtain a final result, a spreadsheet was developed with the simplified and the detailed methods. This spreadsheet can be used for single span configurations with up to nine point loads located along the wire. The spreadsheet requires data corresponding to span length, wind velocity, wire diameter, and initial sag at the point of maximum deflection. In addition, it requires the location and magnitude of the dead and wind components of the point loads. The spreadsheet computes the wire length considering dead loads only. It also computes the force components in the vertical and normal direction for each segment of the wire. With these results, the spreadsheet computes by iteration the transverse force component for all the segments of the wire, obtaining the tension in the wire due to dead and wind loads. When the spreadsheet is performing the analysis considering flexible vertical supports, it adjusts the length of the wire according to the deflection of the poles and iterates the process until the tensions computed in two consecutive cycles converge.

D.4.2 Strain Pole Program (Florida DOT)

The *Strain Pole Program* calculates the forces in the span wire and the applied loads at the vertical support. It computes the required vertical support size, considering the final deflections of the wire and the requirements of vertical clearance for a given intersection. The program is based on the following assumptions:

- The basic wind pressure is computed in accordance with the formula given in section 1.2.5 of the current *Supports Specifications*. The height coefficient is 1.0.
- The wind loading on the poles is computed using the appropriate height coefficients and a drag coefficient of 1.5. The drag coefficient is slightly greater than the specification value of 1.45 for square shapes.
- Each support cable takes all of the applied dead and wind loads without interacting with any other cable or structural element. The effect of the deflection of the pole caused by the loads applied at the cable is neglected.

D.4.3 Approximate Method (Georgia DOT)

Georgia DOT uses an approximate method for the analysis of span wire structures. The method makes use of plane analysis of cables for the dead loads and the wind loads, and then superimposes the results by using vector analysis to obtain the final forces in the vertical support and the components of the tensions.

The plane analysis of cables is based on simple statics of cables. According to the statics of cables, if the maximum sag, and the forces acting on the cable are known, the internal tensions in the cable can be determined by using the equilibrium of a rigid body for a segment of the cable. Cables cannot resist moments; therefore, the static moment at a given point of the cable has to be equilibrated by a couple formed by the horizontal reaction of the cable at the support and the horizontal component of the tension in the cable for that segment. This horizontal component of the tension is constant along the cable. Based on this property of cables, the tensions in the cables are easily determined. The analysis of cables then reduces to the analysis of a simple supported beam. With the results of the beam analysis, the transverse reactions at the supports are determined. To determine the horizontal reactions parallel to the cable, the shear diagram is drawn. From the shear diagram, the point of maximum moment is determined by finding the point where the shear of the beam is equal to zero. Once the location of maximum moment is determined, the maximum moment is determined and decomposed into couples formed by the horizontal reaction at the support and the horizontal component of the tension in the segment under analysis. The maximum tension in the cable is the tension of the cable at the support.

When cables are subjected to dead loads and wind loads, Georgia DOT uses the following procedure to find the tensions in span wires:

1. Determine the tension in the span wire due to dead load only by applying a 5 percent sag at the point of zero shear and perform the planar analysis of the cable.
2. Determine the tension in the span wire due to wind load only by applying a 5 percent sag at the point of zero shear and perform the planar analysis of the cable.
3. At the point of attachment to the vertical support, determine the horizontal reaction parallel to the wire by adding the horizontal reaction due to dead load only plus the horizontal reaction due to wind load only.
4. The vertical reaction at the support is determined from the beam analysis with dead load only, and the transverse horizontal reaction is determined from the beam analysis with wind load only.
5. The maximum tensions in the cable are found by performing the vectorial sum of the reaction components at the point of attachment to the vertical support.

D.4.4 Nonlinear Finite Element Analysis (*COSMOS/M*)

To compare the simplified and detailed methods, a highly refined analysis, using the *NSTAR* module of the finite element program *COSMOS* from Structural Research and Analysis Corporation, has been performed. This program considers the nonlinear behavior of the span wire structures and is capable of considering the flexibility of the vertical supports.

The *NSTAR* module of the *COSMOS* program can handle the geometric nonlinearities due to the effect of *large displacements* that occur in span wire structures. To consider these geometric nonlinearities, the program considers a co-rotational system of axes attached to the cable elements during motion and uses advanced techniques, such as the Newton-Raphson method, to solve the system of nonlinear equations that describe the behavior of the span wire.

D.4.5 Numerical Examples

Several examples with different configurations have been analyzed by using the simplified and detailed methods and compared to the results obtained with the Florida DOT strain pole program, the Georgia DOT approximate method, and the more exact finite element solutions obtained with *COSMOS*. With *COSMOS*, two types of runs have been performed. In the first run, the examples have been analyzed with rigid supports. These results can be compared directly to the results obtained with the simplified method, which neglects the flexibility of the vertical supports. In the second run, the examples have been analyzed with flexible supports. These results can be compared directly to the results obtained with the detailed method, which also considers the flexibility of the vertical supports. Table D-1 shows the examples that were analyzed. Wind loads were calculated according to the current *Supports Specifications* wind load provisions.

Examples 1, 2, and 3 were analyzed for forces resulting from the application of two wind speeds (V_w) of 80 and 100 mph for a single span.

Examples 4, 5, and 6 were analyzed for forces resulting from the application of two wind speeds (V_w) of 80 and 100 mph for a box. Only maximum tensions, obtained when the wind is acting normal to the wire, are shown.

Examples 7, 8, and 9 were analyzed for forces resulting from the application of a wind speed (V_w) of 80 mph for a single span tethered configuration. They were analyzed by using the simplified method. The wind forces were equally distributed between the span wire and the tethered wire. Tethered wires were assumed to have a sag of 1.5 percent of the span. They were not assumed to take any vertical load.

The span wire tensions calculated for each example are summarized in Tables D-2 through D-5 and Figures D-2 through D-5.

Table D-2 and Figure D-2 summarize the maximum tensions in the wire obtained for Examples 1, 2, and 3. Those tensions were obtained for vertical loads and wind loads applied normal to the span wire. The results obtained from the Florida DOT program compared very well with the results obtained with the simplified method. For these three

TABLE D-1 List of examples

Example	Figure	Span (ft)	Configuration	Loads	Wind Speed Curr. Spec. (mph)	Height of Pole (ft)	Sag (%)	Simplified Method	Detailed Method	Strain Pole Program from FL DOT	Approx. Method from Ga DOT	*COSMOS*/M
1	Figure D-7	75	Single span	Two 3 lens 8" signals and 1 sign	80/100	25	5	yes	yes	yes	yes	yes
2	Figure D-8	120	Single span	Two 3 lens 12" signals, one 5 lens 12" signal, one sign	80/100	28	5	yes	yes	yes	yes	yes
3	Figure D-9	170	Single span	Three 3 lens 12" signals, one 5 lens 12" signal, one sign	80/100	31	5.3	yes	yes	yes	yes	yes
4	Figure D-10	75	Box	Two 3 lens 8" signals and 1 sign	80/100	25	5.25	yes	yes	yes	yes	yes
5	Figure D-11	120	Box	Two 3 lens 12" signals, one 5 lens 12" signal, one sign	80/100	28	5.62	yes	yes	yes	yes	yes
6	Figure D-12	170	Box	Three 3 lens 12" signals, one 5 lens 12" signal, one sign	80/100	31	5.83	yes	yes	yes	yes	yes
7	Figure D-13	75	Single span tethered	Two 3 lens 8" signals and 1 sign	80	25	5	yes	no	no	no	no
8	Figure D-14	120	Single span tethered	Two 3 lens 12" signals, one 5 lens 12" signal, one sign	80	28	5	yes	no	no	no	no
9	Figure D-15	170	Single span tethered	Three 3 lens 12" signals, one 5 lens 12" signal, one sign	80	31	5.3	yes	no	no	no	no

TABLE D-2 Tensions in wires (lb) for examples 1 through 3

Example	Wind Velocity V_w (mph)	Span (ft)	Simplified Method (lbs)	Detailed Method (lbs)	FDOT Method (lbs)	GDOT Method (lbs)	Cosmos with Rigid Supports (lbs)	Cosmos with Flexible Supports (lbs)	Ratio of FDOT Method to Simplified Method	Ratio of Detailed Method to Simplified Method	Ratio of GDOT Method to Simplified Method	Ratio of Cosmos with Rigid Supports Method to Simplified Method	Ratio of Cosmos with Flexible Supports Method to Simplified Method
1	80	75	2440	1769	2589	2902	2176	1176	1.06	0.73	1.19	0.89	0.48
2		120	4478	3200	4145	5537	4022	2426	0.93	0.71	1.24	0.90	0.54
3		170	5214	4039	5127	6909	4702	2657	0.98	0.77	1.33	0.90	0.51

TABLE D-3 Tensions in wires (lb) for examples 1 through 3 (V_w = 100 mph)

Example	Wind Velocity V_w (mph)	Span (ft)	Simplified Method (lbs)	Detailed Method (lbs)	FDOT Method (lbs)	GDOT Method (lbs)	Cosmos with Rigid Supports (lbs)	Cosmos with Flexible Supports (lbs)	Ratio of FDOT Method to Simplified Method	Ratio of Detailed Method to Simplified Method	Ratio of GDOT Method to Simplified Method	Ratio of Cosmos with Rigid Supports Method to Simplified Method	Ratio of Cosmos with Flexible Supports Method to Simplified Method
1	100	75	3744	2424	3858	4207	3673	1495	1.03	0.65	1.12	0.98	0.40
2		120	6767	4250	6066	7837	5494	2825	0.90	0.63	1.16	0.81	0.42
3		170	7839	5429	7531	9757	6064	3355	0.96	0.69	1.24	0.77	0.43

TABLE D-4 Tensions in wries (lb) for examples 4 through 6

Example	Wind Velocity V_w (mph)	Span (ft)	Simplified Method (lbs)	Detailed Method (lbs)	FDOT Method (lbs)	GDOT Method (lbs)	Cosmos with Rigid Supports (lbs)	Cosmos with Flexible Supports (lbs)	Ratio of FDOT Method to Simplified Method	Ratio of Detailed Method to Simplified Method	Ratio of GDOT Method to Simplified Method	Ratio of Cosmos with Rigid Supports Method to Simplified Method	Ratio of Cosmos with Flexible Supports Method to Simplified Method
4	80	75	2327	1730	2583	2767	2067	1117	1.11	0.74	1.19	0.89	0.48
5		120	3994	2995	4127	4935	3821	2305	1.03	0.75	1.24	0.96	0.58
6		170	4751	3803	5101	5940	4467	2524	1.07	0.80	1.25	0.94	0.53

TABLE D-5 Tensions in wires (lb) for examples 4 through 6 (V_w = 100 mph)

Example	Wind Velocity Vw (mph)	Span (ft)	Simplified Method (lbs)	Detailed Method (lbs)	FDOT Method (lbs)	GDOT Method (lbs)	Cosmos with Rigid Supports (lbs)	Cosmos with Flexible Supports (lbs)	Ratio of FDOT Method to Simplified Method	Ratio of Detailed Method to Simplified Method	Ratio of GDOT Method to Simplified Method	Ratio of Cosmos with Rigid Supports Method to Simplified Method	Ratio of Cosmos with Flexible Supports Method to Simplified Method
4	100	75	3571	2383	3850	4011	3489	1420	1.08	0.67	1.12	0.98	0.40
5		120	5493	3877	6036	6355	5219	2684	1.10	0.71	1.16	0.95	0.49
6		170	7143	5168	7488	8390	5761	3187	1.05	0.72	1.17	0.81	0.45

examples, the maximum difference is about 6 percent and the average difference is about 1 percent, which indicates close agreement between the two methods. When the results obtained with the simplified method are compared with the results obtained with the detailed method, the maximum difference between the two methods is 29 percent and the average difference is about 26.4 percent, showing that the simplified method is more conservative than the detailed one. When comparing the Georgia DOT method with the simplified method, the differences between the two methods range from 19 percent in example 1 to 33 percent in example 3, with the Georgia DOT method being more conservative than the simplified method. Comparing the results of *COSMOS* with rigid supports with the simplified method, the differences between the two methods range from 11 percent in example 1 to 10 percent in example 3, with the simplified method being more conservative than *COSMOS* with rigid supports. Comparing the results of *COSMOS* with flexible supports with the simplified method, the differences between the two methods range from 52 percent in example 1 to 49 percent in example 3, with the simplified method being more conservative than *COSMOS* with flexible supports.

Table D-3 and Figure D-3 summarize the maximum tensions in the wire obtained for Examples 1, 2, and 3, when analyzed under the action of vertical loads and wind loads corresponding to a wind velocity (V_w) of 100 mph. The tensions were obtained for vertical loads and wind loads applied normal to the span wire. The results show that the Florida DOT program is in close agreement with the simplified method. For these three examples, the maximum difference was 9 percent and the average difference was 4 percent. Comparing the results obtained from the simplified method with those obtained from the detailed method, the maximum difference between the two methods is 37 percent and the average difference is 34 percent, showing that the simplified method is more conservative than the detailed one. Comparing the Georgia DOT method with the simplified method, the differences between the two methods range from 12 percent

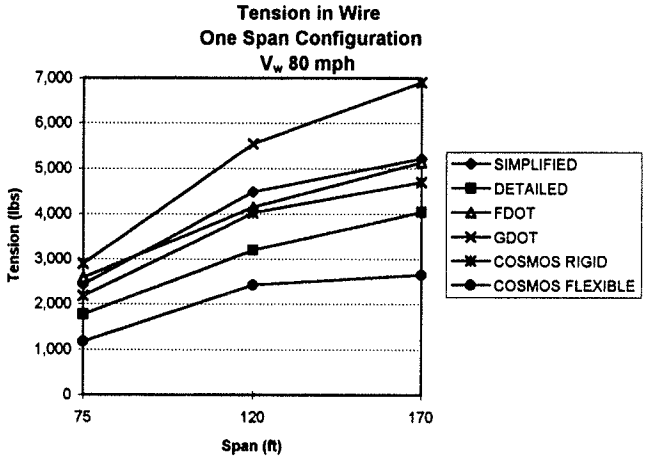

Figure D-2. Tensions in wire for examples 1 through 3.

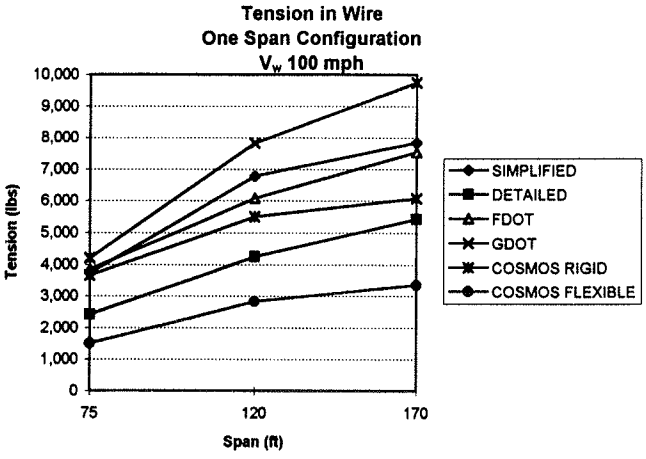

Figure D-3. Tensions in wire for examples 1 through 3 (V_w = 100 mph).

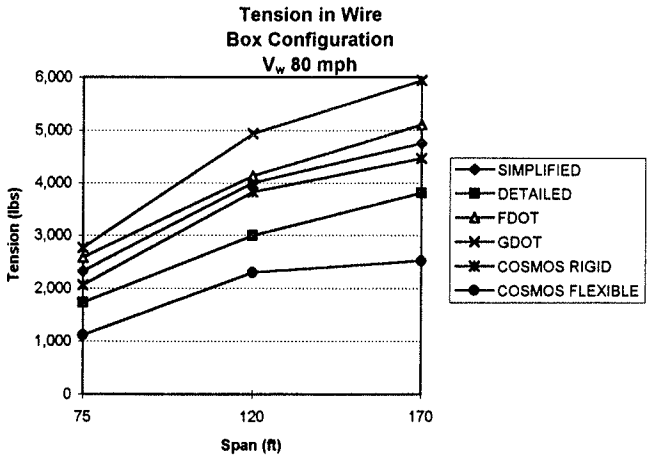

Figure D-4. Tensions in wire for examples 4 through 6.

in example 1 to 24 percent in example 3, with the Georgia DOT method being more conservative than the simplified one. Comparing the results from *COSMOS* with rigid supports to the simplified method, the differences between the two methods range from 2 percent in example 1 to 23 percent in example 3, with the simplified method being more conservative than *COSMOS* with rigid supports. Comparing the results from *COSMOS* with flexible supports to the simplified method, the differences between the two methods range from 60 percent in example 1 to 57 percent in example 3, with the simplified method being more conservative than *COSMOS* with flexible supports.

As shown in Figure D-3, the detailed method is more conservative than *COSMOS* with flexible supports. Assuming the results from *COSMOS* as being "exact," the detailed method overestimates the tensions of span wires when the lateral flexibility of the support is included in the analysis.

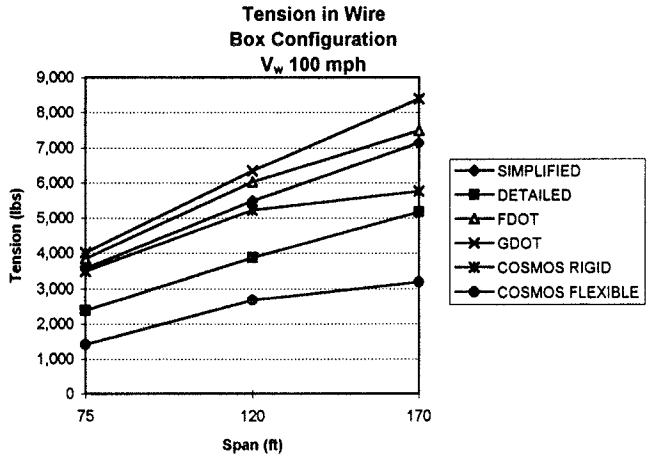

Figure D-5. Tensions in wire for examples 4 through 6 (V_w = 100 mph).

When comparing the results of Table D-2 with the results of Table D-3, the differences between the simplified method and the detailed method are greater for Table D-3. This can be attributed to the increase in lateral deflection of the vertical supports due to the increased tension in the wires because of the increased wind load.

Table D-4 and Figure D-4 summarize the maximum tensions in the wire obtained for Examples 4, 5, and 6, when analyzed for vertical loads and an 80-mph wind speed. The tensions of the wires were obtained for vertical load and wind load applied normal to the span wire. From these data, the results obtained from the Florida DOT program are slightly conservative compared to the simplified method. For these three examples, the maximum difference is 11 percent and the average difference is 8.3 percent. Comparing the results obtained from the simplified method with those obtained from the detailed method, the maximum difference between the two methods is 29 percent and the average difference is 26.4 percent, indicating that the simplified method is conservative compared with the detailed one. Comparing the Georgia DOT method with the simplified one, the differences between the two methods range from 19 percent in example 4 to 25 percent in example 6, with the Georgia DOT method being more conservative than the simplified one. Comparing the results from *COSMOS* with rigid supports to the simplified method, the differences between the two methods range from 11 percent in example 4 to 6 percent in example 6, with the simplified method being more conservative than *COSMOS* with rigid supports. Comparing the results from *COSMOS* with flexible supports with the simplified method, the differences between the two methods range from 52 percent in example 4 to 47 percent in example 6, with the simplified method being more conservative than *COSMOS* with flexible supports.

As shown in Figure D-4, the detailed method is more conservative than *COSMOS* with flexible supports. Considering the results from *COSMOS* as being "exact," the detailed method overestimates the tensions of span wires when the lateral flexibility of the support is included in the analysis.

Table D-5 and Figure D-5 summarize the maximum tensions in the wire obtained for examples 4, 5, and 6, when analyzed for vertical loads and a 100-mph wind speed. The tensions were obtained for vertical load and wind load applied normal to the span wire. From this data, the results obtained from Florida DOT program are slightly conservative compared with the results obtained from the simplified method. For these three examples, the maximum difference is 8 percent and the average difference is 7 percent. Again, this can be attributed to the fact that the simplified method is applied to a single span wire structure without considering the interaction between the adjacent span wires, which is accounted for in the Florida DOT program. Comparing the results obtained from the simplified method with those obtained from the detailed one, the maximum difference between the two methods is 33 percent and the average difference is 27

TABLE D-6 Tensions in wires (lb) for examples 7 through 9

Example	Velocity, V_w, (mph)	Span (ft)	Tethered Wire (lb)	Main Wire (lb)	Ratio of Tethered Wire to Main Wire
7	80	75	2660	1396	1.91
8		120	5220	2684	1.94
9		170	8453	3251	2.60

percent, showing that the simplified method is more conservative than the detailed method. Comparing the Georgia DOT method with the simplified method, the differences between the two methods range from 12 percent in example 4 to 17 percent in example 6, with the Georgia DOT method being more conservative than the simplified method. Comparing the results from *COSMOS* with rigid supports with the simplified method, the differences between the two methods range from 2 percent in example 4 to 19 percent in example 6, with the simplified method being more conservative than *COSMOS* with rigid supports. Comparing the results from *COSMOS* with flexible supports with the simplified method, the differences between the two methods range from 60 percent in example 4 to 55 percent in example 6, with the simplified method being more conservative than *COSMOS* with flexible supports.

Figure D-5 shows that the detailed method is more conservative than *COSMOS* with flexible supports. Considering *COSMOS* results as being "exact," the detailed method overestimates the tensions of span wires when the lateral flexibility of the support is included in the analysis.

Tethered Configurations

Examples 7, 8, and 9 were analyzed to evaluate the effect of tethered wires. Tethered wires are usually placed below the span wires to provide a stabilizing wire for the signs and signals attached to the span wire. Because of the construction sequence, tethered wires are usually placed with very small sags. Because they have smaller sags than span wires, the possibility exists that tethered wires have to support higher tensions due to wind loads acting in the transverse direction of the span.

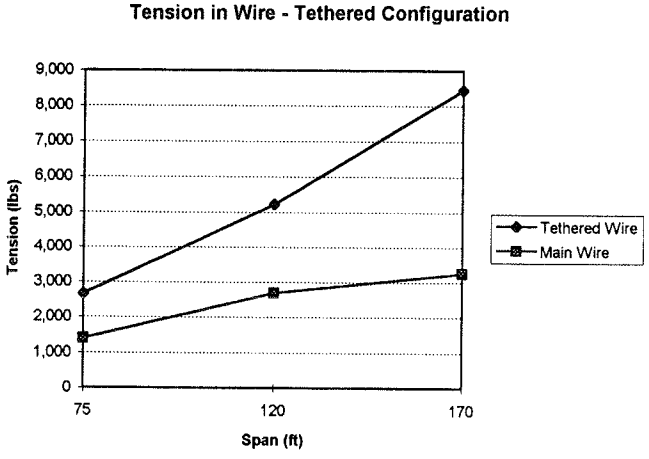

Figure D-6. Tension in wire for examples 7 through 9.

Table D-6 and Figure D-6 summarize the maximum tensions in the span wire and tethered wire for the tethered configurations of examples 7, 8, and 9, when analyzed for vertical loads and an 80-mph wind speed computed according to the current *Supports Specifications*. Wind loads were assumed equally distributed between the span wire and the tethered wire, while vertical loads were applied only to the span wire. Tethered wires were assumed to have a constant sag of 1.5 percent of the span. In tethered configurations, tethered wires tend to develop higher forces than span wires because of the small sag that tethered wires normally have. Comparing the tension forces obtained for span and tethered wires, it is clear that for tethered configurations (when the tethered wires are assumed to support wind loads), the vertical supports have to be stiffer than those required for similar nontethered configurations. Therefore, non-tethered configurations will result in more economical designs.

An alternative design approach, used in some DOTs (New York, Georgia, and Texas) for tethered configurations, assumes that the tethered wire fails under design wind loads. Thus, the forces developed in the tethered wires are not considered in the analysis or design of the span wire structure.

CONCLUSIONS

Figures D-7 through D-15 show the loads and dimensions for examples 1 through 9. From the analysis performed and the results shown, the following conclusions can be drawn:

- The simplified method is significantly more conservative than the detailed method. Span wire forces calculated by both methods showed differences between the two methods that range between 30 and 40 percent for equivalent configurations. These differences can increase or decrease depending on the degree of flexibility of the vertical support. For ideal rigid supports with no flexibility, the detailed method converges to the simplified method. The opposite is also valid for very

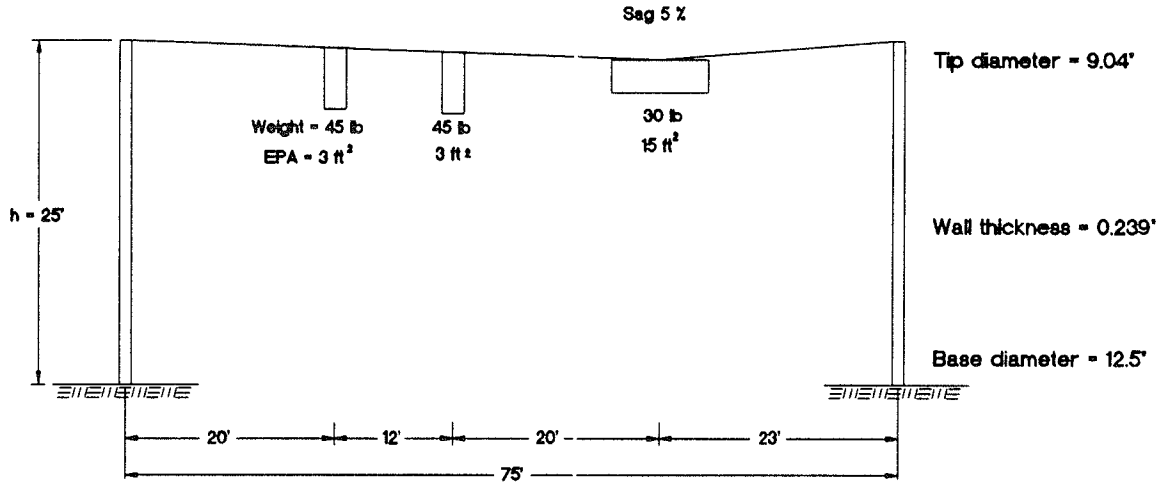

Figure D-7. Example 1.

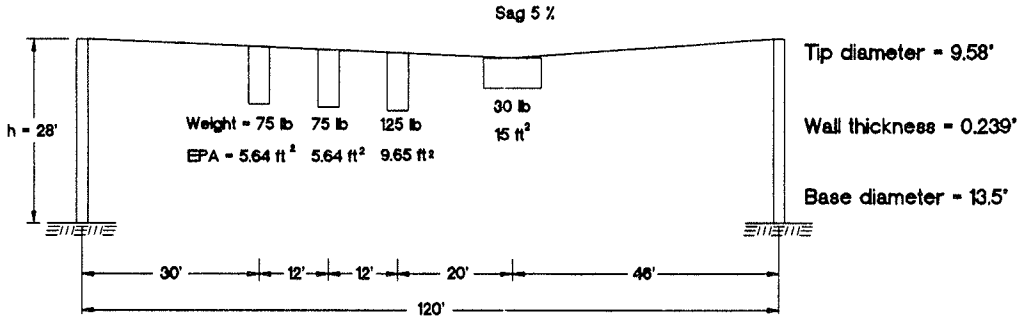

Figure D-8. Example 2.

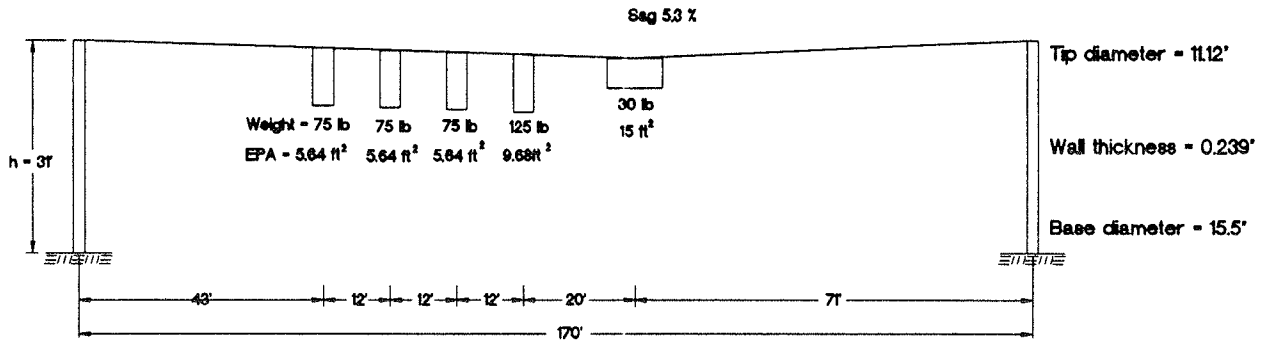

Figure D-9. Example 3.

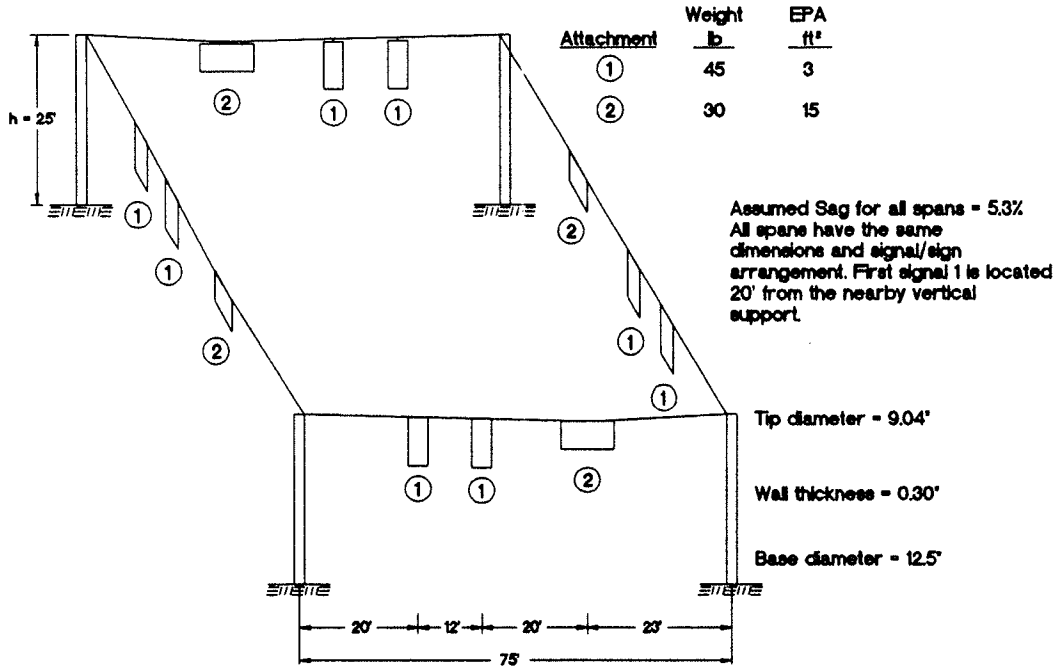

Figure D-10. Example 4.

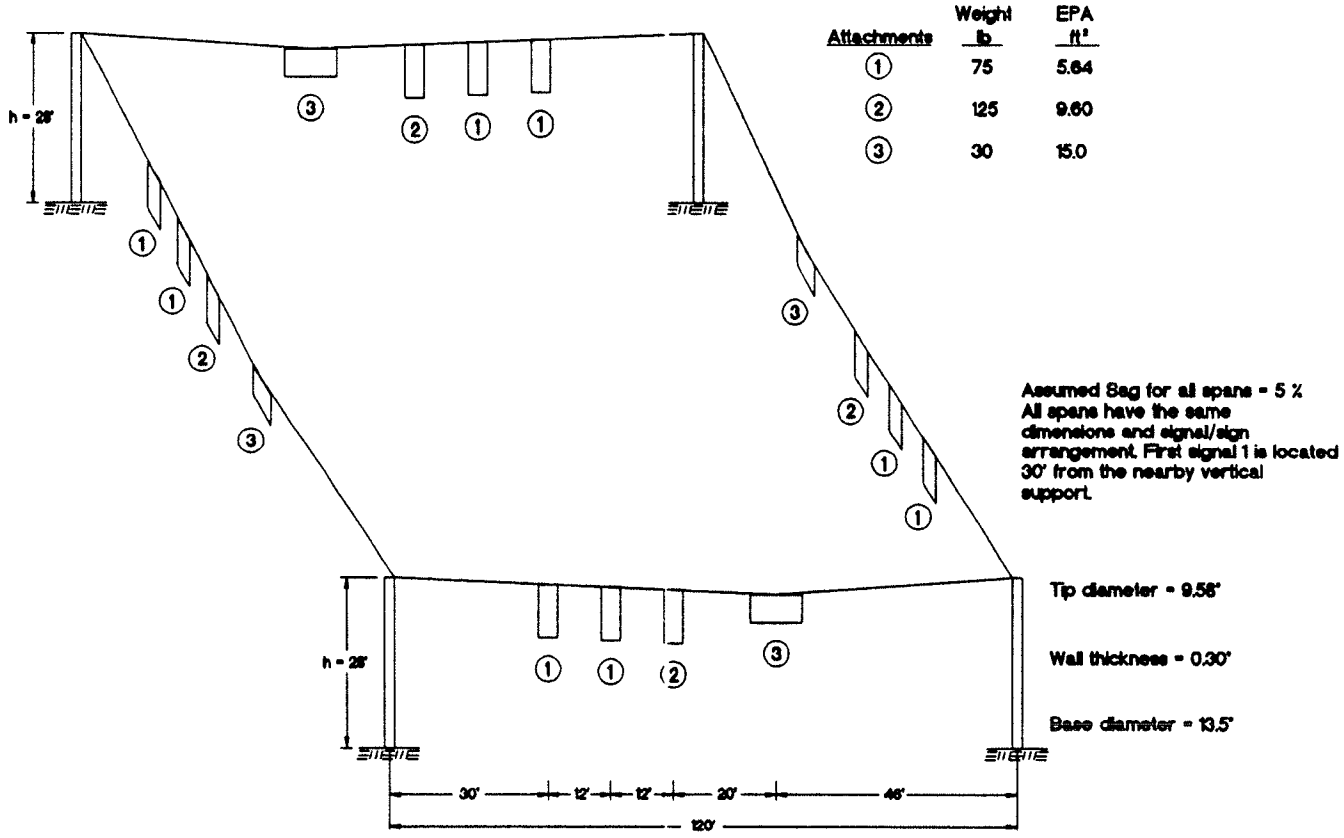

Figure D-11. Example 5.

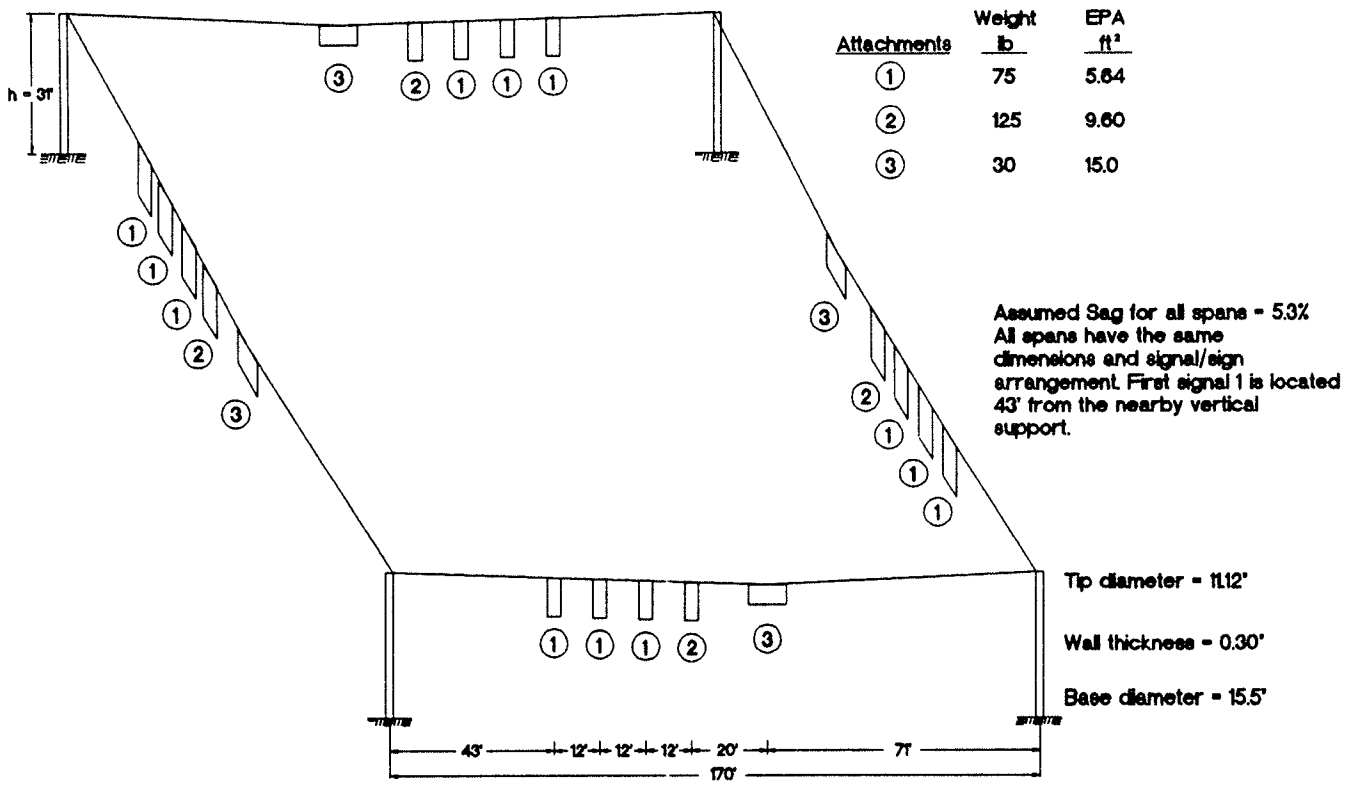

Figure D-12. Example 6.

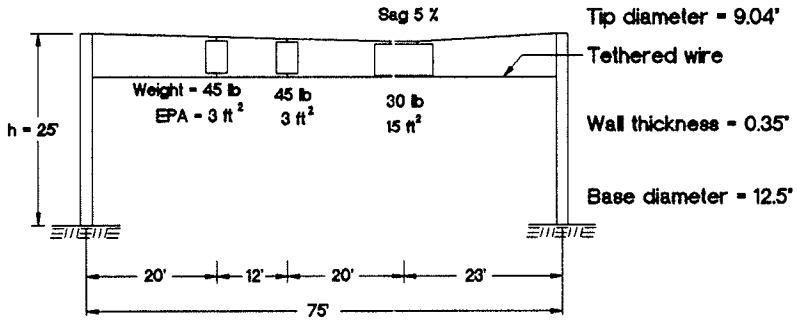

Figure D-13. Example 7.

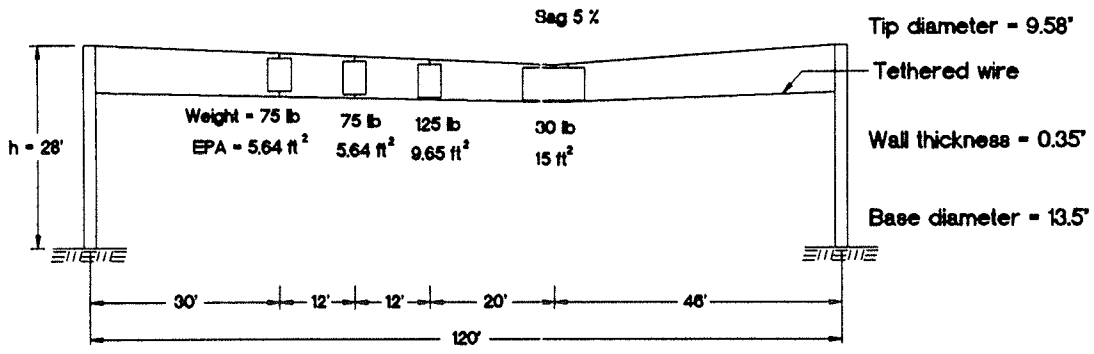

Figure D-14. Example 8.

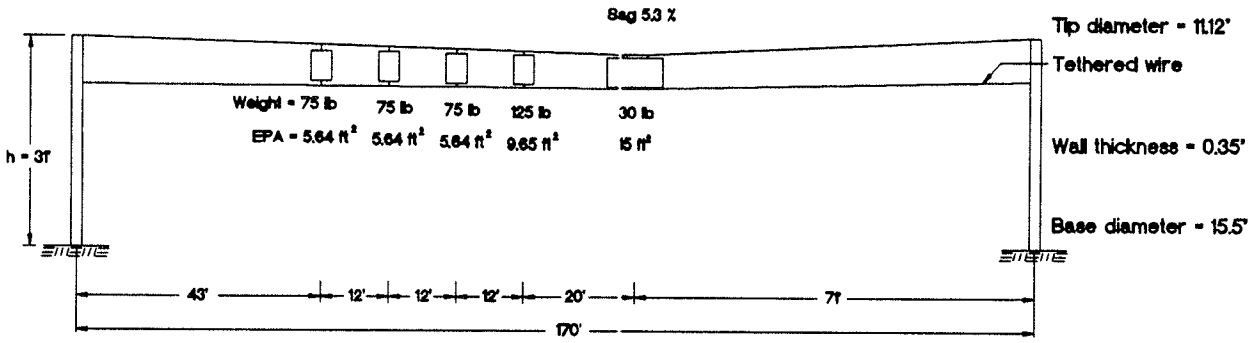

Figure D-15. Example 9.

flexible supports, or in situations in which the vertical support experiences other excitations that cause it to deflect in the direction of the span. In these situations, the simplified method can provide values of tensions 100 percent greater or more than the detailed method. Both methods can be used in the proposed specification,depending on the kind of analysis to be performed and subject to the designer's judgment.

- Considering the results obtained from *COSMOS* software as being "exact," the simplified method is more conservative than *COSMOS* with rigid supports. The amount of error in the estimation of the tensions in the wires ranges from 2 percent for example 1, with a wind speed of 100 mph, to 23 percent for example 3, with a wind speed of 100 mph. Because the analysis with *COSMOS* or similar finite element programs requires highly specialized software, as well as a solid background in nonlinear analysis from the designer, the simplified method appears to offer an appropriate method for analysis of span wire structures when the flexibility of the supports is not included in the analysis.
- Considering the results obtained from *COSMOS* software as being "exact," the detailed method is more conservative than *COSMOS* with flexible supports. The amount of error in the estimation of the tensions in the wires ranges from 30 percent for example 5, with a wind speed of 80 mph, to 67 percent for example 4, with a wind speed of 100 mph. Special considerations, such as deflection of the vertical supports, must be taken by the designer when using the detailed method. The deflection of the supports affects the magnitude of the induced tension in the wires and, hence, plays an important role in the determination of the member size of the vertical support.
- For single span configurations, the critical loading condition for computing the wire tension occurs when the wind is acting normal to the wire.
- Tethered configurations, where the tethered wires are considered as structural elements capable of taking wind loads, result in larger wire forces applied to the vertical support as compared to nontethered span wire configurations.

APPENDIX E

REFERENCES

1. AASHTO, *Standard Specifications for Structural Supports for Highway Signs, Luminaires and Traffic Signals*. Washington, DC (1985).
2. AASHTO, *Standard Specifications for Structural Supports for Highway Signs, Luminaires and Traffic Signals*. Washington, DC (1961).
3. AASHTO, *Standard Specifications for Structural Supports for Highway Signs, Luminaires and Traffic Signals*. Washington, DC (1968).
4. AASHTO, *Standard Specifications for Structural Supports for Highway Signs, Luminaires and Traffic Signals*. Washington, DC (1975).
5. AASHTO, *Standard Specifications for Structural Supports for Highway Signs, Luminaires and Traffic Signals*. Washington, DC (1994).
6. Ross, H.E., Jr., Sicking, D.L., Zimmer, R.A., and Mitchie, J.D., "Recommended Procedures for the Safety Performance Evaluation of Highway Features." *NCHRP Report 350*, Transportation Research Board, National Research Council, Washington, DC (1993) 142 pp.
7. AASHTO, *LRFD Bridge Design Specifications*. 1st Edition, Washington, DC (1994).
8. AISC, *Manual of Steel Construction - Load and Resistance Factor Design*. Chicago, IL (1986).
9. The Aluminum Association, *Aluminum Design Manual*. Washington, DC (1994).
10. ASCE, *LRFD Standard for Engineered Wood Construction*. Public Ballot Draft, New York (November 1994).
11. Ellingwood, B., Galambos, T.V., MacGregor, J.G., and Cornell, C.A., "Development of a Probability Based Load Criterion for American National Standard A58." NBS Special Publication 577, National Bureau of Standards (June 1980).
12. Ravindra, M.K., and Galambos, T.V., "Load and Resistance Factor Design for Steel." *Journal of the Structural Division*, ASCE, Vol. 104, No. ST9 (September 1978).
13. Yura, J.A., Galambos, T.V., and Ravindra, M.K., "The Bending Resistance of Steel Beams." *Journal of the Structural Division*, ASCE, Vol. 104, No. ST9 (September 1978).
14. Bjorhovde, R., Galambos, T.V., and Ravindra, M.K., "LRFD Criteria for Steel Beam-Columns." *Journal of the Structural Division*, ASCE, Vol. 104, No. ST9 (September 1978).
15. Ravindra, M.K., Cornell, C.A., and Galambos, T.V., "Wind and Snow Load Factors for Use in LRFD." *Journal of the Structural Division*, ASCE, Vol. 104, No. ST9 (September 1978).
16. Galambos, T.V., and Ravindra, M.K., "Properties of Steel for Use in LRFD." *Journal of the Structural Division*, ASCE, Vol. 104, No. ST9 (September 1978).
17. Ellingwood, B., MacGregor, J.G., Galambos, T.V., and Cornell, C.A., "Probability Based Load Criteria: Load Factors and Load Combinations." *Journal of the Structural Division*, ASCE, Vol. 108, No. ST5 (May 1982).
18. Galambos, T.V., Ellingwood, B., MacGregor, J.G., and Cornell, C.A., "Probability Based Load Criteria: Assessment of Current Design Practice." *Journal of the Structural Division*, ASCE, Vol. 108, No. ST5 (May 1982).
19. Heger, F.J., "Public Safety - Is It Compromised by New LRFD Design Standards?" *Journal of Structural Engineering*, Vol. 119, No. 4 (April 1993).
20. Milford, R.V., "Load Factors for Limit States Codes." *Journal of Structural Engineering*, Vol. 113, No. 9 (September 1987).
21. Ang, A.H.-S., and Cornell, C.A., "Reliability Bases of Structural Safety and Design." *Journal of the Structural Division*, ASCE, Vol. 100, No. ST9 (September 1974).
22. Ravindra, M.K., Lind, N.C., and Siu, W., "Illustrations of Reliability-Based Design." *Journal of the Structural Division*, ASCE, Vol. 100, No. ST9 (September 1974).
23. Hasofer, A.M., and Lind, N.C., "Exact and Invariant Second-Moment Code Format." *Journal of Engineering Mechanics Division*, Proceedings ASCE, Vol. 100, No. EM1 (February 1974).
24. Ministry of Transportation, *Ontario Highway Bridge Design Code*. Toronto, Ontario, Canada (1992).
25. ASCE, *Design of Steel Transmission Pole Structures*. 2nd Edition, Manuals and Reports on Engineering Practice No. 72, New York (1990).
26. American Inst. of Steel Construction, *Manual of Steel Construction - Allowable Stress Design*. 9th Edition, Chicago, IL (1989).
27. ASCE, *Standard Minimum Design Loads for Buildings and Other Structures*. ANSI/ASCE 7-95, New York (1995).
28. Kaczinski, M.R., Dexter, R.J., and Van Dien, J.P., "Fatigue-Resistant Design of Cantilevered Signal, Sign, and Light Supports." *NCHRP Report 412*, Transportation Research Board, National Research Council, Washington, DC (1998).
29. Gaylord, E.H., and Gaylord, C.N., eds., *Structural Engineering Handbook*. McGraw-Hill, New York (1990).
30. Sharp, M.L., *Behavior and Design of Aluminum Structures*. McGraw-Hill, New York (1993).
31. Task Committee on Wind Forces of the Committee on Loads and Stresses of the Structural Division, "Wind Forces on Structures." *Transactions*, ASCE, New York, Part 2, Vol. 126 (1961).
32. American National Standards Institute, *Building Code Requirements for Minimum Design Loads in Buildings and Other Structures*. ANSI A58.1-1972, New York (1972).
33. American National Standards Institute, *Minimum Design Loads for Buildings and Other Structures*. ANSI A58.1-1982, New York (1982).
34. ASCE, *Standard Minimum Design Loads for Buildings and Other Structures*. ANSI/ASCE 7-88, New York (1990).
35. ASCE, *Standard Minimum Design Loads for Buildings and Other Structures*. ANSI/ASCE 7-93, New York (1994).

36. Durst, C.S., "Wind Speeds over Short Periods of Time." *Meteorology Magazine*, Vol. 89 (1960).
37. Simiu, E., Changery, M.J., and Filliben, J.J., "Extreme Wind Speeds at 129 Stations in the Contiguous United States." Building Science Series Report 118, National Bureau of Standards, Washington, DC (1979).
38. Peterka, J.A., and Shahid, S., "Extreme Gust Wind Speeds in the U.S." Proceedings, 7th U.S. National Conference on Wind Engineering, UCLA, Los Angeles, CA, Vol. 2 (1993).
39. Thom, H.C.S., "New Distribution of Extreme Winds in the United States." *Proceedings of the American Society of Civil Engineers*, Structural Division, Vol. 94, No. ST7, ASCE, New York (1968).
40. Batts, M.E., Cordes, M.R., Russell, L.R., Shaver, J.R., and Simiu, E., "Hurricane Wind Speeds in the United States." NBS Building Science Series 124, National Bureau of Standards, Washington, DC (1980).
41. Georgiou, P.N., Davenport, A.G., and Vickery, B.J., "Design Wind Speeds in Regions Dominated by Tropical Cyclones." *Journal of Wind Engineering and Industrial Aerodynamics*, Vol. 13 (1983).
42. Peterka, J.A., "Improved Extreme Wind Prediction for the United States." *Journal of Wind Engineering and Industrial Aerodynamics*, Vol. 41 (1992).
43. Vickery, B.J., and Twisdale, L.A., "Prediction of Hurricane Wind Speeds in the U.S." Proceedings, 7th National Conference on Wind Engineering, UCLA, Los Angeles, CA, Vol. 2 (1993).
44. Sherlock, R.H., "Gust Factors for the Design of Buildings." *International Association for Bridge and Structural Engineering*, Vol. 8, Zurich, Switzerland (1947).
45. Clark, J., "Design of Aluminum Structural Members." *Structural Engineering Handbook*, Gaylord, E., and Gaylord, C., eds., McGraw-Hill, New York (1990).
46. Marchman, J., III, "Wind Loading on Free-Swinging Traffic Signals." *Transportation Engineering Journal*, Vol. 97, ASCE (May 1971).
47. Cannon, D.D., and LeMaster, R.A., *Local Buckling Strength of Polygonal Tubular Poles*. Transmission Line Mechanical Research Center, Electric Power Research Institute, Haslet, TX (1987).
48. Plantema, F.J., "Collapsing Stresses of Circular Cylinders and Round Tubes." Report S. 280, Nat. Luchtvaartlabatiorium, Amsterdam, The Netherlands (1946).
49. Schilling, C.G., "Buckling Strength of Circular Tubes." *Journal of the Structural Division*, ASCE, Vol. 91, No. ST5, Proceedings 4520 (October 1965).
50. AISC, *Manual of Steel Construction - Load and Resistance Factor Design*. 2nd Edition, Chicago, IL (1994).
51. AASHTO, *Standard Specifications for Highway Bridges*. Washington, DC (1996).
52. Brockenbrough, R.L., "Suggested Structural Design Criteria for Steel Lighting Standards." U.S. Steel Report, Project No. 57 019-450(6) Pittsburgh, PA (1970).
53. Fiss, R.A., "Local Buckling of Tubular Steel Poles in Bending." Paper presented at ASCE Annual and National Environmental Engineering Meeting, St. Louis, MO (1971).
54. AISC, *Manual of Steel Construction*. 8th Edition, Chicago, IL (1978).
55. Brown, J.C., and Tidbury, G.H., "An Investigation of the Collapse of Thin-Walled Rectangular Beams in Biaxial Bending." *International Journal of Mechanical Sciences*, Vol. 25, No. 9-10 (1983).
56. Duan, L., and Chen, W.-F., "A Yield Surface Equation for Doubly Symmetrical Sections." *Engineering Structures*, Vol. 12, No. 2 (1990).
57. Pekoz, T., "Combined Axial Load and Bending in Cold-Formed Steel Members." *Thin-Walled Metal Structures in Buildings*, Stockholm, Sweden (1986).
58. Uchida, Y., and Morino, S., "Biaxial Bending Moment-Curvature Relation of Box Beam-Column with Degrading Stress-Strain Relation." *Research Reports of the Faculty of Engineering*, Mie Univ., Vol. 11, Tsu, Japan (December 1986).
59. Mazzolani, F.M., *Aluminum Alloy Structures*. Pitman Publishing, Inc., Boston (1985).
60. Clark, J.W., and Rolf, R.L., "Buckling of Aluminum Columns, Plates, and Beams." *Journal of the Structural Division*, ASCE, Vol. 92, No. ST3 (June 1966).
61. Clark, J.W., and Rolf, R.L., "Design of Aluminum Tubular Members." *Journal of the Structural Division*, ASCE, Vol. 90, No. ST6 (December 1964).
62. The Aluminum Association, *Specifications for Aluminum Structures*. Publication 30, Washington, DC (1982).
63. ASCE/PCI Joint Committee on Concrete Poles, "Guide for the Design of Prestressed Concrete Poles-Final Draft." ASCE/PCI (1994).
64. PCI Committee on Prestressed Concrete Poles, "Guide for Design of Prestressed Concrete Poles." *Journal of the Prestressed Concrete Institute*, Vol. 28, No. 3 (May-June 1983).
65. Rogers, T.E., Jr., Acree, E., Baker, W.F., Coons, T.W., Gauger, G., Healey, G.S., Imper, R.R., Kniptash, W.R., Langness, S.B., McCalla, W.T., Mees, E.M., and Perry, H.G., "Guide Specifications for Prestressed Concrete Poles." *Journal of the Prestressed Concrete Institute*, Vol. 27, No. 3 (May-June 1982).
66. ASTM, "Final Revisions to ASTM Designation C 1089 Standard Specification for Spun Cast Prestressed Concrete Poles." Philadelphia, PA (1995).
67. ASTM, "Standard Specification for Static Cast Prestressed Concrete Poles." ASTM C935, *Annual Book of ASTM Standards*, Philadelphia, PA (1995).
68. American Concrete Institute, *Building Code Requirements for Reinforced Concrete*. ACI 318-89 (Revised 1992), Detroit, MI (1992).
69. American Concrete Institute, *Building Code Requirements for Structural Concrete*. ACI 318-95, Farmington Hills, MI (1995).
70. AASHTO, *Standard Specifications for Highway Bridges*. Washington, DC (1977).
71. Li, S.-T., and Liu, T.C.-Y., "Prestressed Concrete Piling-Contemporary Design Practice and Recommendations." *ACI Journal* (March 1970).
72. American Forest and Paper Association, *National Design Specifications for Wood Construction - Revised 1991 Edition*. ANSI/NFoPA NDS-1991, Washington, DC (1993).
73. American National Standard Institute, "Specifications and Dimensions for Wood Poles." ANSI 05.1-1992, New York (1992).
74. American Institute of Timber, *Timber Construction Manual*. 4th Edition, John Wiley and Sons, Inc., New York (1994).
75. American Wood-Preservers' Association, *AWPA Book of Standards 1996*. Stevensville, MD (1996).
76. ASTM, "Standard Specification and Test Method for Establishing Recommended Design Stresses for Round Timber Construction Poles." ASTM D3200-74 (Reapproved 1994), *Annual Book of ASTM Standards*, Philadelphia, PA (1995).

77. ASTM, "Standard Methods for Establishing Design Stresses for Round Timber Piles." ASTM D2899-86, *Annual Book of ASTM Standards*, Philadelphia, PA (1995).
78. ASCE, *Structural Plastics Design Manual.* ASCE Manuals and Reports on Engineering Practice, No. 63, New York (1984).
79. Barbero, E.J., and Ritchey, R.A., "A Universal Design Equation for FRP Columns." 48th Annual Conference, Composites Institute, The Society of the Plastics Industry, Inc. (February 8-11, 1993).
80. Johnson, A.F., "Design of RP Cylinders under Buckling Loads." 40th Annual Conference, Reinforced Plastics/Composites Institute, The Society of the Plastics Industry, Inc., London (January 28-February 1, 1985).
81. "Design of Lighting Columns." British Standard BD 26/94, BSI, London, U.K. (September 1994).
82. ASTM, "Standard Specification for Reinforced Thermosetting Plastic Poles." ASTM D4923-92, *Annual Book of ASTM Standards*, Philadelphia, PA (1995).
83. McDonald, J.R., Mehta, K.C., Oler, W.W., and Pulipaka, N., "Wind Load Effects on Signs, Luminaires, and Traffic Signals Structures." Report No. 1303-F, Final Report submitted to Texas Department of Transportation, Wind Engineering Research Center, Lubbock, TX (1995).
84. Lundgren, H.R., "Evaluation of Monotube Sign Support Structure." Report No. FHWA-AZ89-829, Arizona Department of Transportation, Phoenix (1989).
85. Ehsani, M.R., Chakrabarti, S.K., and Bjorhovde, R., "Static and Dynamic Behavior of Monotube Span-Type Sign Structures." Report No. FHWA/AZ-84/194-I, Arizona Department of Transportation, Tempe (1984).
86. Martin, K.A., Ehsani, M.R., and Bjorhovde, R., "Field Testing of Monotube Sign Support Structures." Report No. FHWA/AZ-86/237, Arizona Department of Transportation, Tempe (1985).
87. USS Corporation, "Axial Buckling Loads of Steel Lighting Standards." Technical Report, Pittsburgh (February 1973).
88. Timoshenko, S., and Gere, J., *Theory of Elastic Stability.* McGraw-Hill Book Company, New York (1961).
89. Gere, J., and Carter, W.O., "Critical Buckling Loads for Tapered Columns." *Journal of the Structural Division*, Proceedings 3045 ASCE, Vol. 88, No. ST1 (February 1962).
90. South, J.M., "Fatigue Analysis of Overhead Sign and Signal Structures." Report No. FHWA/IL/PR-115, Illinois Department of Transportation, Springfield (1994).
91. Boulos, S.J., Fu, G., and Alampalli, S., "Load Testing, Finite Element Analysis, and Design of Steel Traffic-Signal Poles." Report No. FHWA/NY/RR-93/159, Federal Highway Administration (1993).
92. Hahin, C., *Fatigue of Large Traffic Signal Structures*, Illinois Department of Transportation, Springfield (1989).
93. American Welding Society, *Structural Welding Code - Steel.* ANSI/AWS D1.1-94, Miami, FL (1994).
94. American Welding Society, *Structural Welding Code - Aluminum.* ANSI/AWS D1.2-90, Miami, FL (1990).
95. American Concrete Institute, "Code Requirements for Nuclear Safety Related Concrete Structures." Appendix B, Steel Embedments, ACI 349-90, Farmington Hills, MI (1995).
96. AASHTO, "Standard Specification for Steel Anchor Bolts." AASHTO M 314-90, *Standard Specifications for Transportation Materials and Methods of Sampling and Testing*, 17th Edition, Washington, DC (1993).
97. ASTM, "Standard Specification for Anchor Bolts, Steel, 36, 55, and 105-ksi Yield Strength." ASTM F 1554-94, *Annual Book of ASTM Standards*, Philadelphia, PA (1995).
98. Cook, R.A., Doerr, G.T., and Klingner, R.E., *Design Guide for Steel-to-Concrete Connections.* Report FHWA/TX-89+1126-4F, Center for Transportation Research, Texas State Department of Highways and Public Transportation, Austin (March 1989).
99. American Concrete Institute, "State-of-the-Art Report on Anchorage to Concrete." ACI 355.1R-91, Farmington Hills, MI (1991).
100. Cannon, R.W., "Straight Talk About Anchorage to Concrete - Part I," *ACI Structural Journal*, Vol. 92, No. 5 (September-October 1995).
101. Jirsa, J.O., Cichy, N.T., Calzadilla, M.R., Smart, W.H., Pavluvick, M.P., and Breen, J.E., "Strength and Behavior of Bolt Installations Anchored in Concrete Piers." Report No. FHWA/TX85/51+305-1F, Texas State Department of Highways and Public Transportation (1984).
102. Eligehausen, R., and Balogh, T., "Behavior of Fasteners Loaded in Tension in Cracked Reinforced Concrete." *ACI Structural Journal*, Vol. 92 (May-June 1995).
103. Fuchs, W., Eligehausen, R., and Breen, J.E., "Concrete Capacity Design (CCD) Approach for Fastening to Concrete." *ACI Structural Journal*, Vol. 92 (January-February 1995).
104. Lynch, T.J., and Burdette, E.G., "Some Design Considerations for Anchors in Concrete." *ACI Structural Journal*, Vol. 88, No. 1 (January-February 1991).
105. Lee, D.W., and Breen, J.E., "Factors Affecting Anchor Bolt Development." Research Report No. 88-1F, Center for Highway Research, Texas Highway Department, Austin (1966).
106. Hasselwander, G.B., Jirsa, J.O., Breen, J.E., and Lo, K., "Strength and Behavior of Anchor Bolts Embedded Near Edges of Concrete Piers." Report No. CFHR 3-5-74-29-2F, Center for Highway Research, Texas State Department of Highways and Public Transportation, Austin (1977).
107. AISC, *Manual of Steel Construction.* 7th Edition, Chicago, IL (1970).
108. American Concrete Institute, "Design and Construction of Drilled Piers." ACI 336.3R-93, *Manual of Concrete Practice*, Farmington, Hills, MI (1995).
109. American Concrete Institute, "Suggested Analysis and Design Procedures for Combined Footings and Mats." ACI 336.2R-88 (Reapproved 1993), *Manual of Concrete Practice*, Farmington, Hills, MI (1995).
110. Broms, B.B., "Design of Laterally Loaded Piles." *Journal of the Soil Mechanics and Foundation Division*, ASCE, Proceedings, Vol. 91, No. SM3 (May 1965).
111. Broms, B.B., "Lateral Resistance of Piles in Cohesionless Soils." *Journal of the Soil Mechanics and Foundation Division*, ASCE, Proceedings 3909, Vol. 90, No. SM3 (May 1964).
112. Broms, B.B., "Lateral Resistance of Piles in Cohesive Soils." *Journal of the Soil Mechanics and Foundation Division*, ASCE, Proceedings 3825, Vol. 90, No. SM2 (March 1964).
113. *Design and Construction of Deep Foundations*, International Conference, U.S. Federal Highway Administration (December 1994).
114. DiGioia, A.M., Rojas-Gonzalez, L., and Newman, F.B., "Statistical Analyses of Drilled Shaft and Embedded Pole Models." *Foundation Engineering: Current Principles and Practices*, ASCE, New York (1989).

115. Hansen, J.B., "The Ultimate Resistance of Rigid Piles Against Transversal Forces." *The Danish Geotechnical Institute Bullitin*, Vol. 12, Copenhagen, Denmark (1961).
116. Ivey, D.L., and Hawkings, L., "Signboard Footings to Resist Wind Loads." Civil Engineering, Vol. 36, No. 12 (December 1966).
117. Poulos, H.G., *Pile Foundation and Design*. John Wiley and Sons, Inc., New York (1980).
118. Reese, L.C., and O'Neill, M.W., "Drilled Shafts: Construction Procedures and Design Methods." Report FHWA-HI-88-042, Federal Highway Administration, McLean, VA (1988).
119. Reese, L.C., *Handbook on Design of Piles and Drilled Shafts Under Lateral Load*. Report FHWA-IP-84-11, Federal Highway Administration, McLean, VA (July 1984).
120. Singh, A., Hu, R.E.-W., and Consineau, R.D., "Lateral Load Capacity of Piles in Sand and Normally Consolidated Clay." *Civil Engineering*, Vol. 41 (August 1971).
121. Teng and Associates, "Tapered Steel and Poles Caisson Foundation Design." U.S. Steel, ADUSS 88-4328-01, Pittsburgh (July 1969).
122. Tomlinson, M.J., *Pile Design and Construction Practice*. Viewpoint Publications, Cement and Concrete Association, London (1977).
123. Kinney, E.E., "Correct Embedment for Pole Structures." *Wood Preserving News* (October 1959).
124. GAI Consultants, Inc., *Laterally Loaded Drilled Pier Research, Volume 1: Design Methodology*. Electric Power Research Institute, Palo Alto, CA (1982).
125. Borden, R.H., and Gabr, M.A., "Analysis of Compact Pole-Type Footings - LTBASE: Computer Program for Laterally Loaded Pier Analysis Including Base and Slope Effects." Report No. FHWA/NC87-001, Department of Civil Engineering, North Carolina State University, Raleigh, Report prepared for the North Carolina Department of Transportation and Federal Highway Administration (1987).
126. Reese, L.C., *Documentation of Computer Program LPILE1*. Ensoft, Inc., Austin, TX (1985).
127. Michie, J.D., "Recommended Procedures for the Safety Performance Evaluation of Highway Appurtenances." *NCHRP Report 230*, Transportation Research Board, National Research Council, Washington, DC (1981) 42 pp.
128. Bronstad, M.E., and Michie, J.D., "Recommended Procedures for Vehicle Crash Testing of Highway Appurtenances." *NCHRP Report 153*, Transportation Research Board, National Research Council, Washington, DC (1974) 19 pp.
129. Structures Design Office, Florida Department of Transportation, *Strain Pole Program Version 1.65*. Tallahassee (April 1992).
130. McDonald, B., and Peyrot, A., "Sag-Tension Calculations Valid for Any Line Geometry." *Journal of Structural Engineering*, Vol. 116, No. 9 (September 1990).
131. Wang, C.M., "Optimal Shape of Cables." *Journal of Engineering Mechanics*, Vol. 110, No. 11 (November 1984).
132. Wang, C.M., and Jin, D., "Basic Problem on Optimal Spatial Cable Layout." *Journal of Engineering Mechanics*, Vol. 115, No. 5 (May 1989).
133. Watson, C.G., *Sags and Tensions in Overhead Lines*. Sir Isaac Pitman, London (1931).
134. Tatum, V.K., Barfield, G.S., and Gratton, E.H., "Evaluation of Program to Calculate Traffic Signal Layouts." Final Report, GDOT Research Project 9111, Georgia DOT, Atlanta (October 1992).
135. AASHTO, "Standard Specification for Zinc (Hot-Dip Galvanized) Coatings on Iron and Steel Products." AASHTO M111-91 (ASTM A123-89a), *Standard Specifications for Transportation Materials and Methods of Sampling and Testing*, 17th Edition, Washington, DC (1993).
136. AASHTO, "Standard Specification for Zinc (Hot-Dip Galvanized) Coatings on Iron and Steel Products." AASHTO M111-87 (ASTM A123-84), *Standard Specifications for Transportation Materials and Methods of Sampling and Testing*, 15th Edition, Washington, DC (1990).
137. AASHTO, "Zinc Coating (Hot-Dip) on Iron and Steel Hardware." AASHTO M232-84 (ASTM A153-82), *Standard Specifications for Transportation Materials and Methods of Sampling and Testing*, 17th Edition, Washington, DC (1993).
138. AASHTO, *Standard Specifications for Highway Bridges*. Washington, DC (1992).
139. Davis, J.R., *Aluminum and Aluminum Alloys*. ASM International, Materials Park, OH (1993).
140. ACI Committee 222, "Corrosion of Metals in Concrete." ACI 222R-89, *Manual of Concrete Practice*, American Concrete Institute, Farmington Hills, MI (1995).
141. ACI Committee 201, "Guide to Durable Concrete." ACI 201.2R-92, *Manual of Concrete Practice*, American Concrete Institute, Farmington Hills, MI (1995).
142. ACI Committee 212, "Chemical Admixtures for Concrete." ACI 212.3R-91, *Manual of Concrete Practice*, American Concrete Institute, Farmington Hills, MI (1995).
143. Corley, W.G., "Designing Corrosion Resistance into Reinforced Concrete." *Materials Performance*, Vol. 34 (September 1995).
144. Hime, W.G., "The Corrosion of Steel - Random Thoughts and Wishful Thinking." *Concrete International*, Vol. 15 (October 1993).
145. Rostam, S., "Service Life Design - The European Approach." *Concrete International*, Vol. 15 (July 1993).
146. Campbell, G.M., and Detwiler, R.J., "Development of Mix Design for Strength and Durability of Steam-Cured Concrete." *Concrete International*, Vol. 15 (July 1993).
147. Rasheeduzzafar Al-Saadoun, S.S., and Al-Gahtani, A.S., "Reinforcement Corrosion-Resisting Characteristics of Silica Fume Blended-Cement Concrete." *ACI Materials Journal* (July-August 1992).
148. Yeomans, S.R., "Performance of Black, Galvanized, and Epoxy-Coated Reinforcing Steels in Chloride-Contaminated Concrete." *Corrosion* (January 1994).
149. Research Engineers, Inc., *STAAD-III/ISDS Revision 14.2*. Orange, CA (1991).
150. Cook, R.D., and Young, W.C., *Advanced Mechanics of Materials*. Macmillan Publishing Company, New York (1985).
151. Fisher, J.W., Nussbaumer, A., Keating, P.B., and Yen, B.T. "Resistance of Welded Details Under Variable Amplitude Long-Life Fatigue Loading." *NCHRP Report 354*, Transportation Research Board, National Research Council, Washington, DC (1993) 38 pp.
152. Timoshenko, S., Young, D.H., and Weaver, J., *Vibration Problems in Engineering*. 4th Edition, John Wiley and Sons, Inc., New York (1974).

The **Transportation Research Board** is a unit of the National Research Council, which serves the National Academy of Sciences and the National Academy of Engineering. The Board's mission is to promote innovation and progress in transportation by stimulating and conducting research, facilitating the dissemination of information, and encouraging the implementation of research results. The Board's varied activities annually draw on approximately 4,000 engineers, scientists, and other transportation researchers and practitioners from the public and private sectors and academia, all of whom contribute their expertise in the public interest. The program is supported by state transportation departments, federal agencies including the component administrations of the U.S. Department of Transportation, and other organizations and individuals interested in the development of transportation.

The National Academy of Sciences is a private, nonprofit, self-perpetuating society of distinguished scholars engaged in scientific and engineering research, dedicated to the furtherance of science and technology and to their use for the general welfare. Upon the authority of the charter granted to it by the Congress in 1863, the Academy has a mandate that requires it to advise the federal government on scientific and technical matters. Dr. Bruce M. Alberts is president of the National Academy of Sciences.

The National Academy of Engineering was established in 1964, under the charter of the National Academy of Sciences, as a parallel organization of outstanding engineers. It is autonomous in its administration and in the selection of its members, sharing with the National Academy of Sciences the responsibility for advising the federal government. The National Academy of Engineering also sponsors engineering programs aimed at meeting national needs, encourages education and research, and recognizes the superior achievements of engineers. Dr. William A. Wulf is president of the National Academy of Engineering.

The Institute of Medicine was established in 1970 by the National Academy of Sciences to secure the services of eminent members of appropriate professions in the examination of policy matters pertaining to the health of the public. The Institute acts under the responsibility given to the National Academy of Sciences by its congressional charter to be an adviser to the federal government and, upon its own initiative, to identify issues of medical care, research, and education. Dr. Kenneth I. Shine is president of the Institute of Medicine.

The National Research Council was organized by the National Academy of Sciences in 1916 to associate the broad community of science and technology with the Academy's purpose of furthering knowledge and advising the federal government. Functioning in accordance with general policies determined by the Academy, the Council has become the principal operating agency of both the National Academy of Sciences and the National Academy of Engineering in providing services to the government, the public, and the scientific and engineering communities. The Council is administered jointly by both the Academies and the Institute of Medicine. Dr. Bruce M. Alberts and Dr. William A. Wulf are chairman and vice chairman, respectively, of the National Research Council.

Abbreviations used without definitions in TRB publications:

AASHO	American Association of State Highway Officials
AASHTO	American Association of State Highway and Transportation Officials
ASCE	American Society of Civil Engineers
ASME	American Society of Mechanical Engineers
ASTM	American Society for Testing and Materials
FAA	Federal Aviation Administration
FHWA	Federal Highway Administration
FRA	Federal Railroad Administration
FTA	Federal Transit Administration
IEEE	Institute of Electrical and Electronics Engineers
ITE	Institute of Transportation Engineers
NCHRP	National Cooperative Highway Research Program
NCTRP	National Cooperative Transit Research and Development Program
NHTSA	National Highway Traffic Safety Administration
SAE	Society of Automotive Engineers
TCRP	Transit Cooperative Research Program
TRB	Transportation Research Board
U.S.DOT	United States Department of Transportation

Transportation Research Board
National Research Council
2101 Constitution Avenue, N.W.
Washington, D.C. 20418

ADDRESS CORRECTION REQUESTED